SLOW-RELEASE CROSS-COUPLING AND AN ADVANCED METHOD FOR β-GLYCOSYLATION: METHODS STIMULATED BY AMPHOTERICIN B

BY

DAVID M. KNAPP

DISSERTATION

Submitted in partial fulfillment of the requirements
for the degree of Doctor of Philosophy in Chemistry
in the Graduate College of the
University of Illinois at Urbana Champaign, 2012

Urbana, Illinois

Doctoral Committee:

Associate Professor Martin D. Burke, Chair
Professor Wilfred A. van der Donk
Professor John A. Katzenellenbogen
Professor Jeffrey S. Moore

ABSTRACT

Amphotericin B (AmB) represents a clinically vital but toxic antibiotic that additionally has the ability to form ion channels in biological membranes, a capacity normally associated with proteins. Better understanding the dynamics of channel formation and how it relates to AmB's antifungal activity would stand to enable both the rational development of derivatives that have a better therapeutic index, and the design of the small molecule prosthetics with the capacity to treat currently incurable human diseases. Efficient access to derivatives of AmB would greatly facilitate these goals.

In this context, several methodological advances have been made that were stimulated by studies toward an efficient and flexible total synthesis of AmB. In response to challenges encountered in the construction of the AmB polyene, a new cross-coupling protocol was developed whereby *N*-methyliminodiacetic acid (MIDA) boronates can be used directly in Suzuki-Miyaura cross-coupling (SMC) reactions, enabling air-stable MIDA boronates to act as surrogates for boronic acids. Additionally, conditions were identified under which MIDA boronates could be slowly hydrolyzed in the SMC reaction, enabling an in situ "slow-release" of the boronic acid. This slow release effect enables the efficient cross-coupling of a variety of otherwise unstable boronic acids. The synthesis and isolation of 2-pyridyl MIDA boronate and its derivatives demonstrates that even the most unstable boronic acids may be rendered stable and competent cross coupling partners by conversion to the corresponding MIDA boronates. Further, the use of "fast-release" conditions enabled the construction of the AmB heptaene as well as a variety of polyenyl natural products both within and outside our research group. To overcome the challenging 1,2-*cis* glycosidic bond found in AmB a mycosamine sugar donor synthesis was developed incorporating a new directing group for neighboring group participation. The use of this new directing group enabled efficient glycosylation of, and ultimately the completion of, a critical building block in the context of the iterative cross-coupling (ICC)-based synthesis of AmB. The potential of this glycosylation strategy for rapidly accessing AmB derivatives was also demonstrated in the synthesis of a C3'-deaminomycosamine sugar donor and its efficient attachment to a protected amphotericin aglycone.

ACKNOWLEDGEMENTS

I would like to start by thanking my advisor Marty Burke for his mentorship over the past six years. His unwavering support and guidance have been instrumental in enabling me to succeed as a graduate student. His insistence on dreaming big is a perspective that I will carry with me wherever life may take me. I would also like to thank my thesis committee: Prof. Wilfred van der Donk, Prof. John Katzenellenbogen and Prof. Jeff Moore for their support, and for always holding me to a high standard of scholarship. My undergraduate research advisor, Prof. Mark Brandt, also deserves credit for inspiring my interest in chemistry. His contagious enthusiasm for trying to understand how the world works defined my college experience and ultimately brought me here. The organic area secretaries, Becky Duffield, Stacy Olsen and Susan Lighty deserve special mention for graciously putting up with my incessant bothering.

To the rest of the Burke group, I do not think I can sufficiently express my gratitude. Your support and friendship have without question made the completion of this degree possible. I want to specifically thank several past and current group members. To my former bay mates Ian Dailey and Eric Gillis, I want thank you for being awesome. Your friendship made this lab an incredible place to work. I won't soon forget the coffee shop commiserations, the music marathons, or the outrageously inappropriate lunch-time discussions, to say nothing of our time in the trenches. I am incredibly happy that you both found such success and happiness in your new lives, but I have to say, it's just not the same around here without you. Additionally, I must thank Brice Uno and Erin Davis for nights at the Pig, Jenna Klubnick for her dance parties, Stephen Davis for his welcome distractions, and Pulin for being Pulin. I also wish to thank Seiko Fujii and Hannah Haley for putting up with the bitter, cynical man that I have undoubtedly become in my twilight years here.

I also must say thank you to my parents, for their unfaltering support over the years, and to my brother for making it pretty much impossible to quit, whether he realizes it or not. I also gratefully acknowledge the many generous sources of funding I have received over the years, including the University of Illinois, the Roger Adams fellowship, the National Institutes of Health, the Chemical Biology Interface Training Grant, and the Lilly Endowment Community Scholarship.

LIST OF ABBREVIATIONS

AmB	amphotericin B
AmdeB	amphoteronolide B
AmE	amphotericin B methyl ester
BLM	black lipid membranes
BRSM	based on recovered starting material
C3'deNAmB	C3'-deamino amphotericin B

C35deOAmB	C35-deoxy amphotericin B	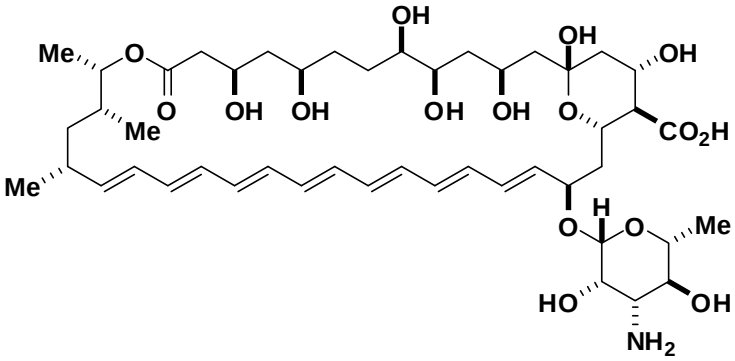
CAM	ceric ammonium molybdate	
cat	catachol	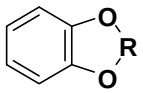
CMP	2-chloro-6-methylpyridine	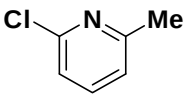
CMPT	2-chloro-6-methylpyridinium triflate	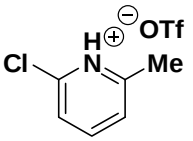
Cp*	pentamethylcyclopentadienyl	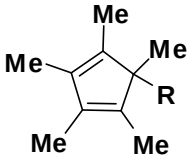
CSA	(±)-camphorsulfonic acid	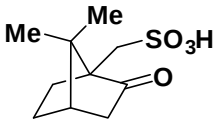
CuTC	copper(I) thiophene-2-carboxylate	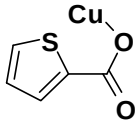
dba	dibenzylidene acetone	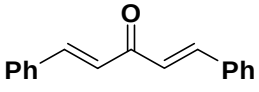
DCC	*N*,*N*'-dicyclohexylcarbodiimide	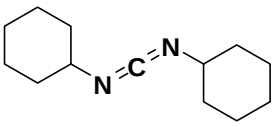

DCVC	dry column vacuum chromatography	
DCM	dichloromethane	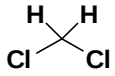
DDQ	2,3-dichloro-5,6-dicyano-1,4-benzoquinone	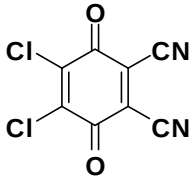
$(DHQ)_2PHAL$	1,4-bis(9-*O*-dihydroquininyl)phthalazine	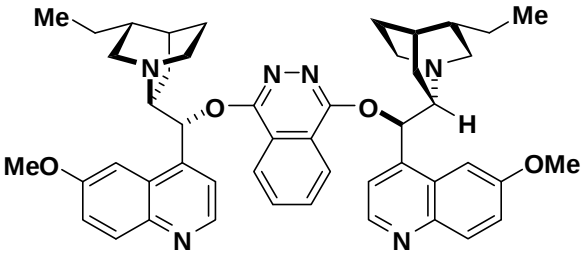
$(DHQ)_2PYR$	2,5-diphenyl-4,6-bis(9-*O*-dihydroquininyl)pyrimidine	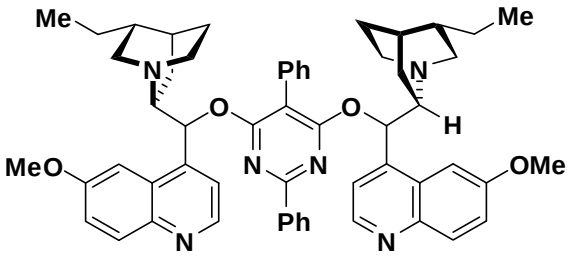
DIBAL	diisobutylaluminum	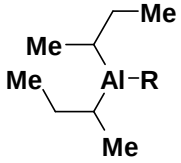
(+)-DIPT	diisopropyltartrate	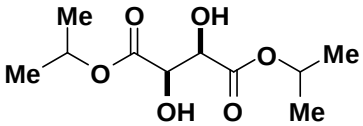
DMAP	dimethylaminopyridine	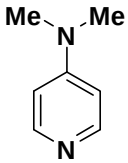
DMB	3,4-dimethoxybenzyl	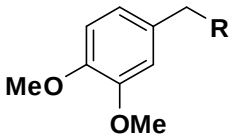

DMP	Dess-Martin periodinane	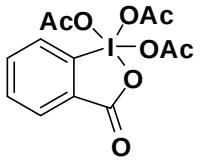
d.r.	diastereomeric ratio	
DTBMP	2,6-di-*tert*-butyl-4-methylpyridine	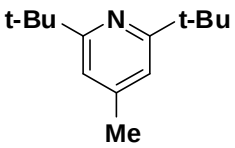
Fmoc	fluorenylmethyloxycarbonyl	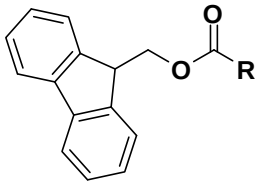
HMPA	hexamethylphosphoramide	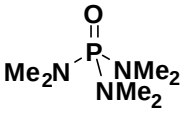
ICC	iterative cross-coupling	
IPA	isopropyl alcohol	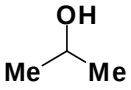
ipc	isopinocampheyl	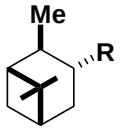
m-CPBA	*meta*-chloroperbenzoic acid	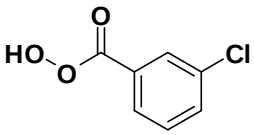
MeAmB	C41-methyl amphotericin B	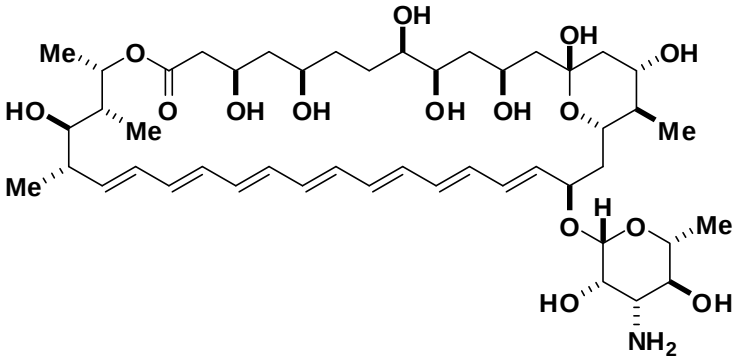

MeAmdeB	C41-methyl amphoteronolide B	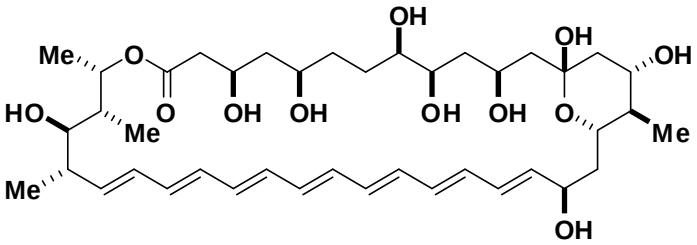
MIC	minimum inhibitory concentration	
MIDA	*N*-methyliminodiacetic acid	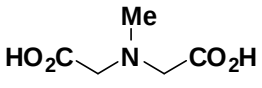
NBS	*N*-bromosuccinimide	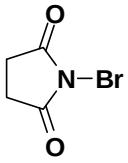
NCS	*N*-chlorosuccinimide	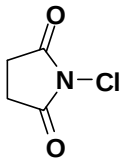
NIS	*N*-iodosuccinimide	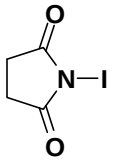
PADC	potassium azodicarboxylate	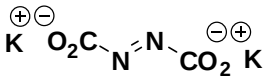
$Pd(dtbpf)Cl_2$	palladium(II) ditert-butylphosphinoferrocene dichloride	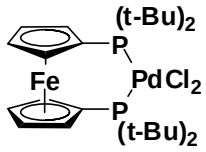
PMB	*para*-methoxybenzyl	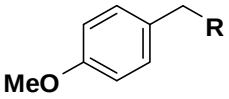
PMP	*para*-methoxyphenyl	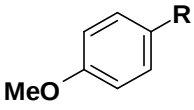

PPTS	pyridinium *para*-toluenesulfonate	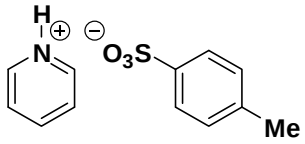
PTFE	polytetrafluoroethylene	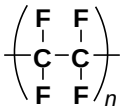
pyr	pyridine	
r.t.	room temperature	
SMC	Suzuki-Miyaura cross-coupling	
S-Phos	2-dicyclohexylphosphino-2',6'-dimethoxybiphenyl	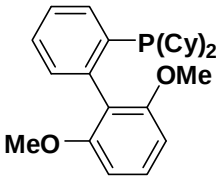
Su	succinimide	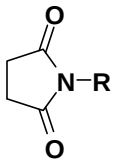
TBAF	tetrabutylammonium fluoride	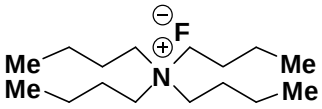
TBAI	tetrabutylammonium iodide	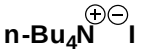
TBDPS	*tert*-butyldiphenylsilyl	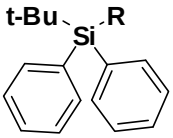
TBS	*tert*-butyldimethylsilyl	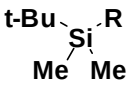
TDMB	4-*tert*-butyldimethylsilyloxy-2,2-dimethylbutyrate	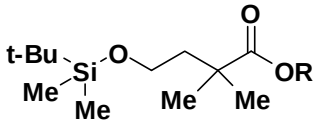

Tf	trifluormethanesulfonyl	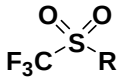
TMSE	trimethylsilylethyl	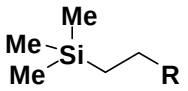
TOF	turn-over-frequency	
Ts	toluenesulfonyl	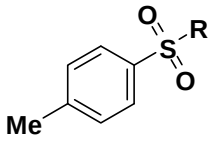
(*R*,*R*)-TsDPEN	(*R*,*R*)-*N*-(*para*-toluenesulfonyl)-1,2-diphenyl-1,2-ethanediamine	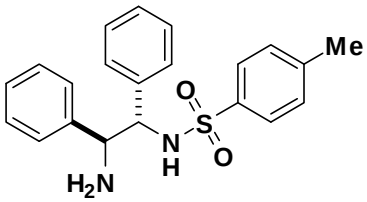
X-Phos	2-dicyclohexylphophino-2',4',6'-triisopropylbiphenyl	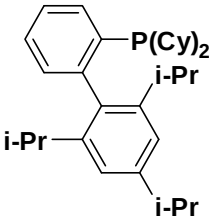

TABLE OF CONTENTS

CHAPTER 1

Understanding of Mycosamine-Containing Polyene Macrolides

1-1 TOTAL SYNTHESIS AS A STIMULUS FOR NEW SYNTHETIC METHODOLOGY

The remarkable complexity and variety of molecular structures found in nature forces the synthetic chemist to consider new tactics and strategies for their synthesis in the laboratory. For this reason natural product synthesis has historically led to the development of a large number of new chemical methods, ranging from new carbon-heteroatom and carbon-carbon bond-forming reactions, to new techniques to control the stereochemical outcome of existing reactions, and even to the discovery of entirely new reactions. The continued discovery and challenge of natural products with difficult-to-access architectures suggests that the potential of small molecules to stimulate new methodology remains high.

Mycosamine-containing polyene macrolides constitute one such class of natural products. Despite being known for more than 60 years, members of this class still pose a formidable synthetic challenge. Polyene macrolides are also notable for their biological activity. They are potent antimycotics, and the most prominent member of the class, amphotericin B, remains the last line of defense against systemic fungal infections in humans. Furthermore, some members, including amphotericin B, are capable of forming ion-channels in biological membranes, a function normally reserved for proteins. We believe this ability to perform protein-like activity represents untapped potential in this class of compounds, but harnessing that potential will require a better understanding of its mechanism of action, something that has eluded the scientific community for more than half a century. The following sections describe the historical context of this remarkable small molecule, the current understanding of its mechanism of action, and some new synthetic methodologies that have been stimulated by our own efforts toward its synthesis and study.

1-2 AMPTHOTERICN B: A CLINICALLY VITAL SMALL MOLECULE

Systemic fungal infections represent a serious and expanding threat to human health. In the United States, the occurrence of fungal septicemias increased by 207% between the years of 1979 and 2000,[1] fungal pathogens account for approximately 10% of all reported hospital acquired infections, and *Candida* species alone are statistically tied for the third most common

source of microbial bloodstream infection.[2] Further, the prevalence of fungal infections may be significantly underestimated due to the challenges inherent to their diagnosis, as well as the high frequency of false-negative results in fungal blood-cultures.[3] For those infected, mortality rates are high, ranging from 30–80%.[4] The associated burden to the U.S. healthcare system is also high, with reports of total cost ranging from $1–4 billion annually.[5-7] Additionally, demographic trends that are associated with an increased risk of fungal septicemia such an aging population, an increase in the length of hospital stays, and a growing population of immunocompromised individuals due to organ transplants and stem cell therapies, are only expected to continue.[8] Further exacerbating this situation is the growing problem of microbial resistance which has narrowed the range of viable treatments.[9] Mirroring the trends seen in bacterial antibiotics,[10] the development of new classes of antifungal agents has also been slow, making microbial resistance an even more serious concern.

Despite these troubling statistics, prior to 1950 the situation was even more dire, with the mortality rate of blood borne fungal infections at nearly 100% due to the lack of any effective treatment.[11] The isolation of the potent antifungal polyene macrolide nystatin (initially named fungicidin) from the soil bacterium *Streptomyces noursei* in 1950[12-13] revolutionized the treatment of fungal infections. Commercialized in 1954, nystatin was the first broad spectrum antifungal agent. In the years following nystatin's isolation, intense research unearthed a number of additional polyene macrolides, including rimocidin in 1951,[14] perimycin in 1952,[15] candicidin in 1953,[16] amphotericin in 1955,[17] and natamycin in 1957.[18]

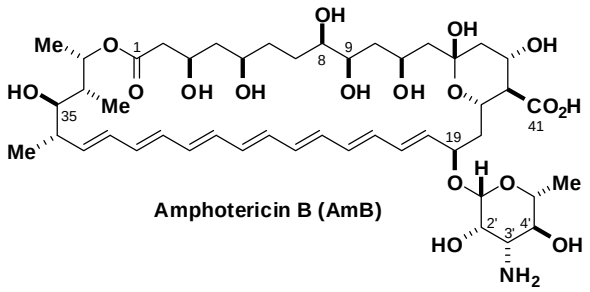

Figure 1.1. Chemical structure of amphotericin B (AmB)

Today, amphotericin B (AmB) (Figure 1.1), also a member of this class, represents the standard of care for systemic fungal infections. First introduced in the clinic in 1958, AmB has enjoyed continuous clinical use for over 50 years. The remarkable success of this antibiotic can

be attributed to two factors: its broad spectrum of activity[19] and its relative insusceptibility to microbial resistance.[20] However, despite its potent antifungal activity, the effective clinical use of AmB has been hampered by its severe dose-limiting toxicity. Specifically, the use of AmB is associated with significant cardiac and renal toxicity, as well as hemolytic anemia. [21] These effects have been partly reduced by liposome formulations,[22] but an unclear understanding of AmB's mechanism of action has to date hampered further improvement of the therapeutic index, or the design of more effective derivatives, of this vital antibiotic.

AmB is also notable for its capacity for form discrete ion-channels in lipid bilayers, a phenomenon that we find to be extremely provocative. Specifically, it suggests to us that AmB might serve as the foundation for the development of "molecular prosthetics," small molecules designed to mimic the function of proteins in living systems. There exist a number of diseases that stem from an acute lack of protein function, including channelopathies like cystic fibrosis.[23] These diseases are essentially untreatable via the current pharmacological paradigm: that of using a small molecule to inhibit a protein target. The use of a molecular prosthetic that could even partially restore the function of a missing or dysfunctional protein might represent a fundamentally new way to treat these diseases.[24-26] We therefore propose that an atomistic understanding of this remarkable small molecule-based channel stands to not only enable the pursuit of less toxic AmB derivatives, but might also enable the development of a new class drugs targeting currently incurable diseases.

1-3 STRUCTURAL CHARACTERISTICS OF THE POLYENE MACROLIDES

AmB belongs to a class of natural products called mycosamine-containing polyene macrolides. Since the discovery of AmB, more than 200 mycosamine-containing polyene macrolides have been reported, though to date only 36 have been structurally characterized to a reasonable degree of certainty.[27-50] Their structural similarity is a consequence of their common biosynthetic origin; all are products of type I polyketide synthase (PKS) machinery found in their producing organisms.[51] Further, this class of natural products is characterized by several notable structural features, all found on the "eastern end" of the molecules. As shown in Figure 1.2, these include a 6-membered endocyclic hemiketal, an exocyclic carboxylic acid, and a mycosamine sugar appendage. The carboxylic acid and mycosamine sugar are both installed by dedicated tailoring enzymes after the parent macrolide is released from the PKS machinery.[52] Interestingly,

within this class of natural products, mycosamine attachment is always accompanied by the presence of the neighboring carboxylic acid, which is itself installed by P-450 mediated oxidation of an exocyclic methyl group. These two functional groups are also notable in their rarity outside of the polyene macrolide family. The only other natural products known to contain a mycosamine sugar are the fluvaricins,[53-55] and the tetramic acid derivative vancoresmycin.[56] Exhaustive oxidation of exocyclic methyl groups is also extremely rare.[52]

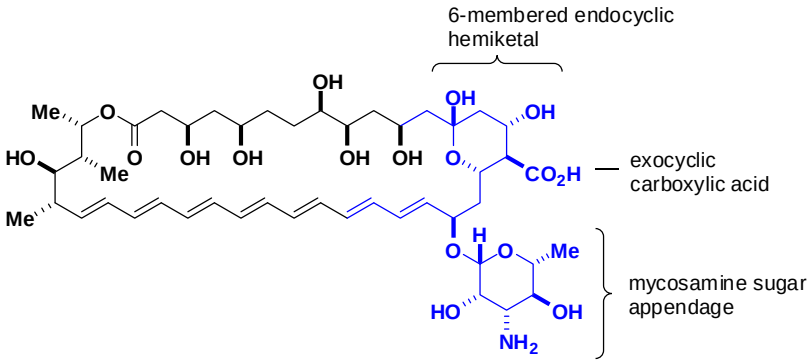

Figure 1.2. Structural features common to mycosamine-containing polyene macrolides, as shown on AmB. Together, these features comprise a highly conserved motif, which is highlighted in blue.

Collectively, these structural features form a highly conserved motif common to all mycosamine-containing polyene macrolides that have been structurally characterized thus far (Figure 1.2). Given the ubiquity of this structural motif across all members of the polyene macrolide family, we hypothesized that these natural products share a common mechanism of action, and that this motif might represent the structural features critical for that mechanism.

1-4 MECHANISTIC UNDERSTANDING OF POLYENE MACROLIDE ANTIBIOTICS

Understanding the mechanism of antifungal activity of AmB and other members of the polyene macrolide family is key to the development antimycotics with improved therapeutic indexes. Additionally, a thorough understanding of AmB's mechanism of action might shed light on how it is uniquely insusceptible to microbial resistance. Such an understanding could enable the design of a new class of pharmaceuticals better able to avoid the growing problem of microbial resistance, which would have a substantial impact beyond just fungal infections. With this potential in mind it is therefore not surprising that a tremendous amount of effort has been

directed at understanding the mechanism of action of polyene macrolides over the last half century.

Initial studies on the mechanism of polyene macrolides were performed in 1958 by Osteux and coworkers, who observed that nystatin induced leakage of low molecular weight contents from *C. albicans*, but that larger contents were retained.[57] Similarly, in 1961 Kinsky and coworkers found that treatment of *N. crassi* with AmB resulted in a significantly reduced dry weight of mycelial mats.[58] Kinsky proposed that AmB permeabilizes membranes, and that this permeabilization is the source of its activity. Since that time, membrane permeabilization has been the general mechanism most often implicated as the mode of activity and toxicity in these compounds.[51,59-60] Indeed, a significant amount of data over the years has correlated the membrane permeabilizing properties of AmB and related polyene macrolides with their biological activity. de Kruijff and co-workers showed that cholesterol laden *A. laidlawii*, known to be sensitive to AmB, lost intracellular potassium when exposed to AmB.[61] Correspondingly, the eubacterium *B. megaterium*, which is completely resistant to AmB, showed no efflux of cellular material.[62-64] In 1976, electrophysiology experiments with black planar lipid bilayers (BLM)[65] showed unequivocal channel formation in both AmB and nystatin.[66] Remarkably, these channels displayed characteristics, such as gating, more generally associated with protein ion channels. Further, it was demonstrated that these channels could be reversibly blocked with tetraethylammonium cation,[67] also similar to known protein ion channels. With evidence mounting for a existence of a discrete channel, Andreoli and coworkers investigated the ability of small solutes to pass through membranes permeabilized with AmB.[68] They found that AmB increased the membrane permeability of small molecules like urea and glycerol, but not larger molecules like glucose. Correlating the hydrodynamic radii of these small molecules with their ability to transit membranes in the presence of AmB, Andreoli and coworkers estimated an AmB pore size of 7–10 Å.

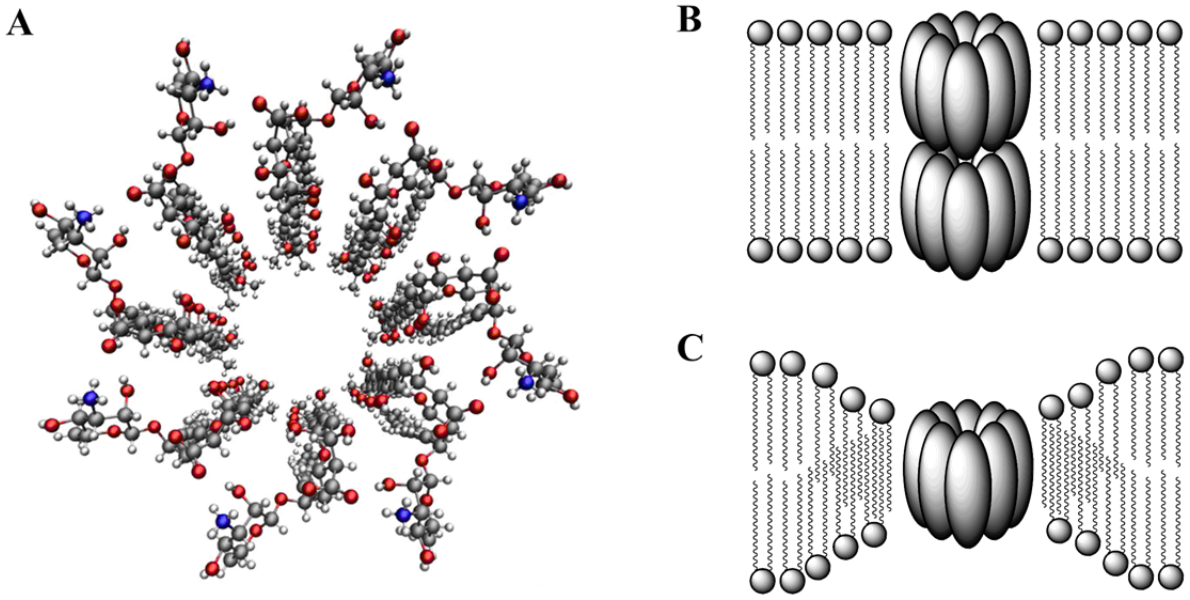

Figure 1.3. (A) Top down view of the barrel-stave channel model proposed for AmB. (B) Side on view of the channel complex double-barrel channel with one half of the barrel in each leaflet of the membrane, stacked on top of one another. (C) The single-barrel channel model, in which one barrel pinches the membrane together.

Collectively, these results led to the now classic barrel-stave channel model, proposed independently by de Kruijff,[69] Andreoli,[70-71] and Finklestein[72] (Figure 1.3). In this model, eight monomers of AmB assemble into a membrane-spanning complex, each with their hydrophilic polyol projecting inward toward the interior of a water-filled pore, and the hydrophobic polyene exposed to the exterior lipid environment. Additionally, there are two basic proposals for how this channel might span a lipid bilayer. In the first, single barrel-hypothesis, a single AmB octomeric complex, or barrel, spans the membrane directly, forcing the surrounding phospholipids to pinch together. In the double-barrel hypothesis, two barrels stack on top of one another to span the bilayer.[73] The double-barrel model appears particularly attractive for AmB, given that the length of the AmB macrolactone (21 Å) is conspicuously almost exactly one half the length of a lipid bilayer (43 Å). Nevertheless, these two models remain debated in the literature.[74]

Several interactions have been predicted to play a key role in the stabilization of this barrel-stave complex. All three involve the mycosamine sugar and C41'-carboxylate, the very same conserved functionality shown previously as unique to mycosamine-containing polyene macrolides. In the first proposal, the C41-carboxylate and the C3'-ammonium of the mycosamine interact to form a stabilizing ring of salt bridges around the periphery of the

channel.[75-77] In the second proposal, the C41-carboxylate and mycosamine sugar have been implicated in intermolecular polar interactions with the head groups of nearby lipids, thereby anchoring the channel in the membrane.[76-78] Finally, it has also been proposed that the mycosamine sugar may engage in a direct binding interaction with membrane sterols, specifically to the C3-β-hydroxyl of the A ring in ergosterol and cholesterol.[76-77,79-82] It should be noted, however, that a competing hypothesis proposes that AmB does not interact directly with membrane embedded sterols at all.[83-84] In this indirect sterol model, sterols change the global membrane properties, thereby creating more favorable conditions for AmB activity.

While there was clear evidence for channel formation, the existence or nature of a direct binding interaction with sterols was more controversial in the literature. Despite this lack of clarity, the dependence of AmB activity on the presence of sterols was well known even in the 1950's. In 1958, Carter and coworkers found that the addition of exogenous sterols isolated from carrots effectively inhibited the activity of many polyene macrolide antibiotics against yeast,[85] though at the time it was not clear why. Kinsky and coworkers noted that rat erythrocytes, which contain cholesterol, and *N.Crassa* protoplasts, which contain ergosterol are both sensitive to AmB, while *B. megaterium*, which lacks any membrane sterols, is completely resistant.[62-64] Further evidence came in comparative studies with the mycobacterium, *A. laidlawii,* which lack the protein machinery to manufacture their own membrane sterols. They will readily incorporate environmental sterols into their own membranes, but the presence of sterols is not necessary for their survival. Feingold and coworkers observed that *laidlawii* grown in strictly sterol-free media were insensitive to AmB, but that they became sensitive upon addition of exogenous sterol.[61] Similar results were observed with the *S. japonicus*, a yeast strain which modulates its ergosterol production based on the availability of oxygen. When these yeast are grown under strictly anaerobic conditions produce no sterols, and when grown as such were found to be insensitive to natamycin. When grown under aerobic conditions, the yeast produce ergosterol, and become sensitive.[86] Additionally, in BLM studies the presence of sterols (ergosterol or cholesterol) is necessary for AmB channel formation.[87] Collectively, these experiments demonstrated a clear dependence of AmB activity on the presence of sterol, but the exact nature of that dependence remained unclear.

1-5 PROBING AMB VIA A FUNCTIONAL GROUP-DELETION APPROACH

Traditionally, attempts to directly probe the nature of the AmB ion channel interaction have relied upon covalent modification of AmB and/or lipids.[88-89] This strategy suffers from fundamental experimental complications, in that covalent attachment of a bulky group to either AmB or a lipid can dramatically alter its conformation and/or chemical reactivity, making the functional effects of the modifications difficult to interpret. Even small changes, such as the inversion of the 3-β-hydroxyl group on a sterol can dramatically alter the effects the sterol has on a lipid bilayer.[90-91] We envisioned a different approach, whereby we would delete protic functional groups from AmB and then assay the functional consequence of the deletion in a manner similar to "alanine scanning" in protein science.[92-93] In this functional group-deletion approach there is no complication from introducing added steric bulk or new reactivity, and assuming that deletion does not change the gross conformation of the target molecule, any change in function would be directly attributable to the excised group.

Palacios and coworkers successfully demonstrated this approach in a study probing the importance of the mycosamine sugar and C41-carboxylate to the antifungal activity of AmB.[94] AmB derivatives MeAmB (lacking the C41-carboxylate), AmdeB (lacking mycosamine) and MeAmdeB (lacking both) were prepared, and the consequences of these modifications were investigated (Figure 1.4). The mycosamine sugar was observed to be required for antifungal activity, as both derivatives lacking the sugar were inactive against yeast strain *C. albicans* and *S. cerevesiae*. Surprisingly though, deletion of the C41-carboxylate alone yielded a compound that was equipotent to AmB. Since a methyl group cannot donate or accept a hydrogen bond, this derivative cannot participate in the intermolecular interaction proposed to stabilize the channel complex. Therefore, either this polar interaction is not required for the channel formation, and/or channel formation is not required for cell killing.

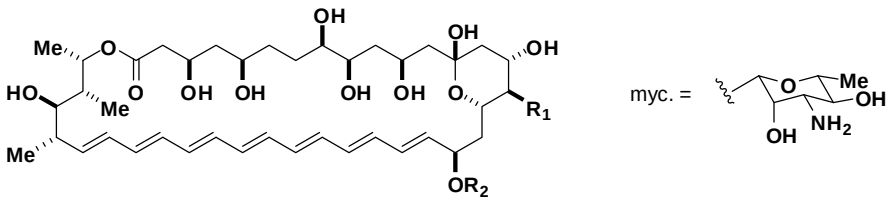

	R_1	R_2	MIC (μM) against *C. albicans*	MIC (μM) against *S. cerevesiae*
AmB	**CO_2H**	myc.	0.25	0.5
MeAmB	**Me**	myc.	0.25	0.5
AmdeB	**CO_2H**	**H**	>50	>50
MeAmdeB	**Me**	**H**	>50	>50

Figure 1.4. Functional group deletion strategy applied to the AmB carboxylate and mycosamine sugar.

The power of this approach was further demonstrated when combined with an isothermal titration calorimetry (ITC) assay that enabled interrogation of a direct binding interaction between AmB and ergosterol.[95] Using the same set of functional group-deficient derivatives, Palacios and coworkers demonstrated that the mycosamine sugar is critical for a direct binding interaction between AmB and ergosterol in lipid bilayers, as well as for channel formation. Interestingly, it was known that some mycosamine-containing polyene macrolides, including natamycin and rimocidin, are potent antimycotics, but do not permeabilize membranes.[69,96-97] Also, in some mutated yeast strains the anti-fungal and membrane permeabilizing effects of mycosamine-containing polyene macrolides is disconnected.[98] Collectively, the above data led to the hypothesis that mycosamine-containing polyene macrolides operate by two distinct mechanisms: sterol-sequestration and membrane-permeabilization via channel formation, both of which require mycosamine-mediated sterol binding as enabled by the conserved structural motif found in all members of this class of natural products (Figure 1.5B).

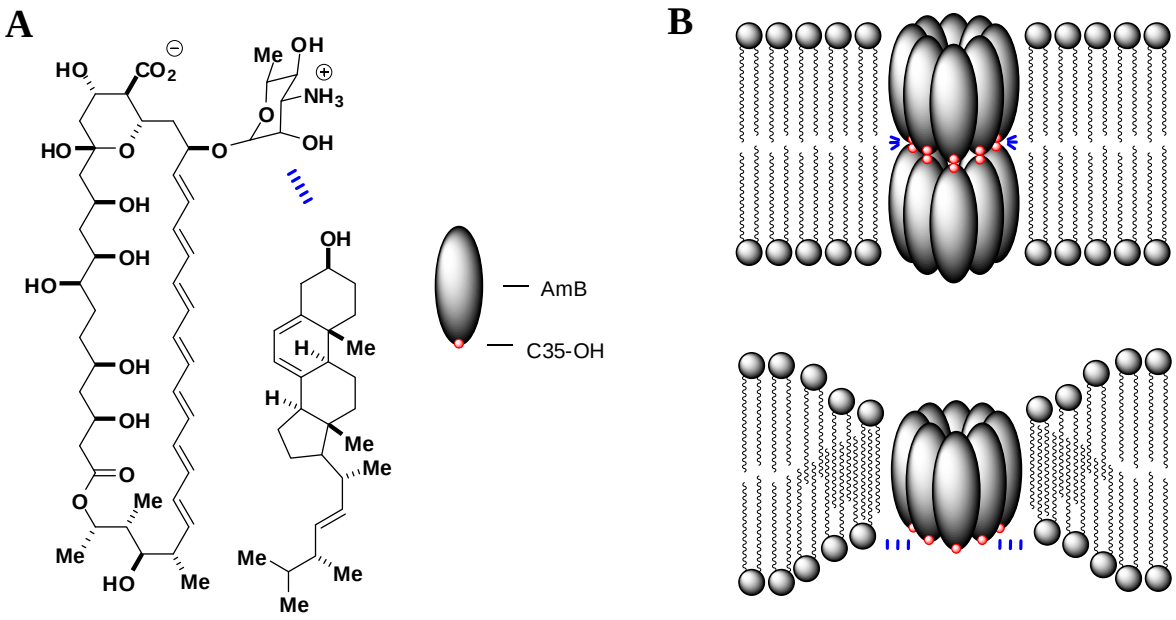

Figure 1.5. (A) Structures of AmB and ergosterol. (B) While the C35-hydroxyl of AmB was not predicted to be necessary for mycosamine mediated sterol binding, it *was* predicted to be critical for either of the two leading models of channel formation.

In a subsequent study,[99] Gray and coworkers prepared a new functional group deficient probe, C35deOAmB. The C35 hydroxyl group of AmB is not predicted to be critical for the proposed mycosamine-mediated binding of ergosterol (Figure 1.5A), but the C35-hydroxyl is expected to be critical for the formation of the AmB channel complex by either of the two leading models for channel formation in lipid bilayers (Figure 1.5B). In the single barrel model, the C35 hydroxyl is expected to participate in polar interaction with the neighboring phospholipid head groups, while in the double-barrel model, the C35 hydroxyl is expected to mediate dimerization of the individual barrel units via a network of intermolecular hydrogen bonds. Deletion of the C35 hydroxyl therefore provides a way of discriminating between these two mechanisms, sterol binding and channel formation. Indeed, C35deOAmB was found to be incapable of permeabilizing membranes, yet retained the ability to bind ergosterol, as determined by ITC. Importantly, C35deOAmB also retained potent antifungal activity. Thus, it was concluded that direct sterol binding, not channel formation, is primarily responsible for the antifungal activity of AmB.

This conclusion has several important implications. First, efforts to date to improve the therapeutic index of AmB have largely focused on the challenging task of promoting the assembly of a multimeric channel in the lipid bilayers of yeast cells over those of human cells.

The identification of ergosterol-binding as the primary mode of cell killing makes the task of finding more effective derivatives, at least in principle, simpler. To find a less toxic derivative of AmB, one needs simply to create an AmB derivative that more selectively binds ergosterol, the principle sterol in yeast, over cholesterol, the principle sterol in humans.

Second, the development of microbial resistance represents a globally emerging threat to human health. The existence of drugs like AmB that have been in continual use for over 50 years without significant microbial resistance suggests that antimicrobial mechanisms exist which are inherently refractory to resistance. AmB kills yeast cells primarily by binding and sequestration of ergosterol, a critical membrane lipid, and this might represent a general strategy for the design of new, more enduring drugs. It should be noted that AmB may also benefit from a dual mode of antimicrobial action. While sterol binding is the primary mechanism of cell killing, channel formation likely contributes as a secondary mechanism, making the development of the microbial resistance even more challenging. This dual mechanism parallels the activity observed in the antibiotic nisin, which displays a similar dual mode of action.[100]

Finally, the ability of C35deOAmB to bind ergosterol without forming channels demonstrates that the two modes of action of AmB are not inextricably linked. This suggests that derivatives might be possible which readily form channels, but do not significantly bind to cholesterol. Discovering such derivatives would be a crucial first step in developing a molecular prosthetic which could mimic the function of a protein ion-channel without the toxicity associated with sterol-binding.

Ultimately, all of the above goals necessitate a still deeper understanding of the principles underlying sterol binding and channel formation. Fortunately, the deletion-based approach represents a powerful way to interrogate the mechanism of small molecules. Further, the now clarified sterol binding model plainly identifies the next targets for study. While the mycosamine sugar is necessary for sterol binding, the functional group(s) responsible for this binding event remain unclear. Future functional deletion targets include AmB derivatives lacking individual hydrogen bonding group on the mycosamine to identify specifically which group(s) are involved in sterol binding. Specifically, individual deletion of the C2' and C4'-hydroxyls and the C3'-amine would provide insight into which of these functional groups is involved in sterol binding. Unfettered access to these derivatives would enable a deeper understanding of this important small molecule-small molecule interaction

1-6 ICC APPROACH TO THE SYNTHESIS OF AMB

In the context of the functional group deletion strategy, synthesizing the defunctionalized probes is by far the hardest step. Once a functionally deficient probe is in hand, the assays necessary to test its activity are relatively straightforward. For example, the synthesis of the key deoxygenated derivative C35deOAmB described in the previous section required the combined contributions of six graduate students over more than 5 years. In contrast, once C35deOAmB was in hand, biological experiments required to assess its activity required less than 4 months, including significant time spent developing a new ITC assay. The development of a more efficient route to small molecules would dramatically speed up the scientific process. Of more fundamental concern, in the context of AmB, many defunctionalized derivatives of interest are not accessible from a degradative approach. As part of a systematic approach to the atomistic dissection of AmB, a synthetic strategy was needed to access derivatives potentially lacking any protic functional group. With this aim in mind, we decided that an efficient, bottom-up synthesis of AmB would greatly facilitate the preparation of new derivatives.

AmB represents a formidable synthetic target, and to date only one total synthesis has been achieved, by Nicolaou and coworkers in 1988.[101-103] Nicolaou's synthesis is undoubtedly a classic, but it lacks the efficiency and flexibility required to generate multiple deoxygenated derivatives in quantities necessary for study. To realistically have a chance at accessing derivatives by total synthesis another approach would be required. To enable a more systematized and efficient approach toward AmB, and small molecules in general, Gillis and coworkers reported in 2007 the development of a system for the iterative cross-coupling (ICC) of bifunctional haloboronic acid building blocks.[104] Complexation of a boronic acid with *N*-methyliminodiacetic acid (MIDA) renders the boron center inert to anhydrous Suzuki-Miyaura cross-coupling (SMC) conditions, as well as a variety of other synthetic transformations.[105] Despite this stability, MIDA boronates can be deprotected under aqueous basic conditions to yield the corresponding boronic acids, which can then be subjected to another SMC reaction, thus enabling an iterative cycle (Figure 1.6).

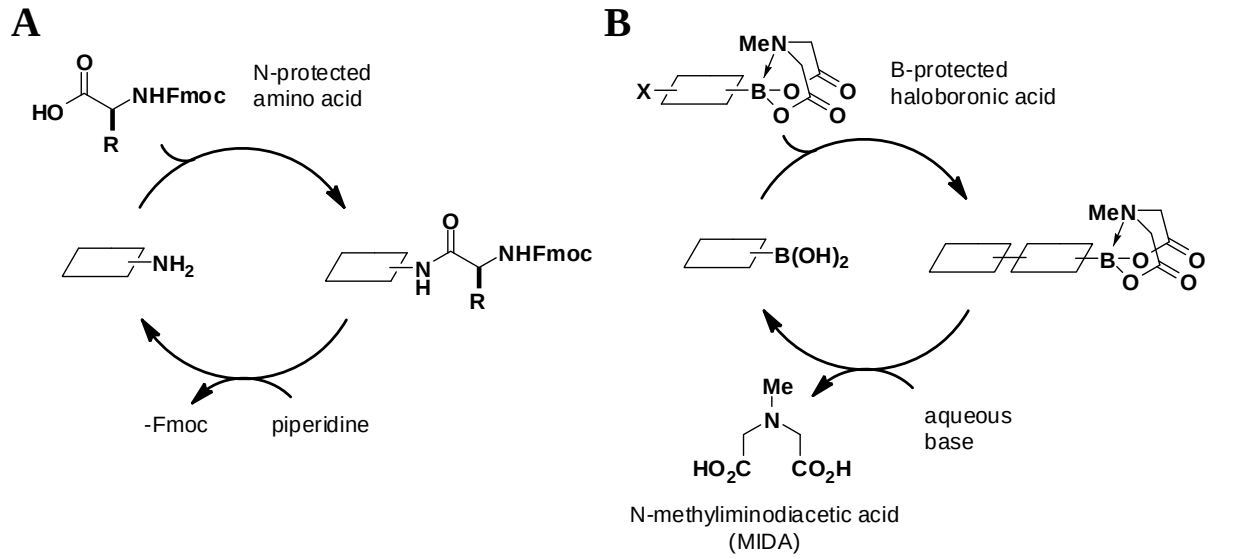

Figure 1.6. (A) The ICC strategy was inspired by the facile manner by which polypeptides are assembled from pre-formed bifunctional building blocks using a single reaction. (B) In ICC, the stability of the MIDA protecting group to anhydrous base enables cross-coupling of a boronic acid selectively to a bifunctional building block containing a halide and a protected boronic acid. Subsequent deprotection of MIDA reveals a new boronic acid, enabling the process to be iterated.

Applying Suzuki transforms to AmB enables it to be deconstructed into four smaller, much more synthetically manageable building blocks. This building block approach is also highly desirable in the context of the synthesis of derivatives, as for any given derivative, only one of the four building blocks needs to be modified. Also notable is BB2, a building block that incorporates all of the conserved functionality inherent to mycosamine-containing polyene macrolide antibiotics. This particular building block would be especially useful, as it could be applied to the ICC-based synthesis of any of the known polyene macrolides.

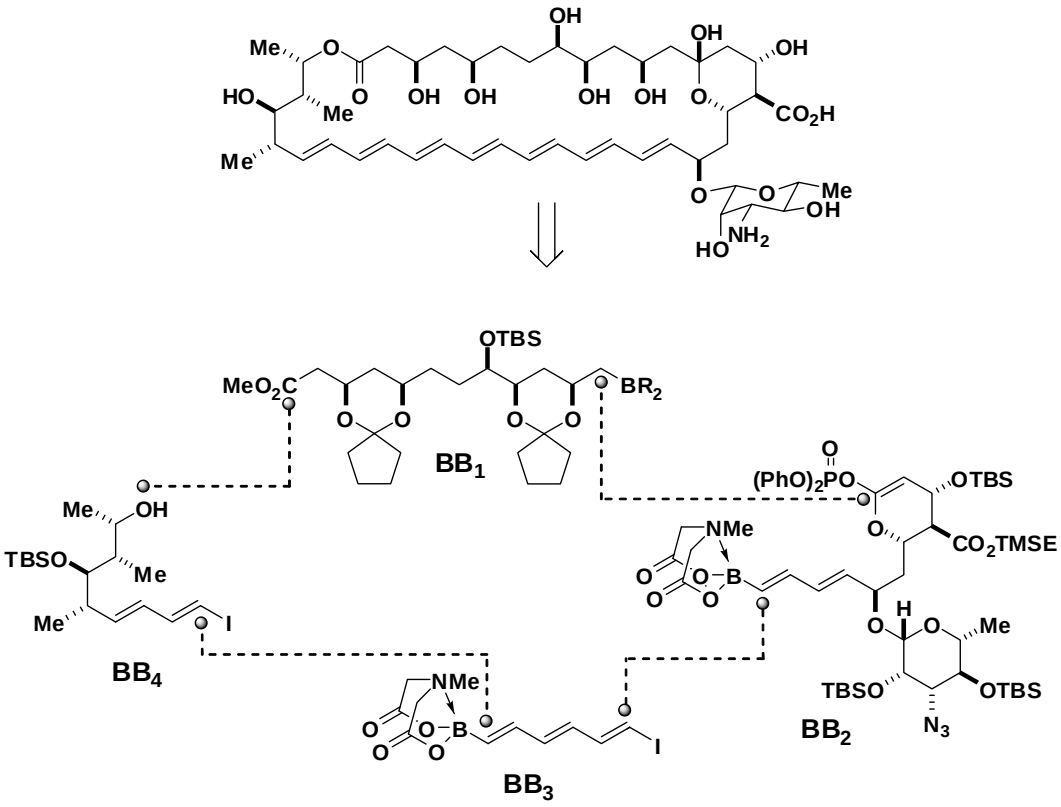

Figure 1.7. ICC-based retrosynthesis of AmB.

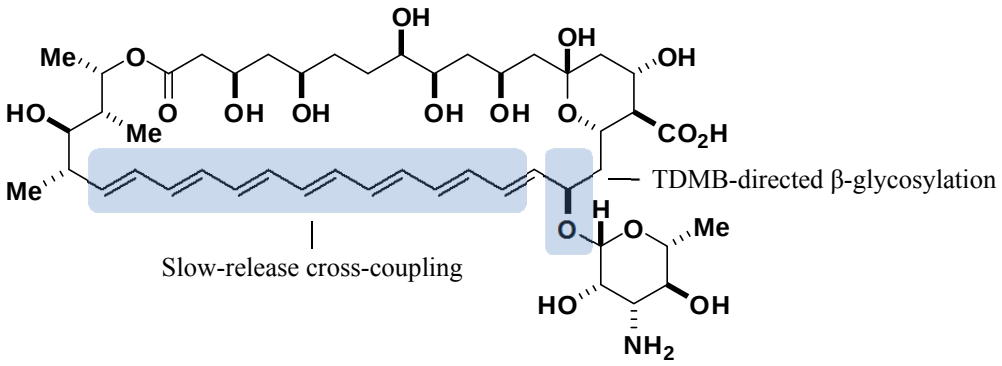

Figure 1.8. The synthesis of AmB has stimulated two important new synthetic methodologies in addition to the general ICC strategy described by Gillis and coworkers: slow-release cross-coupling and TDMB-directed β-glycosylation. The development of these two methodologies is detailed in the following chapters.

The following chapters describe new synthetic methodologies borne out of efforts to overcome synthetic challenges encountered in the synthesis of AmB by this ICC strategy (Figure 1.8). Specifically, the proposed assembly of the AmB polyene by ICC, which requires the cross-

coupling of unstable boronic acids, stimulated the development of a new cross-coupling methodology involving the slow release of unstable boronic acids from air-stable MIDA boronates. Additionally, attachment of the critical mycosamine appendage to BB2 proved to be very challenging and stimulated the development of new glycosylation methodology involving the use of a new directing group for 1,2-*trans*-glycosidations. Importantly, in several cases, the solutions to above problems proved highly useful outside of the context of synthesizing AmB and its derivatives.

1-7 REFERENCES

1. Martin, G. S.; Mannino, D. M.; Eaton, S.; Moss, M. *New Engl. J. Med.* **2003**, *348*, 1546–1554.
2. Wisplinghoff, H.; Bischoff, T.; Tallent, S. M.; Seifert, H.; Wenzel, R. P.; Edmond, M. B. *Clin. Infect. Dis.* **2004**, *39*, 309–317.
3. Kami, M.; Machida, U.; Okuzumi, K.; Matsumura, T.; Mori, S.-i.; Hori, A.; Kashima, T.; Kanda, Y.; Takaue, Y.; Sakamaki, H.; Hirai, H.; Yoneyama, A.; Mutou, Y. *Br. J. Haemotol.* **2002**, *117*, 40–46.
4. Chen, S. C. A.; Playford, E. G.; Sorrell, T. C. *Curr. Opin. Pharmacol.* **2010**, *10*, 522–530.
5. Wilson, L. S.; Reyes, C. M.; Stolpman, M.; Speckman, J.; Allen, K.; Beney, J. *Value Health* **2002**, *5*, 26–34.
6. Zaoutis, T. E.; Argon, J.; Chu, J.; Berlin, J. A.; Walsh, T. J.; Feudtner, C. *Clin. Infect. Dis.* **2005**, *41*, 1232–1239.
7. Miller, L. G.; Hajjeh, R. A.; Edwards, J. E. *Clin. Infect. Dis.* **2001**, *32*, 1110.
8. Perlroth, J.; Choi, B.; Spellberg, B. *Med. Mycol.* **2007**, *45*, 321–346.
9. Seco, E. M.; Miranzo, D.; Nieto, C.; Malpartida, F. *Appl. Microbiol. Biotechnol.* **2010**, *85*, 1797–1807.
10. Taubes, G. *Science* **2008**, *321*, 356–361.
11. Akaike, N.; Harata, N. *Jpn. J. Physiol.* **1994**, *44*, 433–473.
12. Hazen, E. L.; Brown, R. *Science* **1950**, *112*, 419–429.
13. Hazen, E. L.; Brown, R. *Proc. Soc. Exp. Biol. Med.* **1951**, *76*, 93–97.
14. Davisson, J. W.; Tanner, F. W., Jr.; Finlay, A. C.; Solomons, I. A. *Antibiot. Chemother.* **1951**, *1*, 289–290.
15. Oswald, E. J.; Randall, W. A.; Reedy, R. J. *Antibiot. Annu.* **1955**, *3*, 236–239.
16. Lechevalier, H.; Acker, R. F.; Corke, C. T.; Haenseler, C. M.; Waksman, S. A. *Mycologia* **1953**, *45*, 155–171.
17. Donovick, R.; Gold, W.; Pagano, J. F.; Stout, H. A. *Antibiot. Annu.* **1955**, *3*, 579–586.
18. Struyk, A. P.; Hoette, I.; Drost, G.; Waisvisz, J. M.; Van Eek, T.; Hoogerheide, J. C. *Antibiot. Annu.* **1957**, *5*, 878–885.
19. Ellis, D. *J. Antimicrob. Chemother.* **2002**, *49*, 7–10.
20. Rogers, T. R. *Int. J. Antimicrob. Agents* **2006**, *27, Supplement 1*, 7–11.
21. Gallis, H. A.; Drew, R. H.; Pickard, W. W. *Rev. Infect. Dis.* **1990**, *12*, 308–329.
22. Saliba, F.; Dupont, B. *Med. Mycol.* **2008**, *46*, 97–112.
23. Ratjen, F. A. *Respiratory Care* **2009**, *54*, 595–602.

24. Jiang, C. W.; Lee, E. R.; Lane, M. B.; Xiao, Y. F.; Harris, D. J.; Cheng, S. H. *Am. J. Physiol. Lung Cell Mol. Physiol.* **2001**, *281*, L1164–L1172.
25. Gao, L.; Broughman, J. R.; Iwamoto, T.; Tomich, J. M.; Venglarik, C. J.; Forman, H. J. *Am. J. Physiol. Lung Cell Mol. Physiol.* **2001**, *281*, L24–L30.
26. ElEtri, M.; Cuppoletti, J. *Am. J. Physiol. Lung Cell Mol. Physiol.* **1996**, *270*, L386–L392.
27. Omura, S. *Macrolide Antibiotics, Chemistry, Biology, and Practice*; 1st ed.; Academic Press: New York, NY, 1984.
28. Sowinski, P.; Bieszczad, T.; Pawlak, J.; Borowski, E. *J. Antibiot.* **1996**, *49*, 1232–1235.
29. Perez-Zuniga, F. J.; Seco, E. M.; Cuesta, T.; Degenhardt, F.; Rohr, J.; Vallin, C.; Iznaga, Y.; Perez, M. E.; Gonzalez, L.; Malpartida, F. *J. Antibiot.* **2004**, *57*, 197–204.
30. Gupte, T. E.; Chatterjee, N. R.; Nanda, R. K.; Naik, S. R. *Indian J. Chem. B Org.* **2000**, *39*, 936–940.
31. Lancelin, J. M.; Beau, J. M. *J. Am. Chem. Soc.* **1990**, *112*, 4060–4061.
32. Lancelin, J. M.; Beau, J. M. *Tetrahedron Lett.* **1989**, *30*, 4521–4524.
33. Pawlak, J.; Tabin, P.; Sowinski, P.; Borowski, E. *Pol. J. Chem.* **2005**, *79*, 1673–1679.
34. Zielinski, J.; Golik, J.; Pawlak, J.; Borowski, E.; Falkowski, L. *J. Antibiot.* **1988**, *41*, 1289–1291.
35. Sowinski, P.; Pawlak, J.; Borowski, E.; Gariboldi, P. *J. Antibiot.* **1995**, *48*, 1288–1291.
36. Ryu, G.; Choi, W. C.; Hwang, S. J.; Yeo, W. H.; Lee, C. S.; Kim, S. K. *J. Nat. Prod.* **1999**, *62*, 917–919.
37. Hirota, H.; Itoh, A.; Ido, J.; Iwamoto, Y.; Goshima, E.; Miki, T.; Hasuda, K.; Ohashi, Y. *J. Antibiot.* **1991**, *44*, 181–186.
38. Nakagomi, K.; Sakai, S.; Tanaka, H.; Tomizuka, N.; Kawakami, Y.; Nakajima, T. *J. Antibiot.* **1990**, *43*, 470–476.
39. Vertesy, L.; Aretz, W.; Ehlers, E.; Hawser, S.; Isert, D.; Knauf, M.; Kurz, M.; Schiell, M.; Vogel, M.; Wink, J. *J. Antibiot.* **1998**, *51*, 921–928.
40. Wright, J. J.; Greeves, D.; Mallams, A. K.; Picker, D. H. *J. Chem. Soc., Chem. Commun.* **1977**, 710–712.
41. Mechlinski, W.; Schaffner, C. P.; Ganis, P.; Avitabile, G. *Tetrahedron Lett.* **1970**, *44*, 3873–3876.
42. Zielinski, J.; Borowyborowski, H.; Golik, J.; Gumieniak, J.; Ziminski, T.; Kolodziejczyk, P.; Pawlak, J.; Borowski, E. *Tetrahedron Lett.* **1979**, 1791–1794.
43. Pawlak, J.; Sowinski, P.; Borowski, E.; Gariboldi, P. *J. Antibiot.* **1993**, *46*, 1598–1604.
44. Kozhuharova, L.; Gochev, V.; Koleva, L. *World J. Microbiol. Biotechnol.* **2008**, *24*, 1–5.
45. Zhou, Y.; Li, J.; Zhu, J.; Chen, S.; Bai, L.; Zhou, X.; Wu, H.; Deng, Z. *Chem. Biol.* **2008**, *15*, 629–638.
46. Pawlak, J.; Sowinski, P.; Bieszczad, T.; Borowski, E. *Pol. J. Chem.* **2005**, *79*, 1667–1672.
47. Borowski, E.; Golik, J.; Zielinski, J.; Falkowski, L.; Kolodziejczyk, P.; Pawlak, J.; Shenin, Y. *J. Antibiot.* **1978**, *31*, 117–123.
48. Tweit, R. C.; Pandey, R. C.; Rinehart, K. L. *J. Antibiot.* **1982**, *35*, 997–1012.
49. Komori, T. *J. Antibiot.* **1990**, *43*, 778–782.
50. Sowinski, P.; Gariboldi, P.; Pawlak, J. K.; Borowski, E. *J. Antibiot.* **1989**, *42*, 1639–1642.
51. Omura, S. *Macrolide Antibiotics, Chemistry, Biology, and Practice*; 2nd ed.; Academic Press: New York, NY, 2002.
52. Aparicio, J. F.; Caffrey, P.; Gil, J. A.; Zotchev, S. B. *Applied Microbiology and Biotechnology* **2003**, *61*, 179–188.

53. Naruse, N.; Tsuno, T.; Sawada, Y.; Konishi, M.; Oki, T. *J. Antibiot.* **1991**, *44*, 741–755.
54. Hedge, V. R.; Patel, M. G.; Horan, A. C.; King, A. H.; Gentile, F.; Puar, M. S.; Loebenberg, D. *J. Antibiot. (Tokyo)* **1998**, *51*, 464–470.
55. Cooper, R.; Truumees, I.; Yarborough, R.; Loebenberg, D.; Marquez, J.; Horan, A.; Patel, M.; Gullo, V.; Puar, M.; Pramanik, B. *J. Antibiot.* **1992**, *45*, 633–638.
56. Hopmann, C.; Kurz, M.; Bronstrup, M.; Wink, J.; LeBeller, D. *Tetrahedron Lett.* **2002**, *43*, 435–438.
57. Osteux, R.; Tranvanky; Biguet, J. *Comptes Rendus de l'Académie des Sciences* **1958**, *247*, 2475–2477.
58. Kinsky, S. C. *Biochem. Biophys. Res. Commun.* **1961**, *4*, 353–357.
59. Bolard, J. *Biochimica et Biophysica Acta* **1986**, *864*, 257–304.
60. Cereghetti, D. M.; Carreira, E. M. *Synthesis* **2006**, 914–942.
61. de Kruijff, B.; Gerritse, W.; Oerleman, A.; Demel, R. A.; Vandeene, L. *Biochimica et Biophysica Acta* **1974**, *339*, 30–43.
62. Kinsky, S. C.; Avruch, J.; Permutt, M.; Schonder, A. A.; Rogers, H. B. *Biochem. Biophys. Res. Commun.* **1962**, *9*, 503–507.
63. Kinsky, S. C. *Proc. Natl. Acad. Sci. U. S. A.* **1962**, *48*, 1049–1056.
64. Kinsky, S. C. *Arch. Biochem. Biophys.* **1963**, *102*, 180–188.
65. Mueller, P.; Tien, H. T.; Wescott, W. C.; Rudin, D. O. *Circulation* **1962**, *26*, 1167–1171.
66. Ermishkin, L. N.; Kasumov, K. M.; Potzeluyev, V. M. *Nature* **1976**, *262*, 698–699.
67. Borisova, M. P.; Ermishkin, L. N.; Silberstein, A. Y. *Biochimica et Biophysica Acta* **1979**, *553*, 450–459.
68. Andreoli, T. E.; Dennis, V. W.; Weigl, A. M. *J. Gen. Physiol.* **1969**, *53*, 133–156.
69. de Kruijff, B.; Demel, R. A. *Biochimica et Biophysica Acta* **1974**, *339*, 57–70.
70. Andreoli, T. E. *Kidney Int.* **1973**, *4*, 337–345.
71. Andreoli, T. E. *Ann. N. Y. Acad. Sci.* **1974**, *235*, 448–468.
72. Eiseman, G. *In Membranes. Lipid Bilayers and Antibiotics* New York, NY, 1973; Vol. 2 377–408.
73. van Hoogevest, P.; de Kruijff, B. *Biochimica et Biophysica Acta* **1978**, *511*, 397–407.
74. Szpilman, A. M.; Manthorpe, J. M.; Carreira, E. M. *Angew. Chem. Int. Ed.* **2008**, *47*, 4339–4342.
75. Kasumov, K. M.; Borisova, M. P.; Ermishkin, L. N.; Potseluyev, V. M.; Silberstein, A. Y.; Vainshtein, V. A. *Biochimica et Biophysica Acta* **1979**, *551*, 229–237.
76. Baginski, M.; Resat, H.; McCammon, J. A. *Mol. Pharm.* **1997**, *52*, 560–570.
77. Baginski, M.; Resat, H.; Borowski, E. *Biochimica et Biophysica Acta* **2002**, *1567*, 63–78.
78. Balakrishnan, A. R.; Easwaran, K. R. K. *Biochemistry* **1993**, *32*, 4139–4144.
79. Kotler-Brajtburg, J.; Price, H. D.; Medoff, G.; Schlessi, D.; Kobayash, G. *Antimicrob. Agents Chemother.* **1974**, *5*, 377–382.
80. Herve, M.; Debouzy, J. C.; Borowski, E.; Cybulska, B.; Garybobo, C. M. *Biochimica et Biophysica Acta* **1989**, *980*, 261–272.
81. Mazerski, J.; Bolard, J.; Borowski, E. *Biochimica et Biophysica Acta* **1995**, *1236*, 170–176.
82. Neumann, A.; Baginski, M.; Czub, J. *J. Am. Chem. Soc.* **2010**, *132*, 18266–18272.
83. Hsuchen, C. C.; Feingold, D. S. *Biochem. Biophys. Res. Commun.* **1973**, *51*, 972–978.
84. Hsuchen, C. C.; Feingold, D. S. *Antimicrob. Agents Chemother.* **1973**, *4*, 309–315.
85. Gottlieb, D.; Carter, H. E.; Sloneker, J. H.; Ammann, A. *Science* **1958**, *128*, 361–361.
86. Bulder, C. *Antonie Leeuwenhoek* **1971**, *37*, 353–358.

87. Andreoli, T. E.; Monahan, M. *J. Gen. Physiol.* **1968**, *52*, 300–325.
88. Kasai, Y.; Matsumori, N.; Umegawa, Y.; Matsuoka, S.; Ueno, H.; Ikeuchi, H.; Oishi, T.; Murata, M. *Chem.-Eur. J.* **2008**, *14*, 1178–1185.
89. Volmer, A. A.; Szpilman, A. M.; Carreira, E. M. *Nat. Prod. Rep.* **2010**, *27*, 1329–1349.
90. Rog, T.; Pasenkiewicz-Gierula, M.; Vattulainen, I.; Karttunen, M. *Biochimica et Biophysica Acta* **2009**, *1788*, 97–121.
91. Dufourc, E. J.; Parish, E. J.; Chitrakorn, S.; Smith, I. C. P. *Biochemistry* **1984**, *23*, 6062–6071.
92. Wells, J. A. *Methods Enzymol.* **1991**, *202*, 390–411.
93. Cunningham, B. C.; Wells, J. A. *Science* **1989**, *244*, 1081–1085.
94. Palacios, D. S.; Anderson, T. M.; Burke, M. D. *J. Am. Chem. Soc.* **2007**, *129*, 13804–13805.
95. Palacios, D. S.; Dailey, I.; Siebert, D. M.; Wilcock, B. C.; Burke, M. D. *Proc. Natl. Acad. Sci. U. S. A.* **2011**, *108*, 6733–6738.
96. Welscher, Y. M. T.; Ten Napel, H. H.; Balague, M. M.; Souza, C. M.; Riezman, H.; De Kruijff, B.; BreukinkO, E. *J. Biol. Chem.* **2008**, *283*, 6393–6401.
97. Zygmunt, W. A. *Appl. Microbiol.* **1966**, *14*, 953–956.
98. Hsuchen, C. C.; Feingold, D. S. *Nature* **1974**, *251*, 656–659.
99. Gray, K. C.; Palacios, D. S.; Dailey, I.; Endo, M. M.; Uno, B. E.; Wilcock, B. C.; Burke, M. D. *Proc. Natl. Acad. Sci. U. S. A.* **2012**, *109*, 2234–2239.
100. Hasper, H. E.; Kramer, N. E.; Smith, J. L.; Hillman, J. D.; Zachariah, C.; Kuipers, O. P.; de Kruijff, B.; Breukink, E. *Science* **2006**, *313*, 1636–1637.
101. Nicolaou, K. C.; Daines, R. A.; Uenishi, J.; Li, W. S.; Papahatjis, D. P.; Chakraborty, T. K. *J. Am. Chem. Soc.* **1988**, *110*, 4672–4685.
102. Nicolaou, K. C.; Daines, R. A.; Chakraborty, T. K.; Ogawa, Y. *J. Am. Chem. Soc.* **1988**, *110*, 4685–4696.
103. Nicolaou, K. C.; Daines, R. A.; Ogawa, Y.; Chakraborty, T. K. *J. Am. Chem. Soc.* **1988**, *110*, 4696–4705.
104. Gillis, E. P.; Burke, M. D. *J. Am. Chem. Soc.* **2007**, *129*, 6716–6717.
105. Gillis, E. P.; Burke, M. D. *J. Am. Chem. Soc.* **2008**, *130*, 14084–14085.

CHAPTER 2

Direct-Release Cross-Coupling of MIDA Boronates

The SMC reaction was chosen as the basis for the ICC platform due to its well-demonstrated power in the construction of complex small molecules. Nevertheless, the synthesis of AmB and its derivatives presents an exceptional challenge that ultimately demanded the development of new methodology. This chapter describes such methodology; i.e. a new SMC reaction protocol based on the in situ release of boronic acids from their corresponding MIDA boronates under aqueous basic cross-coupling conditions. The author's contribution to the development was inspired by challenges encountered in work toward the AmB total synthesis, but the developed methodology has proven to be much more generally useful, enabling the efficient cross-coupling of a range of classes of otherwise unstable boronic acids. Efficient cross-coupling of polyenyl, vinyl, cyclopropyl, and 2-heterocyclic MIDA boronates is described, as well as the notoriously challenging 2-pyridyl motif. Eric P. Gillis contributed the results presented in Figure 2.2, Table 2.5, Table 2.6, and Table 2.7. Graham R. Dick contributed all of the results presented in section 2-6.

2-1 BACKGROUND

Boronic acids are highly desirable building blocks due to their low cost, minimal environmental impact and lack of toxicity,[1] as well as the relatively mild conditions necessary to activate them for cross-coupling.[2] They serve as excellent building blocks for the synthesis of a wide range of natural products, pharmaceuticals, and materials, and with the development of MIDA boronates and the ICC platform the utility of boronic acids in the construction of complex small molecules has been even further extended.[3-10] Yet, boronic acids are not without their limitations. Most notably, some are highly susceptible to protodeboronation, oxidation, and/or polymerization[11-12] which preclude their benchtop storage and/or efficient coupling, particularly with aryl chlorides.

In light of this, the assembly of the AmB polyene by iterative SMC reactions was anticipated to be a challenging portion of the synthesis, due to the necessity of working with highly conjugated polyenylboronic acid intermediates. Polyenylboronic acids are notoriously unstable,[13-14] which has to some extent precluded their general use in organic synthesis. This

possible hurdle was confirmed in an experiment modeling the final coupling reaction of the AmB polyene synthesis using the ICC strategy (Scheme 2.1). Deprotection of pentaenyl-MIDA boronate **2.1** with aqueous sodium hydroxide and subsequent cross-coupling with dienyl chloride **2.2** proved to be very challenging. This challenge was attributed to the very sensitive nature of the required polyenyl boronic acid intermediate.

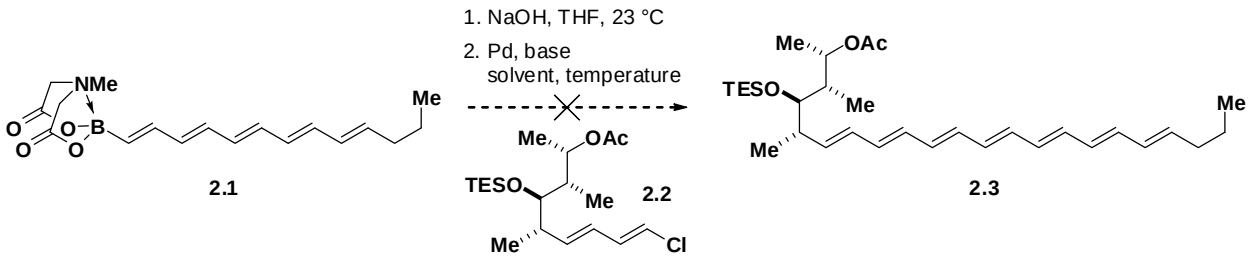

Scheme 2.1. Deprotection of pentaenyl MIDA boronate **2.1** to the corresponding boronic acid and subsequent exposure to SMC reaction conditions with dienyl chloride **2.2** was extremely challenging

This result highlights one of the principal challenges associated with boronic acids: Many of the most desirable boronic acids, including polyenyl, 2-heterocyclic,[15-24] vinyl,[12,25-26] and cyclopropyl[27-30] derivatives are inherently unstable. This instability manifests in two important ways. First, these boronic acids tend to be unstable to storage. Second, protodeboronation, a common decomposition pathway, is known to be accelerated by heat, base, polar solvents and palladium catalysts, making these compounds unstable to the conditions of the SMC reaction itself.[31] To address these challenges, a number of important surrogates for boronic acids have been developed for use in the SMC reaction, including trialkoxy[32-35] or trihydroxyborate salts,[36] diethanolamine adducts,[37-40] sterically bulky boronic esters,[41-43] and boroxines.[44-46] Perhaps the most notable boronic acid substitute is the trifluoroborate salt developed by Molander and co-workers.[47-49] In contrast to boronic acids, trifluoroborate salts are generally air-stable monomeric crystalline solids. In addition, they are capable of direct use in SMC reactions and have been successfully used as surrogates for unstable boronic acids.[50-54] However, trifluoroborate salts suffer from a number of key limitations. Incompatibility with silica gel limits the available options for their isolation and purification.[55] The use of trifluoroborate salts has also been associated with the release of HF, which is both toxic and damaging to glassware.[11,56] Also, while there are a few examples of SMC reactions between heteroaromatic trifluoroborate salts and sterically encumbered and electron rich aryl chlorides,[52] it has not been generally established

that trifluoroborate salts are effective cross-coupling partners with electron rich aryl chlorides. Finally, some very unstable boronic acids, notably 2-pyridylboronic acid, are not effective coupling partners as the corresponding trifluoroborate salts.[50] The apparent lack of a robust, generally effective surrogate for unstable boronic acids struck us as an important unmet need in synthetic methodology. We therefore reasoned that the development of such a reagent could potentially not only address the problems we had encountered with polyene construction in the context of the AmB synthesis, but might also have a profound impact on the state of the art of the SMC reaction in general.

2-2 STABILITY OF BORONIC ACIDS

While the stability of boronic acids has been described anecdotally in the literature, there have been few quantitative reports to date. Therefore, to ground ourselves in a better understanding of this phenomenon we sought to rigorously test the air-stability of a variety of boronic acids. To this end we synthesized a collection of boronic acids representing several classes known to have stability problems (Table 2.1). To maximize their starting purity, each was synthesized via hydrolysis from the corresponding MIDA boronate and determined by ^{1}H-NMR to be >95% pure at the start of the experiment. A sample of each boronic acid was then stored sealed under air at room temperature for a period of 15 days, after which the quantity of remaining boronic acid was determined by ^{1}H-NMR using 4-bromoacetophenone as an internal standard. Every boronic acid tested exhibited some degree of decomposition within this time frame. The 2-furyl, 2-pyrrole-, 2-indole- and vinylboronic acid (**2.4a**, **2.4e**, **2.4f**, and **2.4g**) were observed to be particularly unstable, with very little of the original boronic acid left in the sample. In follow-up experiments vinylboronic acid (**2.4g**) was observed to undergo nearly complete (>95%) decomposition in only *two days*. In sharp contrast, identical experiments performed with the corresponding MIDA boronates (**2.5a**, **2.5e**, **2.5f**, and **2.5g**) showed the MIDA boronates to completely air-stable, with no decomposition observed even after sixty days. For **2.5a**, **2.5d**, and **2.5g**, no decomposition was detectable even after more than 15 weeks at ambient conditions. This remarkable stability is consistent with previous reports[3] and suggests that, at the very least for the purpose of addressing benchtop instability, MIDA boronates may be effective surrogates for unstable boronic acids.

Table 2.1

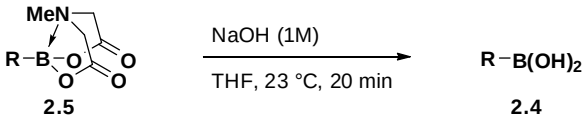

entry	R	% remaining after storage under air at 23 °C[a] **2.4** (15 days)	**2.5** (60 days)
1	 **a**	7	>95[b]
2	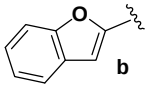 **b**	88	>95
3	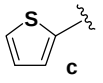 **c**	80	>95
4	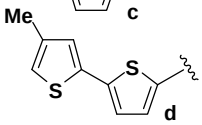 **d**	80	>95[b]
5	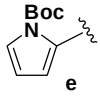 **e**	<5	>95
6	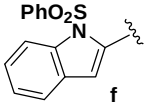 **f**	<5	>95
7	 **g**	5	>95[b]
8	 **h**	31	>95

[a]Freshly prepared boronic acids 2.4 and MIDA boronats 2.5 were stored as solids on the benchtop under air for 15 and 60 days, respectively. [b]Stored for 107 days.

2-3 DIRECT-RELEASE CROSS-COUPLING OF MIDA BORONATES

Having established that complexation with MIDA effectively renders otherwise unstable boronic acids stable to storage, we next investigated whether we could harness this phenomenon to improve the efficiency with which these boronic acids could be utilized in the SMC reaction. Traditionally, using a MIDA boronate as surrogate for an unstable boronic acid would involve deprotection with aqueous sodium hydroxide, isolation of the resulting boronic acid, and then exposure of that boronic acid to SMC reaction conditions. We recognized that SMC reaction conditions, i.e. palladium catalyst and aqueous or anhydrous base, and the unique stability profile of MIDA boronates might provide an opportunity to streamline this process. While MIDA

boronates are quite stable to anhydrous bases, they are labile to *aqueous* bases. Thus, we reasoned that by subjecting a MIDA boronate directly to aqueous basic SMC reaction conditions we might achieve in situ hydrolysis of the MIDA boronate, revealing the boronic acid which would subsequently undergo cross-coupling. If successful, such a direct addition would completely eliminate the need to handle the unstable boronic acid, and would thus minimize time available for decomposition since the boronic acid would capable of reacting immediately upon MIDA boronate deprotection.

It should be noted that this "direct-release" protocol would be incompatible with the selective cross-coupling of MIDA-protected haloboronic acids as part of an ICC sequence, due to the necessity of preserving the integrity of the MIDA ligand in such a reaction. However, this protocol could be quite useful for any aqueous non-selective coupling. Further, direct-release coupling would be compatible with the *final step* of an ICC sequence, a useful feature given that the last cross-coupling in an ICC sequence is often the most challenging due to the highly conjugated nature of the boronic acid involved.

The success of a direct-release coupling requires that the MIDA ligand released upon MIDA boronate hydrolysis does not interfere with the subsequent cross-coupling reactions. MIDA is known to be a competent ligand for a number of transition metals, including palladium(II) species,[57] and the amount of MIDA present in the SMC reaction would far exceed the amount of the palladium catalyst. Thus, to test the viability of using MIDA boronates directly in SMC reactions, we exposed MIDA boronate **2.6** directly to bromoacetophenone (**2.7**) under standard aqueous cross-coupling conditions (Scheme 2.2). By ^{1}H-NMR we observed complete consumption of **2.7**, and after column chromatography obtained the desired biaryl cross-coupling product **2.8** in 97% yield, suggesting that the presence of stoichiometric quantities of MIDA had no deleterious impact on the reaction.

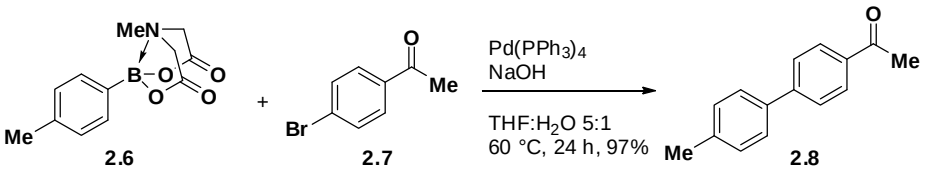

Scheme 2.2. Direct exposure of MIDA boronate **2.6** to bromoacetophenone (**2.7**) and standard SMC reaction conditions resulted in a 97% yield of biaryl product **2.8**, suggesting that the MIDA released from in situ hydrolysis of the MIDA boronate was not detrimental to the activity of the catalyst.

To better assess the generality of direct-release coupling, we next synthesized a collection of simple MIDA boronates, and compared their efficiency in direct release cross-coupling reactions to the corresponding boronic acids (Table 2.2). Note that these otherwise standard SMC reaction conditions included an increased amount of base to account for the hydrolysis of the MIDA boronate. As seen in Table 2.2 there was little difference in yields between the MIDA boronates and boronic acids, with only some variation involving boronic acids **2.9c** and **2.9d**. This may have been a result of imperfect purity of these boronic acids, as these were obtained commercially and used as received without further purification. Collectively, these results added additional evidence that the MIDA ligand does not significantly reduce the activity of the palladium catalyst under direct release SMC conditions.

Table 2.2

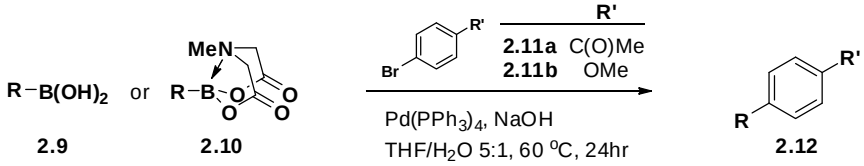

Entry	R	Halide	Product	% Yield from 2.9	% Yield from 2.10
1	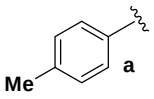	**2.11a**	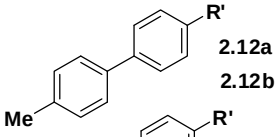 **2.12a**	96	97
2		**2.11b**	**2.12b**	96	93
3	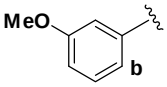	**2.11a**	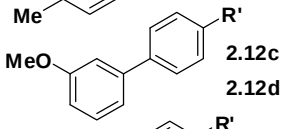 **2.12c**	98	98
4		**2.11b**	**2.12d**	94	96
5	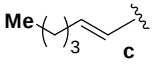	**2.11a**	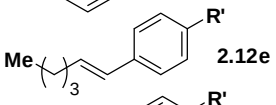 **2.12e**	90	96
6	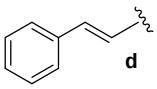	**2.11a**	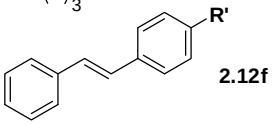 **2.12f**	87	95

Reaction conditions: 1.0 equiv **2.11**, 1.5 equiv **2.9** or **2.10**, 7.5 equiv NaOH.

Hydrolysis of MIDA boronates with strong bases such as sodium hydroxide proceeds in under 10 minutes at room temperature.[3] For the purpose of clarity, such direct-release conditions employing strong bases such as sodium hydroxide, potassium hydroxide, etc. will hereafter be referred to as "fast-release" conditions. An important consequence of this phenomenon is that, if

the released MIDA ligand acts as a spectator, within several minutes at 60 °C there is essentially no difference between fast-release conditions and conditions using boronic acids, assuming the latter are pure. The fast-release protocol has the clear advantage of mitigating the problems associated with boronic acid storage, and it ensures the delivery of pure boronic acid to the SMC reaction. However, we would not expect fast-release conditions to effectively address the problem of boronic acids which exhibit significant instability to the conditions of the SMC reaction itself.

This hypothesis was confirmed when we attempted SMC reactions using more unstable boronic acids and slower reacting aryl chlorides. For example, even when using the powerful biaryldialkylphosphine ligands developed by Buchwald and co-workers,[58] the reaction of **2.4a** with the deactivated aryl chloride **2.13** proceeded in modest yield, (Scheme 2.3), despite the boronic acid having been freshly prepared prior to the reaction. An identical experiment carried out using the corresponding MIDA boronate (**2.5a**) under fast-release conditions resulted in a similar yield. These results are consistent with the known challenge of using 2-heterocyclic boronic acids in SMC reactions with aryl chlorides,[31] and our own experiments have shown that **2.4a** undergoes protodeboronation when exposed to the aqueous basic conditions of the SMC reaction (vide infra). These results demonstrate that fast-release conditions, while beneficial to the handling and storage of boronic acids, do not fully address the challenges associated with the use of unstable boronic acids.

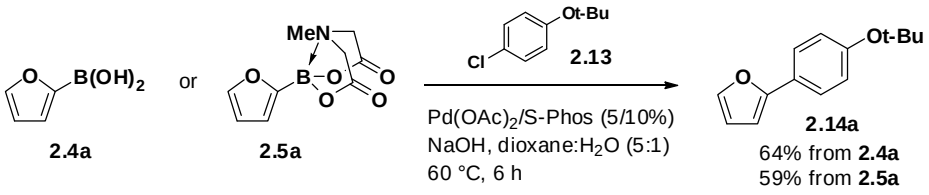

Scheme 2.3. Both 2-furylboronic acid (**2.4a**) and 2-furyl MIDA boronate (**2.5a**) gave similarly modest yields in an attempted cross-coupling with **2.13**, showing that direct couplings of MIDA boronates using strong bases like NaOH may not be more effective than using the corresponding boronic acid in reactions involving slower reacting aryl chlorides.

2-4 SLOW-RELEASE CROSS-COUPLING OF MIDA BORONATES

A likely reason for the low yields in Scheme 2.3 is that decomposition of the boronic acid by protodeboronation is competitive with productive cross-coupling. One factor that likely exacerbates this problem is the low catalyst loading typical in the SMC reaction. For example,

with a 5% catalyst loading, at the start of the reaction, only 5% of the boronic acid is able to react productively with the catalyst, while the remaining 95% must wait for the catalytic cycle to turn over, during which time it is free to undergo other competing, non-productive pathways. One obvious way to address this problem is to increase the catalyst loading, thereby increasing the ratio of catalyst to boronic acid, and speeding up productive coupling over protodeboronation. Intuitively, it seemed that a reasonable alternative would be to decrease the concentration of the boronic acid, achieving a similar change in the ratio of catalyst to boronic acid. For example, if the boronic acid were added to the reaction at a rate slower than the turn-over frequency (TOF) of the catalyst, then the catalyst would at all times remain superstoichiometric to the boronic acid, enabling the boronic acid to most efficiently undergo productive coupling. This hypothesis is consistent with a literature report by Buchwald and coworkers, whereby the yield of an SMC reaction was improved by the slow addition of an unstable boronic acid to the reaction mixture.[31]

Additionally, it is worth considering the resting state of the catalyst. The SMC reaction proceeds through a three-step catalytic cycle, involving oxidative addition, transmetallation, and reductive elimination (Figure 2.1). Keeping the concentration of the boronic acid very low forces the turnover limiting step of the catalytic cycle to be transmetallation, and in the presence of a still high concentration of halide, the resting state of the catalyst will be at the oxidative addition product (**2**). Thus, at very low boronic acid concentrations, virtually all of the catalyst will be sitting at **2**, primed to immediately undergo transmetallation with the boronic acid as it is added to the reaction. If one assumes that protodeboronation is a first order process with respect to the boronic acid, then the relative rates of transmetallation vs. protodeboronation are directly dependent on the concentration of species **2**. Increasing the concentration of species **2** by forcing a change in the catalyst resting state will increase the rate of transmetallation, but have no impact on the competing protodeboronation. A similar resting state analysis was recently employed by researchers at GlaxoSmithKline in an elegant process-level optimization of an SMC reaction plagued by undesired homocoupling.[59]

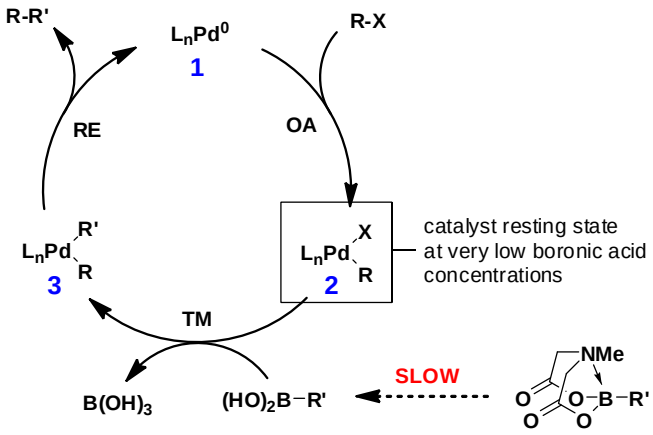

Figure 2.1. A proposal to explain the beneficial nature of slow-release cross-coupling. The low concentration of boronic acid in solution forces the catalyst resting state to [**2**]. The increased concentration of [**2**] correspondingly accelerates the rate of transmetallation with the boronic acid. This resting state proposal also helps to explain why slow-release phenomenon has been show to limit other SMC byproducts like oxidative homocoupling.

To test the hypothesis that slow addition of an unstable boronic acid would improve the efficiency of the SMC reaction, we repeated the experiment shown in Scheme 2.3, adding the boronic acid slowly via syringe pump over three hours. Despite only using a single equivalent of unstable **2.4a**, a 98% yield of the desired product **2.14a** was obtained after column chromatography. While the use of a syringe pump is not overly challenging, it does introduce undesired complexity to the reaction setup, and again necessitates the isolation and handling of the unstable boronic acid. Instead, we proposed that a similar effect could be achieved if the boronic acid were delivered to the reaction internally, via a slow hydrolysis from the corresponding MIDA boronate.

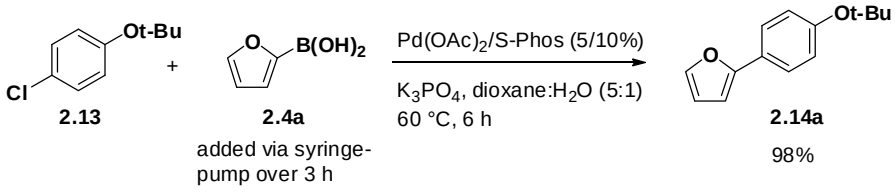

Scheme 2.4. The use of a syringe pump to deliver 1.0 equiv of boronic acid **2.4a** steadily over 3 h enabled a nearly quantitative yield of the biaryl product **2.14a**. We attribute this high yield to slow addition of the boronic acid.

To test whether a "slow-release" of an unstable boronic acid from the corresponding MIDA boronate could improve the efficiency of a cross-coupling reaction, we needed to identify conditions that would still promote efficient cross-coupling, but that would result in a much

slower hydrolysis of the MIDA boronate. Ideally, the rate of hydrolysis would be slower than the turnover-rate of the catalyst used in the SMC reaction. Before investigating potential conditions, we needed to accurately determine the rate of the reaction in question. Therefore, we again set up the reaction of boronic acid **2.4a** with **2.13**, under our standard SMC conditions, and monitored the course of the reaction by analyzing aliquots taken from the reaction by GC (Figure 2.2). As seen in Figure 2.2, the reaction appears to reach a maximum conversion of the halide of 62% within one hour, which is consistent with the yield obtained in Scheme 2.3. It is likely that the halide ceases to convert after one hour due to the fact that all of boronic acid has been consumed, either via productive conversion to **2.14a** or destructive protodeboronation. To test if protodeboronation occurs under these conditions at a rate commensurate with this hypothesis, we set up an experiment wherein boronic acid **2.4a** was exposed to mock cross-coupling conditions (aqueous K_3PO_4 in dioxane at 60 ˚C) and the amount of boronic acid remaining in the mixture was determined over the course of six hours by ^{1}H-NMR (Figure 2.3). Consistent with our hypothesis, the amount of **2.4a** decreased steadily over six hours as it converts to furan (**2.15**), demonstrating its instability to aqueous base at elevated temperature. The amount of **2.4a** remaining after one hour, ~40%, is also roughly consistent with the conversion of halide obtained in the actual SMC reaction in Figure 2.2. Collectively, these experiments suggested to us that in order to match the catalyst TOF a MIDA boronate would need to be hydrolyzed over at least 30 minutes at 60 ˚C.

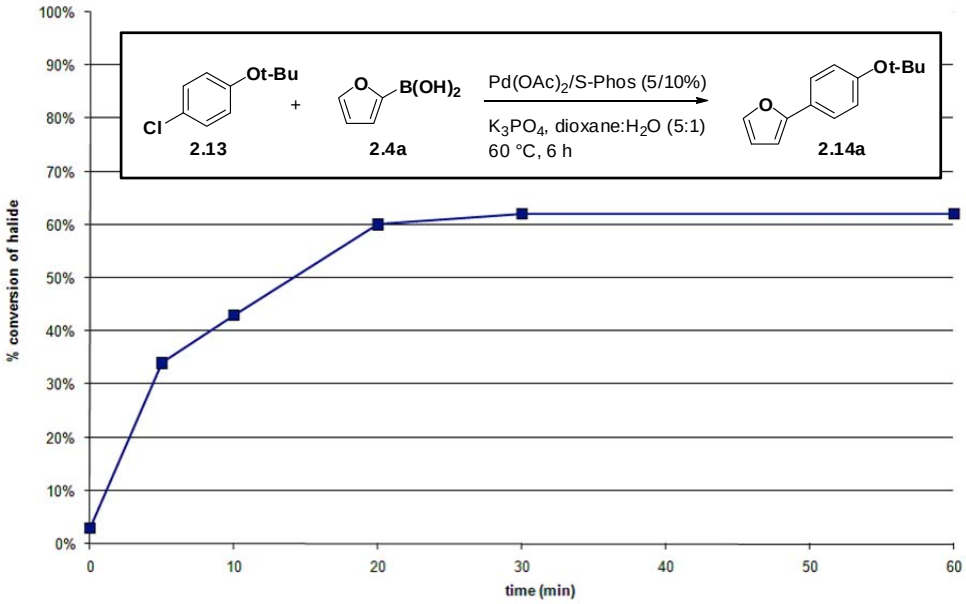

Figure 2.2. The reaction of **2.13** with **2.4a**, when monitored by GC, was seen to stalls out at ~60% conversion of halide, consistent with the observation that under similar conditions this reaction affords **2.14a** in 64% yield.

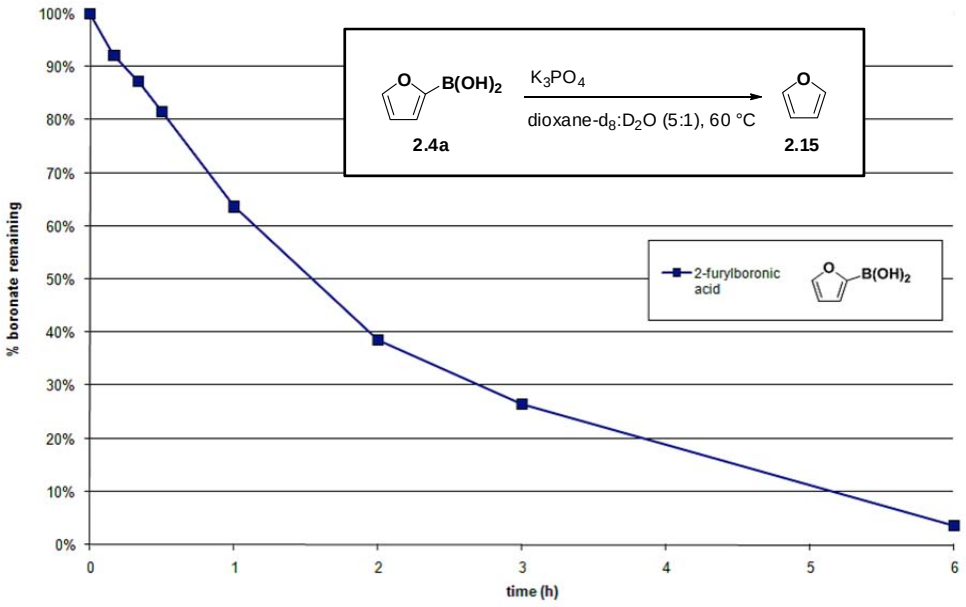

Figure 2.3. Exposure of boronic acid **2.4a** to mock cross-coupling conditions results in steady decomposition via protodeboronation. The progress of decomposition was monitored by ^{1}H-NMR over the course of 6 h.

Previous experiments in our laboratory had demonstrated that weak bases hydrolyze MIDA boronates more slowly than strong bases such as sodium hydroxide,[60] so we tested K_3PO_4, an inexpensive base commonly employed in SMC reactions, at a variety of temperatures to evaluate its suitability for use in slow-release SMC reaction (Figure 2.4). When MIDA boronate **2.5a** was exposed to aqueous K_3PO_4 in dioxane at 60 ˚C we observed that hydrolysis was greater than 95% complete after two hours, well above the target of thirty minutes that we had previously established. Notably, even at 100 ˚C, complete hydrolysis took longer than thirty minutes, suggesting that slow-release conditions might be effective even at significantly elevated temperatures. Deprotection at room temperature was considerably slower, requiring greater than 24 hours to complete (Figure 2.5). Based on these results, K_3PO_4 appeared very suitable for use in slow-release SMC reactions performed between 23 and 100 °C.

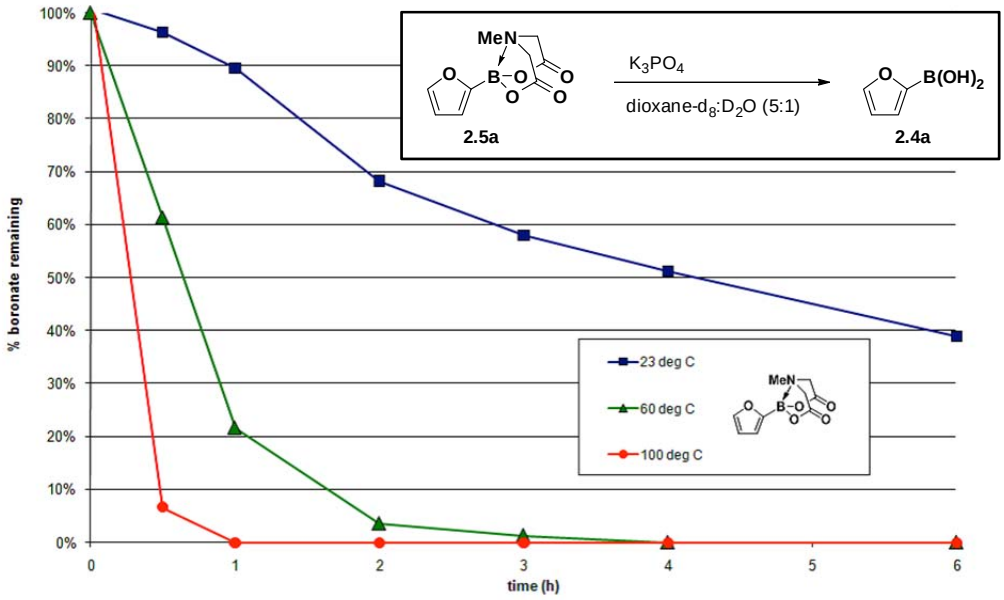

Figure 2.4. Exposure of MIDA boronate **2.5a** to mock cross-coupling conditions demonstrates a steady release of the boronic acid in a temperature-dependent fashion. These results suggest that the slow-release effect may be useful even at temperatures up to 100 °C, and that temperatures below room temperature are likely to be impractical with this particular base due to the long time necessary to achieve full deprotection.

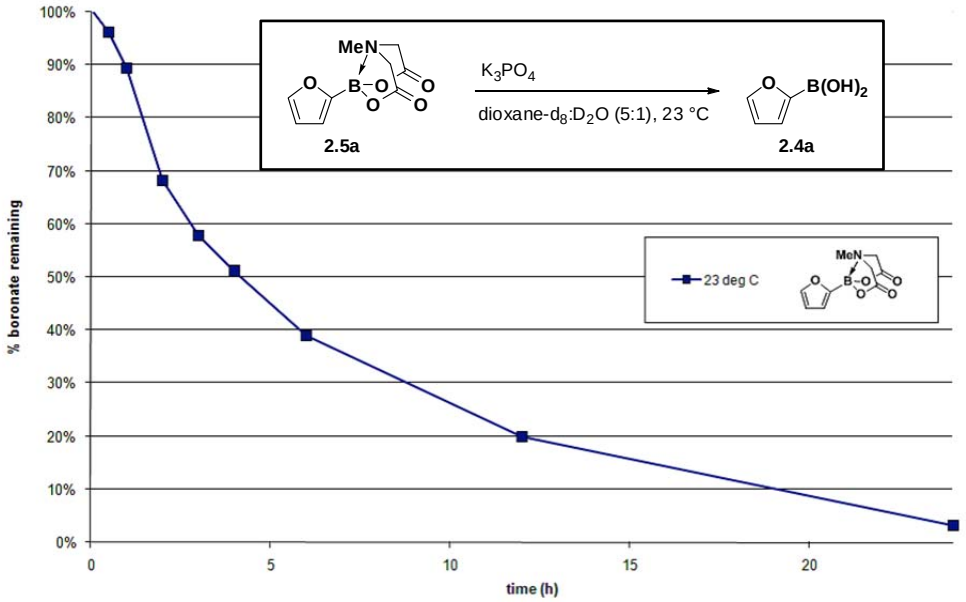

Figure 2.5. The deprotection of MIDA boronate **2.5a** under mock reaction conditions takes approximately 24 hours at room temperature.

We also investigated the sensitivity of the MIDA boronate hydrolysis kinetics to the organic group appended to boron. We exposed several different MIDA boronates containing vinyl, cyclopropyl, aryl and heteroaryl moieties to aqueous K_3PO_4 in dioxane at 60 ˚C. Remarkably, the deprotection rates were very similar for all MIDA boronates tested. This suggested to us that any improvement in SMC reaction efficiency imparted by the slow-release conditions might be quite general. Notably, it has recently been demonstrated that the release rates for trifluoroborate salts vary substantially as a function of the organic group.[56]

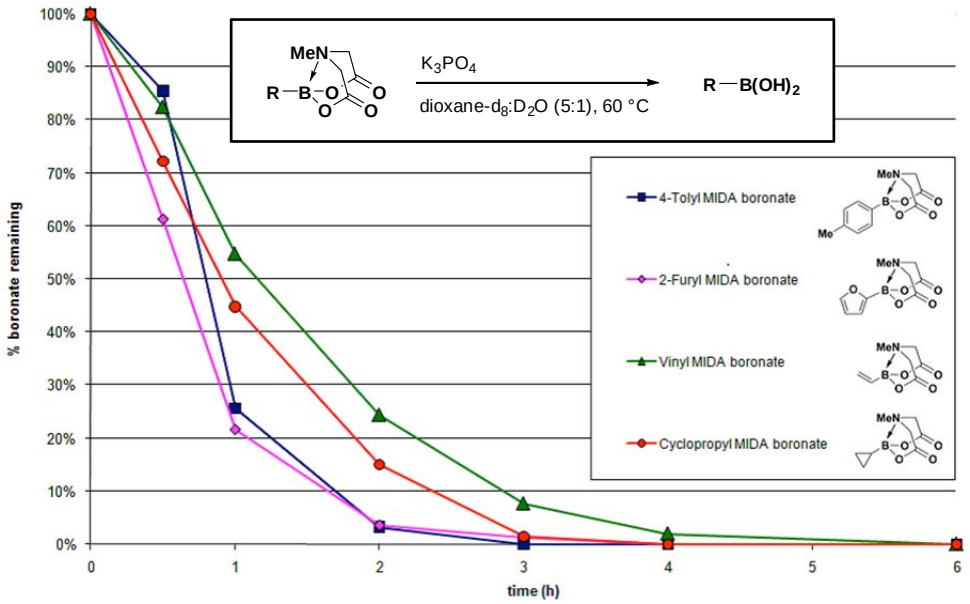

Figure 2.6. The rate of deprotection of MIDA boronates does not seem to be dependent on the nature of the organic group appended to boron as seen in the above substrates representing aryl, heteroaryl, vinyl and cyclopropyl functionalities.

To test whether the candidate slow-release conditions could improve the efficiency of SMC reactions involving unstable boronic acids, we repeated the experiment from Scheme 2.4, using MIDA boronate **2.5a** directly in the reaction with K_3PO_4 as a base (Table 2.3, entry 1). Strikingly, the product was obtained in a very high 94% yield after chromatography, matching the result obtained with the syringe pump.

To better understand the generality of this approach, a collection of additional MIDA boronates were synthesized, representing several classes of boronic acids previously described to exhibit significant instability. MIDA boronates **2.5a-h** were thus exposed to the slow-release SMC conditions, and the yields obtained were compared to those obtained with the corresponding boronic acids (Table 2.3). Importantly, all boronic acids were freshly prepared immediately before use by hydrolysis from the corresponding MIDA boronate and confirmed to be ≥95% pure by ^{1}H NMR. Additionally, only a single equivalent of MIDA boronate or boronic acid was used relative to the halide coupling partner, so that any decomposition of the organoborane in the reaction would manifest as a decrease in yield. The yields obtained with the

MIDA boronates were uniformly high (≥90%), despite the use of only a *single equivalent* of organoborane, while the yields obtained with boronic acids **2.4a-h** were much lower. In some cases the differences were striking. For example, thiophenylboronic acid **2.4c** generated a 37% yield, compared to a 94% yield from corresponding MIDA boronate **2.5f**. Similarly, indolylboronic acid **2.4f** generated only a 14% yield, compared to a 93% yield from the corresponding MIDA boronate **2.5f**. Interestingly, there was not a significant difference between **2.4h** and **2.5h**, suggesting that difficulties with **2.4h** noted in the literature are due to its instability to storage. Collectively, these results clearly demonstrate that MIDA boronates can not only serve as effective direct surrogates for boronic acids in SMC reactions, but that under slow-release conditions they can effectively improve the efficiency with which one can use otherwise unstable boronic acids.

Table 2.3

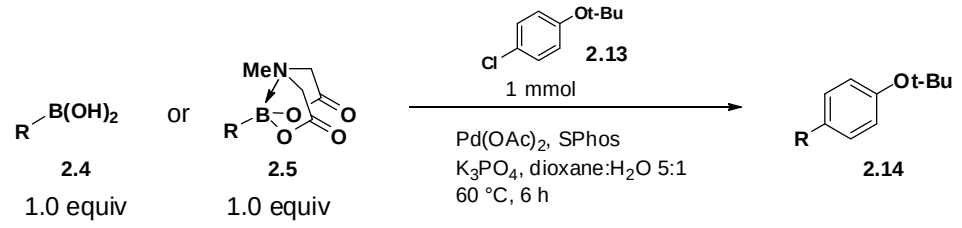

Entry	R	Product	Isolated yield[a] from: 2.4	2.5
1	 a	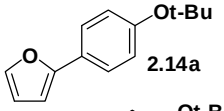 2.14a	68	**94**
2	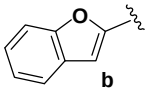 b	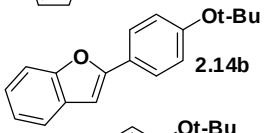 2.14b	50	**92**
3	 c	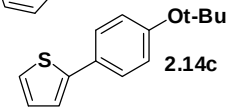 2.14c	37	**94**
4	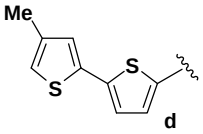 d	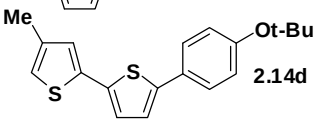 2.14d	45	**96**
5	 e	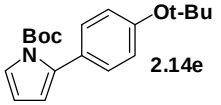 2.14e	61	**90**
6	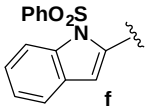 f	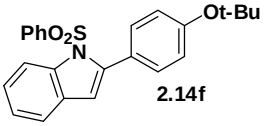 2.14f	14	**93**
7[b]	 g	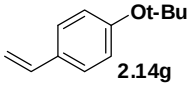 2.14g	79	**98**
8[b]	 h	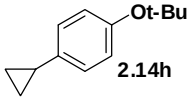 2.14h	95	**96**

[a]Reaction conditions: 1.0 equiv 2.13, 1.0 equiv 2.5 (freshly prepared, >95% purity) or 1.0 equiv 2.4, 5 mol% $Pd(OAc)_2$, 10 mol% S-Phos, 7.5 equiv K_3PO_4, 0.07M in dioxane:H_2O 5:1, 60 °C, 6 h.[b]Cross-couplings performed at 100 °C.

While the generality of the slow-release SMC reaction conditions appeared quite good with respect to the identity of the organoborane, we were still interested in further exploring the scope of this protocol with respect the identity of the halide. We had attempted to set a high bar

for ourselves by performing all initial experiments with an electronically deactivated aryl chloride (**2.13**), and so chose maintain that level of rigor by testing the same MIDA boronates from Table 2.3 against a variety of aryl chlorides (**2.15a-h**) encompassing substrates that were electron-rich (**2.15a**, **2.15c**, **2.15e**, **2.15f**, **2.15g**), electron-poor (**2.15d**, **2.15h**), sterically encumbered (**2.15a**, **2.15b**, **2.15d**) and heteroaromatic (**2.15c**, **2.15e**, **2.15f**, **2.15g**, **2.15h)** (Table 2.4). Across 21 examples, the average yield was 92%, demonstrating the efficiency and generality of the slow-release protocol. Reactions were set up without the use of a glovebox, using the same standard conditions developed in Table 2.3 and 1.2 equivalents of the MIDA boronates, and used only a single catalyst system. Reactions were generally complete within six hours. Some exceptions were as follows: The best results for vinyl MIDA boronate (**2.5g**) and cyclopropyl MIDA boronate (**2.5h**) were obtained at 100 ˚C (entries 16 -21), and entries 7, 8 and 20 used 1.5 equivalents of MIDA boronate. Interestingly, in contrast to results reported for potassium vinyltrifluoroborate, for SMC reactions performed with vinyl MIDA boronate (**2.5g**), in no case did we observe byproducts from a competitive Heck coupling reaction.

It should also be noted that during the course of our experimentation with the slow-release SMC conditions we attempted to reduce the amount of base used in the reaction. While isolated experiments showed that as few as 3 equivalents of K_3PO_4 could sometimes give full conversion and high yields, extensive attempts to optimize the protocol with between 3 to 5 equivalents of base inevitably gave highly irreproducible results. In contrast, using 7.5 equivalents of base appears to render the protocol robust and highly reproducible.

Table 2.4

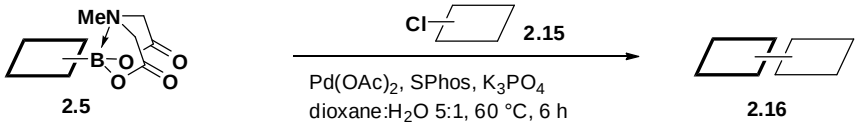

Entry	2.5	2.15	2.16	isolated yield (%)
1	**2.5a**	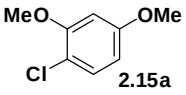 **2.15a**	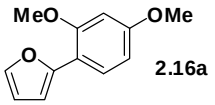 **2.16a**	99
2	**2.5a**	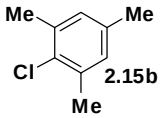 **2.15b**	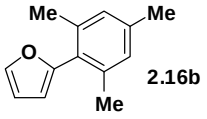 **2.16b**	97
3	**2.5a**	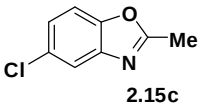 **2.15c**	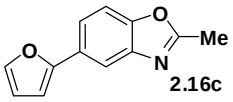 **2.16c**	99
4	**2.5a**	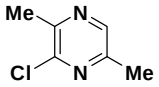 **2.15d**	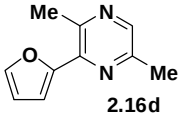 **2.16d**	91
5	**2.5b**	**2.15a**	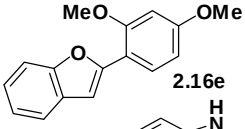 **2.16e**	94
6	**2.5b**	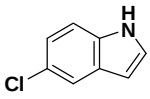 **2.15e**	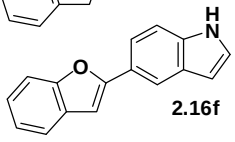 **2.16f**	94
7[b]	**2.5b**	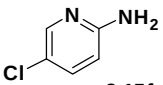 **2.15f**	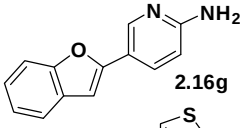 **2.16g**	85
8[b]	**2.5b**	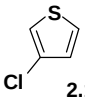 **2.15g**	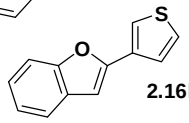 **2.16h**	85
9	**2.5c**	**2.15a**	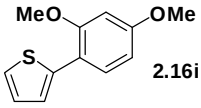 **2.16i**	98
10	**2.5c**	**2.15c**	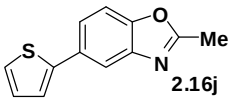 **2.16j**	99
11	**2.5c**	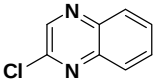 **2.15h**	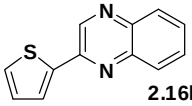 **2.16k**	97

[a]General reaction conditions: 1 equiv of aryl halide (1 mmol), 1.2 equiv of MIDA boronate, 5 mol % $Pd(OAc)_2$, 10 mol % SPhos, 7.5 equiv of K_3PO_4, 0.07 M in dioxane:H_2O 5:1, 60 °C, 6 h. [b]1.5 equiv of MIDA boronate. [c]0.5 mmol of aryl halide, 0.6 mmol of MIDA boronate (1.2 equiv). [d]100 °C . [e]2 h. [f]24 h

Table 2.4 cont.

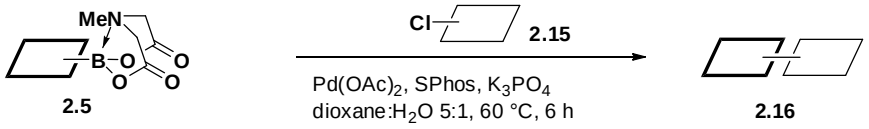

Entry	2.5	2.15	2.16	isolated yield (%)
12[c]	**2.5e**	**2.15a**	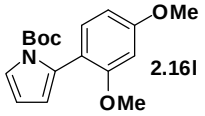 **2.16l**	81
13[c]	**2.5e**	**2.15c**	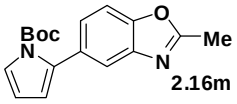 **2.16m**	98
14	**2.5f**	**2.15a**	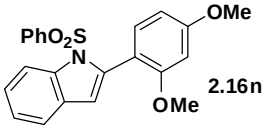 **2.16n**	97
15	**2.5f**	**2.15c**	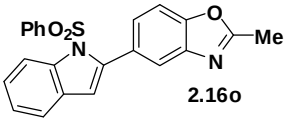 **2.16o**	93
16[d,e]	**2.5g**	**2.15b**	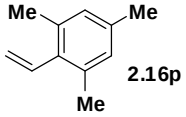 **2.16p**	91
17[d,e]	**2.5g**	**2.15h**	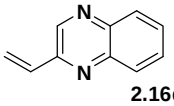 **2.16q**	87
18[d,e]	**2.5g**	**2.15f**	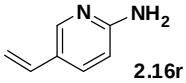 **2.16r**	76
19[d,e]	**2.5g**	**2.15c**	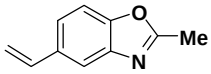 **2.16s**	96
20[b,d,f]	**2.5h**	**2.15b**	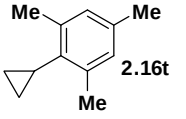 **2.16t**	79
21[d]	**2.5h**	**2.15a**	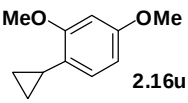 **2.16u**	97

[a]General reaction conditions: 1 equiv of aryl halide (1 mmol), 1.2 equiv of MIDA boronate, 5 mol % $Pd(OAc)_2$, 10 mol % SPhos, 7.5 equiv of K_3PO_4, 0.07 M in dioxane:H_2O 5:1, 60 °C, 6 h. [b]1.5 equiv of MIDA boronate. [c]0.5 mmol of aryl halide, 0.6 mmol of MIDA boronate (1.2 equiv). [d]100 °C . [e]2 h. [f]24 h

2-5 SYNTHESIS AND CROSS-COUPLING OF 2-PYRIDYL MIDA BORONATE

Encouraged by the success of the slow-release SMC protocol, we wished to explore the limits of the methodology. In this vein, 2-pyridylboronic acid presented itself as a worthy target. From an applications standpoint, the 2-pyridyl subunit is a very important motif found in a variety of pharmaceuticals,[61-62] natural products,[63-65] unnatural nucleotides,[66-67] fluorescent probes,[68] materials,[69-71] and metal-complexing ligands.[71-73] Unfortunately, 2-pyridyl boronic is extremely unstable,[74-75] precluding its use in SMC reactions. As a testament to its potential value, however, tremendous effort has been directed over the past several decades toward the development of a 2-pyridyl organometallic equivalent that can be efficiently used in cross-coupling reactions.[32,37-40,50,76-78] Unfortunately, each of these methods suffers from one or more important limitations, including a lack of air-stability,[32,50,78] use of toxic metals,[76-77] an inability to fully characterize or isolate the building block in a chemically pure form,[37-38] and/or inefficiency in couplings with more challenging yet desirable halide coupling partners like deactivated aryl chlorides.[37-40]

Recognizing a challenging and unmet need in the synthetic methodology, we first questioned if we could synthesize 2-pyridyl MIDA boronate (**2.19**), and if so, whether it might exhibit the same degree of air-stability that had to date appeared ubiquitous to the MIDA boronate class. Consistent with its reported instability, we initially had considerable difficulty isolating **2.19**. Traditional Dean-Stark complexation was not possible due to our inability to access the free boronic acid, and attempts to transmetallate from silicon to boron[9,79] were unsuccessful, despite numerous variations of the procedure (Brice Uno, unpublished results). Alternatively, we were intrigued by several reports of the modest stability of 2-pyridyltrialkoxyborate salts like **2.18**.[32,75] We reasoned that a transligation from the relatively stable alkoxyborate salt directly to the MIDA boronate might be possible. Indeed, preparation of **2.18**, followed by reaction with MIDA in DMSO and azeotropic removal of i-PrOH with refluxing toluene afforded our first successful synthesis of **2.19**, albeit in only 2% yield (Table 2.5). Further optimization by employing low pressure vacuum distillation, and finally portion-wise solid addition of a mixture of **2.18** and Celite to a mixture of DMSO and MIDA at 45 ˚C and 1 Torr increased the yield to 13% and 27% respectively. While we remained far from satisfied with this yield, it did enable us access to gram-quantities of **2.19**. Remarkably, in stark contrast to 2-pyridylboronic acid, **2.19** was isolated as a colorless, free-flowing crystalline solid,

in terms of its physical characteristics no different than the other MIDA boronates described above. Its high crystallinity enabled X-ray crystallographic analysis, which afforded an unambiguous structural confirmation (Figure 2.7), though surprisingly it also showed good solubility in acetone, MeCN and DMF. Additionally, **2.19** was also observed to be stable under air at room temperature for at least two months. To the best of our knowledge, 2-pyridyl MIDA boronate (**2.19**) represents the first example of an air-stable 2-pyridyl borane that can be isolated in chemically pure form.

Table 2.5

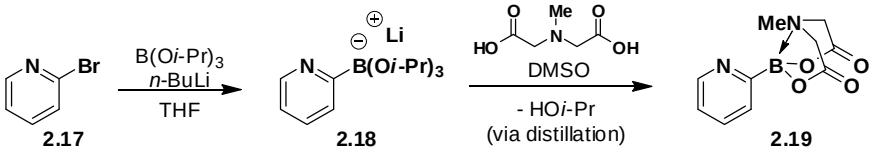

2.17 2.18 2.19

Entry	Distillation temp (°C)	Distillation Pressure (Torr)	% Yield of **2.18**
1	110	740	2
2	45	1	18
3	45	1	**27**[a]

[a] **2.18** was added portion-wise as mixture adsorbed onto Celite

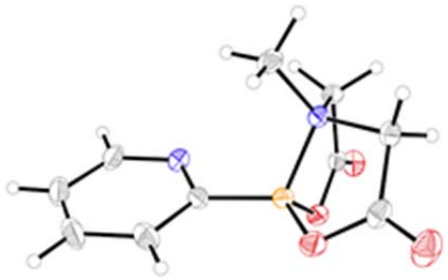

Figure 2.7. Crystal structure of 2-pyridyl MIDA boronate (**2.19**).

Having developed a preparative synthesis of **2.19**, we next sought to explore whether it could be an effective cross-coupling partner using the slow-release SMC methodology. Using conditions similar to those from Table 2.4, when **2.19** was exposed to 4-bromoacetophenone (**2.7**), no conversion to the desired SMC product was observed (Table 2.6, entry 1). Copper has been shown to be useful in promoting SMC reactions.[34,40,43] The addition of 0.2 equivalents of CuI afforded 11% conversion as determined by ^{1}H NMR (entry 2). Switching to a more polar

solvent, DMF with K_2CO_3 improved the yield to 30% (entry 3). Finally, changing the ratio of DMF:IPA to 1:1 and changing to the catalyst $Pd(dtbpf)Cl_2$ improved conversion to 100% (entry 4). Unfortunately, applying these conditions to activated aryl chloride 4-chloroacetophenone (**2.20a**) afforded a rather poor 21% conversion (entry 5).

Table 2.6

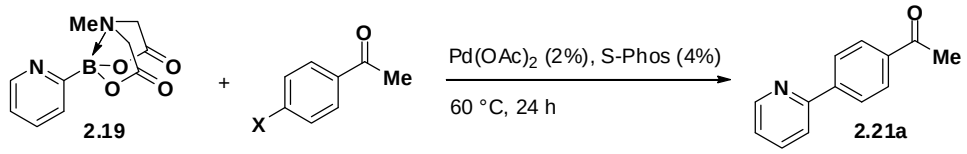

Entry	X	Solvent	Base	Equiv CuI	Conversion to **2.21a**
1	Br **(2.7)**	THF:H_2O (5:1)	K_3PO_4	0	0%
2	Br **(2.7)**	THF:H_2O (5:1)	K_3PO_4	0.2	11%
3	Br **(2.7)**	DMF:i-PrOH (5:1)	K_2CO_3	0.2	30%
4[a]	Br **(2.7)**	DMF:i-PrOH (1:1)	K_2CO_3	0.2	100%
5[a]	Cl **(2.20a)**	DMF:i-PrOH (1:1)	K_2CO_3	0.2	21%

[a] In place of $Pd(OAc)_2$ and S-Phos, $Pd(dtbpf)Cl_2$ was used

It became clear that for the more difficult aryl chlorides a broader, more systematic screening effort would be necessary. Therefore we surveyed a range of copper sources (CuI, $CuSO_4$, CuO, Cu_2O, $CuNO_3$, CuTC), bases ($Ba(OH)_2$, KOAc, K_2CO_3, Cs_2CO_3, $CaCO_3$, TBAF, CsF, K_3PO_4), temperatures, solvents and catalysts. From these experiments we identified $Cu(OAc)_2$ as being more effective than CuI in promoting the desired reaction. $CsCO_3$ and K_2CO_3 were equally superior to the rest of the bases, and the combination of the X-Phos and Pd_2dba_3 was uniquely effective, as was the solvent combination of DMF:IPA (4:1) at 100 ˚C. Combining these results we were able to identify optimal conditions for the reaction of **2.20a** with **2.19**, which gave the desired product after column chromatography in 72% yield (Table 2.7, entry 1). We next tested these conditions with a variety of aryl and heteroaryl chlorides and bromides, and found them to be fairly general (Table 2.7). Interestingly, yields with aryl bromides **2.20f-h** were not significantly better than the aryl chlorides (**2.20a-e**), though it is possible that after such intense optimization for reaction with **2.20a** we had arrived at conditions imperfectly suited for bromides, especially given the excellent earlier result with bromoacetophenone (Table 2.6, entry 4). Also worth noting are bipyridine **2.21h**, isoquinoline **2.21e**, pyrazine **2.21d** and quinoxaline

2.21c. In each of these products, cross-coupling has formed a bond between two carbons each adjacent to nitrogen. Through the use of cross-coupling, these products could only be obtained by using an inherently unstable nitrogen 2-heterocyclic nucleophile. Collectively, these results strongly suggest that 2-pyridyl MIDA boronate (**2.19**) is a stable and efficient surrogate for the highly unstable 2-pyridyl boronic acid in SMC reactions. It should be noted that using these reaction conditions, limitations still existed in cross-coupling to deactivated aryl chlorides. A recent publication[80] by Dick and coworkers, addresses this limitation through the use of a diethanolamine additive. This is clearly an important advance but lies outside the scope of this dissertation.

Table 2.7

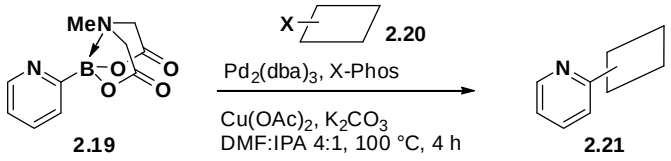

Entry	**2.20**	**2.21**	Isolated yield of **2.21** (%)[a]
1	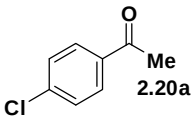 **2.20a**	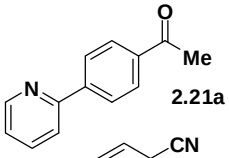 **2.21a**	72
2	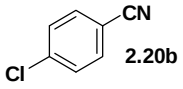 **2.20b**	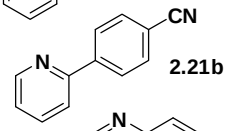 **2.21b**	60
3	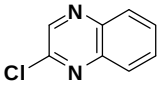 **2.20c**	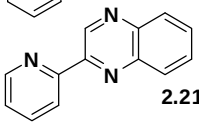 **2.21c**	79
4	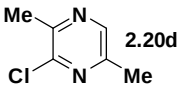 **2.20d**	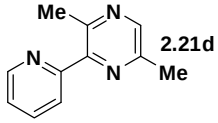 **2.21d**	52
5	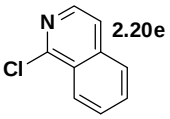 **2.20e**	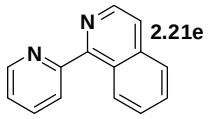 **2.21e**	74
6	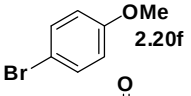 **2.20f**	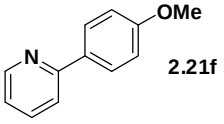 **2.21f**	57
7	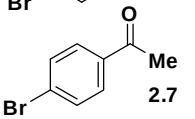 **2.7**	**2.21a**	42
8	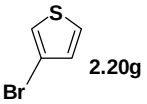 **2.20g**	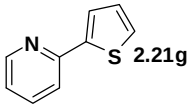 **2.21g**	66
9	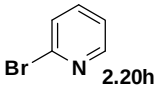 **2.20h**	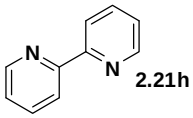 **2.21h**	41

[a]Reaction conditions: 1.0 equiv halide **2.20** (1 mmol), 1.5 equiv MIDA boronate **2.19**, 1.5 mol% $Pd_2(dba)_3$, 6 mol% X-Phos, 50 mol% $Cu(OAc)_2$, 5 equiv K_2CO_3, 0.1 M in DMF:IPA 4:1, 100 °C, 4h.

2-6 IMPROVED SYNTHESIS OF 2-PYRIDYL MIDA BORONATE AND DERIVATIVES

Having demonstrated the utility of **2.19**, we returned our attention to the unfinished problem of its synthesis. While the current synthesis (Table 2.5, entry 3) enabled the generation of small amounts of material, the yield remained poor, and the reaction was operationally challenging, difficult to scale, and involved arduous column chromatography which ideally would be eliminated. Initial experimentation involved elimination of the technically challenging solid addition of **2.18**, instead adding it as a suspension in THF. Additionally, we attempted lowering the temperature of the distillation with the goal of suppressing undesired protodeboronation of **2.18** and/or the corresponding diisopropylboronic ester. This strategy had previously seemed beneficial (Table 2.5, entries 1 and 2), but the yields for reactions run between 23 and 55 ˚C were low and inconsistent. A breakthrough was subsequently made in the discovery that **2.19** can be heated in anhydrous DMSO for greater than one hour without detectable decomposition by ^{1}H NMR. This result prompted us to investigate higher temperatures (Figure 2.8). Surprisingly, we found that the reaction performed much better at higher temperatures, with the highest observed yield at 130 ˚C. In practice, we found 115 ˚C to be an acceptable compromise between yield and practicality.

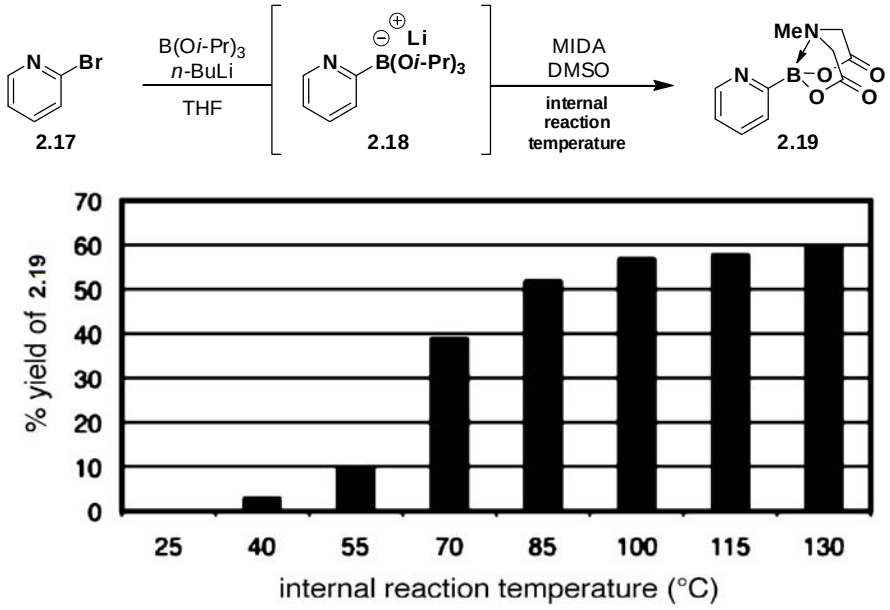

Figure 2.8. Yield of **2.19** as a function of temperature (each bar represents the average of two runs)

Application of this optimized procedure, semi-officially dubbed the "hot protocol" enabled isolation of **2.19** in 59% yield (Table 2.8, entry 1), a significant improvement over the previous-generation synthesis. Additionally, a procedure was developed whereby the product could be purified by trituration and subsequent re-crystallization, with no need for SiO_2 chromatography. In light of the significantly improved efficiency of this reaction, we were prompted to investigate whether derivatives of **2.19** might be accessible. Beginning with 2-pyridyl bromides **2.22a-i**, application of the hot protocol enabled isolation of 2-pyridyl MIDA boronate derivatives **2.23a-i** in fair to good yield (Table 2.8, entries 2-10). Furthermore, beginning with bromides **2.24** and **2.26**, we were able obtain 2-thiazole MIDA boronate (**2.25**) and pyrazinyl MIDA boronate (**2.27**) in 30% and 43% yields, respectively (Scheme 2.5). To our knowledge **2.27** represents the first example of an air-stable pyrazinyl organoborane.

Table 2.8

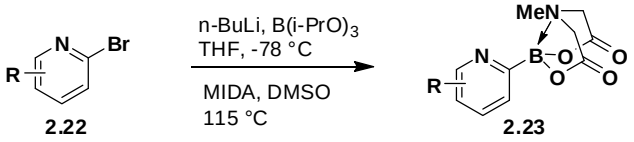

Entry	2.22	2.23	Isolated Yield (%)
1	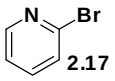	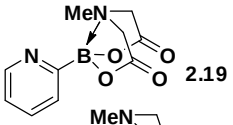	59
2	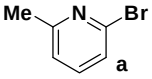	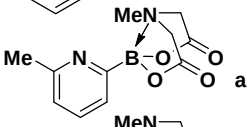	58
3	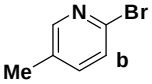	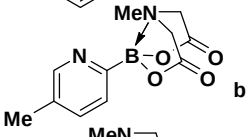	51
4	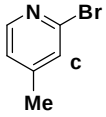	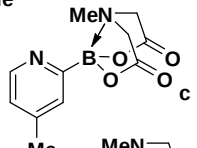	42
5	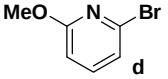	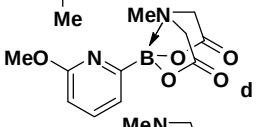	81
6	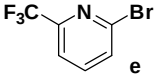	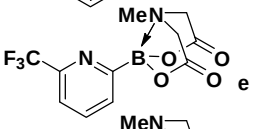	89
7	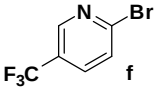	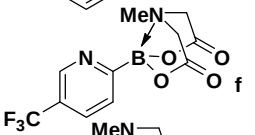	56
8	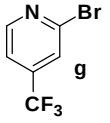	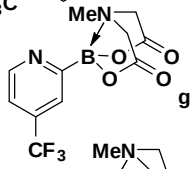	53
9	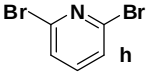	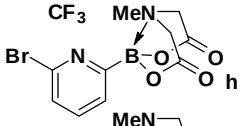	47
10	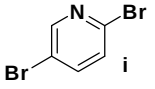	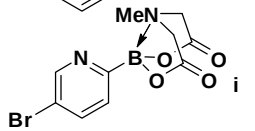	69

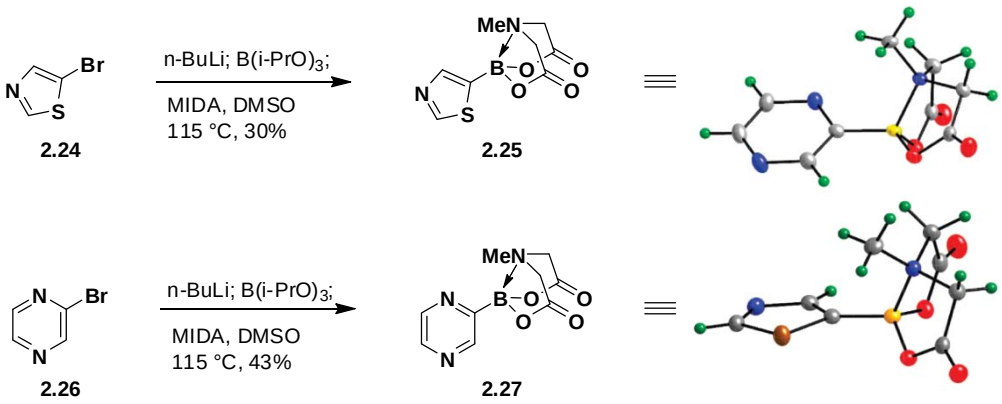

Scheme 2.5. Synthesis of 5-thiazole MIDA boronate (**2.25**) and 2-pyrazinyl MIDA boronate (**2.27**). Also shown are the corresponding crystal structures obtained via X-ray crystallography.

2-7 APPLICATION OF DIRECT-RELEASE SMC REACTIONS TO NATURAL PRODUCT SYNTHESIS

Given the positive results obtained with vinyl, cyclohexyl and heterocyclic boronic acids in the direct release SMC protocol, we wanted to see if this methodology might offer a solution to one of the synthetic problems that originally stimulated the project. Repeating the coupling from Scheme 2.1, instead using the MIDA boronate directly with *aqueous* NaOH (Scheme 2.6), the desired heptaene product (**2.3**) was obtained in 48% yield. **2.3** represents fully one half of the AmB macrolactone, and at the time of this result represented, to our knowledge, the longest polyene ever synthesized via an SMC reaction. Since then that record has been surpassed, first by Eric Woerly in his synthesis of the carotenoid peridinin also using a direct-release SMC reaction,[10] and later by Seiko Fujii in her synthesis of the carotenoid synechoxanthin using a novel bidirectional variation of the direct-release protocol.[81]

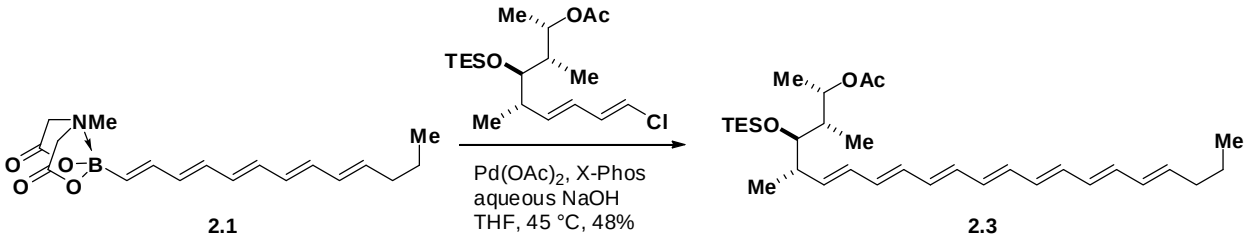

Scheme 2.6. Application of the "fast-release" cross-coupling conditions enabled synthesis of the previously inaccessible heptaene **2.3**.

In addition to the AmB polyene and the aforementioned carotenoids, peridinin and synechoxanthin, the direct release protocol has found use in a number of other natural product syntheses, both within and outside of our laboratory, including crocacin C,[5] myxalamide A,[82] methyl-eicosapentaenoate,[83] renierapurpurin (Hannah Haley, unpublished results), the polyene core of vacidin A,[6] and a deoxygenated derivative of AmB[84] (Figure 2.9). Interestingly, despite the clear benefit of the slow-release conditions for SMC reactions involving heterocyclic, cyclopropyl and vinyl boronic acids, fast-release conditions with sodium hydroxide have repeatedly proven to be superior for the construction of extended polyenes. This may be because the longer reaction times necessitated by the slow-release conditions allow time for decomposition of either the unstable vinyl halide substrate or the polyene product. The number of examples of syntheses incorporating direct-release coupling of MIDA boronates at the end of an ICC sequence, particularly in the context of polyenes, clearly demonstrates the utility of this methodology in natural product synthesis.

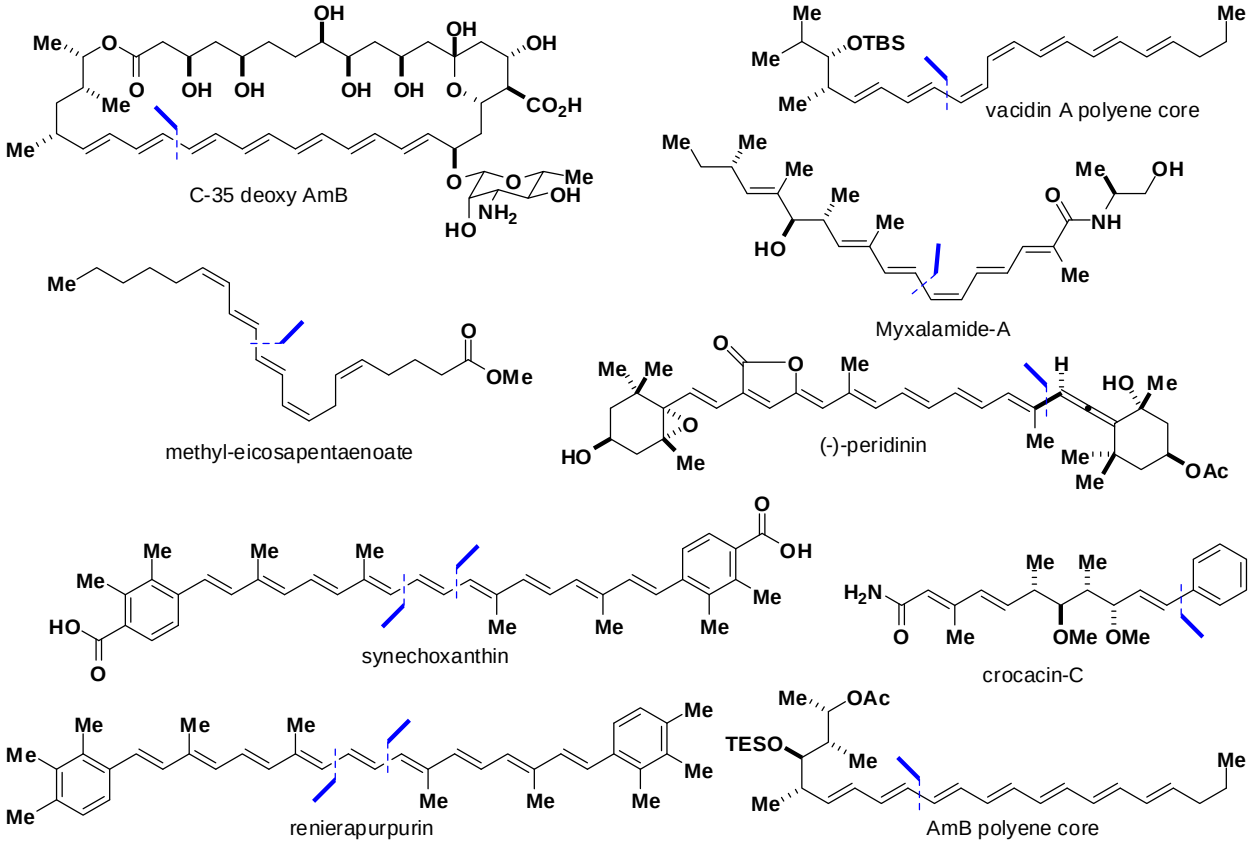

Figure 2.9. Examples of natural product-based syntheses which have utilized the direct release cross-coupling protocol. The relevant bond disconnection(s) are noted for each molecule.

2-8 SUMMARY

Stimulated by challenges encountered in the AmB polyene synthesis, it has been demonstrated that MIDA boronates can be utilized as direct surrogates for unstable boronic acids. Unlike many of their boronic acid counterparts, MIDA boronates are uniformly air-stable, free-flowing, crystalline solids, completely stable to storage under ambient conditions. Further, a new SMC reaction protocol has been developed in which MIDA boronates can be directly utilized in *aqueous basic* SMC reactions, whereby in situ hydrolysis of the MIDA boronate generates the boronic acid for cross-coupling. The use of weak bases like K_3PO_4 promotes a slow-release of the boronic acid, which minimizes competitive protodeboronation and allows for very efficient cross-coupling compared to reactions using unprotected free boronic acids, even in couplings to deactivated and/or sterically encumbered aryl chlorides. Alternatively, the use of "fast-release" conditions using strong bases like NaOH has been identified as particularly useful in the context of polyene construction, where the stability of the polyenyl halide coupling partner or polyene product is as much of a concern as that of the polyenylboronic acid. This methodology has also been extended to include the notoriously unstable 2-pyridylboronic acid, which as the corresponding MIDA boronate represents the first air-stable and chemically pure 2-pyridyl organoborane. The necessity of aqueous or protic co-solvents restricts this direct-release protocol to the final step of an ICC sequence (often the most challenging), but makes it very useful for the cross-coupling of any monofunctional halide or pseudohalide. By taking advantage of their favorable physical properties, uniform air stability, and their capacity for in situ slow-release in SMC reactions, MIDA boronates thus fully address both of the key problems associated with the use of unstable boronic acids in the SMC reaction, i.e. their instability to storage *and* instability under SMC reaction conditions. This advance stands to not only greatly expand the range of useful organoboranes available for use in cross-coupling but also to generally enhance the utility of the SMC reaction in organic synthesis. Additionally, following the publication of these results, others have found the slow-release approach useful in the synthesis and cross-coupling of other heterocyclic organoboranes[85-86] unnatural amino acids,[87] and in the context of other reactions.[11,88-90]

2-9 EXPERIMENTAL SECTION

Materials.

Commercial reagents were purchased from Sigma-Aldrich, Fisher Scientific, Alfa Aesar, TCI America Frontier Scientific, Oakwood Products or Combi-Blocks and were used without further purification unless otherwise noted. Solvents were purified via passage through packed columns as described by Pangborn and coworkers[91] (THF, Et_2O, MeCN, DCM: dry neutral alumina; hexane, benzene, and toluene: dry neutral alumina and Q-5 reactant (copper(II) oxide on alumina); DMSO, DMF: activated molecular sieves). All water was deionized prior to use. Triethylamine, diisopropylamine, diethylamine, pyridine, and 2,6-lutidine were freshly distilled under an atmosphere of nitrogen from CaH_2. The following compounds were prepared according to procedures reported in the literature: *N*-methyliminodiacetic acid,[4] 4-tolyl MIDA boronate (**2.10a**),[3] vinyl MIDA boronate (**2.5g**),[9] and 5-bromo-2-thiopheneboronic acid MIDA ester.[3]

General Experimental Procedures.

Unless otherwise noted, all reactions were performed in flame-dried glassware under argon. Organic solutions were concentrated via rotary evaporation under reduced pressure with a bath temperature of 35-40 ºC. Reactions were monitored by analytical thin layer chromatography (TLC) performed using the indicated solvent on E. Merck silica gel 60 F254 plates (0.25mm). Compounds were visualized by: exposure to a UV lamp (λ = 254 or 366 nm), incubation in a glass chamber containing iodine, and/or treatment with a solution of $KMnO_4$, an acidic solution of p-anisaldehyde or a solution of ceric ammonium molybdate (CAM) followed by brief heating with a Varitemp heat gun. MIDA boronates are compatible with standard silica gel chromatography, including standard loading techniques. Column chromatography was performed using standard methods[92] or with a Teledyne-Isco CombiFlash R_f purification system. Both methods were performed using Merck silica gel grade 9385 60 Å (230-400 mesh).

Structural analysis.

^{1}H-NMR spectra were recorded at 23 °C on a Varian Unity or a Varian Unity Inova 500 MHz spectrometer. Chemical shifts (δ) are reported in parts per million (ppm) downfield from tetramethylsilane and referenced to residual protium in the NMR solvent ($CHCl_3$, δ = 7.26; CD_2HCN, δ = 1.93, center line; acetone-d_6 δ = 2.04, center line). Alternatively, NMR-solvents

designated as "w/ TMS" were referenced to tetramethylsilane (δ = 0.00 ppm) added as an internal standard. Data are reported as follows: chemical shift, multiplicity (s = singlet, d = doublet, t = triplet, q = quartet, quint = quintet, sept = septet, m = multiplet, br = broad, app = apparent), coupling constant (*J*) in Hertz (Hz), and integration. ^{13}C NMR spectra were recorded at 23 °C on a Varian Unity 500 MHz spectrometer. Chemical shifts (δ) are reported in ppm downfield from tetramethylsilane and referenced to carbon resonances in the NMR solvent ($CDCl_3$, δ = 77.0, center line; CD_3CN, δ = 1.30, center line, acetone-d_6 δ = 29.80, center line) or to added tetramethylsilane (δ = 0.00). Carbons bearing boron substituents were not observed (quadrupolar relaxation). ^{11}B NMR were recorded using a General Electric GN300WB instrument and referenced to an external standard of ($BF_3 \cdot Et_2O$). High resolution mass spectra (HRMS) were performed by Furong Sun and Dr. Steve Mullen at the University of Illinois School of Chemical Sciences Mass Spectrometry Laboratory. Infrared spectra were collected from a thin film on NaCl plates or as KBr pellets on a Perkin-Elmer Spectrum BX FT-IR spectrometer, a Mattson Galaxy Series FT-IR 5000 spectrometer or a Mattson Infinity Gold FT-IR spectrometer. Absorption maxima (ν_{max}) are reported in wavenumbers (cm^{-1}). X-ray crystallographic analysis of **2.19** was carried out by Dr. Scott Wilson and Dr. Danielle Gray at the University of Illinois George L. Clark X-Ray facility.

Kinetics of boronic acid cross-coupling (Figure 2.3).

Under ambient atmosphere, to a 25 mL Schlenk flask equipped with a stir bar was added 2-dicyclohexylphosphino-2',6'-dimethoxybiphenyl (S-Phos) (41 mg, 0.10 mmol), $Pd(OAc)_2$ (11 mg, 0.050 mmol) and freshly-prepared 2-furylboronic acid (**2.4a**) (106 mg, 0.949 mmol). The flask was placed under argon atmosphere and to the flask was added dioxane (12.5 mL). To the solution was added dodecane (100 μL, internal standard) and 1-*tert*-butoxy-4-chlorobenzene (**2.13**) (175 μL, 0.980 mmol), and the solution was stirred at 23 °C for 10 minutes. The solution was sampled and analyzed by GC to determine the ratio of halide:internal standard. To the dark amber solution was added aq K_3PO_4 (3.0 M, 2.5 mL, degassed by sparging with argon for 30 min) and the dark mixture was stirred for 5 minutes. The organic phase was sampled as the initial time-point (t=0), and the mixture was then immediately placed in a 60 °C oil bath with stirring. The organic phase was sampled periodically and the consumption of the halide was determined by GC analysis versus the internal standard.

Rates of in-situ boronic acid decomposition (Figure 2.4).

A stock solution of 2-furylboronic acid (**2.4a**) and 4-bromoanisole (internal standard) in dioxane-d_8 was prepared as follows: 2-furylboronic acid (9 mg, 0.08 mmol) and 4-bromoanisole (15 mg, 0.080 mmol) were dissolved in dioxane-d_8 (1.0 mL). To each of eight argon-filled 1.5 mL vials, equipped with stir bars and sealed with PTFE-lined septum-screw caps was added the boronic acid stock solution (100 μL), followed by a solution of K_3PO_4 in D_2O (3.0 M, 20 μL) by syringe. The mixtures were maintained, with stirring at 60 °C for the specified time (10 min, 20 min, 30 min, 1 h, etc.) The mixtures were then immediately quenched by the addition of a solution of pH 7 potassium phosphate buffer in D_2O (2M, 120 μL) allowed to cool to 23 °C and diluted with DMSO-d_6 (0.5 mL, containing TMS internal standard). The resulting solutions were immediately analyzed by ^{1}H-NMR. The percent boronic acid remaining was calculated by comparing the ratio of the integrated 4-bromoanisole C-H signal (doublet, 7.41 ppm) to that of the boronic acid C-H signal (doublet, 7.74 ppm).

Rates of slow-release of boronic acids from MIDA boronates (Figures 2.5-2.7).

Stock solutions of the MIDA boronate and 4-bromoanisole (internal standard) in dioxane-d_8 were prepared as follows: 4-tolyl MIDA boronate[Error! Bookmark not defined.] (16 mg, 0.064 mmol) and 4-bromoanisole (12 mg, 0.065 mmol) were dissolved in dioxane-d_8 (800 μL); 2-furyl MIDA boronate (**2.5a)** (54 mg, 0.24 mmol) and 4-bromoanisole (45 mg, 24 mmol) were dissolved in dioxane-d_8 (3.0 mL); vinyl MIDA boronate (**2.5g)** (11.7 mg, 0.064 mmol) and 4-bromoanisole (12 mg, 0.065 mmol) were dissolved in dioxane-d_8 (800 μL); cyclopropyl MIDA boronate (**2.5h**) (12.8 mg, 0.065 mmol) and 4-bromoanisole (12.0 mg, 0.064 mmol) were dissolved in dioxane-d_8 (800 μL). To each 1.5 mL vial equipped with a small stir bar was added the boronate stock solution (100 μL) followed by a solution of K_3PO_4 in D_2O (3.0 M, 20 μL). The mixtures were stirred at the specified temperature (23 °C, 60 °C, or 100 °C) for the specified time (0.5 h, 1.0 h, 2.0 h, etc.). The mixtures were then immediately cooled to room temperature and were diluted with CD_3CN (0.5 mL containing TMS internal standard). The solutions were immediately analyzed by ^{1}H-NMR. The percent MIDA boronate remaining was calculated by comparing the ratio of the integrated 4-bromoanisole OCH_3 singlet (3.76 ppm, internal standard) to that of the MIDA boronate NCH_3 singlet (tolyl = 2.47 ppm; furyl = 2.60 ppm; vinyl = 2.77 ppm; cyclopropyl = 2.98 ppm).

Yield of 2-pyridyl MIDA based on internal reaction temperature (Figure 2.9).

To a 25 mL Schlenk flask equipped with a stir bar was added 2-bromopyridine (0.30 mL, 3.1 mmol), triisopropylborate (0.70 mL, 3.0 mmol), and THF (6 mL). The resulting stirred solution was cooled to -78 °C. To the cooled solution was added dropwise over 5 min *n*-butyllithium (2.58 M in hexanes, 1.2 mL, 3.1 mmol). Following the addition, the reaction was stirred at -78 °C for 1 h, then warmed to 23 °C with stirring for 3 h. Separately, to a 3-neck 50 mL flask equipped with a 25 mL pressure equalizing addition funnel, a water-cooled short-path distillation apparatus, a thermometer, and a stir bar was added *N*-methyiminodiacetic acid (0.75 g, 5.1 mmol) and DMSO-d_6 (6 mL). The mixture was heated with stirring to the internal temperature as indicated (25 °C, 40 °C, 55 °C, 70 °C, 85 °C, 100 °C, 115 °C, or 130 °C). The borate mixture contained in the Schlenk flask was transferred to the addition funnel, washing with THF (6 mL). To the hot, stirred DMSO solution was added dropwise the borate solution at a rate necessary to maintain the internal temperature ± 5 °C from the indicated temperature (ca. 30 min.). Following the addition, the mixture was cooled to room temperature. Where necessary, residual THF was removed in vacuo. To the DMSO-d_6 solution was added 4-bromoanisole (0.190 mL, internal standard). The mixture was filtered through a short pad of Celite and the filtrate was then analyzed by ^{1}H-NMR to find the yield of **2.18** as determined by reference to the internal standard. Specifically, the H_3C-N resonance of **2.18** at 2.53 ppm was compared to the aromatic resonance of 4-bromoanisole at 6.88 ppm.

Syringe pump addition of boronic acid (Scheme 2.4).

Under ambient atmosphere, to a 40 mL I-Chem vial equipped with a stir bar was added 1-*tert*-butoxy-4-chlorobenzene (**2.13**) (0.185 g, 1.00 mmol), dicyclohexylphosphino-2',6'-dimethoxy-1,1'-biphenyl (S-Phos) (41 mg, 0.10 mmol) and $Pd(OAc)_2$ (11 mg, 0.050 mmol). The vial was sealed with a PTFE-lined septum screw-cap, and then placed under an argon atmosphere. To the vial was added dioxane (9.5 mL) and the resulting mixture was stirred at 23 °C for 10 min. To the vial was added aq K_3PO_4 (3.0 M, 2.5 mL, degassed by sparging with argon for 30 min). The vial was placed in a 60 °C oil bath, and to the stirring mixture was added dropwise over 3 h via syringe pump freshly prepared 2-furylboronic acid (**2.4a**) (0.112 g, 1.00 mmol) as a solution in dioxane (3.0 mL). After the addition was complete, the reaction mixture was stirred at 60 °C for an additional 3 h. The mixture was cooled to room temperature and was

then transferred to a 60 mL separatory funnel and was diluted with aq NaOH (1.0 M, 10 mL). The mixture was extracted with Et_2O (3 × 10 mL). The combined organic fractions were dried over $MgSO_4$, filtered and then concentrated in vacuo. The resulting residue was purified by flash chromatography (hexanes:EtOAc, 100:0 → 9:1) to afford a colorless oil (0.213 g, 98%). (see 2.3 for characterization of product).

Benchtop stability of boronic acids and MIDA boronates (Table 2.1).

To quantify the stability of boronic acids or MIDA boronates to storage on the benchtop as solids under air at 23 °C, the following general procedure was followed: Two 7-mL vials were charged with 10 mg of freshly prepared boronic acid or MIDA boronate at 23 °C under ambient. The vials containing these solid samples were then sealed with PTFE-lined screw caps under ambient atmosphere and placed on the benchtop at 23 ºC. The solid sample present in one of the two vials was then immediately analyzed via ^{1}H NMR to verify the purity and quantity of boronic acid present at time zero (see below for details of NMR assay). After 15 days (boronic acids) or 60 days (MIDA boronates), the solid sample in the second vial was then analyzed via ^{1}H NMR, again by the method described below, to determine the quantity of boronic acid remaining at the indicated time. The NMR assay was performed as follows: An NMR stock solution was prepared as follows: To a 25 mL volumetric flask was added bromoacetophenone (0.336 g, 1.69 mmol) as an internal standard for quantification of the boronic acid, tetramethylsilane (1 mL) as an internal standard for the NMR shifts, and DMSO-d_6:D_2O 95:5 to a final solution volume of 25.00 mL. To a vial containing solid boronic acid or solid MIDA boronate (see above) was added 1.00 mL of this NMR stock solution, and the resulting solution was analyzed by ^{1}H NMR. The mmol of boronic acid or MIDA boronate present in the sample was determined by comparing the ratio of the integrated 4-bromoacetophenone aryl C–H doublets (7.90 ppm relative to TMS) to that of the boronic acid or MIDA boronate C–H signals.

Synthesis of MIDA boronates (Table 2.1).

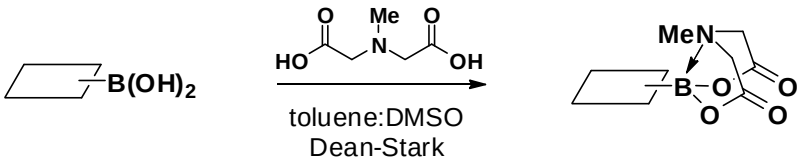

General procedure for the synthesis of MIDA boronates. To a round-bottom flask equipped with a stir bar was added the boronic acid (1 equiv), *N*-methyliminodiacetic acid (1-1.5 equiv), DMSO and either toluene or benzene. The flask was fitted with a Dean-Stark trap and the Dean-Stark trap was fitted with a reflux condenser vented to ambient atmosphere. The stirred mixture was heated to reflux with azeotropic removal of water for 2-18 h. The solution was concentrated in vacuo (1 Torr, 100 °C). Unless otherwise noted, the resulting residue was adsorbed onto Celite in vacuo from an acetone suspension and the resulting powder was subjected to flash chromatography ($Et_2O \rightarrow Et_2O$:MeCN).

2-furyl MIDA boronate (**2.5a**). The general procedure was followed using furan-2-boronic acid (5.029 g, 44.95 mmol, purchased from Sigma-Aldrich), *N*-methyliminodiacetic acid (7.275 g, 49.44 mmol), toluene (210 mL) and DMSO (40 mL). The mixture was refluxed for 8 h. The product was eluted with $Et_2O \rightarrow Et_2O$:acetone 1:1. The solid thus obtained was dissolved in a minimum of acetone to which Et_2O was slowly added to promote crystallization. Filtration of the mixture afforded **2.5a** as an off-white crystalline solid (8.98 g, 90%).

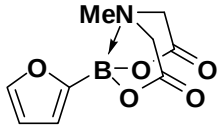

2.5a

TLC (EtOAc)

R_f = 0.33, stained with $KMnO_4$

^{1}H-NMR (500 MHz, CD_3CN)

δ 7.66 (dd, *J* = 2.0, 1.0 Hz, 1H), 6.71 (dd, *J* = 3.0, 1.0 Hz, 1H), 6.43 (dd, *J* = 3.0, 2.0 Hz, 1H), 4.06 (d, *J* = 17 Hz, 2H), 3.89 (d, *J* = 17 Hz, 2H), 2.60 (s, 3H)

^{13}C-NMR (125 MHz, CD_3CN)

δ 169.2, 147.0, 119.1, 110.8, 62.4, 47.9

^{11}B-NMR (96 MHz, CH_3CN)

δ 9.5

HRMS (EI+)

Calculated for $C_9H_{10}BNO_5$ $(M)^+$: 223.0652

Found: 223.0651

IR (thin film, cm^{-1})

3136, 3109, 3002, 2990, 2962, 1751, 1570, 1481, 1457, 1419, 1346, 1336, 1302, 1245, 1227, 1197, 1153, 1085, 1057, 1004, 965, 932, 873, 839, 828, 823

2-benzofuranyl MIDA boronate (**2.5b**). The general procedure was followed using benzofuran-2-boronic acid (5.247 g, 32.39 mmol, purchased from Sigma-Aldrich), *N*-methyliminodiacetic acid (5.005 g, 34.02 mmol), toluene (135 mL) and DMSO (15 mL). The mixture was refluxed for 8 h. The product was eluted with Et_2O → Et_2O:MeCN 2:1. The solid thus obtained was dissolved in a minimum of acetone to which Et_2O was slowly added to promote crystallization. Filtration of the mixture afforded **2.5b** as a colorless crystalline solid (7.61 g, 86%).

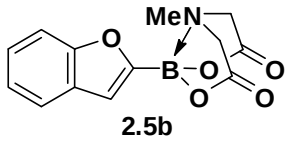

2.5b

TLC (EtOAc)

R_f = 0.45, visualized by UV (λ = 254 nm) and $KMnO_4$ stain

^{1}H-NMR (500 MHz, CD_3CN)

δ 7.63 (app dq, *J* = 7.5, 1.0 Hz, 1H), 7.51 (app. dt, *J* = 8.5, 1.0 Hz, 1H), 7.30 (m, 1H), 7.22 (app tt, *J* = 7.5, 0.5 Hz, 1H), 7.11 (s, 1H), 4.14 (d, *J* = 17 Hz, 2H), 3.97 (d, *J* = 17 Hz, 2H), 2.69 (s, 3H)

^{13}C-NMR (125 MHz, CD_3CN)

δ 169.2, 158.2, 129.1, 125.7, 123.6, 122.4, 115.8, 112.2, 62.6, 48.1

^{11}B-NMR (96 MHz, CD_3CN)

δ 9.5

HRMS (EI+)

Calculated for $C_{13}H_{12}BNO_5$ $(M)^+$: 273.0809

Found: 273.0810

IR (thin film, cm^{-1})

3008, 2956, 1765, 1560, 1448, 1335, 1282, 1249, 1191, 1157, 1138, 1052, 1005, 942, 853

2-thiophenyl MIDA boronate (**2.5c**). The general procedure was followed using thiophene-2-boronic acid (4.871 g, 38.06 mmol, purchased from Sigma-Aldrich), *N*-methyliminodiacetic acid (5.884 g, 39.99 mmol), benzene (180 mL) and DMSO (20 mL). The mixture was refluxed for 8 h. The product was eluted with Et_2O → Et_2O:MeCN 2:1. The solid thus obtained was dissolved in a minimum of acetone to which Et_2O was slowly added to promote crystallization. Filtration of the mixture afforded **2.5c** as a colorless crystalline solid (7.13 g, 78%).

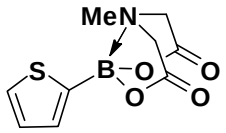

2.5c

TLC (EtOAc)

R_f = 0.34, visualized by UV (λ = 254 and 366 nm) and $KMnO_4$ stain

^{1}H-NMR (500 MHz, CD_3CN)

δ 7.62 (dd, *J* = 5.0, 1.0 Hz, 1H), 7.28 (dd, *J* = 3.5, 1.0 Hz, 1H), 7.19 (dd, *J* = 5.0, 3.5 Hz, 1H), 4.07 (d, *J* = 17 Hz, 2H), 3.90 (d, *J* = 18 Hz, 2H), 2.58 (s, 3H)

^{13}C-NMR (125 MHz, CD_3CN)

δ 169.1, 134.2, 130.7, 129.5, 62.4, 48.3

^{11}B-NMR (96 MHz, CD_3CN)

δ 11.2

HRMS (EI+)

Calculated for $C_9H_{10}BNO_4S$ $(M)^+$: 239.0424

Found: 239.0432

IR (thin film, cm^{-1})

3007, 2954, 1773, 1704, 1514, 1457, 1421, 1337, 1285, 1226, 1172, 1029, 979, 894, 860, 814, 713

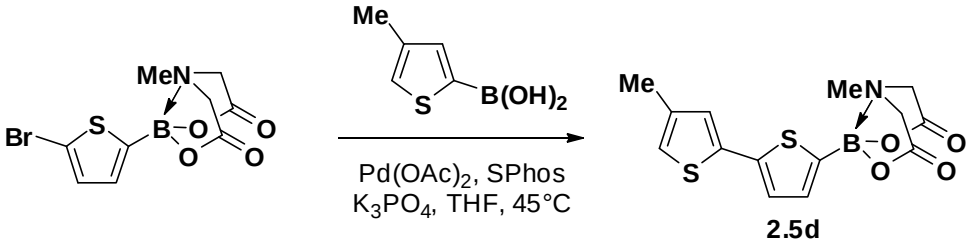

2.5d

bis-thiophenyl MIDA boronate (**2.5d**)**.**

Preparation of catalyst stock solution: In a glove box, to a 40 mL vial equipped with a stir bar was added $Pd(OAc)_2$ (0.137 g, 0.610 mmol), dicyclohexylphosphino-2',6'-dimethoxy-1,1'-biphenyl (S-Phos) (0.502 g, 1.22 mmol) and THF (25 mL). The solution was stirred for 30 minutes upon which the color of the solution changed from orange to yellow.

Cross-coupling reaction: To a 500 mL two-neck flask equipped with a stir bar was added 2-bromothiophene-5-MIDA boronate ester[3] (4.862 g, 15.29 mmol), 4-methylthiophene-2-boronic acid (4.808 g, 30.58 mmol) and K_3PO_4 (anhydrous, finely ground, 9.739 g, 45.89 mmol). The flask was fitted with a reflux condenser and the second arm was fitted with a rubber septum. The flask was placed under argon atmosphere and to the flask was added THF (150 mL). To the flask was added via cannula the catalyst stock solution (25 mL). The mixture was heated to 45 °C with stirring for 12 h. The mixture was cooled to room temperature and then was filtered through a thin pad of silica gel eluting with a copious volume of MeCN. The filtrate was concentrated in vacuo and the crude residue was adsorbed onto Celite from an acetone solution. The resulting powder was subjected to flash chromatography on silica gel (Et_2O, then Et_2O:MeCN 2:1) to afford a green foam, which was further purified by dissolving the product in a minimum of

acetone followed by slow addition of Et_2O to promote crystallization. Filtration of the resulting mixture afforded **2.5d** as a pale green solid (3.744 g, 73%).

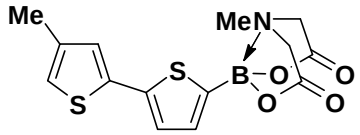

2.5d

TLC (EtOAc)

R_f = 0.38, visualized by UV (λ = 254 and 366 nm) and $KMnO_4$ stain

^{1}H-NMR (500 MHz, CD_3CN)

δ 7.24 (d, *J* = 3.5 Hz, 1H), 7.17 (d, *J* = 3.5 Hz, 1H), 7.09 (d, *J* = 1.5 Hz, 1H), 6.91 (app quint, *J* = 1.0 Hz, 1H), 4.07 (d, *J* = 17 Hz, 2H), 3.91 (d, *J* = 17 Hz, 2H), 2.66 (s, 3H), 2.22 (d, *J* = 1.0 Hz, 3H)

^{13}C-NMR (125 MHz, CD_3CN)

δ 169.1, 142.5, 139.8, 137.6, 135.3, 127.3, 125.9, 121.2, 62.4, 48.4, 15.7

^{11}B-NMR (96 MHz, CD_3CN)

δ 10.9

HRMS (EI+)

Calculated for $C_{14}H_{14}BNO_4S_2$ $(M)^+$:	335.0457
Found:	335.0457

IR (thin film, cm^{-1})

3004, 2953, 1773, 1453, 1419, 1336, 1285, 1231, 1193, 1169, 1037, 980, 858, 806

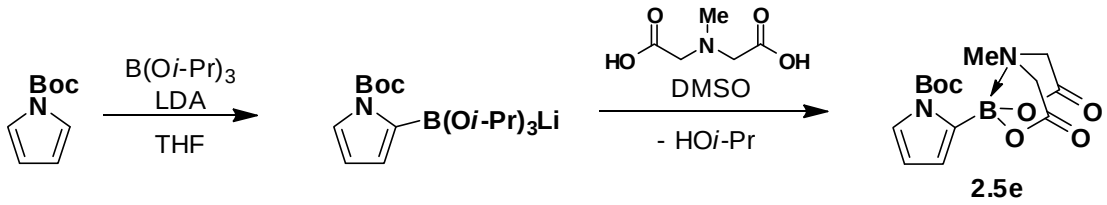

2.5e

2-(N-*tert*-butoxycarbonyl)pyrrole MIDA boronate (**2.5e**). In an unoptimized procedure, to a 50 mL Schlenk flask equipped with a stir bar was added THF (15 mL) and diisopropylamine (920 μL). The solution was cooled to -78 °C and then to the stirred solution was added dropwise *n*-BuLi (2.5 M in hexanes, 2.75 mL). The solution was maintained at -78 °C for 10 min, and then was allowed to warm to room temperature with stirring for 3 h. The solution was cooled to -78 °C, and to the stirred solution was added dropwise via cannula N-*tert*-butoxycarbonylpyrrole (1.016 g, 6.074 mmol) as a solution in THF (15 mL + 10 mL washing). The solution was stirred for 30 min. To the yellow solution was added dropwise triisopropylborate (1.40 mL, 6.07 mmol). The solution was stirred for 10 min at -78 °C and then was allow to warm to room temperature with stirring overnight (11 h). To the near-black solution was added DMSO (15 mL). The THF was then removed in vacuo and the resulting DMSO solution was transferred to a 50 mL pressure-equalizing addition funnel. The funnel was fitted onto a 100 mL 3-neck round-bottom flask charged with *N*-methyliminodiacetic acid (1.407 g, 9.563 mmol) and DMSO (20 mL). To a second neck was fitted a short-path distillation apparatus connected to vacuum. The third neck of the flask was sealed with a septum. The system was placed under vacuum (1 Torr) and the mixture was heated to 75 °C upon which the DMSO began to distill. The DMSO solution of lithium triisopropyl 2-(N-*tert*-butoxycarbonyl)pyrrole borate was added to the distilling mixture dropwise over 1 h. The mixture was further distilled to near dryness (1 h). The resulting residue was suspended in acetone and concentrated in vacuo onto Celite (10 g). The resulting powder was lyophilized for one day to remove additional DMSO and then was subjected to flash chromatography on silica gel (Et_2O:MeCN, 100:0 → 80:20) to afford **2.5e** as an off-white crystalline solid (565 mg, 29%).

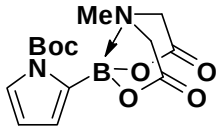

2.5e

TLC (EtOAc)

R_f = 0.35 stained with $KMnO_4$

^{1}H-NMR (500 MHz, CD_3CN)

δ 7.38 (dd, *J* = 3.0, 1.5 Hz, 1H), 6.61 (dd, *J* = 3.0, 1.5 Hz, 1H), 6.20 (t, *J* = 3.0 Hz, 1H), 4.09 (d, *J* = 17 Hz, 2H), 4.05 (d, 17 Hz, 2H), 2.79 (s, 3H), 1.54 (s, 9H)

^{13}C-NMR (125 MHz, CD_3CN)

δ 169.9, 151.2, 126.2, 124.9, 112.1, 84.9, 65.9, 49.9, 28.0

^{11}B-NMR (96 MHz, CD_3CN)

δ 11.1

HRMS (ESI+)

Calculated for $C_{14}H_{20}BN_2O_6$ $(M+H)^+$: 323.1414

Found: 323.1414

IR (KBr, cm^{-1})

3174, 3118, 3012, 2982, 2941, 1743, 1457, 1337, 1304, 1296, 1253, 1235, 1146, 1027, 1008, 815, 747

1-(Phenylsulfonyl)-2-indole MIDA boronate (**2.5f**). The general procedure was followed using 1-(phenylsulfonyl)-2-indoleboronic acid (1.396 g, 4.64 mmol, purchased from Sigma-Aldrich), *N*-methyliminodiacetic acid (0.717 g, 4.88 mmol), toluene (30 mL) and DMSO (15 mL). The mixture was refluxed for 3 h. The mixture was cooled to room temperature and the toluene was removed in vacuo. The resulting DMSO solution was transferred to a separatory funnel and was diluted with H_2O (50 mL). The aqueous phase was extracted with THF:Et_2O (1:1, 3 × 25 mL).

The combined organics were washed with brine (2 × 25 mL), dried over $MgSO_4$, filtered and concentrated in vacuo. The residue was adsorbed onto Celite from an acetone solution and the resulting powder was subjected to flash chromatography on silica gel (Et_2O:MeCN 100:0 → 2:1) to afford **2.5f** as a colorless crystalline solid (1.326 g, 69%).

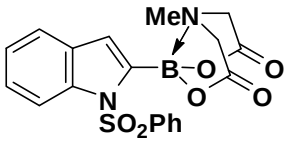

2.5f

TLC (EtOAc)

R_f = 0.42, visualized by UV (λ = 254 nm)

^{1}H-NMR (500 MHz, CD_3CN)

δ 8.18 (d, *J* = 8.5 Hz, 1H), 7.99 (d, *J* = 7.0, 2H), 7.59 (m, 2H), 7.49 (t, *J* = 8.5 Hz, 2H), 7.36 (ddd, *J* = 8.5, 7.5, 1.5 Hz, 1H), 7.26 (app. td, *J* = 7.0, 1.0 Hz, 1H), 7.16 (d, *J* = 0.5 Hz, 1H), 4.16 (d, *J* = 18 Hz, 2H), 4.11 (d, *J* = 18 Hz, 2H), 3.00 (s, 3H)

^{13}C-NMR (125 MHz, CD_3CN)

δ 140.4, 139.7, 135.3, 131.3, 130.4, 127.8, 126.6, 124.8, 123.8, 122.6, 115.7, 65.9, 50.7

^{11}B-NMR (96 MHz, CD_3CN)

δ 10.9

HRMS (EI+)

Calculated for $C_{19}H_{17}O_6N_2SB$ $(M)^+$: 412.0900

Found: 412.0897

IR (KBr, cm^{-1})

3068, 3014, 1769, 1528, 1469, 1448, 1363, 1340, 1299, 1228, 1176, 1124, 1091, 1042, 1010, 966, 865, 750, 727, 686, 656, 589, 573, 561

cyclopropyl MIDA boronate (**2.5h**). The general procedure was followed using cyclopropyl boronic acid (5.139 g, 59.82 mmol, purchased from Oakwood Products), *N*-methyliminodiacetic acid (10.56 g, 71.79 mmol), DMSO (20 mL) and toluene (20 mL). The mixture was refluxed for 2 h. The mixture was cooled to room temperature and then was concentrated in vacuo (1 Torr, 100 °C). Although the product is stable to chromatography, for convenience the purification step was modified to employ crystallization. The residue oil was suspended in EtOAc (500 mL) and was transferred to a 2 L separatory funnel. The mixture was washed with water (250 mL). The aqueous phase was extracted with EtOAc (3 × 250 mL). The combined organics were washed with brine (50 mL) and then were dried over $MgSO_4$, filtered, and concentrated in vacuo. The resulting crude product was dissolved in acetone (app. 100 mL), and then was diluted slowly over 1 h with Et_2O (1.5 L) to promote crystallization of the product. The mixture was filtered to isolate **2.5h** as a colorless, crystalline solid (8.775 g, 74%).

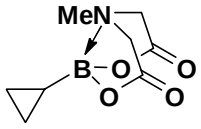

2.5h

TLC (EtOAc)

R_f = 0.21, stained with $KMnO_4$

^{1}H-NMR (500 MHz, CD_3CN)

δ 3.92 (d, *J* = 17 Hz, 2H), 3.80 (d, *J* = 17 Hz, 2H), 2.98 (s, 3H), 0.46 (dq, *J* = 9.5, 3.0 Hz, 2H), 0.12 (m, 2H), -0.33 (m, 1H)

^{13}C-NMR (125 MHz, acetone-d_6)

δ 169.0, 62.7, 46.8, 1.2

^{11}B-NMR (96 MHz, CD_3CN)

δ 13.2

HRMS (FAB+)

Calculated for $C_8H_{13}BNO_4$ $(M+H)^+$: 198.0938

Found: 198.0937

IR (thin film, cm^{-1})

2998, 1744, 1457, 1358, 1337, 2197, 1246, 1129, 1048, 985, 956, 892, 880, 845, 704

Synthesis of boronic acids (Table 2.1).

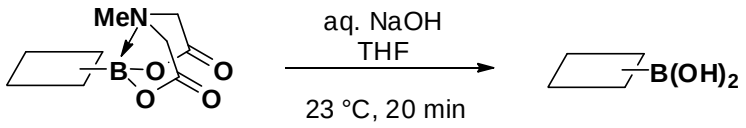

General Procedure for the synthesis of boronic acids. Under ambient atmosphere, to a 100 mL flask equipped with a stir bar and charged with MIDA boronate (**2.5**) (5 mmol) as a solution in THF (50 mL) was added aq NaOH (1.0 M, 15 mL). The mixture was vigorously stirred for 20 min. The mixture was then transferred to a separatory funnel and was diluted with Et_2O (50 mL) and 0.5 M pH 7 sodium phosphate buffer (50 mL). The mixture was shaken, and the phases were separated. The aqueous phase was extracted with THF:Et_2O (1:1, 2 × 25 mL). The combined organics were dried over $MgSO_4$, filtered and concentrated in vacuo. Residual solvent was co-evaporated with MeCN, and the resulting solid was placed under vacuum (~1 Torr) for 30 min. All boronic acids thus obtained were judged to be >95% pure by ^{1}H-NMR (See accompanying ^{1}H NMR spectra) and were utilized in cross-coupling reactions immediately after preparation.

Boronic acid 2.4a. The general procedure was followed using MIDA boronate **2.5a** (1.127 g, 5.002 mmol) to yield the **2.4a** as an off white solid (0.531 g, 95%).

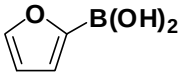

2.4a

TLC (EtOAc)

R_f = 0.46, stained with $KMnO_4$

^{1}H-NMR (500 MHz, DMSO-d_6:D_2O 95:5 w/ TMS)

δ 7.81 (dd, *J* = 1.5, 0.5 Hz, 1H), 7.07 (dd, *J* = 3.0, 0.5 Hz, 1H), 6.48 (dd, *J* = 3.5, 2.0 Hz, 1H)

^{13}C-NMR (125 MHz, DMSO-d_6:D_2O 95:5 w/ TMS)

δ 146.4, 121.5, 110.3

HRMS (EI+)

Calculated for $C_4H_5O_3B$ $(M)^+$:	112.0332
Found:	112.0332

^{1}H NMR Spectrum of **2.4a**

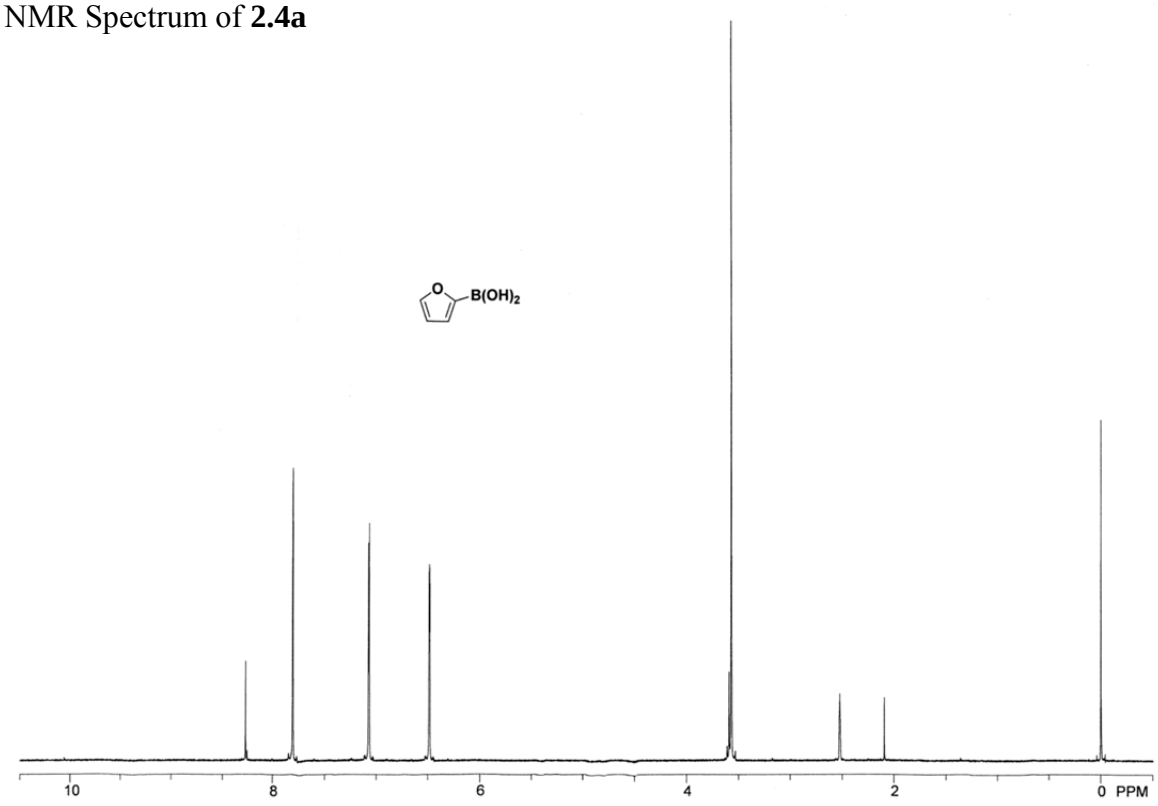

Boronic acid 2.4b. The general procedure was followed using MIDA boronate **2.5b** (1.374 g, 5.033 mmol) to yield **2.4b** as an off white solid (0.728 g, 89%).

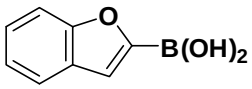

2.4b

TLC (EtOAc)

R_f = 0.14, visualized by UV (λ = 254 and 366 nm) and $KMnO_4$ stain

^{1}H-NMR (500 MHz, DMSO-d_6:D_2O 95:5 w/ TMS)

δ 7.71 (d, *J* = 8.0 Hz, 1H), 7.60 (d, *J* = 8.5 Hz, 1H), 7.50 (s, 1H), 7.37 (t, *J* = 8.0 Hz, 1H), 7.26 (t, *J* = 7.5 Hz, 1H)

^{13}C-NMR (125 MHz, DMSO-d_6:D_2O 95:5 w/ TMS)

δ 156.4, 127.6, 125.3, 122.5, 121.8, 117.5, 111.4

^{1}H NMR Spectrum of **2.4b**

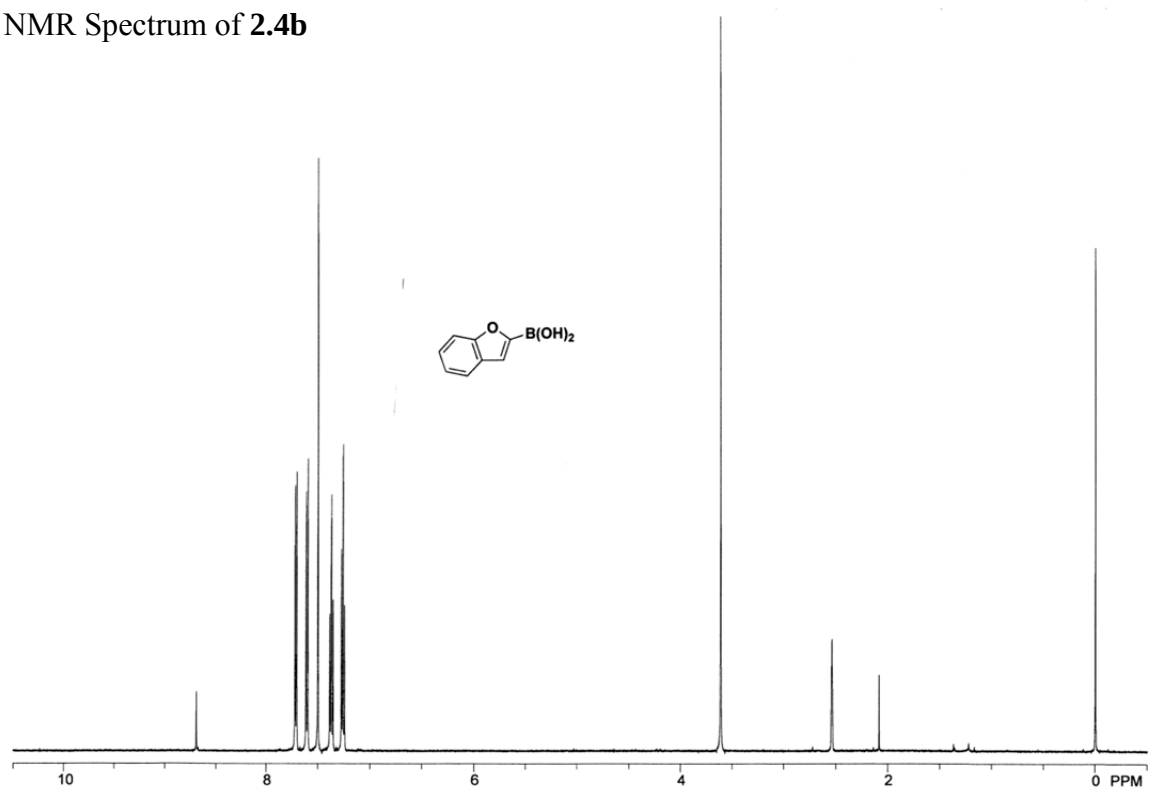

Boronic acid 2.4c. The general procedure was followed using MIDA boronate **2.5c** (1.207 g, 5.048 mmol) to yield **2.4c** as a white solid (0.641 g, 99%).

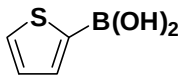

2.4c

TLC (EtOAc)

R_f = 0.23, visualized by UV (λ = 254 nm) and $KMnO_4$ stain

^{1}H-NMR (500 MHz, DMSO-d_6:D_2O 95:5 w/ TMS)

δ 7.75 (d, *J* = 5.0 Hz, 1H), 7.69 (d, *J* = 3.5 Hz, 1H), 7.18 Hz (app t, *J* = 4.0 Hz, 1H)

^{13}C-NMR (125 MHz, DMSO-d_6:D_2O 95:5 w/ TMS)

δ 135.9, 131.5, 128.1

^{1}H NMR Spectrum of **2.4c**

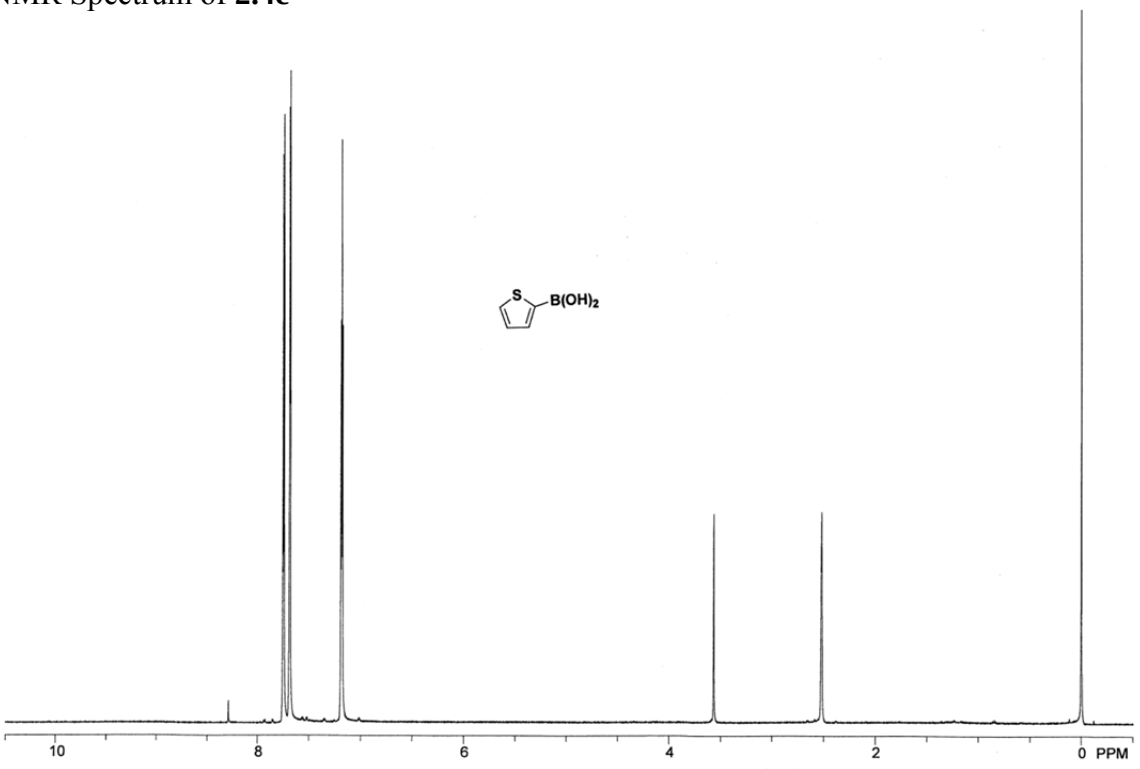

Boronic acid 2.4d. The general procedure was followed using MIDA boronate **2.5d** (1.099 g, 3.277 mmol) and aq NaOH (1.0 M, 10 mL) to yield **2.4d** was as a green solid (0.667 g, 91%).

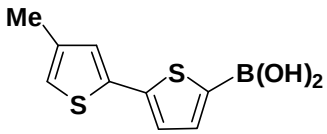

2.4d

TLC (EtOAc)

R_f = 0.34, visualized by UV (λ = 254 and 366 nm) and $KMnO_4$ stain

^{1}H-NMR (500 MHz, DMSO-d_6:D_2O 95:5 w/ TMS)

δ 7.59 (d, *J* = 3.5 Hz, 1H), 7.29 (d, *J* = 3.5 Hz, 1H), 7.17 (d, *J* = 1.0 Hz, 1H), 7.08 (s, 1H), 2.22 (s, 3H)

^{13}C-NMR (125 MHz, DMSO-d_6:D_2O 95:5 w/ TMS)

δ 142.0, 138.3, 137.0, 136.3, 126.3, 124.6, 120.6, 15.3

^{1}H NMR Spectrum of **2.4d**

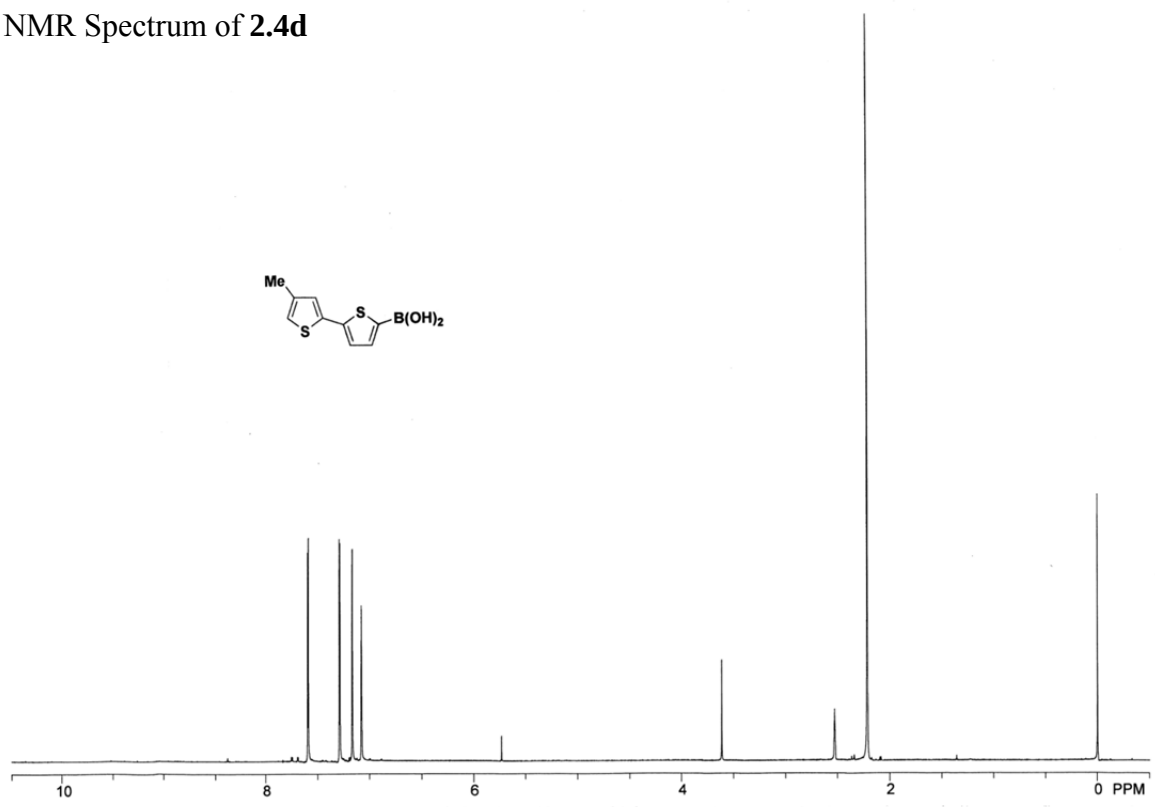

Boronic acid 2.4e. The general procedure was followed using MIDA boronate **2.5e** (0.691 g, 2.144 mmol) and aq NaOH (1.0 M, 6.5 mL). Reaction volumes were scaled accordingly. After addition of NaOH, the reaction was stirred at 23 °C for 10 min. The reaction mixture was transferred to a separatory funnel and was diluted with Et_2O (20 mL) and 1M aq NaOH (20 mL). The mixture was shaken and the organic phase was separated and discarded. The aqueous phase was diluted with THF:Et_2O (1:1, 20 mL) and saturated aq NH_4Cl (20 mL). The mixture was shaken and the phases were separated. The aqueous phase was extracted with THF:Et_2O (1:1, 2 × 10 mL). The combined organics were dried over $MgSO_4$, filtered and concentrated in vacuo to afford **1e** as a colorless solid (0.403 g, 89%).

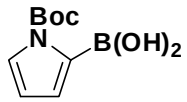

2.4e

TLC (EtOAc)

R_f = 0.50, visualized by UV (λ = 254 nm) and $KMnO_4$ stain

^{1}H-NMR (500 MHz, DMSO-d_6:D_2O 95:5 w/ TMS)

δ 7.34 (dd, *J* = 1.5 Hz, 1H), 6.46 (dd, *J* = 3.5, 2.0 Hz, 1H), 6.23 (t, *J* = 3.0 Hz, 1H), 1.54 (s, 9H)

^{13}C-NMR (125 MHz, DMSO-d_6:D_2O 95:5 w/ TMS)

δ 149.8, 123.0, 120.6, 111.7, 84.1, 27.3

^{1}H NMR Spectrum of **2.4e**

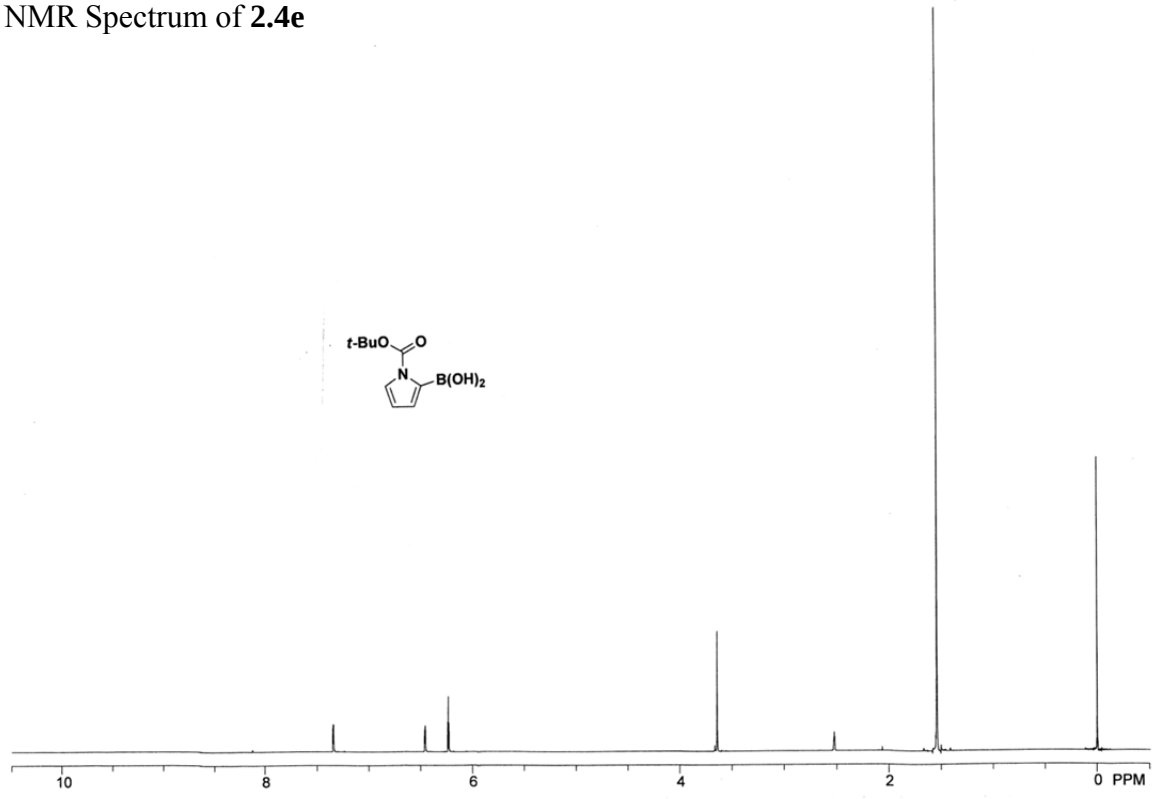

Boronic acid 2.4f. The general procedure was followed using MIDA boronate **2.5f** (1.236 g, 2.999 mmol) THF (30 mL), and aq NaOH (1.0 M, 9 mL). The mixture was stirred 5 min. The mixture was transferred to a separatory funnel and was diluted with Et_2O (30 mL) and aq NaOH (1.0 M, 30 mL). The mixture was shaken and the organic phase was separated and discarded. The aqueous phase was diluted with THF:Et_2O (1:1, 30 mL) and saturated aq NH_4Cl (30 mL). The mixture was shaken and the phases were separated. The aqueous phase was extracted with THF:Et_2O (1:1, 2 × 15 mL). The combined organics were dried over $MgSO_4$, filtered and concentrated in vacuo to afford **2f** as a pale yellow solid (584 mg, 65%).

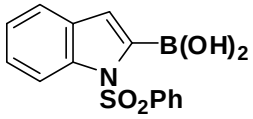

2.4f

TLC (EtOAc)

R_f = 0.53, visualized by UV (λ = 254 and 366 nm)

^{1}H-NMR (500 MHz, DMSO-d_6:D_2O 95:5 w/ TMS)

δ 8.02 (d, *J* = 7.5 Hz, 2H), 7.84 (d, *J* = 8.0 Hz, 1H), 7.65 (t, *J* = 7.5 Hz, 1H), 7.56 (t, *J* = 7.5 Hz, 3H), 7.28 (t, *J* = 7.5 Hz, 1H), 7.20 (t, *J* = 8.0 Hz, 1H), 6.81 (s, 1H)

^{13}C-NMR (125 MHz, DMSO-d_6:D_2O 95:5 w/ TMS)

δ 137.1, 135.4, 134.2, 131.1, 129.4, 126.9, 124.3, 123.3, 121.1, 114.4, 113.3

^{1}H NMR Spectrum of **2.4f**

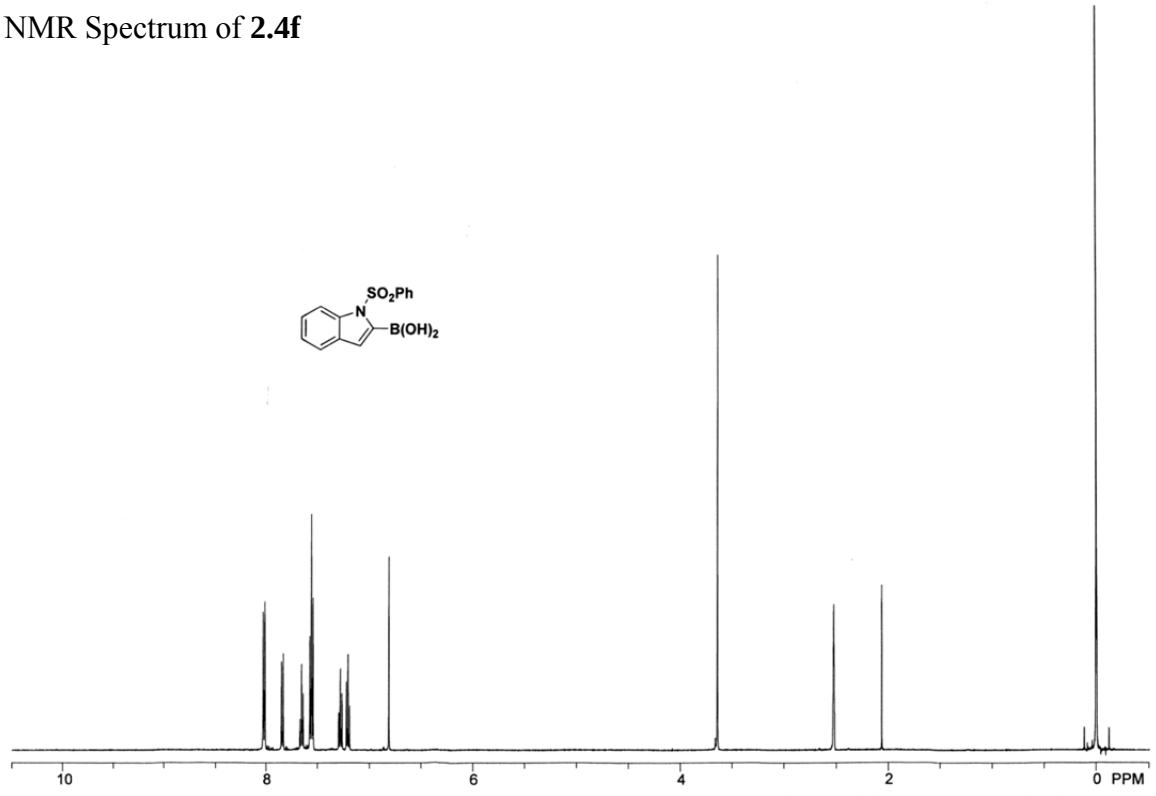

Boronic acid 2.4g. The general procedure was followed using MIDA boronate **2.5g** (0.915 g, 5.00 mmol) and aq NaOH (1.0 mL, 15 mL). Due to the volatility of the product, solvent removal was performed at 23 °C. Residual solvent was co-evaporated with CH_2Cl_2. To further remove solvent, the product was briefly (< 1 minute) placed under vacuum (~1 Torr). Boronic acid **2.4g** was isolated as a white solid (0.161 g, 45%).

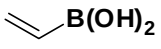

2.4g

TLC (EtOAc)

R_f = 0.31, stained with $KMnO_4$

^{1}H-NMR (500 MHz, DMSO-d_6:D_2O 95:5 w/ TMS)

δ 6.01 (dd, *J* = 19, 5.5 Hz, 1H), 5.80 (m, 2H)

^{13}C-NMR (125 MHz, DMSO-d_6:D_2O 95:5 w/ TMS)

δ 133.7

HRMS (CI+)

Calculated for $C_2H_6O_2B$ $(M+H)^+$:	73.04609
Found:	73.04602

^{1}H NMR Spectrum of **2.4g**

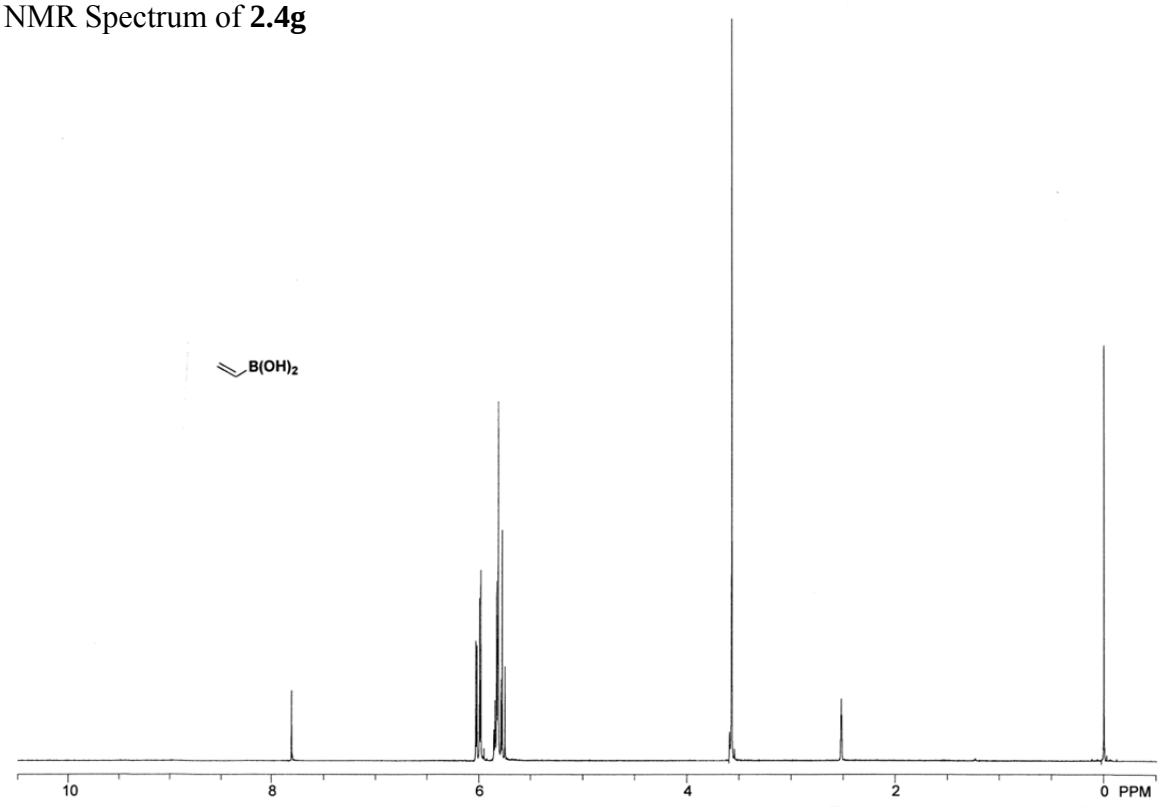

Boronic acid 2.4h. The general procedure was followed using boronate **2.5h** (0.789 g, 4.00 mmol) and aq NaOH (1.0 M, 12 mL). Reaction and workup volumes were scaled accordingly. Boronic acid **2.4h** was isolated as an off-white solid (0.183 g, 53%).

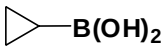

2.4h

TLC (EtOAc)

R_f = 0.22, stained with $KMnO_4$

^{1}H-NMR (500 MHz, DMSO-d_6:D_2O 95:5 w/ TMS)

δ 0.43 (m, 2H), 0.33 (m, 2H), -0.39 (m, 1H)

^{13}C-NMR (125 MHz, DMSO-d_6:D_2O 95:5 w/ TMS)

δ 3.29

^{1}H NMR Spectrum of **2.4h**

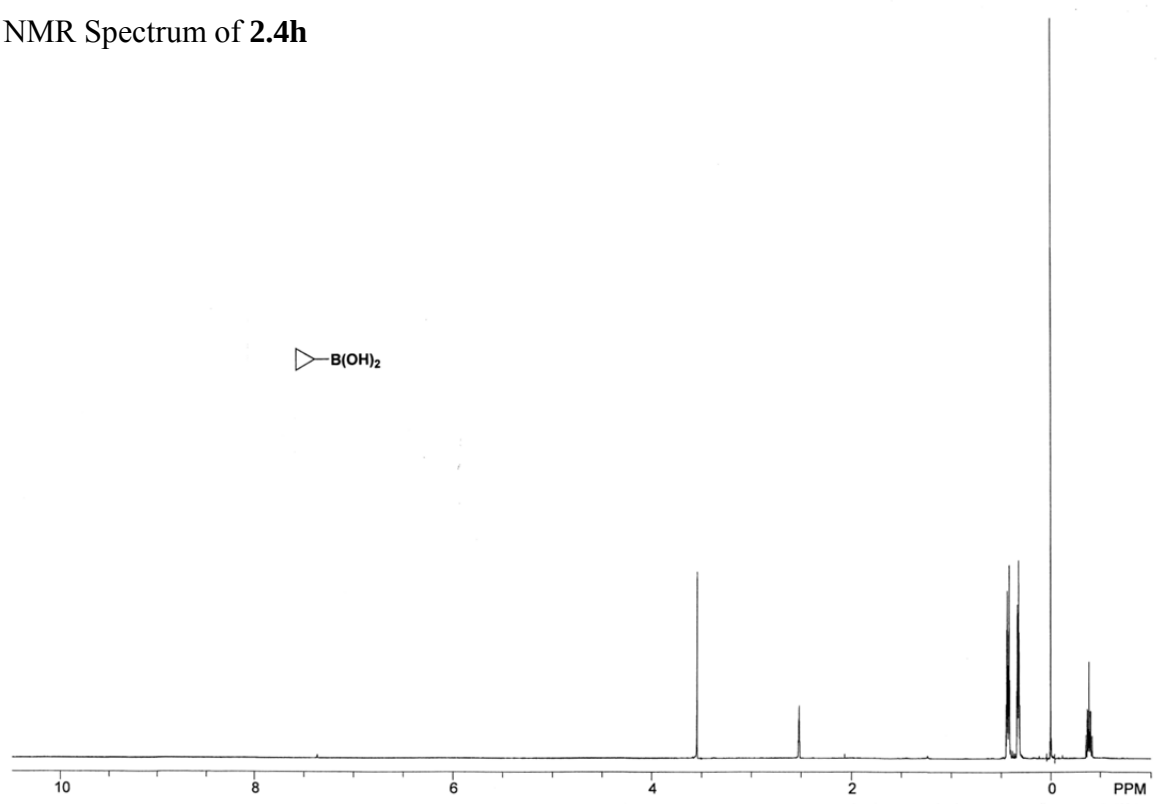

Synthesis of MIDA boronates (Table 2.2)

3-methoxyphenyl MIDA boronate (2.10b). A 500 mL flask equipped with a stir bar was charged with 3-methoxyphenylboronic acid (1.325 g, 8.72 mmol), *N*-methyliminodiacetic acid (1.290 g, 10.13 mmol), toluene (260 mL) and DMSO (26 mL). The flask was fitted with a Dean-Stark apparatus filled with toluene and a reflux condenser open to ambient atmosphere, and the mixture was refluxed with stirring for 16 h, followed by concentration in vacuo (35 °C at 20 mTorr, then 100 °C at 1 mTorr). The crude product was adsorbed onto Florisil® from an acetone solution, and the resulting powder was dry-loaded on top of a silica gel column slurry-packed with Et_2O. The column was flushed with a copious volume of Et_2O and eluted with Et_2O:MeCN 1:1 to yield the boronate ester **2.10b** as a colorless, crystalline solid (2.25 g, 98%).

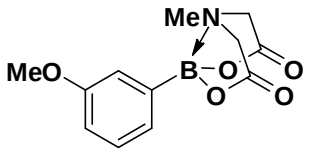

2.10b

TLC (EtOAc)

R_f = 0.33, visualized by UV (254 nm) and $KMnO_4$

^{1}H-NMR (500 MHz, CD_3CN)

δ 7.30 (ddd, J = 8.2, 7.3, 0.4, 1H), 7.03 (dt, J = 7.3, 1.2, 1H), 7.01 (dd, J = 2.5, 0.6, 1H), 6.94 (ddd, J = 8.3, 2.8, 1.1, 1H), 4.05 (d, J = 17, 2H), 3.88 (d, J = 17, 2H), 3.78 (s, 3H), 2.50 (s, 3H)

^{13}C-NMR (500 MHz, CD_3CN)

δ 169.6, 160.3, 130.2, 125.5, 118.3, 115.8, 62.8, 55.7, 48.4

^{11}B-NMR (600 MHz, CD_3CN)

δ 12.0

HRMS (EI+)

Calculated for $C_{12}H_{14}BNO_5$ $(M)^+$: 263.0965

Found: 263.0963

IR (thin film, cm^{-1})

3005, 2956, 1765, 1608, 1576, 1487, 1461, 1419, 1341, 1320, 1292, 1248, 1203, 1170, 1149, 1094, 1050, 1030, 1014, 1002, 965, 896, 861

trans-1-hexenyl MIDA boronate (2.10c). A 500 mL flask equipped with a stir bar was charged with E-hexen-1-ylboronic acid (0.457 g, 3.57 mmol), *N*-methyliminodiacetic acid (0.526 g, 3.58 mmol), toluene (63 mL) and DMSO (7 mL). The flask was fitted with a Dean-Stark apparatus filled with toluene and a reflux condenser open to ambient atmosphere. The mixture was refluxed with stirring for 18 h, followed by concentration in vacuo (35 °C at 20 mTorr, then 100 °C at 1 mTorr). The crude product was adsorbed onto Florisil® from an acetone solution, and the resulting powder was dry-loaded on top of a silica gel column slurry-packed with Et_2O. The column was flushed with a copious volume of Et_2O and eluted with Et_2O:MeCN 1:1 to yield the boronate ester **2.10c** as a colorless, crystalline solid (0.722 g, 85%).

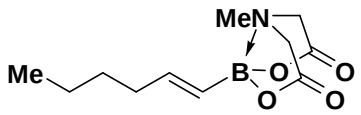

2.10c

TLC (EtOAc)

R_f = 0.37, visualized by $KMnO_4$

^{1}H-NMR (500 MHz, CD_3CN)

δ 6.06 (dt, J = 18, 6.5, 1H), 5.40 (dt, J = 18, 1.5, 1H), 3.92 (d, J = 17, 2H), 3.75 (d, J =17, 2H), 2.74 (s, 3H), 2.11 (q, J = 7.1, 2H), 1.38 (quint, J = 7.1, 2H), 1.31 (sext, J = 7.2, 2H), 0.89 (t, J = 7.3, 3H)

^{13}C-NMR (500 MHz, CD_3CN)

δ 169.5, 146.9, 62.2, 47.6, 35.8, 31.7, 22.9, 14.2.

^{11}B-NMR (600 MHz, CD_3CN)

δ 11.1

HRMS (CI+)

Calculated for $C_{11}H_{19}BNO_4$ $(M+H)^+$: 240.1407

Found: 240.1406

IR (thin film, cm^{-1})

2956, 2923, 1750, 1643, 1451, 1339, 1304, 1249, 1132, 1027, 995, 959, 867

trans-styrenyl MIDA boronate (2.10d). A 500 mL flask equipped with a stir bar was charged with trans-2-phenylvinylboronic acid (3.27 g, 22.1 mmol, 1 equiv.), *N*-methyliminodiacetic acid (3.26 g, 22.2 mmol, 1 equiv), benzene (360 mL) and DMSO (40 mL). The flask was fitted with a Dean-Stark apparatus filled with benzene and a reflux condenser open to ambient atmosphere, and the mixture was refluxed with stirring for 18 h, followed by concentration in vacuo (35 °C at 20 mTorr, then 100 °C at 1 mTorr). The crude product was adsorbed onto Florisil® from an acetone solution, and the resulting powder was dry-loaded on top of a silica gel column slurry-packed with Et_2O. The column was flushed with a copious volume of Et_2O and eluted with Et_2O:MeCN 1:1 to yield the boronate ester **2.10d** as a colorless, crystalline solid (5.50 g, 96%).

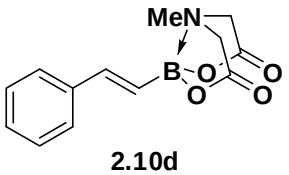

2.10d

TLC (EtOAc)

R_f =0.37, visualized by UV (254 nm) and $KMnO_4$

^{1}H-NMR (500 MHz, CD_3CN)

δ 7.52 (app. d, J = 7.6, 2H), 7.35 (app. t, J = 7.5), 7.27 (app. t, J = 7.5, 1H), 6.97 (d, J = 18, 1H), 6.30 (d, J = 18, 1H), 4.02 (d, J = 17, 2H), 3.86 (d, J = 17, 2H), 2.81 (s, 3H).

^{13}C-NMR (500 MHz, CD_3CN)

δ 169.6, 143.2, 139.0, 129.5, 129.0, 127.6, 62.4, 47.7.

^{11}B-NMR (600 MHz, CD_3CN)

δ 11.5

HRMS (EI+)

Calculated for $C_{13}H_{14}BNO_4$ $(M)^+$: 259.1016

Found: 259.1017

IR (thin film, cm^{-1})

2999, 1757, 1624, 1448, 1336, 1298, 1238, 1152, 1113, 1087, 1029, 998, 955, 874, 748, 696.

Fast-release cross-coupling of boronic acids and MIDA boronates (Table 2.2).

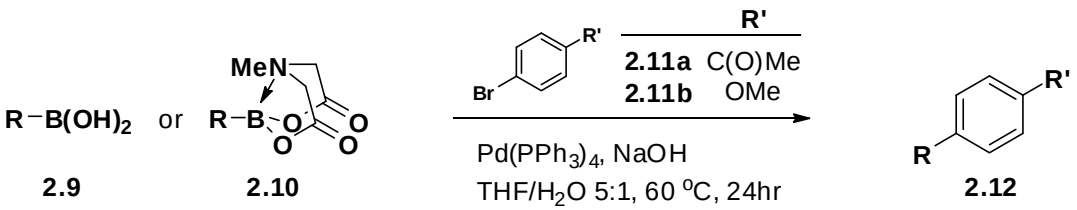

2.9 **2.10** **2.12**

General procedures for the direct coupling of boronic acids or MIDA boronate esters. To a 20 mL vial equipped with a stir bar was added the halide (1.0 mmol), solid base (7.5 mmol), and either the boronate ester (1.5 mmol) or the corresponding boronic acid (1.5 mmol). The vial was capped with a Kimwipe® and elastic band and brought into a glove box. To the vial was added 0.02 mmol $Pd(PPh_3)_4$ from a 0.02 M stock solution in THF. Additional THF was added to bring

the total solvent volume to 10.0 mL. The vial was sealed with a PTFE-lined septum-screw cap and removed from the glove box. H_2O (2 mL), degassed for 30 minutes by sparging with argon or nitrogen, was added by syringe, and the resulting biphasic mixture was maintained, with vigorous stirring, at 60°C for 24 h. The reaction mixture was allowed to cool to 23°C, and was diluted with 1M aq NaOH (10 mL) and Et_2O (10 mL). The aqueous phase was separated and extracted with Et_2O (3 × 10 mL). The combined organic fractions were washed with saturated aq NaCl (10 mL) and dried over $MgSO_4$. Solvent was removed in vacuo. The resulting crude product was purified by flash column chromatography (SiO_2).

4'-Methyl-4-acetylbiphenyl (2.12b) [Table 2.2, Entry 1]. The general procedure was followed using 4-bromoacetophenone (0.201 g, 1.01 mmol), p-tolylboronic acid (0.206 g, 1.51 mmol), and NaOH (0.307 g, 7.68 mmol). Products were eluted with hexanes:EtOAc 6:1 to yield the title compound as a white crystalline solid (0.204 g, 96%).

A parallel reaction using 4-bromoacetophenone (0.201 g, 1.01 mmol), **2.10a** (0.376 g, 1.52 mmol), and NaOH (0.305 g, 7.62 mmol) afforded the title compound as a white crystalline solid (0.204 g, 96%).

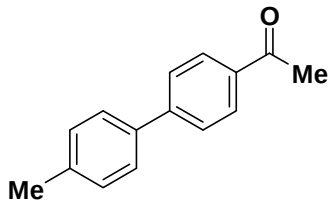

2.12a

TLC (hexanes:EtOAc 6:1)

R_f = 0.26, visualized by UV (254 nm) and $KMnO_4$

^{1}H-NMR (500 MHz, $CDCl_3$)

δ 8.02 (app. d, J = 8.4, 2H), 7.67 (app. d, J = 8.5, 2H), 7.54 (app. d, J = 8.0, 2H), 7.28 (app. d, J = 7.9), 2.64 (s, 3H), 2.41 (s, 3H)

^{13}C-NMR (500 MHz, $CDCl_3$)

δ 197.6, 145.6, 138.1, 136.8, 135.5, 129.6, 128.8, 127.0, 126.8, 26.5, 21.1

HRMS (CI+)

Calculated for $C_{15}H_{15}O$ $(M+H)^+$: 211.11230

Found: 211.11214

IR (thin film, cm^{-1})

1680, 1601, 1398, 1361, 1324, 1267, 1201, 1133, 959, 847

4'-Methoxy-4-methylbiphenyl (2.12b) [Table 2.2, Entry 2]. The general procedure was followed using 4-bromoanisole (0.188 g, 1.01 mmol), 4-tolylboronic acid (0.205 g, 1.51 mmol), and NaOH (0.302 g, 7.55 mmol). The product was eluted with a gradient of hexanes:CH_2Cl_2 3:1 → 100% CH_2Cl_2 to yield the title compound as a colorless solid (0.195 g, 98%).

A parallel reaction using 4-bromoanisole (0.188 g, 1.01 mmol), **2.10a** (0.372 g, 1.51 mmol) and NaOH (0.301 g, 7.53 mmol) conditions afforded the title compound as a colorless solid (0.189 g, 95%).

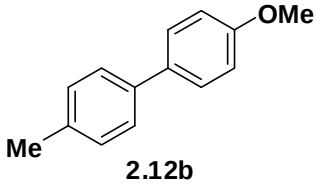

2.12b

TLC (hexanes:EtOAc 6:1)

R_f = 0.47, visualized by UV (254 nm) and $KMnO_4$

^{1}H-NMR (500 MHz, $CDCl_3$)

δ 7.52 (app. d, J = 8.8, 2H), 7.46 (app. d, J = 8.2, 2H), 7.24 (app. d, J = 7.8, 2H), 6.98 (app. d, J = 8.8, 2H), 3.86 (s, 3H), 2.39 (s, 3H)

^{13}C-NMR (500 MHz, $CDCl_3$)

δ 158.9, 137.9, 136.3, 133.7, 129.4, 127.9, 126.5, 114.1, 55.3, 21.0

HRMS (EI+)

Calculated for $C_{14}H_{14}O$ $(M)^+$: 198.1045

Found: 198.1046

IR (thin film, cm^{-1})

2957, 2836, 1608, 1502, 1288, 1269, 1252, 1183, 1038, 1012, 841, 807

4-Acetyl-3'-methoxybiphenyl (2.12c) [Table 2.2, Entry 3]. The general procedure was followed using 4-bromoacetophenone (0.200 g, 1.00 mmol), 3-methoxyphenylboronic acid (0.229 g, 1.51 mmol), and NaOH (0.303 g, 7.58 mmol). The product was eluted with hexanes:CH_2Cl_2:EtOAc 50:45:5 to yield the title compound as a clear colorless oil which crystallized under vacuum (0.222 g, 98%).

A parallel reaction using 4-bromoacetophenone (0.201 g, 1.01 mmol), **2.10b** (0.397 g, 1.51 mmol) and NaOH (0.303 g, 7.58 mmol) afforded the title compound as a clear colorless oil which crystallized under vacuum (0.219 g, 96%).

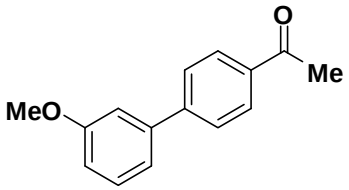

2.12c

TLC (hexanes:EtOAc 6:1)

R_f = 0.19, visualized by UV (254 nm) and $KMnO_4$

^{1}H-NMR (500 MHz, $CDCl_3$)

δ 8.03 (app. d, J = 8.3, 2H), 7.68 (app. d, J = 8.2, 2H), 7.39 (t, J = 7.8, 1H), 7.21 (app. d, J = 7.7, 1H), 7.15 (m, 1H), 6.95 (dd, J = 8.3, 2.6, 1H), 3.87 (s, 3H), 2.63 (s, 3H)

^{13}C-NMR (500 MHz, $CDCl_3$)

δ 197.4, 159.9, 145.3, 141.1, 135.7, 129.8, 128.7, 127.0, 119.5, 113.3, 112.9, 55.1, 26.4

HRMS (CI+)

Calculated for $C_{15}H_{15}O_2$ $(M+H)^+$: 227.10721

Found: 227.10732

IR (thin film, cm^{-1})

2959, 2836, 1678, 1597, 1487, 1465, 1427, 1399, 1325, 1304, 1274, 1222, 1182, 1118, 1049, 1030, 958, 831

3,4'-Dimethoxybiphenyl (2.12d) [Table 2.2, Entry 4]. The general procedure was followed using 4-bromoanisole (0.187 g, 1.00 mmol), 3-methoxyphenylboronic acid (0.228 g, 1.50 mmol), and NaOH (0.300 g, 7.50 mmol). The product was eluted with hexanes:EtOAc 6:1 to yield the title compound as a clear colorless oil (0.201 g, 94%).

A parallel reaction using 4-bromoanisole (0.188 g, 1.01 mmol), **2.10b** (0.397 g, 1.51 mmol) and NaOH (0.302 g, 7.55 mmol) afforded the title compound as a clear colorless oil (0.208 g, 96%).

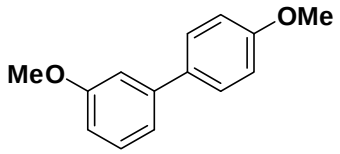

2.12d

TLC (hexanes:EtOAc 6:1)

R_f = 0.42, visualized by UV (254 nm) and $KMnO_4$

^{1}H-NMR (500 MHz, $CDCl_3$)

δ 7.57 (app. d, J = 8.7, 2H), 7.37 (t, J = 7.9, 1H), 7.19 (d, J = 7.7, 1H), 7.14 (app. s, 1H), 7.01 (app. d, J = 8.7, 2H), 6.90 (dd, J = 8.2, 2.4), 3.89 (s, 3H), 3.87 (s, 3H)

^{13}C-NMR (500 MHz, $CDCl_3$)

δ 159.9, 159.2, 142.3, 133.5, 129.7, 128.1, 119.2, 114.1, 112.5, 111.9, 55.3, 55.2

HRMS (EI+)

Calculated for $C_{14}H_{14}O_2$ $(M)^+$: 214.0994

Found: 214.0992

IR (thin film, cm^{-1})

3010, 2962, 2938, 2836, 1598, 1591, 1570, 1517, 1488, 1463, 1401, 1323, 1309, 1288, 1269, 1246, 1220, 1179, 1112, 1085, 1054, 1033, 870, 856, 828, 811

1-[4-(1E)-1-hexenylphenyl]-ethanone (2.12e) [Table 2.2, Entry 5]. The general procedure was followed using 4-bromoacetophenone (0.200 g, 1.01 mmol), E-hexen-1-ylboronic acid (0.192 g, 1.50 mmol), and NaOH (0.316 g, 7.65 mmol). The product was eluted with hexane:EtOAc 8:1 to yield the title compound as a clear colorless oil (0.183 g, 90%).

A parallel reaction using 4-bromoacetophenone (0.200 g, 1.01 mmol), **2.10c** (0.360 g, 1.51 mmol), and NaOH (0.310 g, 7.75 mmol) afforded the title compound as a clear colorless oil (0.196 g, 96%).

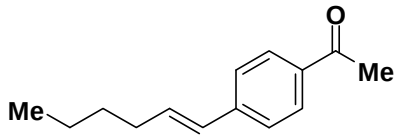

2.12e

TLC (hexanes:EtOAc 6:1)

R_f = 0.43 visualized by UV and $KMnO_4$

^{1}H-NMR (400 MHz, $CDCl_3$)

δ 7.85 (app. d, J = 8.6, 2H), 7.36 (app. d, J = 8.4, 2H), 6.35 (m, 2H), 2.53 (s, 3H), 2.21 (app. q, J = 7.0, 2H), 1.44 (quint, J = 7.1, 2H), 1.35 (sext, J = 7.3, 2H), 0.91 (t, J = 7.3, 3H)

^{13}C-NMR (500 MHz, $CDCl_3$)

δ 197.2, 142.5, 135.2, 134.3, 128.8, 128.6, 125.7, 32.7, 31.1, 26.3, 22.1, 13.8

HRMS (CI+)

Calculated for $C_{14}H_{19}O$ $(M+H)^+$: 203.14360

Found: 203.14360

trans-4-acetylstilbene (2.12f) [Table 2.2, Entry 6]. The general procedure was followed using 4-bromoacetophenone (0.201 g, 1.01 mmol), *trans*-2-phenylvinylboronic acid (0.224 g, 1.51 mmol), and NaOH (0.303 g, 7.58 mmol). The product was eluted with hexanes:CH_2Cl_2:EtOAc 75:20:5 to yield the title compound as a colorless solid. (0.198 g 88%).

A parallel reaction using 4-bromoacetophenone (0.201 g, 1.01 mmol), **2.10d** (0.392 g, 1.51 mmol) and NaOH (0.308 g, 7.70 mmol) afforded the title compound as a colorless solid. (0.214 g, 96%).

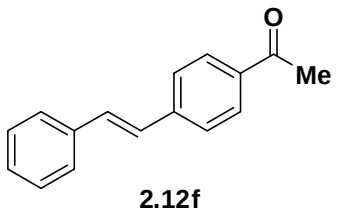

2.12f

TLC (hexanes:EtOAc 6:1)

R_f = 0.24, visualized by UV (254 and 366 nm) and $KMnO_4$

^{1}H-NMR (400 MHz, $CDCl_3$)

δ 7.96 (app. d, J = 8.4, 2H), 7.59 (app. d, J = 8.3, 2H), 7.54 (app. d, J = 7.2, 2H), 7.39 (app. t, J = 7.2, 2H), 7.31 (app. t, J = 7.2, 1H), 7.23 (d, J = 16, 1H), 7.13 (d, J = 16, 1H), 2.61 (s, 3H)

^{13}C-NMR (500 MHz, $CDCl_3$)

δ 197.4, 142.0, 136.6, 135.9, 131.4, 128.8, 128.8, 128.3, 127.4, 126.8, 126.5, 26.6

HRMS (CI+)

Calculated for $C_{16}H_{15}O$ $(M+H)^+$: 223.11230

Found: 223.11214

IR (thin film, cm^{-1})

1676, 1410, 1358, 1333, 1113, 1073, 1020, 965, 953, 867, 820

Slow-release cross-coupling of boronic acids and MIDA boronates (Table 2.3).

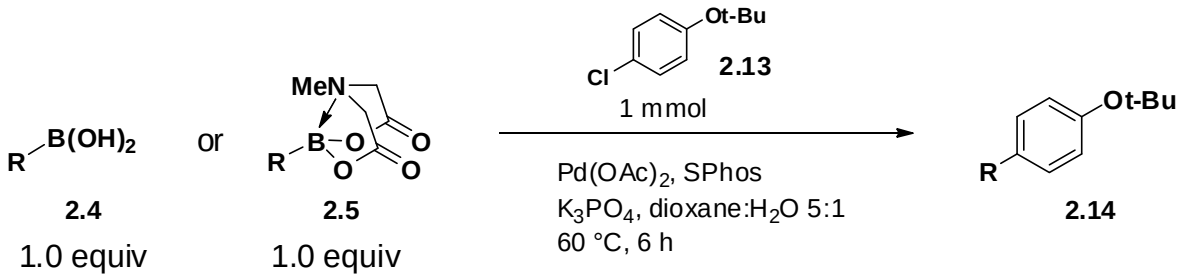

General Procedure:

Under ambient atmosphere, to a 40 mL I-Chem vial equipped with a stir bar was added 1-*tert*-butoxy-4-chlorobenzene (**2.13**) (185 mg, 1.00 mmol), the MIDA boronate or freshly-prepared boronic acid (1.00 mmol), 2-dicyclohexylphosphino-2',6'-dimethoxybiphenyl (S-Phos) (41 mg, 0.10 mmol) and $Pd(OAc)_2$ (11 mg, 0.050 mmol). The vial was sealed with a PTFE-lined septum screw-cap and was placed under argon atmosphere. To the vial was added dioxane (12.5 mL) and the resulting mixture was stirred at 23 °C for 10 min. To the vial was then added aq K_3PO_4 (3.0 M, 2.5 mL, degassed by sparging with argon for 30 min). The vial was placed in a 60 °C oil bath with stirring for 6 h. After cooling to room temperature the mixture was transferred to a 60 mL separatory funnel and was diluted with aq NaOH (1.0 M, 10 mL) and Et_2O (10 mL). The mixture was shaken and the phases were separated. The aqueous phase was extracted with Et_2O (3 × 10 mL). The combined organic fractions were dried over $MgSO_4$, filtered, and concentrated in vacuo. The crude residue was adsorbed onto Celite and the resulting powder was subjected to flash-chromatography on silica gel (hexanes:EtOAc).

2-(4-*tert*-butoxyphenyl)furan (**2.14a**) [Table 2.3, Entry 1]. The general procedure was followed using MIDA boronate **2.5a** (223 mg, 1.00 mmol) to afford **2.14a** as a colorless oil (203 mg, 94%).

A parallel reaction using freshly-prepared boronic acid **2.4a** (112 mg, 1.00 mmol) under otherwise identical conditions afforded **2.14a** as a colorless oil (147 mg, 68%).

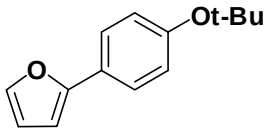

2.14a

TLC (hexanes:EtOAc 20:1)

R_f = 0.33, visualized by UV (λ = 254 nm)

^{1}H-NMR (500 MHz, $CDCl_3$)

δ 7.60 (d, *J* = 8.5 Hz, 2H), 7.45 (dd, *J* = 1.5, 0.5 Hz, 1H), 7.04 (d, *J* = 8.5 Hz, 2H), 6.58 (d, *J* = 3.0 Hz, 1H), 6.46 (dd, *J* = 3.0, 1.5 Hz, 1H), 1.38 (s, 9H)

^{13}C-NMR (125 MHz, $CDCl_3$)

δ 154.8, 153.9, 141.6, 126.3, 124.4, 124.3, 111.5, 104.0, 78.7, 28.8

HRMS (CI+)

Calculated for $C_{14}H_{16}O_2$ $(M)^+$:	216.1150
Found:	216.1151

IR (thin film, cm^{-1})

2977, 1612, 1587, 1566, 1512, 1481, 1414, 1390, 1366, 1245, 1162, 1106, 1078, 1007, 904, 895, 854, 798, 730, 667, 594

2-(4-*tert*-butoxyphenyl)benzofuran (**2.14b**) [Table 2.3, Entry 2]. The general procedure was followed using MIDA boronate **2.5b** (273 mg, 1.00 mmol) to afford **2.14b** as a colorless solid (246 mg, 92%).

A parallel reaction using freshly-prepared boronic acid **2.4b** (162 mg, 1.00 mmol) under

otherwise identical conditions afforded **2.14b** as a pale yellow solid (134 mg, 50%).

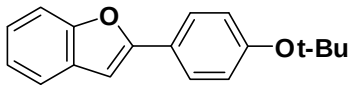

2.14b

TLC (hexanes:EtOAc 20:1)

R_f = 0.28, visualized by UV (λ = 254 nm)

^{1}H-NMR (500 MHz, $CDCl_3$)

δ 7.83 (d, *J* = 8.5 Hz, 2H), 7.62 (d, *J* = 8.0 Hz, 1H), 7.58 (d, *J* = 8.0 Hz, 1H), 7.33 (t, *J* = 7.0 Hz, 1H), 7.29 (t, *J* = 7.0 Hz, 1H), 7.14 (d, *J* = 8.5 Hz, 2H), 6.96 (s, 1H), 1.46 (s, 9H)

^{13}C-NMR (125 MHz, $CDCl_3$)

δ 156.0, 156.9, 154.7, 129.3, 125.6, 125.5, 124.1, 123.8, 122.8, 120.6, 111.0, 110.3, 78.9, 28.8

HRMS (EI+)

Calculated for $C_{18}H_{18}O_2$ $(M)^+$:	266.1307
Found:	266.1303

IR (thin film, cm^{-1})

2978, 1609, 1499, 1451, 1364, 1298, 1239, 1209, 1157, 1099, 1029, 1007, 918, 893, 853, 806, 750, 713

2-(4-*tert*-butoxyphenyl)thiophene (**2.14c**) [Table 2.3, Entry 3]. The general procedure was followed using MIDA boronate **2.5c** (239 mg, 1.00 mmol) to afford **2.14c** as a pale yellow solid (217 mg, 94%).

A parallel reaction using freshly-prepared boronic acid **2.4c** (128 mg, 1.00 mmol) under otherwise identical conditions afforded **2.14c** as a pale yellow oil (87 mg, 37%).

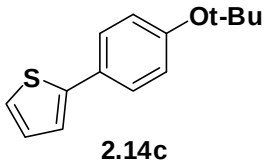

2.14c

TLC (hexanes:EtOAc (10:1)

R_f = 0.50, visualized by UV (λ = 254 nm)

^{1}H-NMR (500 MHz, $CDCl_3$)

δ 7.52 (d, *J* = 7.0 Hz, 2H), 7.24 (s, 1H), 7.23 (d, *J* =1.0 Hz, 1H), 7.06 (dd, *J* = 5.0, 4.0 Hz, 1H), 7.00 (d, *J* = 8.5 Hz, 2H), 1.37 (s, 9H)

^{13}C-NMR (125 MHz, $CDCl_3$)

δ 154.9, 144.1, 129.6, 127.9, 126.4, 124.4, 124.2, 122.4, 78.7, 28.8

HRMS (EI+)

Calculated for $C_{14}H_{16}OS$ $(M)^+$:	232.0922
Found:	232.0921

IR (thin film, cm^{-1})

2978, 1604, 1534, 1498, 1432, 1366, 1243, 1164, 1102, 922, 895, 850, 819, 694, 606, 540

5'-(4-*tert*-butoxyphenyl)-4-methyl-2,2'-bithiophene (**2.14d**) [Table 2.3, Entry 4]. The general procedure was followed using MIDA boronate **2.5d** (335 mg, 1.00 mmol) to afford **2.14d** as a yellow solid (317 mg, 96%).

A parallel reaction using freshly-prepared boronic acid **2.4d** (224 mg, 1.00 mmol) under otherwise identical conditions afforded **2.14d** as a yellow solid (158 mg, 45%; yield corrected for residual **2.13**).

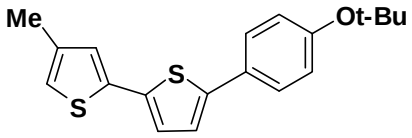

2.14d

TLC (hexanes:EtOAc 10:1)

R_f = 0.41, visualized by UV (λ = 254 and 366 nm)

^{1}H-NMR (500 MHz, $CDCl_3$)

δ 7.50 (d, *J* = 8.5 Hz, 2H), 7.14 (d, *J* = 4.0 Hz, 1H), 7.10 (d, *J* = 4.0 Hz, 1H), 7.01 (m, 3H), 6.79 (s, 1H), 2.27 (s, 3H), 1.39 (s, 9H)

^{13}C-NMR (125 MHz, $CDCl_3$)

δ 155.0, 142.6, 138.3, 137.1, 136.3, 129.2, 126.0, 125.6, 124.3, 124.2, 123.0, 119.4, 78.7, 28.7, 15.6

HRMS (EI+)

Calculated for $C_{19}H_{20}OS_2$ $(M)^+$:	328.0956
Found:	328.0958

IR (thin film, cm^{-1})

2973, 1502, 1466, 1365, 1246, 1160, 1106, 897, 850, 836, 804, 733, 717, 589, 528

N-(*tert*-butoxycarbonyl)-2-(4-*tert*-butoxyphenyl)pyrrole (**2.14e**) [Table 2.3, Entry 5]. The general procedure was followed using MIDA boronate **2.5e** (322 mg, 1.00 mmol) to afford **2.14e** as a pale yellow solid (284 mg, 90%).

A parallel reaction using freshly-prepared boronic acid **2.4e** (211 mg, 1.00 mmol) under otherwise identical conditions afforded **2.14e** as a pale yellow oil (192 mg, 61%).

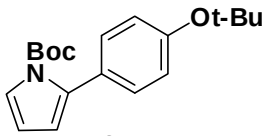

2.14e

TLC (hexanes:EtOAc 10:1)

R_f = 0.37, visualized by UV (λ = 254 nm)

^{1}H-NMR (500 MHz, $CDCl_3$)

δ 7.36 (dd, *J* = 3.0, 1.5 Hz, 1H), 7.23 (d, *J* = 8.5 Hz, 2H), 6.97 (d, *J* = 8.5 Hz, 2H), 6.22 (t, *J* = 1.5 Hz, 1H), 6.15 (dd, *J* = 3.5, 2.0 Hz, 1H), 1.38 (s, 9H), 1.34 (s, 9H)

^{13}C-NMR (125 MHz, $CDCl_3$)

δ 154.5, 149.5, 134.6, 129.7, 129.6, 123.1, 122.3, 114.2, 110.4, 83.5, 78.4, 28.8, 27.6

HRMS (CI+)

Calculated for $C_{19}H_{25}O_3N$ $(M)^+$:	315.1834
Found:	315.1834

IR (thin film, cm^{-1})

2978, 2934, 1739, 1511, 1474, 1392, 1369, 1337, 1314, 1238, 1162, 1074, 1040, 975, 897, 855, 814, 773, 7.29

N-phenylsulfonyl-2-(4-*tert*-butoxyphenyl)indole (**2.14f**) [Table 2.3, Entry 6]. The general procedure was followed using MIDA boronate **2.5f** (412 mg, 1.00 mmol). Purification by flash chromatography (SiO_2 hexanes:EtOAc 100:0 → 80:20 followed by C_{18} silica gel (H_2O:MeCN 1:1 → 1:9) afforded **2.14f** as a colorless solid (376 mg, 93%).

A parallel reaction using freshly-prepared boronic acid **2.4f** (301 mg, 1.00 mmol) under otherwise identical reaction and purification conditions afforded **2.14f** as a colorless solid (59 mg, 14%).

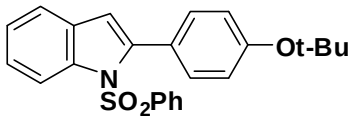

2.14f

TLC (hexanes:EtOAc 10:1)

R_f = 0.20, visualized by UV (λ = 254 and 366 nm)

^{1}H-NMR (500 MHz, $CDCl_3$ w/ TMS)

δ 8.32 (d, *J* = 8.5 Hz, 1H), 7.43 (m, 2H), 7.34 (m, 5H), 7.25 (m, 3H), 7.01 (d, *J* = 9.0 Hz, 2H), 6.50 (s, 1H), 1.43 (s, 9H)

^{13}C-NMR (125 MHz, $CDCl_3$)

δ 156.1, 141.8, 138.2, 137.7, 133.4, 131.1, 130.4, 128.5, 126.7, 126.6, 124.6, 124.2, 122.6, 120.5, 116.5, 112.9, 78.8, 28.9

HRMS (EI+)

Calculated for $C_{24}H_{23}O_3NS$ $(M)^+$: 405.13987

Found: 405.13919

IR (thin film, cm^{-1})

2979, 2971, 1496, 1446, 1367, 1256, 1238, 1217, 1182, 1171, 1163, 1152, 1120, 1087, 1055, 992, 899, 858, 822, 756, 729, 682, 593, 568, 547

1-*tert*-butoxy-4-vinylbenzene (**2.14g**) [Table 2.3, Entry 7]. The general procedure was followed using MIDA boronate **2.5g** (183 mg, 1.00 mmol) with the modification that the reaction was run at 100 ºC to afford **2.14g** as a pale yellow liquid (172 mg, 98%).

A parallel reaction using freshly-prepared boronic acid **2.4g** (72 mg, 1.0 mmol) under otherwise identical conditions afforded **2.14g** as pale yellow liquid (0.17 g, 79%; yield corrected for residual **3a**).

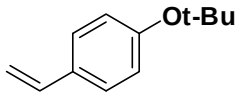

2.14g

TLC (hexanes:EtOAc 10:1)

R_f = 0.51, visualized by UV (λ = 254 nm)

^{1}H-NMR (500 MHz, $CDCl_3$)

δ 7.34 (d, *J* = 8.5 Hz, 2H), 6.97 (d, *J* = 8.5 Hz, 2H), 6.70 (dd, *J* = 18, 11 Hz, 1H), 5.67 (d, *J* = 18 Hz, 1H), 5.19 (d, *J* = 11 Hz, 1H), 1.37 (s, 9H)

^{13}C-NMR (125 MHz, $CDCl_3$)

δ 155.2, 136.3, 132.7, 126.7, 124.1, 112.4, 78.5, 28.8

HRMS (CI+)

Calculated for $C_{12}H_{16}O$ $(M)^+$:	176.1201
Found:	176.1198

IR (thin film, cm^{-1})

2978, 2931, 1630, 1603, 1505, 1473, 1390, 1366, 1243, 1161, 1107, 989, 923, 898, 858, 840

1-*tert*-butoxy-4-cyclopropylbenzene (**2.14h**) [Table 2.3, Entry 8]. The general procedure was followed using MIDA boronate **2.5h** (183 mg, 1.00 mmol) with the modification that the reaction was run at 100 ºC to afford **2.14h** as a pale yellow liquid (183 mg, 96%).

A parallel reaction using freshly-prepared boronic acid **2.4h** (86 mg, 1.0 mmol) under otherwise identical conditions afforded **2.14h** as pale yellow liquid (0.18 g, 95%).

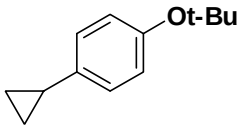

2.14h

TLC (hexanes:EtOAc 10:1)

R_f = 0.51, visualized by UV (λ = 254 nm)

^{1}H-NMR (500 MHz, $CDCl_3$)

δ 6.98 (d, *J* = 8.5 Hz, 2H), 6.90 (d, *J* = 8.5 Hz, 2H), 1.87 (m, 1H), 1.34 (s, 9H), 0.94 (m, 2H), 0.67 (m, 2H)

^{13}C-NMR (125 MHz, $CDCl_3$)

δ 152.9, 138.6, 125.9, 124.1, 78.0, 28.7, 14.8, 8.9

HRMS (CI+)

Calculated for $C_{13}H_{18}O$ $(M)^+$:	190.1358
Found:	190.1357

IR (thin film, cm^{-1})

3082, 2977, 2932, 1609, 1510, 1474, 1460, 1389, 1365, 1239, 1164, 1105, 1046, 1015, 923, 900, 845, 813

Scope of slow-release cross-coupling conditions (Table 2.4).

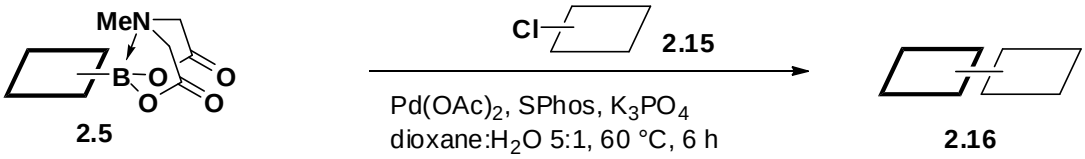

2.5 **2.16**

General Procedure:

Under ambient atmosphere, to a 40 mL I-Chem vial equipped with a stir bar was added the aryl chloride (1.00 mmol), the MIDA boronate (1.20 mmol), dicyclohexylphosphino-2',6'-

dimethoxy-1,1'-biphenyl (S-Phos) (41 mg, 0.10 mmol) and $Pd(OAc)_2$ (11 mg, 0.050 mmol). The vial was sealed with a PTFE-lined septum screw-cap, and then placed under an argon atmosphere. To the vial was added dioxane (12.5 mL) and the resulting mixture was stirred at 23 °C for 10 min. To the vial was added aq K_3PO_4 (3.0 M, 2.5 mL, degassed by sparging with argon for 30 min). The vial was placed in a 60 °C oil bath with stirring for 6 h. The mixture was cooled to room temperature, and was then transferred to a 60 mL separatory funnel and diluted with aq NaOH (1.0 M, 10 mL). The mixture was extracted with Et_2O (3 x 10 mL). The combined organic fractions were dried over $MgSO_4$, filtered, and then concentrated in vacuo. The resulting residue was adsorbed onto Celite (app. 10 g). The resulting powder was subjected to flash-chromatography on silica gel (hexanes:EtOAc).

2-(2,4-dimethoxyphenyl)furan (**2.16a**) [Table 2.4, Entry 1]. The general procedure was followed using 1-chloro-2,4-dimethoxybenzene (**2.15a**) (173 mg, 1.00 mmol), 2-furan MIDA boronate (**2.5a**) (267 mg, 1.20 mmol), S-Phos (41 mg, 0.10 mmol) and $Pd(OAc)_2$ (12 mg, 0.052 mmol) to afford **2.16a** as a pale orange liquid (202 mg, 99%).

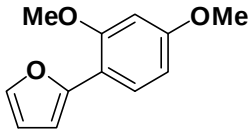

2.16a

TLC (hexanes:EtOAc 9:1)

R_f = 0.36, visualized by UV (λ = 254 nm)

^{1}H-NMR (500 MHz, $CDCl_3$ w/ TMS)

δ 7.74 (d, *J* = 8.5 Hz, 1H), 7.41 (d, *J* = 1.0 Hz, 1H), 6.79 (d, *J* = 3.5 Hz, 1H), 6.55 (dd, *J* = 8.5, 2.5 Hz, 1H), 6.52 (d, *J* = 2.0 Hz, 1H), 6.46 (q, *J* = 2.0 Hz, 1H), 3.89 (s, 3H), 3.82 (s, 3H)

^{13}C-NMR (125 MHz, $CDCl_3$)

δ 159.9, 156.5, 150.4, 140.4, 126.8, 113.4, 111.4, 107.8, 104.6, 98.7, 55.4 (2 carbons)

HRMS (EI+)

Calculated for $C_{12}H_{12}O_3$ $(M)^+$: 204.0787

Found: 204.0790

IR (thin film, cm^{-1})

3002, 2960, 2937, 2836, 1614, 1585, 1514, 1468, 1418, 1307, 1288, 1270, 1208, 1160, 1054, 1029, 1003, 827, 798, 735

2-(2,4,6-trimethylphenyl)furan (**2.16b**) [Table 2.4, Entry 2]. The general procedure was followed using mesityl chloride (**2.15b**) (154 mg, 1.00 mmol), 2-furyl MIDA boronate (**2.5a**) (267 mg, 1.20 mmol), S-Phos (42 mg, 0.10 mmol) and $Pd(OAc)_2$ (11 mg, 0.049 mmol) to afford **2.16b** as a colorless crystalline solid (181 mg, 97%).

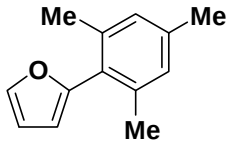

2.16b

TLC (hexanes)

R_f = 0.40, visualized by UV (λ = 254 nm)

^{1}H-NMR (500 MHz, $CDCl_3$ w/ TMS)

δ 7.46 (s, 1H), 6.90 (s, 2H), 6.44 (t, *J* = 3.0 Hz, 1H), 6.23 (d, *J* = 3.0 Hz, 1H), 2.28 (s, 3H), 2.15 (s, 6H)

^{13}C-NMR (125 MHz, $CDCl_3$)

δ 152.4, 141.4, 138.3, 138.3, 128.2, 128.2, 110.3, 109.0, 21.0, 20.4

HRMS (EI+)

Calculated for $C_{13}H_{14}O$ $(M)^+$: 186.1045

Found: 186.1043

IR (thin film, cm^{-1})

2975, 2954, 2919, 1612, 1505, 1473, 1440, 1373, 1257, 1212, 1169, 1148, 1028, 1005, 898, 863, 743

5-(2-furanyl)-2-methylbenzoxazole (**2.16c**) [Table 2.4, Entry 3]. The general procedure was followed using 5-chloro-2-methylbenzoxazole (**2.15c**) (168 mg, 1.00 mmol), 2-furyl MIDA boronate (**2.5a**) (266 mg, 1.19 mmol), S-Phos (41 mg, 0.10 mmol) and $Pd(OAc)_2$ (11 mg, 0.049 mmol) to afford **2.16c** as a pale orange crystalline solid (198 mg, 99%).

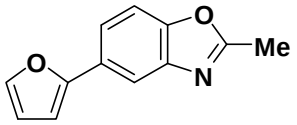

2.16c

TLC (hexanes:EtOAc 3:1)

R_f = 0.30, visualized by UV (λ = 254 nm)

^{1}H-NMR (500 MHz, $CDCl_3$ w/ TMS)

δ 7.93 (d, *J* = 1.0 Hz, 1H), 7.61 (dd, *J* = 8.5, 1.5 Hz, 1H), 7.47 (d, *J* = 1.0 Hz, 1H), 7.44 (d, *J* = 8.5 Hz, 1H), 6.63 (d, *J* = 3.5 Hz, 1H), 6.47 (dd, *J* = 3.5, 2.0 Hz, 1H), 2.62 (s, 3H)

^{13}C-NMR (125 MHz, $CDCl_3$)

δ 164.5, 153.7, 150.3, 141.9, 141.9, 127.6, 120.8, 114.6, 111.6, 110.3, 104.6, 14.5

HRMS (EI+)

Calculated for $C_{12}H_9NO_2$ $(M)^+$:	199.0633
Found:	199.0634

IR (KBr, cm^{-1})

2934, 2857, 1576, 1504, 1458, 1383, 1300, 1269, 1228, 1170, 1011, 885, 811

3-(2-furanyl)-2,5-dimethylpyrazine (**2.16d**) [Table 2.4, Entry 4]. The general procedure was followed using 3-chloro-2,5-dimethylpyrazine (**2.15d**) (143 mg, 1.00 mmol), 2-furyl MIDA boronate (**2.5a**) (267 mg, 1.20 mmol), S-Phos (41 mg, 0.10 mmol) and $Pd(OAc)_2$ (11 mg, 0.049 mmol) to afford **2.16d** as a golden liquid (159 mg, 91%).

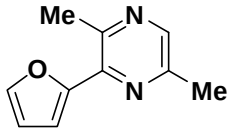

2.16d

TLC (hexanes:EtOAc 3:1)

R_f = 0.28, visualized by UV (λ = 254 nm)

^{1}H-NMR (500 MHz, $CDCl_3$ w/ TMS)

δ 8.20 (s, 1H), 7.61 (d, *J* = 1.0 Hz, 1H), 7.00 (d, *J* = 3.5 Hz, 1H), 6.54 (dd, *J* = 3.0, 1.5 Hz, 1H), 2.74 (s, 3H), 2.54 (s, 3H)

^{13}C-NMR (125 MHz, $CDCl_3$)

δ 151.7, 150.2, 146.5, 143.9, 142.5, 141.2, 112.3, 111.7, 23.3, 21.2

HRMS (EI+)

Calculated for $C_{10}H_{10}N_2O$ $(M)^+$:	174.0793
Found:	174.0799

IR (thin film, cm^{-1})

3116, 3038, 2966, 2926, 2858, 2359, 2228, 1553, 1537, 1449, 1446, 1389, 1357, 1289, 1255, 1220, 1203, 1174, 1149, 1095, 1061, 1012, 973, 928, 886, 867, 821, 735, 596

2-(2,4-dimethoxyphenyl)benzofuran (**2.16e**) [Table 2.4, Entry 5]. The general procedure was followed using 1-chloro-2,4-dimethoxybenzene (**2.15a**) (172 mg, 1.00 mmol), 2-benzofuranyl MIDA boronate (**2.5b**) (328 mg, 1.20 mmol), S-Phos (41 mg, 0.10 mmol) and $Pd(OAc)_2$ (12 mg, 0.051 mmol) to afford **2.16e** as a colorless liquid (239 mg, 94%)

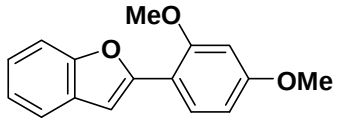

2.16e

TLC (hexanes:EtOAc 9:1)

R_f = 0.25, visualized by UV (λ = 254 nm)

^{1}H-NMR (500 MHz, $CDCl_3$ w/ TMS)

δ 7.97 (d, *J* = 8.5 Hz, 1H), 7.56 (d, *J* = 7.5 Hz, 1H), 7.48 (d, *J* = 7.5 Hz, 1H), 7.24-7.17 (m, 3H), 6.60 (dd, *J* = 8.5, 2.5 Hz, 1H), 6.55 (d, *J* = 2.0 Hz, 1H), 3.95 (s, 3H), 3.84 (s, 3H)

^{13}C-NMR (125 MHz, $CDCl_3$)

δ 160.8, 157.7, 153.6, 152.4, 130.0, 127.9, 123.5, 122.5, 120.7, 112.7, 110.6, 104.8, 104.2, 98.7, 55.4, 55.4

HRMS (EI+)

Calculated for $C_{16}H_{14}O_3$ $(M)^+$:	254.0943
Found:	254.0941

IR (thin film, cm^{-1})

3002, 2960, 2937, 2834, 1611, 1586, 1503, 1452, 1291, 1255, 1211, 1160, 1050, 1032, 1013

5-(2-benzofuranyl)indole (**2.16f**) [Table 2.4, Entry 6]. The general procedure was followed using 5-chloroindole (**2.15e**) (153 mg, 1.01 mmol), 2-benzofuranyl MIDA boronate (**2.5b**) (329 mg, 1.20 mmol), S-Phos (41 mg, 0.10 mmol) and $Pd(OAc)_2$ (12 mg, 0.053 mmol). The extraction step was modified to use Et_2O (10 mL), then EtOAc (2 x 10 mL). Benzofuran **2.16f** was isolated as a pale yellow solid (220 mg, 94%).

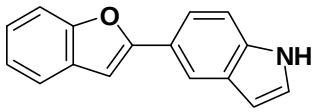

2.16f

TLC (hexanes:EtOAc 3:1)

R_f = 0.31, visualized by UV (λ = 254 nm)

^{1}H-NMR (500 MHz, acetone-d_6)

δ 10.44 (br s, 1H), 8.23 (s, 1H), 7.74 (dd, *J* = 8.5, 1.5 Hz, 1H), 7.59 (d, *J* = 7.0 Hz, 1H), 7.56 (app. d, *J* = 8.5 Hz, 2H), 7.41 (t, *J* = 3.0 Hz, 1H), 7.26 (td, *J* = 7.5, 1.0 Hz, 1H), 7.22 (td, *J* = 7.5, 1.0 Hz, 1H), 7.13 (s, 1H), 6.62 (t, *J* = 2.0 Hz, 1H)

^{13}C-NMR (125 MHz, acetone-d_6)

δ 158.7, 155.4, 137.4, 130.7, 129.2, 126.9, 124.3, 123.6, 122.6, 121.3, 119.7, 118.0, 112.7, 111.5, 103.1, 100.0

HRMS (EI+)

Calculated for $C_{16}H_{11}NO$ $(M)^+$:	233.0841
Found:	233.0843

IR (KBr, cm^{-1})

3439, 1582, 1475, 1458, 1444, 1417, 1332, 1295, 1254, 1020, 1006, 890, 877, 807, 753, 728, 594, 487, 442, 410

5-(2-benzofuranyl)-2-pyridinamine (**2.16g**) [Table 2.4, Entry 7]. The general procedure was followed using 2-amino-5-chloropyridine (**2.15f**) (128 mg, 1.00 mmol), 2-benzofuranyl MIDA boronate (**2.5b**) (359 mg, 1.50 mmol), S-Phos (41 mg, 0.10 mmol) and $Pd(OAc)_2$ (12 mg, 0.052 mmol). The extraction step was modified to use Et_2O (10 mL), then EtOAc (2 x 10 mL). Benzofuran **2.16g** was isolated as a pale orange solid (180 mg, 85%).

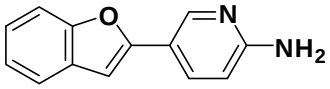

2.16g

TLC (EtOAc)

R_f = 0.45, visualized by UV (λ = 254 nm)

^{1}H-NMR (500 MHz, acetone-d_6)

δ 8.57 (d, *J* = 2.0 Hz, 1H), 7.89 (dd, *J* = 9.0, 2.5 Hz, 1H), 7.57 (d, *J* = 8.5 Hz, 1H), 7.50 (d, *J* = 8.5 Hz, 1H), 7.24 (td, *J* = 7.5, 1.5 Hz, 1H), 7.20 (td, *J* = 7.5, 1.5 Hz, 1H), 7.03 (d, *J* = 1.0 Hz, 1H), 6.66 (d, *J* = 8.5 Hz, 1H), 5.85 (br s, 2H)

^{13}C-NMR (125 MHz, acetone-d_6)

δ 160.8, 155.9, 155.3, 146.1, 134.6, 130.4, 124.4, 123.8, 121.3, 116.6, 111.5, 108.8, 99.4

HRMS (EI+)

Calculated for $C_{13}H_{10}N_2O$ $(M)^+$: 210.0793

Found: 210.0793

IR (KBr, cm^{-1})

3436, 3308, 3114, 3106, 2964, 1650, 1614, 1574, 1500, 1451, 1399, 1352, 1321, 1294, 1271, 1254, 1207, 1151, 1142, 1040, 1007, 934, 918, 835, 806, 747, 532, 515, 450, 412

2-(3-thienyl)benzofuran (**2.16h**) [Table 2.4, Entry 8]. The general procedure was followed using 3-chlorothiophene (**2.15g**) (119 mg, 1.01 mmol), 2-benzofuranyl MIDA boronate (**2.5b**) (360 mg, 1.50 mmol), S-Phos (41 mg, 0.10 mmol) and $Pd(OAc)_2$ (11 mg, 0.050 mmol) to afford **2.16h** as a colorless solid (171 mg, 85%).

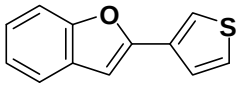

2.16h

TLC (hexanes:EtOAc 9:1)

R_f = 0.53, visualized by UV (λ = 254 nm)

^{1}H-NMR (500 MHz, $CDCl_3$ w/ TMS)

δ 7.67 (d, *J* = 1.5 Hz, 1H), 7.52 (d, *J* = 8.0 Hz, 1H), 7.47 (d, *J* = 8.0 Hz, 1H), 7.40 (d, *J* = 4.5 Hz, 1H), 7.32 (dd, *J* = 4.5, 3.0 Hz, 1H), 7.24 (t, *J* = 7.5 Hz, 1H), 7.19 (t, *J* = 7.5 Hz, 1H), 6.77 (s, 1H)

^{13}C-NMR (125 MHz, $CDCl_3$)

δ 154.5, 152.6, 132.2, 129.0, 126.5, 125.0, 124.0, 122.9, 121.4, 120.8, 111.0, 101.0

HRMS (EI+)

Calculated for $C_{12}H_8OS$ $(M)^+$:	200.0296
Found:	200.0295

IR (KBr, cm^{-1})

3100, 1607, 1452, 1280, 1255, 1041, 944, 854, 807, 785, 749, 601, 436

2-(2,4-dimethoxyphenyl)thiophene (**2.16i**) [Table 2.4, Entry 9]. The general procedure was followed using 1-chloro-2,4-dimethoxybenzene (**2.15a**) (173 mg, 1.00 mmol), 2-thiophenyl MIDA boronate (**2.5c**) (285 mg, 1.19 mmol), S-Phos (41 mg, 0.10 mmol) and $Pd(OAc)_2$ (11 mg, 0.051 mmol) to afford **2.16i** as a pale golden liquid (215 mg, 98%).

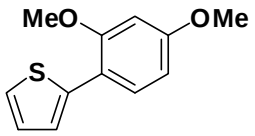

2.16i

TLC (hexanes:EtOAc 9:1)

R_f = 0.27, visualized by UV (λ = 254 nm)

^{1}H-NMR (500 MHz, $CDCl_3$ w/ TMS)

δ 7.53 (d, *J* = 9.5 Hz, 1H), 7.37 (d, *J* = 3.5 Hz, 1H), 7.25 (d, *J* = 5.5 Hz, 1H), 7.05 (t, *J* = 4.5 Hz, 1H), 6.53-6.51 (m, 2H), 3.88 (s, 3H), 3.82 (s, 3H)

^{13}C-NMR (125 MHz, $CDCl_3$)

δ 160.1, 156.7, 139.6, 129.3, 126.7, 124.3, 124.2, 116.5, 105.0, 98.9, 55.5, 55.4

HRMS (EI+)

Calculated for $C_{12}H_{12}O_2S$ $(M)^+$: 220.0558

Found: 220.0563

IR (thin film, cm^{-1})

3102, 3069, 3000, 3959, 3937, 2835, 1610, 1577, 1528, 1464, 1432, 1417, 1354, 1303, 1273, 1242, 1210, 1160, 1114, 1031, 959, 927, 848, 824, 798, 697, 577

2-methyl-5-(2-thienyl)benzoxazole (**2.16j**) [Table 2.4, Entry 10]. The general procedure was followed using 5-chloro-2-methylbenzoxazole (**2.15c**) (168 mg, 1.00 mmol), 2-thiophenyl MIDA boronate (**2.5c**) (287 mg, 1.20 mmol), S-Phos (41 mg, 0.10 mmol) and $Pd(OAc)_2$ (11 mg, 0.051 mmol) to afford **2.16j** as a crystalline pale yellow solid (213 mg, 99%).

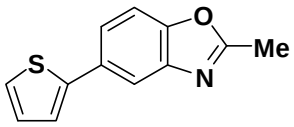

2.16j

TLC (hexanes:EtOAc 3:1)

R_f = 0.35, visualized by UV (λ = 254 nm)

^{1}H-NMR (500 MHz, $CDCl_3$ w/ TMS)

δ 7.85 (d, *J* = 1.0 Hz, 1H), 7.50 (dd, *J* = 8.0, 1.5 Hz, 1H), 7.39 (d, *J* = 8.5 Hz, 1H), 7.26 (d, *J* = 3.0 Hz, 1H), 7.24 (d, *J* = 5.0 Hz, 1H), 7.04 (dd, *J* = 5.0, 3.5 Hz, 1H), 2.59 (s, 3H)

^{13}C-NMR (125 MHz, $CDCl_3$)

δ 164.4, 150.3, 144.0, 142.1, 130.9, 127.9, 124.6, 123.0, 122.8, 116.6, 110.2, 14.4

HRMS (EI+)

Calculated for $C_{12}H_9NOS$ $(M)^+$: 215.0405

Found: 215.0403

IR (KBr, cm^{-1})

3098, 3064, 1622, 1577, 1473, 1428, 1380, 1271, 1160, 1050, 923, 867, 798

2-(2-thienyl)quinoxaline (**2.16k**) [Table 2.4, Entry 11]. The general procedure was followed using 1-chloroisoquinoline (**2.15h**) (165 mg, 1.00 mmol), 2-thiophenyl MIDA boronate (**2.5c**) (287 mg, 1.20 mmol), S-Phos (41 mg, 0.10 mmol) and $Pd(OAc)_2$ (11 mg, 0.050 mmol) to afford **2.16k** as a yellow solid (206 mg, 97%).

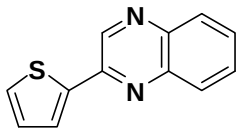

2.16k

TLC (hexanes:EtOAc 3:1)

R_f = 0.42, visualized by UV (λ = 254 nm)

^{1}H-NMR (500 MHz, $CDCl_3$ w/ TMS)

δ 9.20 (s, 1H), 8.04 (app d, *J* = 8.0 Hz, 2H), 7.82 (s, 1H), 7.71 (t, *J* = 7.0 Hz, 1H), 7.66 (t, *J* = 7.0 Hz, 1H), 7.52 (d, *J* = 4.0 Hz, 1H), 7.17 (s, 1H)

^{13}C-NMR (125 MHz, $CDCl_3$)

δ 147.2, 142.1, 142.0, 141.9, 141.2, 130.3, 129.7, 129.1, 129.0, 129.0, 128.3, 126.8

HRMS (EI+)

Calculated for $C_{12}H_8N_2S$ $(M)^+$: 212.0408

Found: 212.0407

IR (thin film, cm^{-1})

3118, 3093, 1573, 1547, 1491, 1428, 1321, 1238, 1208, 1134, 1054, 998, 941, 926, 852

N-(*tert*-butoxycarbonyl)-2-(2,3-dimethoxyphenyl)pyrrole (**2.16l**) [Table 2.4, Entry 12]. The general procedure was followed using 1-chloro-2,4-dimethoxybenzene (**2.15a**) (87 mg, 0.51 mmol), 2-(N-*tert*-butoxycarbonyl)pyrrole MIDA boronate (**2.5e**) (196 mg, 0.61 mmol), S-Phos (20 mg, 0.048 mmol), $Pd(OAc)_2$ (6 mg, 0.03 mmol), K_3PO_4 (3.0 M, 1.25 mL) and dioxane (6.0 mL) to afford **2.16l** as a very pale yellow oil (124 mg, 81%).

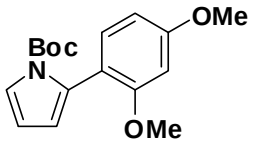

2.16l

TLC (hexanes:EtOAc 3:1)

R_f = 0.59, visualized by UV (λ = 254 nm)

^{1}H-NMR (500 MHz, $CDCl_3$ w/ TMS)

δ 7.32 (s, 1H), 7.17 (d, *J* = 8.0 Hz, 1H), 6.48 (d, *J* = 8.5 Hz, 1H), 6.45 (s, 1H), 6.22 (t, *J* = 3.0 Hz, 1H), 6.10 (s, 1H), 3.82 (s, 3H), 3.72 (s, 3H), 1.36 (s, 9H)

^{13}C-NMR (125 MHz, $CDCl_3$)

δ 160.7, 158.3, 149.4, 131.1, 130.6, 121.6, 117.0, 113.5, 110.2, 103.4, 98.2, 82.6, 55.3, 55.2, 27.6

HRMS (EI+)

Calculated for $C_{17}H_{21}NO_4$ $(M)^+$: 303.1471

Found: 303.1469

IR (thin film, cm^{-1})

2976, 2938, 2834, 1736, 1617, 1584, 1512, 1464, 1437, 1419, 1394, 1370, 1341, 1316, 1209, 1159, 1127, 1034, 974, 840, 726

5-(N-*tert*-butoxycarbonyl-pyrrole)-2-methylbenzoxazole (**2.16m**) [Table 2.4, Entry 13]. The general procedure was followed using 5-chloro-2-methylbenzoxazole (**2.15c**) (84 mg, 0.50 mmol), 2-(N-*tert*-butoxycarbonyl)pyrrole MIDA boronate (**2.5e**) (195 mg, 0.61 mmol), S-Phos (21 mg, 0.050 mmol), $Pd(OAc)_2$ (6 mg, 0.03 mmol), K_3PO_4 (3.0 M, 1.25 mL) and dioxane (6.0 mL) to afford **2.16m** as a very pale yellow oil (146 mg, 98%).

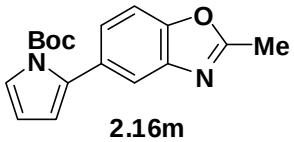

2.16m

TLC (hexanes:EtOAc 3:1)

R_f = 0.42, visualized by UV (λ = 254 nm)

^{1}H-NMR (500 MHz, $CDCl_3$ w/ TMS)

δ 7.63 (s, 1H), 7.43 (d, *J* = 8.5 Hz, 1H), 7.36 (s, 1H), 7.28 (d, *J* = 8.5 Hz, 1H), 6.23 (t, *J* = 3.0 Hz, 1H), 6.20 (s, 1H), 2.64 (s, 3H), 1.34 (s, 9H)

^{13}C-NMR (125 MHz, $CDCl_3$)

δ 164.2, 150.2, 149.1, 140.9, 134.4, 130.6, 126.1, 122.4, 120.0, 114.7, 110.4, 109.0, 83.5, 27.5, 14.5

HRMS (EI+)

Calculated for $C_{17}H_{18}N_2O_3$ $(M)^+$: 298.1318

Found: 298.1317

IR (thin film, cm^{-1})

2982, 1739, 1584, 1584, 1456, 1395, 1365, 1370, 1336, 1313, 1264, 1166, 1140, 985, 906, 836, 809

N-phenylsulfonyl-2-(2,3-dimethoxyphenyl)indole (**2.16n**) [Table 2.4, Entry 14]. The general procedure was followed using 1-chloro-2,4-dimethoxybenzene (**2.15a**) (173 mg, 1.00 mmol), 1-

(phenylsulfonyl)indole-2-MIDA boronate (**2.5f**) (495 mg, 1.20 mmol), S-Phos (42 mg, 0.10 mmol) and $Pd(OAc)_2$ (11 mg, 0.049 mmol) to afford **2.16n** as an off-white solid (382 mg, 97%).

2.16n

TLC (hexanes:EtOAc 3:1)

R_f = 0.37, visualized by UV (λ = 254 nm)

^{1}H-NMR (500 MHz, acetone-d_6)

δ 8.19 (d, *J* = 8.0 Hz, 1H), 7.57-7.53 (m, 3H), 7.50 (d, *J* = 7.5 Hz, 1H), 7.43 (t, *J* = 7.5 Hz, 2H), 7.32 (dt, *J* = 7.0, 1.0 Hz, 1H), 7.23 (t, *J* = 7.5 Hz, 1H), 7.17 (d, *J* = 8.0 Hz, 1H), 6.62 (d, *J* = 2.0 Hz, 1H), 6.58 (dd, *J* = 8.0, 2.0 Hz, 1H), 6.56 (s, 1H), 3.87 (s, 3H), 3.72 (s, 3H)

^{13}C-NMR (125 MHz, acetone-d_6)

δ 163.0, 160.6, 139.4, 139.3, 138.1, 134.5, 133.2, 131.3, 129.8, 127.4, 125.0, 124.5, 121.5, 116.1, 115.0, 113.0, 104.7, 98.8, 55.7, 55.7

HRMS (EI+)

Calculated for $C_{12}H_{19}NO_4S$ $(M)^+$: 393.1035

Found: 393.1036

IR (KBr, cm^{-1})

3000, 2978, 2938, 2842, 1617, 1501, 1449, 1445, 1360, 1284, 1239, 1187, 1163, 1121, 1093, 1069, 1048, 832, 752, 728, 681, 582, 559

5-(N-phenylsulfonyl-indole)-2-methylbenzoxazole (**2.16o**) [Table 2.4, Entry 15]. The general procedure was followed using 5-chloro-2-methylbenzoxazole (**2.15c**) (168 mg, 1.00 mmol), 1-

(phenylsulfonyl)indole-2-MIDA boronate (**2.5f**) (495 mg, 1.20 mmol), S-Phos (41 mg, 0.10 mmol) and $Pd(OAc)_2$ (12 mg, 0.052 mmol) to afford **2.16o** as an off-white solid (366 mg, 93%).

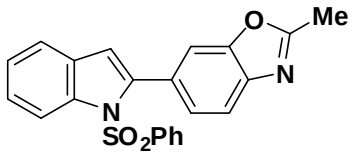

2.16o

TLC (hexanes:EtOAc 1:1)

R_f = 0.36, visualized by UV (λ = 254 nm)

^{1}H-NMR (500 MHz, acetone-d_6)

δ 8.27 (d, *J* = 8.5 Hz, 1H), 7.78 (d, *J* = 1.0 Hz, 1H), 7.61 (d, *J* = 8.5 Hz, 1H), 7.55 (t, *J* = *7*.5 Hz, 1H), 7.51 (d, *J* = 8.0 Hz, 2H), 7.45 (app. d, *J* = 8.0 Hz, 2H), 7.39 (app. t, *J* = 8.0 Hz, 3H), 7.28 (dt, *J* = 7.0, 1.0 Hz, 1H), 6.75 (s, 1H), 2.65 (s, 3H)

^{13}C-NMR (125 MHz, acetone-d_6)

δ 165.6, 152.3, 142.9, 142.4, 139.3, 138.6, 134.8, 131.7, 129.9, 129.6, 128.2, 127.5, 125.8, 125.4, 122.0, 121.9, 117.3, 114.9, 110.1, 14.4

HRMS (EI+)

Calculated for $C_{22}H_{16}N_2O_3S$ $(M)^+$: 388.0882

Found: 388.0880

IR (thin film, cm^{-1})

3063, 3012, 1712, 1623, 1581, 1477, 1449, 1432, 1365, 1262, 1220, 1177, 1157, 1122, 1092, 1065, 1021, 999, 921, 823

2,4,6-trimethylstyrene (**2.16p**) [Table 2.4, Entry 16]. The general procedure was followed using mesityl chloride (**2.15b**) (155 mg, 1.01 mmol), vinyl MIDA boronate (**2.5g**) (220 mg, 1.20 mmol), S-Phos (41 mg, 0.10 mmol) and $Pd(OAc)_2$ (12 mg, 0.051 mmol). The reaction time and

temperature were modified so that the reaction mixture was heated to 100 °C for 2 h. Styrene **2.16p** was isolated as a colorless liquid (150 mg, 91%; yield corrected for residual **2.15b**).

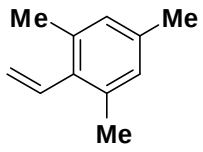

2.16p

TLC (hexanes)

R_f = 0.64, visualized by UV (λ = 254 nm)

^{1}H-NMR (500 MHz, $CDCl_3$ w/ TMS)

δ 6.86 (s, 2H), 6.66 (dd, *J* = 18.0, 11.5 Hz, 1H), 5.50 (dt, *J* = 11.5, 2.0 Hz, 1H), 5.23 (dt, *J* = 18.0, 2.0 Hz, 1H), 2.27 (s, 6H), 2.26 (s, 3H)

^{13}C-NMR (125 MHz, $CDCl_3$)

δ 136.1, 135.7, 135.0, 134.8, 128.5, 119.0, 20.9, 20.8

HRMS (EI+)

Calculated for $C_{11}H_{14}$ $(M)^+$:	146.1096
Found:	146.1098

IR (thin film, cm^{-1})

3080, 2999, 2952, 2918, 2856, 1631, 1612, 1481, 1442, 1376, 994, 919, 850

2-vinylquinoxaline (**2.16q**) [Table 2.4, Entry 17]. The general procedure was followed using 2-chloroquinoxaline (**2.15h**) (165 mg, 1.00 mmol), vinyl MIDA boronate (**2.5g**) (219 mg, 1.20 mmol), S-Phos (41 mg, 0.10 mmol) and $Pd(OAc)_2$ (11 mg, 0.051 mmol). The reaction time and temperature were modified so that the reaction mixture was heated to 100 °C for 2 h. Following the aqueous workup, the crude residue was subjected to purification on C_{18} silica gel (43g RediSep column) eluting with H_2O:THF (95:5 → 55:45, 24 mL/min over 25 min) to afford **2.16q** as an orange oil (133 mg, 87%).

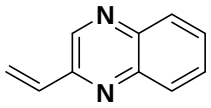

2.16q

TLC (hexanes:EtOAc 3:1)

R_f = 0.31, visualized by UV (λ = 254 nm)

^{1}H-NMR (500 MHz, $CDCl_3$ w/ TMS)

δ 9.00 (s, 1H), 8.08 (app. t, *J* = 9.0 Hz, 2H), 7.77-7.70 (m, 2H), 7.04 (dd, *J* = 17.5, 11.0 Hz, 1H), 6.48 (d, *J* = 17.5 Hz, 1H), 5.79 (d, *J* = 11.0 Hz, 1H)

^{13}C-NMR (125 MHz, $CDCl_3$)

δ 150.4, 143.5, 142.1, 141.7, 134.8, 130.2, 129.5, 129.3, 129.1, 122.1

HRMS (ESI+)

Calculated for $C_{10}H_9N_2$ $(M+H)^+$: 157.0766

Found: 157.0768

IR (thin film, cm^{-1})

3064.0, 3018, 2928, 2847, 1631, 1596, 1546, 1492, 1466, 1414, 1365, 1342, 1331, 1303, 1282, 1258, 1212, 1185, 1121, 1065, 1014, 989, 972, 927, 762

2-amino-5-vinylpyridine (**2.16r**) [Table 2.4, Entry 18]. The general procedure was followed using 2-amino-5-chloropyridine (**2.15f**) (129 mg, 1.00 mmol), vinyl MIDA boronate (**2.5g**) (220 mg, 1.20 mmol), S-Phos (42 mg, 0.10 mmol) and $Pd(OAc)_2$ (11 mg, 0.050 mmol). The reaction time and temperature were modified so that the reaction mixture was heated to 100 °C for 2 h. The extraction step was modified to use Et_2O (10 mL), then EtOAc (2 x 10 mL). Pyridine **2.16r** was isolated as a pale orange crystalline solid (91 mg, 76%).

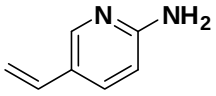

2.16r

TLC (EtOAc)

R_f = 0.48, visualized by UV (λ = 254 nm)

^{1}H-NMR (500 MHz, $CDCl_3$ w/ TMS)

δ 8.05 (s, 1H), 7.56 (dd, *J* = 8.5, 2.0 Hz, 1H), 6.58 (dd, *J* = 17.5, 11.0 Hz, 1H), 6.48 (d, *J* = 9.0 Hz, 1H), 5.56 (d, *J* = 17.5 Hz, 1H), 5.11 (d, *J* = 11.0 Hz, 1H), 4.60 (br s, 2H)

^{13}C-NMR (125 MHz, $CDCl_3$)

δ 157.9, 147.0, 134.4, 133.3, 124.0, 111.2, 108.5

HRMS (EI+)

Calculated for $C_7H_8N_2$ $(M)^+$:	120.0688
Found:	120.0688

IR (KBr, cm^{-1})

3448, 3296, 3128, 1631, 1599, 1509, 1388, 1324, 1274, 1144, 1002, 888, 828

5-vinyl-2-methylbenzoxazole (**2.16s**) [Table 2.4, Entry 19]. The general procedure was followed using 5-chloro-2-methylbenzoxazole (**2.15c**) (167 mg, 1.01 mmol), vinyl MIDA boronate (**2.5g**) (218 mg, 1.19 mmol), S-Phos (42 mg, 0.10 mmol) and $Pd(OAc)_2$ (11 mg, 0.050 mmol). The reaction time and temperature were modified so that the reaction mixture was heated to 100 °C for 2 h. Benzoxazole **2.16s** was isolated as a pale golden liquid (152 mg, 96%).

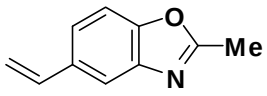

2.16s

TLC (hexanes:EtOAc 3:1)

R_f = 0.46, visualized by UV (λ = 254 nm)

^{1}H-NMR (500 MHz, $CDCl_3$ w/ TMS)

δ 7.67 (s, 1H), 7.38 (d, *J* = 8.0 Hz, 1H), 7.34 (d, *J* = 8.0 Hz, 1H), 6.79 (dd, *J* = 17.5, 11.0 Hz, 1H), 5.74 (d, *J* = 17.5 Hz, 1H), 5.24 (d, *J* = 11.0 Hz, 1H), 2.61 (s, 3H)

^{13}C-NMR (125 MHz, $CDCl_3$)

δ 164.3, 150.6, 141.9, 136.5, 134.2, 122.9, 116.8, 113.4, 109.9, 14.5

HRMS (EI+)

Calculated for $C_{10}H_9NO$ $(M)^+$: 159.0684

Found: 159.0685

IR (thin film, cm^{-1})

3087, 3006, 2984, 2928, 1623, 1622, 1578, 1477, 1433, 1381, 1335, 1262, 1179, 1114, 1040, 989, 918, 881, 840, 815

2,4,6-trimethyl-cyclopropylbenzene (**2.16t**) [Table 2.4, Entry 20]. The general procedure was followed using mesityl chloride (**2.15b**) (155 mg, 1.00 mmol), cyclopropyl MIDA boronate (**2.5h**) (296 mg, 1.50 mmol), S-Phos (42 mg, 0.10 mmol) and $Pd(OAc)_2$ (11 mg, 0.047 mmol). The reaction time and temperature were modified so that the reaction mixture was heated to 100 °C for 24 h. The title compound was isolated as a colorless liquid (127 mg, 79%).

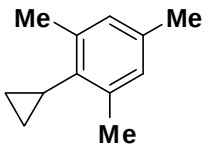

2.16t

TLC (hexanes)

R_f = 0.66, visualized by UV (λ = 254 nm)

^{1}H-NMR (500 MHz, $CDCl_3$ w/ TMS)

δ 6.81 (s, 2H), 2.38 (s, 6H), 2.24 (s, 3H), 1.64 (m, 1H), 0.96 (m, 2H), 0.49 (m, 2H)

^{13}C-NMR (125 MHz, $CDCl_3$)

δ 138.8, 136.0, 135.5, 128.6, 20.8, 20.5, 11.7, 8.0

HRMS (EI+)

Calculated for $C_{12}H_{16}$ $(M)^+$: 160.1252

Found: 160.1252

IR (thin film, cm^{-1})

3080, 3003, 2969, 2954, 2918, 2859, 1612, 1485, 1457, 1375, 1223, 1057, 1025, 901, 850, 814

2,4-dimethoxy-cyclopropylbenzene (**2.16u**) [Table 2.4, Entry 21]. The general procedure was followed using 1-chloro-2,4-dimethoxybenzene (**2.15a**) (173 mg, 1.00 mmol), cyclopropyl MIDA boronate (**2.5h**) (236 mg, 1.20 mmol), S-Phos (41 mg, 0.10 mmol) and $Pd(OAc)_2$ (11 mg, 0.048 mmol). The reaction temperature was modified so that the reaction mixture was heated to 100 °C for 6 h. The title compound was isolated as a colorless liquid (175 mg, 97%).

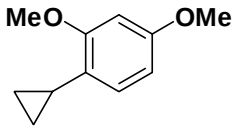

2.16u

TLC (hexanes:EtOAc 9:1)

R_f = 0.65, visualized by UV (λ = 254 nm)

^{1}H-NMR (500 MHz, $CDCl_3$ w/ TMS)

δ 6.77 (d, *J* = 8.5 Hz, 1H), 6.44 (d, *J* = 2.5 Hz, 1H), 6.39 (dd, *J* = 8.5, 2.5 Hz, 1H), 3.83 (s, 3H), 3.77 (s, 3H), 2.03 (m, 1H), 0.85 (m, 2H), 0.57 (m, 2H)

^{13}C-NMR (125 MHz, $CDCl_3$)

δ 159.2, 158.6, 125.7, 124.2, 103.8, 98.4, 55.5, 55.3, 9.0, 6.9

HRMS (EI+)

Calculated for $C_{11}H_{14}O_2$ $(M)^+$: 178.0994

Found: 178.0995

IR (thin film, cm^{-1})

3080, 3000, 2955, 2940, 2835, 1615, 1585, 1510, 1464, 1439, 1416, 1370, 1319, 1290, 1261, 1209, 1172, 1158, 1117, 1062, 1037, 938, 884, 834, 823, 799

Synthesis of 2-pyridyl MIDA boronate (Table 2.5, entry 3).

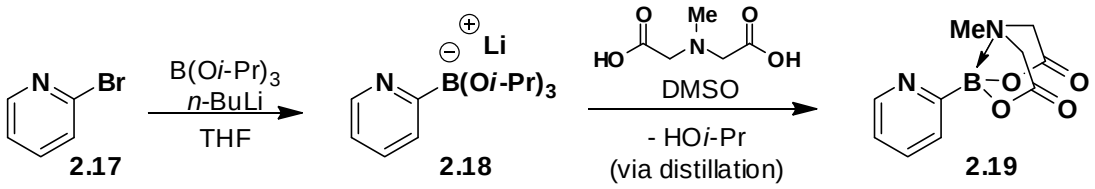

2-pyridyl MIDA boronate (**2.19**). In an unoptimized procedure, to a 250 mL Schlenk flask equipped with a stir bar was added 2-bromopyridine (6.00 mL, 62.9 mmol), triisopropylborate (15.0 mL, 65.2 mmol) and THF (100 mL). The solution was cooled to -78 °C. To the stirred solution was added dropwise *n*-BuLi (25.0 mL, 2.5M in hexanes) at a rate sufficiently slow as to avoid the accumulation of a red color in the mixture (app. 20 minutes). The resulting beige mixture was stirred for 30 min and then was allowed to warm to room temperature with stirring overnight (12 h). The mixture was concentrated in vacuo onto Celite (10 g) to afford a free-flowing powder. Separately, a 500 mL 3-neck round-bottom flask equipped with a stir bar was charged with *N*-methyliminodiacetic acid (15.77 g, 107.2 mmol) and DMSO (100 mL). To one neck of the flask was fitted a solid addition funnel charged with the Celite-adsorbed lithium triisopropyl 2-pyridylborate. To a second neck was fitted a short-path distillation apparatus connected to vacuum. The third neck of the flask was sealed with a septum. The system was placed under vacuum (1 Torr) and the mixture was heated to 75 °C upon which the DMSO began to distill. The lithium triisopropyl 2-pyridylborate was added to the distilling mixture portion-wise over 1 h. The mixture was further distilled to near dryness (1 h). The resulting residue was

suspended in acetone, and then concentrated in vacuo onto additional Celite (10 g). The resulting powder was lyophilized for 3 days to remove additional DMSO, and then was subjected to flash chromatography on silica gel (40 g silica gel cartridge, Et_2O:MeCN, 100:0 → 0:100). The product thus obtained was suspended in acetone (5 mL) and then diluted with Et_2O (100 mL) to promote crystallization. The mixture was filtered to isolate **2.19** as an off-white crystalline solid (4.024 g, 27%).

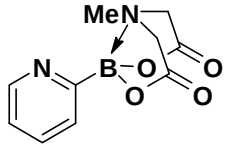

2.19

TLC (MeCN)

R_f = 0.26, visualized by UV (λ = 254 nm) and $KMnO_4$ stain

^{1}H-NMR (500 MHz, CD_3CN)

δ 8.67 (ddd, *J* = 2.5, 1.5, 1.0 Hz, 1H), 7.70 (td, *J* = 7.5, 1.5 Hz, 1H), 7.62 (dt, *J* = 7.5, 1.0 Hz, 1H), 7.28 (ddd, *J* = 8.5, 1.5 Hz, 1H), 8.67 (ddd, *J* = 4.5, 1.5, 1.0 Hz, 1H), 4,09 (d, *J* = 17 Hz, 2H), 3.98 (d, *J* = 17 Hz, 2H), 2.55 (s, 3H)

^{13}C-NMR (125 MHz, CD_3CN)

δ 169.6, 150.8, 135.8, 128.1, 124.3, 62.9, 47.6

^{11}B-NMR (96 MHz, CD_3CN)

δ 10.3

HRMS (CI+)

Calculated for $C_{10}H_{12}O_4N_2B$ $(M+H)^+$:	235.0890
Found:	235.0895

IR (KBr, cm^{-1})

3004, 2956, 1774, 1749, 1633, 1590, 1466, 1340, 1289, 1279, 1214, 1152, 1095, 1054, 1045, 998, 964, 894, 866, 775, 754, 708, 683

Cross-coupling reactions of 2-pyridyl MIDA boronate (Table 2.7).

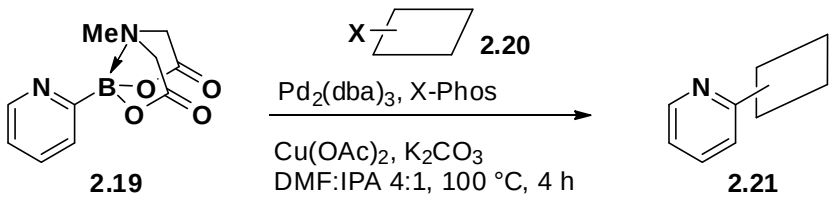

General Procedure. Under ambient atmosphere, to a 15 mL vial equipped with a stir bar was added the halide (1.0 mmol), 2-pyridyl MIDA boronate (**2.19**) (1.5 mmol), K_2CO_3 (5.0 mmol) and $Cu(OAc)_2$ (0.50 mmol). In a glove box, to the vial was added a DMF mixture of 2-dicyclohexylphosphino-2',4',6'-triisopropylbiphenyl (X-Phos) (0.06 mmol) and Pd_2dba_3 (0.015 mmol) (8.0 mL DMF, pre-mixed and incubated for 5 min at 100 °C, then transferred at ~40 °C to avoid incomplete solubility at room temperature.) The reaction mixture was stirred at 100 °C for 4 h. The mixture was cooled to room temperature and then was transferred to a 60 mL separatory funnel and was diluted with aq NaOH (1.0 M, 10 mL). The mixture was extracted with Et_2O (3 × 10 mL). The combined organics were dried over $MgSO_4$, filtered and concentrated in vacuo. The crude residue was adsorbed onto Celite and the resulting powder was subjected to flash-chromatography on silica gel (hexanes:EtOAc).

4-(2-pyridinyl)acetophenone (**2.21a**) [Table 2.8, Entry 1]. The general procedure was followed using 4-chloroacetophenone (**2.20a**) (155 mg, 1.00 mmol), 2-pyridyl MIDA boronate (**2.19**) (349 mg, 1.49 mmol), K_2CO_3 (694 mg, 5.02 mmol) and $Cu(OAc)_2$ (90 mg, 0.50 mmol). Flash chromatography on silica gel (hexanes:EtOAc, 100:0 → 80:20) afforded **2.21a** as a colorless solid (142 mg, 72%).

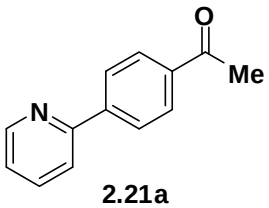

2.21a

TLC (hexanes:EtOAc 1:1)

R_f = 0.47, visualized by UV (λ = 254 nm)

^{1}H-NMR (500 MHz, $CDCl_3$)

δ 8.73 (d, *J* = 5.0 Hz, 1H), 8.10 (d, *J* = 8.5 Hz, 2H), 8.06 (d, *J* = 8.5 Hz, 2H), 7.79 (m, 2H), 7.29 (q, *J* = 4.5 Hz, 1H), 2.65 (s, 3H)

^{13}C-NMR (125 MHz, $CDCl_3$)

δ 197.8, 156.0, 149.9, 143.5, 137.1, 136.9, 128.8, 127.0, 122.9, 121.0, 26.7

HRMS (CI+)

Calculated for $C_{13}H_{12}ON$ $(M+H)^+$: 198.0919

Found: 198.0919

IR (KBr, cm^{-1})

3048, 2999, 1679, 1604, 1584, 1574, 1558, 1466, 1434, 1400, 1356, 1315, 1266, 1156, 1113, 1013, 989, 960, 849, 785, 723, 696, 618, 600, 592

4-(2-pyridinyl)benzonitrile (**2.21b**) [Table 2.8, Entry 2]. The general procedure was followed using 4-chlorobenzonitrile (**2.20b**) (137 mg, 1.00 mmol), 2-pyridyl MIDA boronate (**2.19**) (352 mg, 1.50 mmol), K_2CO_3 (693 mg, 5.01 mmol) and $Cu(OAc)_2$ (91 mg, 0.50 mmol). Flash chromatography on silica gel (hexanes:EtOAc, 9:1) afforded **2.21b** as a pale yellow solid (109 mg, 60%).

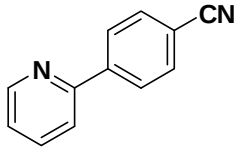

2.21b

TLC (hexanes:EtOAc 1:1)

R_f = 0.59, visualized by UV (λ = 254 nm)

^{1}H-NMR (500 MHz, $CDCl_3$)

δ 8.73 (d, *J* = 5.0 Hz, 1H), 8.11 (d, *J* = 9.0 Hz, 2H), 7.81 (td, *J* = 7.5, 1.5 Hz, 1H), 7.75 (m, 3H), 7.31 (ddd, *J* = 7, 4.5, 1 Hz, 1H)

^{13}C-NMR (125 MHz, $CDCl_3$)

δ 155.2, 150.0, 143.4, 137.1, 132.5, 127.4, 123.3, 121.0, 118.8, 112.5

HRMS (CI+)

Calculated for $C_{12}H_9N_2$ $(M+H)^+$: 181.0766

Found: 181.0765

IR (KBr, cm^{-1})

2228, 1588, 1466, 1433, 1393, 1303, 1152, 1152, 990, 852, 776, 738, 718, 620, 563, 518

2-(2-pyridinyl)quinoxaline (**2.21c**) [Table 2.8, Entry 3]. The general procedure was followed using 2-chloroquinoxaline (**2.20c**) (165 mg, 1.00 mmol), 2-pyridyl MIDA boronate (**2.19**) (353 mg, 1.51 mmol), K_2CO_3 (693 mg, 5.01 mmol) and $Cu(OAc)_2$ (91 mg, 0.50 mmol). Flash chromatography on silica gel (hexanes:EtOAc, 100:0 → 80:20) afforded **2.21c** as a pale orange solid (164 mg, 79%).

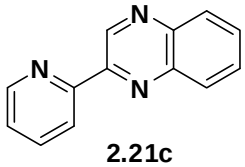

2.21c

TLC (hexanes:EtOAc (1:1)

R_f = 0.56, visualized by UV (λ = 254 nm)

^{1}H-NMR (500 MHz, $CDCl_3$)

δ 9.95 (s, 1H), 8.77 (ddd, *J* = 5.0, 1.5, 1.0 Hz, 1H), 8.58 (d, *J* = 8.0 Hz, 1H), 8.15 (m, 2H), 7.88 (td, *J* = 7.5, 1.5 Hz, 1H), 7.77 (m, 2H), 7.39 (ddd, *J* = 7.5, 4.5, 1.0 Hz, 1H)

^{13}C-NMR (125 MHz, $CDCl_3$)

δ 154.5, 150.1, 149.4, 144.1, 142.5, 141.7, 137.1, 130.1, 130.0, 129.7, 129.3, 124.6, 122.0

HRMS (CI+)

Calculated for $C_{13}H_{10}N_3$ $(M+H)^+$: 208.0875

Found: 208.0871

IR (KBr, cm^{-1})

3050, 3004, 1591, 1548, 1492, 1479, 1457, 1437, 1403, 1367, 1143, 1131, 1059, 1043, 996, 961, 806, 785, 772, 742, 716, 670, 556

2,5-dimethyl-3-(2-pyridinyl)pyrazine (**2.21d**) [Table 2.8, Entry 4]. The general procedure was followed using 3-chloro-2,5-dimethylpyrazine (**2.20d**) (142 mg, 1.00 mmol), 2-pyridyl MIDA boronate (**2.19**) (352 mg, 1.50 mmol), K_2CO_3 (694 mg, 5.02 mmol) and $Cu(OAc)_2$ (90 mg, 0.50 mmol). The aqueous phase was extracted an additional time with EtOAc (10 mL). Flash chromatography on silica gel (hexanes:EtOAc, 100:0 → 55:45) afforded **2.21d** as a pale amber liquid (96 mg, 52%).

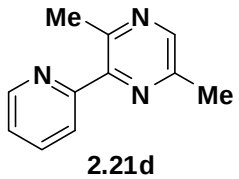

2.21d

TLC (hexanes:EtOAc 1:1)

R_f = 0.39, visualized by UV (λ = 254 nm)

^{1}H-NMR (500 MHz, $CDCl_3$ w/ TMS)

δ 8.72 (d, *J* = 3.5 Hz, 1H), 8.38 (s, 1H), 7.83 (m, 2H), 7.33 (m, 1H), 2.73 (s, 3H), 2.59 (s, 3H)

^{13}C-NMR (125 MHz, $CDCl_3$)

δ 157.2, 150.2, 149.9, 149.4, 148.7, 142.6, 136.6, 124.1, 123.0, 120.1, 22.6, 21.0

HRMS (CI+)

Calculated for $C_{11}H_{12}N_3$ $(M+H)^+$:	186.1031
Found:	186.1034

IR (thin film, cm^{-1})

3055, 2927, 1693, 1589, 1561, 1474, 1452, 1422, 1371, 1292, 1171, 1071, 1048, 995, 804, 752, 744

1-(2-pyridinyl)isoquinoline (**2.21e**) [Table 2.8, Entry 5]. The general procedure was followed using 1-chloroisoquinoline (**2.20e**) (164 mg, 1.00 mmol), 2-pyridyl MIDA boronate (**2.19**) (350 mg, 1.49 mmol), K_2CO_3 (697 mg, 5.05 mmol) and $Cu(OAc)_2$ (89 mg, 0.49 mmol). The aqueous phase was extracted an additional time with EtOAc (10 mL). Flash chromatography on silica gel (hexanes:EtOAc, 70:30 → 30:70) afforded **2.21e** as an off-white solid (152 mg, 74%).

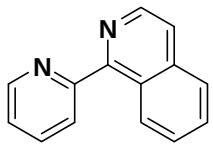

2.21e

TLC (EtOAc)

R_f = 0.47, visualized by UV (λ = 254 and 366 nm)

^{1}H-NMR (500 MHz, $CDCl_3$)

δ 8.79 (ddd, *J* = 5.0, 1.5, 1.0 Hz, 1H), 8.63 (d, *J* = 5.5 Hz, 1H), 8.60 (d, *J* = 8.5 Hz, 1H), 7.99 (dt, *J* = 8.0 Hz, 1.0 Hz, 1H), 7.91 (td, *J* = 7.5, 2.0 Hz, 1H), 7.87 (d, *J* = 8.0 Hz, 1H), 7.70 (d, *J* = 5.5 Hz, 1H), 7.69 (ddd, *J* = 8.0, 7.0, 1.5, 1H), 7.59 (ddd, *J* = 8.5, 7.0, 1 Hz, 1H), 7.40 (ddd, *J* = 7.5, 5.0, 1.0 Hz, 1H)

^{13}C-NMR (125 MHz, $CDCl_3$)

δ 158.2, 157.6, 148.6, 141.8, 137.0, 136.9, 130.0, 127.7, 127.6, 126.8, 126.6, 125.2, 123.2, 121.2

HRMS (CI+)

Calculated for $C_{14}H_{11}N_2$ $(M+H)^+$: 207.0922

Found: 207.0926

IR (KBr, cm^{-1})

3051, 3012, 1581, 1562, 1551, 1470, 1455, 1434, 1379, 1350, 1322, 1245, 1129, 1095, 992, 979, 966, 826, 811, 780, 753, 742, 713, 674, 644, 618, 573, 465, 441

Synthesis of 2-pyridyl MIDA boronate derivatives (Table 2.8).

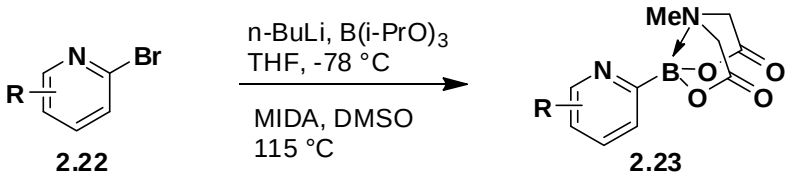

General procedure for the synthesis of MIDA boronates. To a 50 mL Schlenk flask equipped with a stir bar was added halide (8.6 mmol), triisopropyl borate (2.4 mL, 10 mmol), and THF (17 mL). The resulting stirred solution was cooled to -78 °C. To the cooled solution was added dropwise *n*-butyllithium (2.5 M in hexanes, 8.5 mmol) (ca. 0.25 mL/min). Following the addition, the reaction was stirred at -78 °C for 1 h, then warmed to 23 °C with stirring for 3 h. Separately, to a 3-neck 100 mL flask equipped with a 50 mL pressure equalizing addition funnel, a water-cooled short-path distillation apparatus, a thermometer and a stir bar was added *N*-methyiminodiacetic acid (2.151 g, 14.62 mmol) and DMSO (17 mL). The mixture was heated with stirring to an internal temperature of 115 °C. The borate mixture contained in the Schlenk flask was transferred to the addition funnel, washing with a THF (9 mL). To the hot, stirred DMSO solution was added dropwise the borate solution at a rate necessary to maintain the internal temperature at 110-120 °C (ca. 1 h). During the addition the THF was rapidly distilled (distillate temperature of app. 85 °C). Following the addition, the mixture was cooled to 50 °C and the DMSO was removed via distillation (250 mTorr at 50 °C). The resulting residue was cooled to 23 °C and then was adsorbed onto Celite from an acetonitrile suspension and placed under vacuum for 12 h to further remove residual DMSO. The Celite mixture was then subjected to column chromatography on SiO_2 to afford the purified product. Product mixtures containing undesired MIDA boronate byproducts could be recrystallized to afford the pure product as follows: The isolated product was dissolved in hot MeCN (app. 4 mL/mmol product), cooled to room temperature, and precipitated by the dropwise addition of CH_2Cl_2 (app. 16 mL/mmol) to the stirred solution, followed by dropwise addition of Et_2O (app. 50 mL/mmol).

2-pyridyl MIDA boronate (2.19) [Table 2.9, Entry 1]. The general procedure was followed using 2-bromopyridine (0.860 mL, 8.82 mmol), triisopropyl borate (2.4 mL, 10 mmol), *n*-BuLi

(4.15 mL, 2.29 M in hexanes), and *N*-methyliminodiacetic acid (2.463 g, 16.74 mmol). The product was purified via SiO_2 chromatography (Et_2O:MeCN 95:5 → 0:100) to afford **2.19** as an off-white crystalline solid (1.212 g, 59%). Spectral characterization was consistent with literature data.[93]

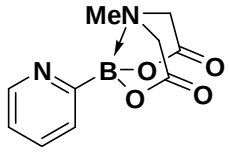

2.19

See Table 2.6 for characterization data.

MIDA boronate (2.23a) [Table 2.9, Entry 2]. The general procedure was followed using 2-bromo-6-methylpyridine (0.98 mL, 8.6 mmol), triisopropyl borate (2.0 mL, 8.7 mmol), *n*-BuLi (3.75 mL, 2.29 M in hexanes), and *N*-methyliminodiacetic acid (2.311 g, 15.71 mmol). The product was purified by SiO_2 chromatography (EtOAc:MeCN 100:0 → 45:55) to afford **2.23a** as an off-white crystalline solid (1.243 g, 58%).

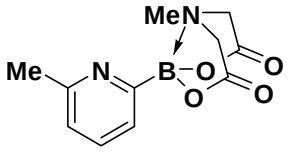

2.23a

TLC (MeCN)

R_f = 0.54, visualized by UV (λ = 254 nm) and $KMnO_4$ stain

^{1}H-NMR (400 MHz, CD_3CN)

δ 7.57 (app t, *J* = 7.6 Hz, 1H), 7.40 (d, *J* = 7.2, 1H), 7.14 (d, *J* = 7.6 Hz, 1H), 4.07 (d, *J* = 17 Hz, 2H), 4.00 (d, *J* = 17 Hz, 2H), 2.55 (s, 3H), 2.48 (s, 3H)

^{13}C-NMR (100 MHz, DMSO-d_6)

δ 169.3, 157.6, 135.0, 124.1, 122.5, 61.9, 46.8, 24.5

^{11}B-NMR (128 MHz, DMSO-d_6)

δ 9.6

HRMS (ES+)

Calculated for $C_{11}H_{14}O_4N_2B$ $(M+H)^+$: 249.1047

Found: 249.1051

MIDA boronate (2.23b) [Table 2.9, Entry 3]. The general procedure was followed using 2-bromo-5-methylpyridine (1.489 g, 8.655 mmol), triisopropyl borate (2.4 mL, 10 mmol), *n*-BuLi (4.15 mL, 2.29 M in hexanes), and *N*-methyliminodiacetic acid (2.227 g, 15.14 mmol). The product was purified via SiO_2 chromatography (Et_2O:MeCN 95:5 → 0:100) to afford **2.23b** as an off-white crystalline solid (1.090 g, 51%).

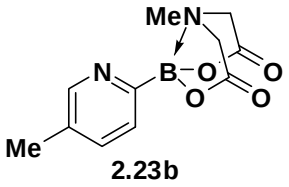

2.23b

TLC (MeCN)

R_f = 0.43, visualized by UV (λ = 254 nm) and $KMnO_4$ stain

^{1}H-NMR (500 MHz, CD_3CN)

δ 8.53 (s, 1H), 7.51 (s, 2H), 4.07 (d, *J* = 17 Hz, 2H), 3.96 (d, *J* = 17 Hz, 2H), 2.53 (s, 3H), 2.31 (s,3H)

^{13}C-NMR (100 MHz, DMSO-d_6)

δ 169.3, 150.2, 135.1, 132.2, 126.6, 61.9, 46.8, 18.0

^{11}B-NMR (128 MHz, DMSO-d_6)

δ 9.6

HRMS (ES+)

Calculated for $C_{11}H_{14}O_4N_2B$ $(M+H)^+$: 249.1047

Found: 249.1039

MIDA boronate (2.23c) [Table 2.9, Entry 4]. The general procedure was followed using 2-bromo-4-methylpyridine (0.960 mL, 8.62 mmol), triisopropyl borate (2.4 mL, 10 mmol), *n*-BuLi (4.15 mL, 2.29 M in hexanes), and *N*-methyliminodiacetic acid (2.264 g, 15.39 mmol). The product was purified by SiO_2 chromatography (Et_2O:MeCN 95:5 → 0:100) to afford **2.23c** as an off-white crystalline solid (897 mg, 42%).

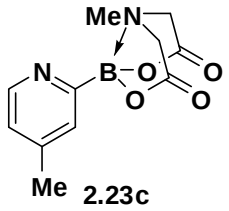

2.23c

TLC (MeCN)

R_f = 0.29, visualized by UV (λ = 254 nm) and $KMnO_4$ stain

^{1}H-NMR (500 MHz, CD_3CN)

δ 8.51 (d, *J* = 5.0 Hz, 1H), 7.47 (s, 1H), 7.11 (d, *J* = 5.0 Hz, 1H), 4.08 (d, *J* = 17 Hz, 2H), 3.97 (d, *J* = 17 Hz, 2H), 2.54 (s, 3H), 2.33 (s,3H)

^{13}C-NMR (125 MHz, DMSO-d_6)

δ 169.3, 149.5, 145.2, 128.0, 123.9, 62.0, 46.8, 20.6

^{11}B-NMR (128 MHz, DMSO-d_6)

δ 9.8

HRMS (ES+)

Calculated for $C_{11}H_{14}O_4N_2B$ $(M+H)^+$:	249.1047
Found:	249.1052

MIDA boronate (2.23d) [Table 2.9, Entry 5]. The general procedure was followed using 2-bromo-6-methoxypyridine (1.05 mL, 8.55 mmol), triisopropyl borate (2.0 mL, 8.7 mmol), *n*-BuLi (6.3 mL, 1.37 M in hexanes), and *N*-methyliminodiacetic acid (2.437 g, 16.56 mmol). The product was purified via SiO_2 chromatography (EtOAc:MeCN 100:0 → 60:40). The isolated product was dissolved in hot MeCN (20 mL), cooled to room temperature, and precipitated by

the dropwise addition of Et_2O (200 mL) to the stirred solution. The crystals were collected to afford **2.23d** as an off-white crystalline solid (1.830 g, 81%).

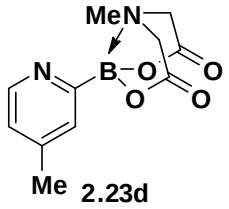

2.23d

TLC (EtOAc)

R_f = 0.34, visualized by UV (λ = 254 nm) and $KMnO_4$ stain

^{1}H-NMR (500 MHz, CD_3CN)

δ 7.60 (dd, *J* = 7.5, 7 Hz, 1H), 7.22 (d, *J* = 7.0 Hz, 1H), 6.70 (d, *J* = 8 Hz, 1H), 4.09 (d, *J* = 17 Hz, 2H), 3.99 (d, *J* = 16.5 Hz, 2H), 3.83 (s, 3H), 2.60 (s, 3H)

^{13}C-NMR (100 MHz, DMSO-d_6)

δ 169.2, 163.1, 138.0, 120.4, 110.4, 61.8, 52.6, 46.5

^{11}B-NMR (128 MHz, DMSO-d_6)

δ 9.3

HRMS (ES+)

Calculated for $C_{11}H_{14}O_5N_2B$ $(M+H)^+$:	265.0996
Found:	265.0989

MIDA boronate (2.23e) [Table 2.9, Entry 6]. The general procedure was followed using 2-bromo-6-trifluoromethylpyridine (1.951g, 8.633 mmol), triisopropyl borate (2.4 mL, 10 mmol), *n*-BuLi (4.15 mL, 2.29 M in hexanes), and *N*-methyliminodiacetic acid (2.293 g, 15.58 mmol). The product was purified via SiO_2 chromatography (hexanes:EtOAc 100:0 → 0:100) to afford **2.23e** as a tan crystalline solid (2.328 g, 89%).

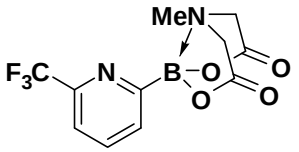

2.23e

TLC (EtOAc)

R_f = 0.57, visualized by UV (λ = 254 nm) and $KMnO_4$ stain

^{1}H-NMR (400 MHz, CD_3CN)

δ 7.95 (app t, *J* = 7.6 Hz, 1H), 7.88 (d, *J* = 7.2 Hz, 1H), 7.72 (dd, *J* = 7.6, 0.8 Hz, 1H), 4.13 (d, *J* = 17 Hz, 2H), 3.98 (d, *J* = 17 Hz, 2H), 2.57 (s, 3H)

^{13}C-NMR (125 MHz, DMSO-d_6)

δ 169.1, 146.7 (q, *J* = 33 Hz), 137.1, 130.4, 121.8 (q, *J* = 270 Hz), 120.0 (d, *J* = 2.8 Hz), 62.1, 47.1

^{11}B-NMR (128 MHz, DMSO-d_6)

δ 9.5

HRMS (ES+)

Calculated for $C_{11}H_{11}O_4N_2BF_3$ $(M+H)^+$:	303.0764
Found:	303.0753

MIDA boronate (2.23f) [Table 2.9, Entry 7]. The general procedure was followed using 2-bromo-5-trifluoromethylpyridine (1.936 g, 8.567 mmol), triisopropyl borate (2.0 mL, 8.7 mmol), *n*-BuLi (3.35 mL, 2.56 M in hexanes), and *N*-methyliminodiacetic acid (2.222 g, 15.10 mmol). The product was purified via SiO_2 chromatography (EtOAc:MeCN 100:0 → 90:10). The isolated product was dissolved in hot MeCN (8 mL), cooled to room temperature, and precipitated by the dropwise addition of Et_2O (80 mL) to the stirred solution. The crystals were collected to afford **2.23f** as an off-white crystalline solid (1.448 g, 56%).

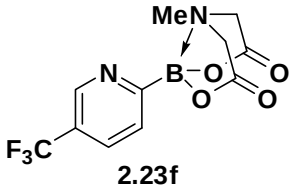

2.23f

TLC (EtOAc)

R_f = 0.43, visualized by UV (λ = 254 nm) and $KMnO_4$ stain

^{1}H-NMR (500 MHz, CD_3CN)

δ 8.99 (s, 1H), 8.00 (dd, *J* = 8.0, 1.5Hz, 1H), 7.82 (d, *J* = 8.0 Hz, 1H), 4.13 (d, *J* = 17 Hz, 2H), 4.00 (d, *J* = 17 Hz, 2H), 2.56 (s, 3H)

^{13}C-NMR (125 MHz, DMSO-d_6)

δ 169.2, 145.9, 132.1, 127.2, 124.3 (q, *J* = 32 Hz), 123.9 (q, *J* = 270 Hz), 62.1, 47.0

^{11}B-NMR (128 MHz, DMSO-d_6)

δ 8.3

HRMS (ES+)

Calculated for $C_{11}H_{11}O_4N_2BF_3$ $(M+H)^+$:	303.0764
Found:	303.0755

MIDA boronate (2.23g) [Table 2.9, Entry 8]. The general procedure was followed using 2-bromo-4-trifluoromethylpyridine (1.05 mL, 8.49 mmol), triisopropyl borate (2.0 mL, 8.7 mmol), *n*-BuLi (6.3 mL, 1.37 M in hexanes), and *N*-methyliminodiacetic acid (2.418g, 16.43 mmol). [Note: The triisopropylborate mixture was transferred to the addition funnel using DMSO (43 mL) rather than THF.] The product was purified via SiO_2 chromatography (Et_2O:MeCN 95:5 → 75:25 → 50:50). The isolated product was dissolved in hot MeCN (5 mL), cooled to room temperature, and precipitated by the dropwise addition of Et_2O (50 mL) to the stirred solution. The precipitation procedure was repeated to afford **2.23g** as an off-white crystalline solid (1.350 g, 53%).

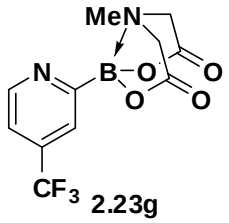

2.23g

TLC (EtOAc)

R_f = 0.17, visualized by UV (λ = 254 nm) and $KMnO_4$ stain

^{1}H-NMR (500 MHz, CD_3CN)

δ 8.92 (d, *J* = 5.0 Hz, 1H), 7.86 (s, 1H), 7.57 (d, *J* = 5.0 Hz, 1H), 4.13 (d, *J* = 17 Hz, 2H), 4.00 (d, *J* = 17 Hz, 2H), 2.56 (s, 3H)

^{13}C-NMR (125 MHz, DMSO-d_6)

δ 169.2, 151.2, 135.3 (q, *J* = 33 Hz), 123.3 (q, *J* = 270 Hz), 121.8, 118.5, 62.2, 47.1

^{11}B-NMR (128 MHz, DMSO-d_6)

δ 9.5

HRMS (ES+)

Calculated for $C_{11}H_{11}O_4N_2BF_3$ $(M+H)^+$:	303.0764
Found:	303.0750

MIDA boronate (2.23h) [Table 2.9, Entry 9]. The general procedure was followed using 2,6-dibromopyridine (2.036g, 8.594 mmol), triisopropyl borate (2.0 mL, 8.7 mmol), *n*-BuLi (3.4 mL, 2.54 M in hexanes), and *N*-methyliminodiacetic acid (2.2049 g, 14.99 mmol). The product was purified via SiO_2 chromatography (hexanes:EtOAc 25:75 → 0:100). The isolated product was dissolved in hot MeCN (3.5 mL), cooled to room temperature, and precipitated by the dropwise addition of CH_2Cl_2 (15 mL) to the stirred solution, followed by dropwise addition of Et_2O (40 mL). The crystals were collected to afford **2.23h** as a white crystalline solid (1.269 g, 47%).

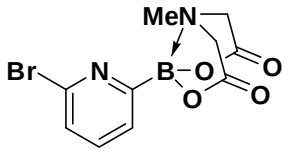

2.23h

TLC (EtOAc)

R_f = 0.46, visualized by UV (λ = 254 nm) and $KMnO_4$ stain

^{1}H-NMR (400 MHz, CD_3CN)

δ 7.61 (m, 2H), 7.49 (m, 1H), 4.10 (d, *J* = 17 Hz, 2H), 3.96 (d, *J* = 17 Hz, 2H), 2.58 (s, 3H)

^{13}C-NMR (100 MHz, DMSO-d_6)

δ 169.1, 142.2, 138.5, 127.6, 126.9, 62.0, 47.2

^{11}B-NMR (128 MHz, DMSO-d_6)

δ 9.3

HRMS (ES+)

Calculated for $C_{10}H_{11}O_4N_2BBr$ $(M+H)^+$:	312.9995
Found:	312.9996

MIDA boronate (2.23i) [Table 2.9, Entry 10]. The general procedure was followed using 2,5-dibromopyridine (2.042 g, 8.620 mmol), triisopropyl borate (2.0 mL, 8.7 mmol), *n*-BuLi (3.35 mL, 2.58 M in hexanes), and *N*-methyliminodiacetic acid (2.260 g, 15.36 mmol). The product was purified via SiO_2 chromatography (Et_2O:MeCN 95:5 → 50:50). The isolated product was dissolved in hot MeCN (3.5 mL), cooled to room temperature, and precipitated by the dropwise addition of CH_2Cl_2 (15 mL) to the stirred solution, followed by the dropwise addition of Et_2O (40 mL). The crystals were collected to afford **2.23i** as a white crystalline solid (1.856 g, 69%).

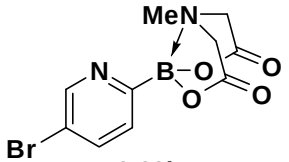

2.23i

TLC (EtOAc)

R_f = 0.24, visualized by UV (λ = 254 nm) and $KMnO_4$ stain

^{1}H-NMR (500 MHz, CD_3CN)

δ 8.42 (d, *J* = 1.5 Hz, 1H), 7.73 (dd, *J* = 8 Hz, 1.5 Hz, 1H), 7.54 (d, *J* = 8 Hz, 1H), 4.09 (d, *J* = 17 Hz, 2H), 3.96 (d, *J* = 17 Hz, 2H), 2.56 (s, 3H)

^{13}C-NMR (125 MHz, DMSO-d_6)

δ 169.1, 154.3, 143.8, 142.8, 127.4, 62.0, 47.8

^{11}B-NMR (128 MHz, DMSO-d_6)

δ 11.0

HRMS (ES+)

Calculated for $C_{10}H_{11}O_4N_2BBr$ $(M+H)^+$:	312.9995
Found:	312.9998

Synthesis of 5-thiazolyl and 2-pyrazinyl MIDA boronate (Scheme 2.5).

5-thiazolyl MIDA boronate (2.25). The general procedure was followed using 5-bromothiazole (0.270 mL, 3.02 mmol), triisopropyl borate (0.670 mL, 2.91 mmol), *n*-BuLi (1.2 mL, 2.58 M in hexanes), and *N*-methyliminodiacetic acid (775 mg, 5.27 mmol). The product was purified via SiO_2 chromatography (Et_2O:MecN 95:5 → 0:100). The isolated product was dissolved in hot MeCN (5 mL), cooled to room temperature, and precipitated by the dropwise addition of CH_2Cl_2 (20 mL) to the stirred solution, followed by dropwise addition of Et_2O (60 mL). The crystals were collected to afford **2.25** as a tan crystalline solid (213 mg, 30%).

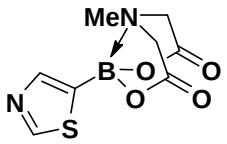

2.25

TLC (MeCN)

R_f = 0.67, visualized by UV (λ = 254 nm) and $KMnO_4$ stain

^{1}H-NMR (500 MHz, CD_3CN)

δ 9.03 (s, 1H), 7.98 (s, 1H), 4.10 (d, *J* = 18 Hz, 2H), 3.93 (d, *J* = 18 Hz, 2H), 2.63 (s, 3H)

^{13}C-NMR (125 MHz, CD_3CN)

δ 168.8, 158.1, 150.0, 62.6, 48.5

^{11}B-NMR (128 MHz, DMSO-d_6)

δ 10.7

HRMS (ES+)

Calculated for $C_8H_{10}O_4N_2BS$ $(M+H)^+$:	241.0454
Found:	241.0452

2-pyrazinyl MIDA boronate (2.27). The general procedure was followed using 2-bromopyrazine (0.275 mL, 2.96 mmol), triisopropyl borate (0.690 mL, 3.00 mmol), *n*-BuLi (1.2 mL, 2.54 M in hexanes), and *N*-methyliminodiacetic acid (774 mg, 5.26 mmol). The product was purified via SiO_2 chromatography (Et_2O:MeCN 95:5 → 0:100) to afford **2.27** as an orange crystalline solid (300 mg, 43%).

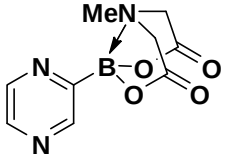

2.27

TLC (MeCN)

R_f = 0.56, visualized by UV (λ = 254 nm) and $KMnO_4$ stain

^{1}H-NMR (500 MHz, CD_3CN)

δ 8.77 (d, *J* = 1.5 Hz, 1H), 8.67 (dd, J = 2.0, 1.5 Hz, 1H), 8.53 (d, *J* = 2.5 Hz, 1H), 4.13 (d, *J* = 17 Hz, 2H), 3.98 (d, *J* = 17 Hz, 2H), 2.59 (s, 3H)

^{13}C-NMR (125 MHz, DMSO-d_6)

δ 169.1, 147.6, 145.4, 144.6, 62.0, 47.2

^{11}B-NMR (128 MHz, DMSO-d_6)

δ 9.6

HRMS (ES+)

Calculated for $C_9H_{11}O_4N_3B$ $(M+H)^+$:	236.0843
Found:	236.0840

2-10 REFERENCES

1. Hall, D. G. *Boronic Acids*; Wiley-VCH: Weinheim, Germany, 2005.
2. Hatanaka, Y.; Hiyama, T. *J. Org. Chem.* **1988**, *53*, 918–920.
3. Gillis, E. P.; Burke, M. D. *J. Am. Chem. Soc.* **2007**, *129*, 6716–6717.
4. Ballmer, S. G.; Gillis, E. P.; Burke, M. D. *Org. Synth.* **2009**, *86*, 344–359.
5. Gillis, E. P.; Burke, M. D. *J. Am. Chem. Soc.* **2008**, *130*, 14084–14085.
6. Lee, S. J.; Anderson, T. M.; Burke, M. D. *Angew. Chem. Int. Ed.* **2010**, *49*, 8860–8863.
7. Lee, S. J.; Gray, K. C.; Paek, J. S.; Burke, M. D. *J. Am. Chem. Soc.* **2008**, *130*, 466–468.
8. Struble, J. R.; Lee, S. J.; Burke, M. D. *Tetrahedron* **2010**, *66*, 4710–4718.
9. Uno, B. E.; Gillis, E. P.; Burke, M. D. *Tetrahedron* **2009**, *65*, 3130–3138.
10. Woerly, E. M.; Cherney, A. H.; Davis, E. K.; Burke, M. D. *J. Am. Chem. Soc.* **2010**, *132*, 6941–6943.
11. Butters, M.; Harvey, J. N.; Jover, J.; Lennox, A. J. J.; Lloyd-Jones, G. C.; Murray, P. M. *Angew. Chem. Int. Ed.* **2010**, *49*, 5156–5160.
12. Matteson, D. S. *J. Am. Chem. Soc.* **1960**, *82*, 4228–4233.
13. Roush, W. R.; Brown, B. B. *J. Am. Chem. Soc.* **1993**, *115*, 2268–2278.
14. Torrado, A.; Iglesias, B.; Lopez, S.; Delera, A. R. *Tetrahedron* **1995**, *51*, 2435–2454.
15. Fleckenstein, C. A.; Plenio, H. *J. Org. Chem.* **2008**, *73*, 3236–3244.
16. Burns, M. J.; Fairlamb, I. J. S.; Kapdi, A. R.; Sehnal, P.; Taylor, R. J. K. *Org. Lett.* **2007**, *9*, 5397–5400.
17. Xin, B.; Zhang, Y.; Cheng, K. *J. Org. Chem.* **2006**, *71*, 5725–5731.
18. Pagano, N.; Maksimoska, J.; Bregman, H.; Williams, D. S.; Webster, R. D.; Xue, F.; Meggers, E. *Org. Biomol. Chem.* **2007**, *5*, 1218–1227.
19. Li, J. H.; Zhu, Q. M.; Xie, Y. X. *Tetrahedron* **2006**, *62*, 10888–10895.

20. Takimiya, K.; Kunugi, Y.; Toyoshima, Y.; Otsubo, T. *J. Am. Chem. Soc.* **2005**, *127*, 3605–3612.
21. Thomas, S. W.; Venkatesan, K.; Müller, P.; Swager, T. M. *J. Am. Chem. Soc.* **2006**, *128*, 16641–16648.
22. Collis, G. E.; Burrell, A. K.; Blandford, E. J.; Officer, D. L. *Tetrahedron* **2007**, *63*, 11141–11152.
23. Qin, P.; Zhu, H.; Edvinsson, T.; Boschloo, G.; Hagfeldt, A.; Sun, L. *J. Am. Chem. Soc.* **2008**, *130*, 8570–8571.
24. Maeda, H.; Haketa, Y.; Nakanishi, T. *J. Am. Chem. Soc.* **2007**, *129*, 13661–13674.
25. Peyroux, E.; Berthiol, F.; Doucet, H.; Santelli, M. *Eur. J. Org. Chem.* **2004**, 1075–1082.
26. Denmark, S. E.; Butler, C. R. *Chem. Commun.* **2009**, 20–33.
27. Todd, R. C.; Josyula, K. V. B.; Gorr, K.; Priebe, K.; Gao, P. *Abstr. Pap. Am. Chem. Soc.* **2007**, *233*.
28. Wallace, D. J.; Chen, C. Y. *Tetrahedron Lett.* **2002**, *43*, 6987–6990.
29. Lemhadri, M.; Doucet, H.; Santelli, M. *Synth. Commun.* **2006**, *36*, 121–128.
30. Chen, H.; Deng, M.-Z. *Org. Lett.* **2000**, *2*, 1649–1651.
31. Billingsley, K.; Buchwald, S. L. *J. Am. Chem. Soc.* **2007**, *129*, 3358–3366.
32. Billingsley, K. L.; Buchwald, S. L. *Angew. Chem. Int. Ed.* **2008**, *47*, 4695–4698.
33. O'Neill, B. T.; Yohannes, D.; Bundesmann, M. W.; Arnold, E. P. *Org. Lett.* **2000**, *2*, 4201–4204.
34. Yamamoto, Y.; Takizawa, M.; Yu, X. Q.; Miyaura, N. *Angew. Chem. Int. Ed.* **2008**, *47*, 928–931.
35. Sindkhedkar, M. D.; Mulla, H. R.; Wurth, M. A.; Cammers-Goodwin, A. *Tetrahedron* **2001**, *57*, 2991–2996.
36. Cammidge, A. N.; Goddard, V. H. M.; Gopee, H.; Harrison, N. L.; Hughes, D. L.; Schubert, C. J.; Sutton, B. M.; Watts, G. L.; Whitehead, A. J. *Org. Lett.* **2006**, *8*, 4071–4074.
37. Hodgson, P. B.; Salingue, F. H. *Tetrahedron Lett.* **2004**, *45*, 685–687.
38. Jones, N. A.; Antoon, J. W.; Bowie, A. L.; Borak, J. B.; Stevens, E. P. *J. Heterocycl. Chem.* **2007**, *44*, 363–367.
39. Gravel, M.; Thompson, K. A.; Zak, M.; Bérubé, C.; Hall, D. G. *J. Org. Chem.* **2001**, *67*, 3–15.
40. Gros, P.; Doudouh, A.; Fort, Y. *Tetrahedron Lett.* **2004**, *45*, 6239–6241.
41. Lightfoot, A. P.; Twiddle, S. J. R.; Whiting, A. *Synlett* **2005**, 529–531.
42. Yang, D. X.; Colletti, S. L.; Wu, K.; Song, M.; Li, G. Y.; Shen, H. C. *Org. Lett.* **2008**, *11*, 381–384.
43. Deng, J. Z.; Paone, D. V.; Ginnetti, A. T.; Kurihara, H.; Dreher, S. D.; Weissman, S. A.; Stauffer, S. R.; Burgey, C. S. *Org. Lett.* **2008**, *11*, 345–347.
44. Cioffi, C. L.; Spencer, W. T.; Richards, J. J.; Herr, R. J. *J. Org. Chem.* **2004**, *69*, 2210–2212.
45. Kerins, F.; O'Shea, D. F. *J. Org. Chem.* **2002**, *67*, 4968–4971.
46. Perkins, J. R.; Carter, R. G. *J. Am. Chem. Soc.* **2008**, *130*, 3290–3291.
47. Darses, S.; Genet, J.-P. *Chem. Rev.* **2007**, *108*, 288–325.
48. Molander, G. A.; Ellis, N. *Acc. Chem. Res.* **2007**, *40*, 275–286.
49. Stefani, H. A.; Cella, R.; Vieira, A. S. *Tetrahedron* **2007**, *63*, 3623–3658.
50. Molander, G. A.; Biolatto, B. *J. Org. Chem.* **2003**, *68*, 4302–4314.
51. Molander, G. A.; Brown, A. R. *J. Org. Chem.* **2006**, *71*, 9681–9686.
52. Molander, G. A.; Canturk, B.; Kennedy, L. E. *J. Org. Chem.* **2009**, *74*, 973–980.

53. Molander, G. A.; Gormisky, P. E. *J. Org. Chem.* **2008**, *73*, 7481–7485.
54. Molander, G. A.; Rivero, M. R. *Org. Lett.* **2002**, *4*, 107–109.
55. Molander, G. A.; Cavalcanti, L. N.; Canturk, B.; Pan, P.-S.; Kennedy, L. E. *J. Org. Chem.* **2009**, *74*, 7364–7369.
56. Lennox, A. J. J.; Lloyd-Jones, G. C. *J. Am. Chem. Soc.* **2012**, *134*, 7431–7441.
57. Smith, B. B.; Sawyer, D. T. *Inorg. Chem.* **1968**, *7*, 1526–1532.
58. Billingsley, K. L.; Anderson, K. W.; Buchwald, S. L. *Angew. Chem. Int. Ed.* **2006**, *45*, 3484–3488.
59. Kedia, S. B.; Mitchell, M. B. *Org. Process Res. Dev.* **2009**, *13*, 420–428.
60. Gillis, E. P. Iterative cross-coupling with MIDA boronates. Ph.D. Dissertation, University of Illinois at Urbana-Champaign, 2010.
61. DeGoey, D. A.; Grampovnik, D. J.; Flentge, C. A.; Flosi, W. J.; Chen, H.-j.; Yeung, C. M.; Randolph, J. T.; Klein, L. L.; Dekhtyar, T.; Colletti, L.; Marsh, K. C.; Stoll, V.; Mamo, M.; Morfitt, D. C.; Nguyen, B.; Schmidt, J. M.; Swanson, S. J.; Mo, H.; Kati, W. M.; Molla, A.; Kempf, D. J. *J. Med. Chem.* **2009**, *52*, 2571–2586.
62. Heim-Riether, A.; Taylor, S. J.; Liang, S.; Gao, D. A.; Xiong, Z.; Michael, A. E.; Collins, B. K.; Farmer, B. T., 2nd; Haverty, K.; Hill-Drzewi, M.; Junker, H.-D.; Mariana, M. S.; Moss, N.; Neumann, T.; Proudfoot, J. R.; Keenan, L. S.; Sekul, R.; Zhang, Q.; Li, J.; Farrow, N. A. *Bioorg. Med. Chem. Lett.* **2009**, *19*, 5321–5324.
63. Aida, W.; Ohtsuki, T.; Li, X.; Ishibashi, M. *Tetrahedron* **2008**, *65*, 369–373.
64. Kubota, N. K.; Ohta, E.; Ohta, S.; Koizumi, F.; Suzuki, M.; Ichimura, M.; Ikegami, S. *Bioorg. Med. Chem.* **2003**, *11*, 4569–4575.
65. Nicolaou, K. C.; Scarpelli, R.; Bollbuck, B.; Werschkun, B.; Pereira, M. M. A.; Wartmann, M.; Altmann, K. H.; Zaharevitz, D.; Gussio, R.; Giannakakou, P. *Chem. Biol.* **2000**, *7*, 593–599.
66. Gutierrez, A. J.; Terhorst, T. J.; Matteucci, M. D.; Froehler, B. C. *J. Am. Chem. Soc.* **1994**, *116*, 5540–5544.
67. Hwang, G. T.; Hari, Y.; Romesberg, F. E. *Nucleic Acids Res.* **2009**, *37*, 4757–4763.
68. Tang, B.; Yu, F.; Li, P.; Tong, L.; Duan, X.; Xie, T.; Wang, X. *J. Am. Chem. Soc.* **2009**, *131*, 3016–3023.
69. Chi, C.-C.; Chiang, C.-L.; Liu, S.-W.; Yueh, H.; Chen, C.-T.; Chen, C.-T. *J. Mater. Chem.* **2009**, *19*, 5561–5571.
70. Schubert, U. S.; Eschbaumer, C. *Org. Lett.* **1999**, *1*, 1027–1029.
71. Whittell, G. R.; Manners, I. *Adv. Mater.* **2007**, *19*, 3439–3468.
72. Havas, F.; Leygue, N.; Danel, M.; Mestre, B.; Galaup, C.; Picard, C. *Tetrahedron* **2009**, *65*, 7673–7686.
73. Yamaguchi, Y.; Kobayashi, S.; Miyamura, S.; Okamoto, Y.; Wakamiya, T.; Matsubara, Y.; Yoshida, Z.-i. *Angew. Chem.* **2004**, *116*, 370–373.
74. Fischer, F. C.; Havinga, E. *Recl. Trav. Chim. Pays-Bas-J. Roy. Neth. Chem. Soc.* **1974**, *93*, 21–24.
75. Tyrrell, E.; Brookes, P. *Synthesis* **2003**, 469–483.
76. Bailey, T. R. *Tetrahedron Lett.* **1986**, *27*, 4407–4410.
77. Littke, A. F.; Schwarz, L.; Fu, G. C. *J. Am. Chem. Soc.* **2002**, *124*, 6343–6348.
78. Luzung, M. R.; Patel, J. S.; Yin, J. *J. Org. Chem.* **2010**, *75*, 8330–8332.
79. Li, H.; Sundararaman, A.; Venkatasubbaiah, K.; Jäkle, F. *J. Am. Chem. Soc.* **2007**, *129*, 5792–5793.

80. Dick, G. R.; Woerly, E. M.; Burke, M. D. *Angew. Chem. Int. Ed.* **2012**, *51*, 2667–2672.
81. Fujii, S.; Chang, S. Y.; Burke, M. D. *Angew. Chem. Int. Ed.* **2011**, *50*, 7862–7864.
82. Fujita, K.; Matsui, R.; Suzuki, T.; Kobayashi, S. *Angew. Chem. Int. Ed.* **2012**, Early View.
83. Mohamed, Y. M. A.; Hansen, T. V. *Tetrahedron Lett.* **2011**, *52*, 1057–1059.
84. Gray, K. C.; Palacios, D. S.; Dailey, I.; Endo, M. M.; Uno, B. E.; Wilcock, B. C.; Burke, M. D. *Proc. Natl. Acad. Sci. U. S. A.* **2012**, *109*, 2234–2239.
85. Grob, J. E.; Nunez, J.; Dechantsreiter, M. A.; Hamann, L. G. *J. Org. Chem.* **2011**, *76*, 10241–10248.
86. Delaunay, T.; Es-Sayed, M.; Vors, J. P.; Monteiro, N.; Balme, G. *Chem. Lett.* **2011**, *40*, 1434–1436.
87. Colgin, N.; Flinn, T.; Cobb, S. L. *Org. Biomol. Chem.* **2011**, *9*, 1864–1870.
88. Brak, K.; Ellman, J. A. *J. Org. Chem.* **2010**, *75*, 3147–3150.
89. Pattison, G.; Piraux, G.; Lam, H. W. *J. Am. Chem. Soc.* **2010**, *132*, 14373–14375.
90. Brak, K.; Ellman, J. A. *Org. Lett.* **2010**, *12*, 2004–2007.
91. Pangborn, A. B.; Giardello, M. A.; Grubbs, R. H.; Rosen, R. K.; Timmers, F. J. *Organometallics* **1996**, *15*, 1518–1520.
92. Still, W. C.; Kahn, M.; Mitra, A. *J. Org. Chem.* **1978**, *43*, 2923–2925.
93. Knapp, D. M.; Gillis, E. P.; Burke, M. D. *J. Am. Chem. Soc.* **2009**, *131*, 6961–6963.

CHAPTER 3

Attempted Glycosylation of AmB via Intramolecular Aglycone Delivery

This chapter describes the design and execution of two separate syntheses targeting a mycosamine sugar donor which could be used in the glycosylation of BB2 as part of the ICC approach to the AmB total synthesis. The second of these syntheses successfully yielded a mycosamine donor which was used to investigate the feasibility of a glycosylation approach known as intramolecular aglycone delivery (IAD) to attach the mycosamine sugar appendage to BB2 with the requisite stereochemistry. Ultimately, this IAD approach did not yield a practical solution to this important problem. Ian Dailey prepared compounds **3.5**, **3.51a**, **3.51b**, and contributed the results presented in Scheme 3.8. Justin Struble prepared compound **3.42** and contributed to the development of the mycosamine synthesis detailed in Schemes 3.5–3.6.

3-1 BACKGROUND

In the context of our goal of obtaining single-deletion derivatives of AmB, the synthesis and attachment of the mycosamine sugar is of particular significance. The mycosamine sugar has been shown to be critical AmB's ability to bind ergosterol and its activity against yeast cells.[1] To further probe the specific mechanistic role of the sugar, three of the derivatives targeted by our laboratory involve its modification. This demands flexibility in any proposed mycosamine sugar synthesis. In addition, a "wild type" sugar donor is also necessary to complete each of the remaining derivatives lacking a hydroxyl group on the macrolactone ring. Despite its importance, attempts to date at installing mycosamine donors onto polyene macrolides have not produced satisfactory results, in large part due to the fact that the mycosamine is bound to AmB macrolactone by a 1,2-*cis* linkage, which is notoriously difficult to form.[2-3] This difficulty in glycosylation arises primarily due to the axial orientation of the alcohol substituent at the C2' position of the mycosamine sugar. This axial substituent shields the β-face of the sugar, leading primarily to α-selective glycosylation.

Various methods have been developed to overcome this inherent challenge, including S_N2-type displacement of anomeric halides,[4-5] use of participating solvents,[6] long-range substituent participation,[7-8] and steric direction.[9-11] Unfortunately, these methods still often lead to anomeric mixtures of products. More recently, the strategy of "intramolecular aglycone

delivery" (IAD) has emerged.[12-15] The general strategy is shown in Figure 3.1, in which the nucleophile is tethered to the sugar donor, and upon activation at the anomeric position nucleophilic attack proceeds in an intramolecular, stereospecific manner, with the stereochemical outcome determined by the configuration at C2. IAD reactions generally proceed with complete stereocontrol, and currently represent the state of the art in the formation of 1,2-*cis* glycosidic linkages, though limitation still remain with respect to the generality of activating conditions and formation of undesired byproducts.[16]

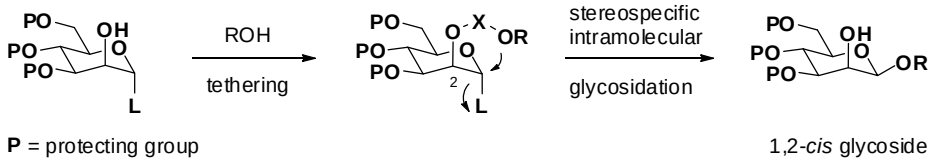

Figure 3.1. Intramolecular aglycone delivery (IAD) enables direct formation of 1,2-*cis* glycosides. After tethering of the nucleophile to a neighboring hydroxyl via a linker, **X**, subsequent delivery of the nucleophile upon activation of the leaving group proceeds stereospecifically from the tethered face of the sugar.

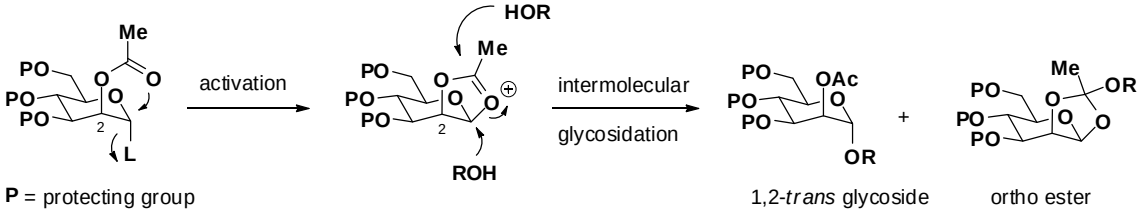

Figure 3.2. Neighboring group participation (also known as anchimeric assistance) provides excellent stereocontrol for the formation of 1,2-*trans* glycosides. In this strategy, a participating protecting group, such as the acetate shown, coordinates to the anomeric carbon following activation, thus blocking top face of the sugar from nucleophilic attack. Note that alternative attack directly onto the acetoxonium ion produces an undesired ortho ester byproduct.

In his classic 1988 synthesis of AmB, Nicolaou and coworkers addressed the problem of the 1,2-*cis* glycosidic bond in AmB by instead initially glycosylating their AmB aglycone with a C2'-epimycosamine donor (**3.2**), using neighboring group participation.[17] As seen in Figure 3.2 in this approach activation of the anomeric tricholoroacetimidate leads to a cyclic oxonium ion, in which the C2-acetate group effectively blocks one face of the sugar, leading to very selective formation of the 1,2-*trans* glycosidic bond.[6,16] Subsequent inversion of the C2 substituent provides the desired 1,2-*cis* configuration. Unfortunately, despite the excellent stereoselectivity obtained, this approach suffered from a low overall yield due to poor conversion in the

glycosylation reaction, as well as a significant amount of ortho ester byproduct (Scheme 3.1).[17] In a later synthesis of C35deOAmB methyl ester, Carreira and coworkers refined this approach to somewhat improve the overall yield, but were unable to solve the problem of competing ortho ester formation, which in this case proved inseparable from the successfully glycosylated product.[18] Underscoring the difficulty inherent to this glycosylation, Rychnovsky and coworkers struggled to attach the sugar to the rimocidin agylcone.[19] Attempting to utilize the Stork variant of the IAD approach, they concluded that the rimocidin aglycone was too poor of a nucleophile to form the desired glycosidic bond with this approach.

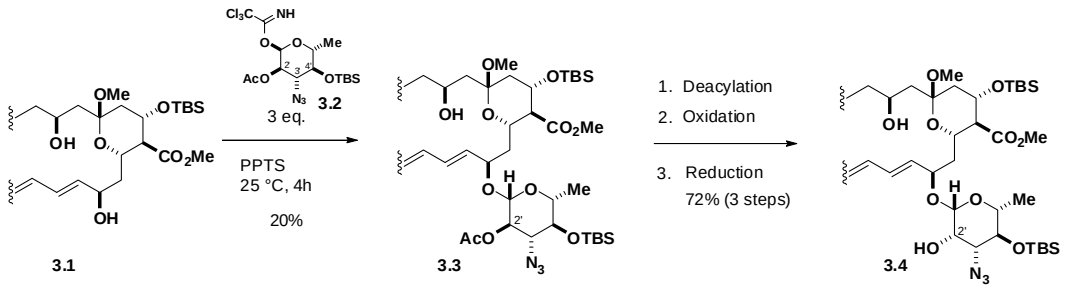

Scheme 3.1. Nicolaou's glycosylation strategy. The low yield in the glycosylation step was due to both poor conversion of **3.1** and formation of an undesired ortho ester byproduct.

With this precedent in mind we decided to attempt to utilize the more recently developed parамethoxybenzyl (PMB) variant of the IAD reaction.[20] In this approach, developed by Ito and coworkers, the sugar and nucleophile are tethered by a PMB-acetal linker. Yields for the PMB IAD variant are generally superior to those for the Hindsgaul and Stork approaches.[16] Additionally, the PMB linker provides a handle to tune the electronics of the system, in that placement of additional electron donating groups on the benzyl ring can improve the glycosylation yield.[21] Further, to maximize the overall efficiency and modularity of the AmB synthesis, we decided to incorporate the sugar not onto the AmB aglycone at the conclusion of the synthesis, but rather as part of BB2 (Scheme 3.2) prior to assembly of the building blocks via ICC (Figure 3.3). We believed this would also serve to address the known problem of poor nucleophilicity of the AmB aglycone by allowing us to use the smaller, less electron deficient **3.5** in our glycosylation reaction.

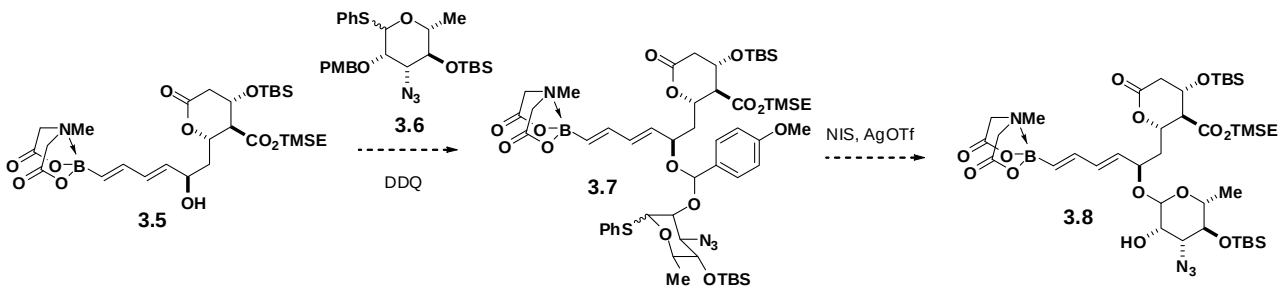

Scheme 3.2. Proposed IAD strategy for glycosylation of BB2.

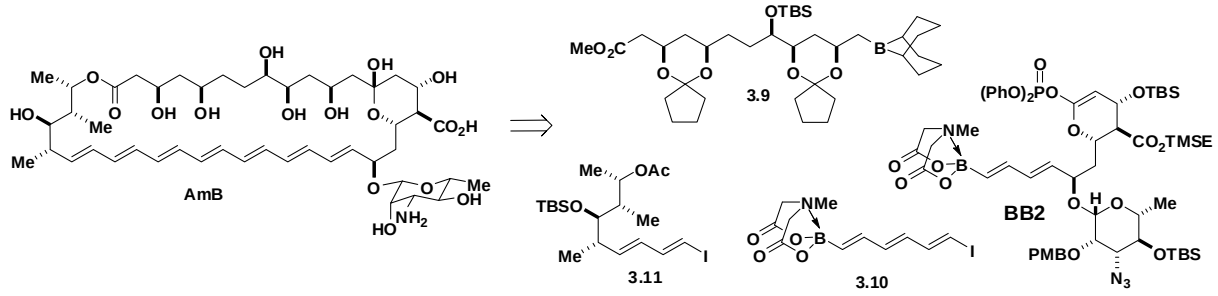

Figure 3.3. AmB retrosynthesis by ICC.

3-2 1ST GENERATION MYCOSAMINE SYNTHESIS

Rather than synthesize the necessary glycoside donor for this procedure from a naturally occurring sugar, we elected to design a de novo synthesis to maximize its flexibility and the ability to access functionally deficient derivatives. Retrosynthetic analysis (Figure 3.4) of the target donor **3.6** starts with opening of the ring to aldehyde **3.12**. We noted that **3.12** could be accessed by periodate cleavage of diol **3.13**. This critical complexity-generating transform allows most of the stereocenters to be established through the stereoselective installation and opening of epoxides, directed by the adjacent hydroxyl groups. This brings us back to the relatively simple diene **3.16**, which can be accessed via SMC reaction from two relatively simple building blocks **3.17** and **3.18**. This synthetic plan was also anticipated to facilitate access to derivatives lacking functional groups targeted for deletion. Specifically, C3'deaminomycosamine could be accessed by a hydride mediated opening of epoxide **3.15**, while C4'deoxymycosamine could be accessed by desilylation and subsequent Barton deoxygenation of **3.6**.

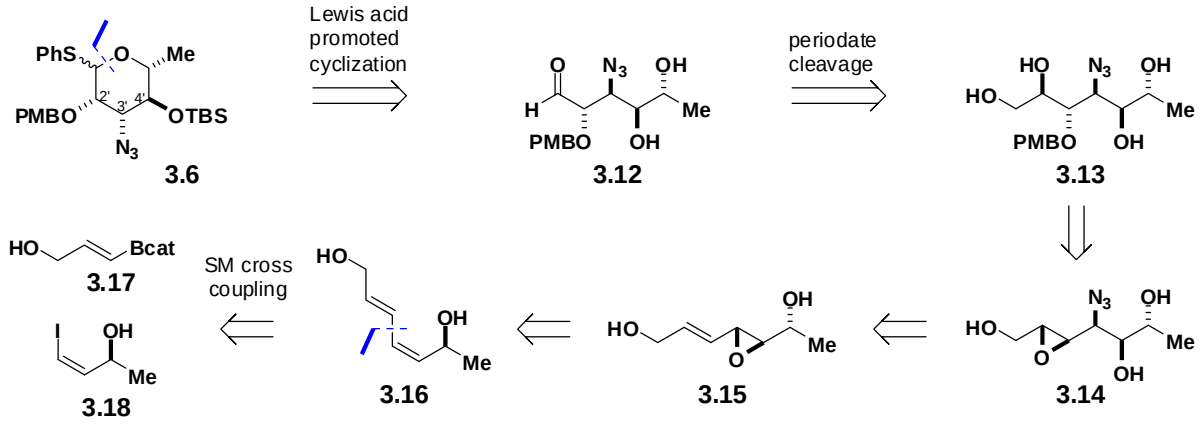

Figure 3.4. 1st generation mycosamine retrosynthesis.

To investigate the feasibility of the proposed route, an initial racemic synthesis of **3.6** commenced with the construction of coupling partners ±**3.18** and **3.19** (Scheme 3.3). Silylation of propargyl alcohol and subsequent hydroboration with catecholborane provided catacholboronic ester **3.19** as a viscous oil. Iodination of commercially available 3-butyn-2-ol, followed by syn-reduction of the alkyne with potassium azodicarboxylate (PADC) afforded the (*Z*)-vinyl iodide ±**3.18** in 84% yield. ±**3.18** and **3.19** were then cross-coupled with $Pd(PPh_3)_4$ to give diene ±**3.20**, effectively completing the carbon framework of the sugar.

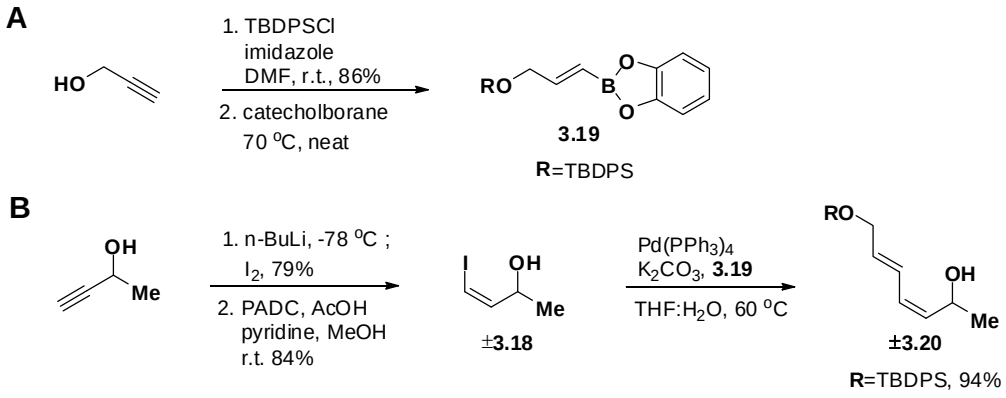

Scheme 3.3. (A) Synthesis of building block **3.19** (B) Synthesis of diene ±**3.20.**

Encouraged by these initially auspicious results, we proceeded forward with the planned functionalization **3** As seen in Figure 3.5A, treatment of diene ±**3.20** with *m*-CPBA resulted in a diastereo- and regioselective epoxidation, directed by the allylic hydroxyl group, to afford the *threo* epoxyalcohol, which was then inverted by a Parikh-Doering oxidation of the alcohol to the

corresponding ketone and a subsequent selective reduction with $Zn(BH_4)_2$ to afford the *erythro* epoxy alcohol ±**3.21**.[22-23] In the initial design of the route, the amine on the sugar was to be installed and carried through the synthesis as an azide, and in fact the opening of the epoxide with NaN_3 at 0 °C proceeded smoothly, installing the nitrogen with excellent selectivity at the allylic position to give ±**3.22**. However, upon warming the reaction solution to room temperature, the resulting ±**3.22** underwent an unanticipated [3,3]-sigmatropic rearrangement to afford ±**3.23** (Figure 3.5A). Despite the reversibility of this process, the undesired constitutional isomer was heavily favored, and the rearrangement was fast at room temperature. To avoid this rearrangement the route was modified by instead opening epoxide ±**3.21** with ammonia and protecting the resulting secondary amine as the Fmoc carbamate, ±**3.24** (Figure 3.5B).

Ketalization of ±**3.24** with 2,2-dimethoxypropane and catalytic PPTS, followed by desilylation with HF·pyridine yielded the racemic allylic alcohol ±**3.25**. Subsequent Sharpless epoxidation proceeded smoothly giving a 1:1 mixture of diastereomeric products **3.26** and **3.27** (the diastereomeric mixture being the expected result of performing the catalyst controlled, asymmetric epoxidation on a racemic substrate), but the resulting epoxy alcohol appeared recalcitrant to opening with PMBOH and $Ti(O\text{-}i\text{-}Pr)_4$, despite literature precedent suggesting the facility of this transformation.[24-26] The use of $ZnCl_2$ and various other solvents were similarly ineffective, while temperatures above 60 °C resulted in rapid Fmoc deprotection. Additionally, it was observed that while Fmoc group was stable at or below 40 °C, at these temperatures **3.26** and **3.27** rapidly decomposed to a variety of unidentified products, with no desired product observed even by mass spectrometry. We hypothesized that the unanticipated addition of an adjacent carbamate may have interfered with proper Lewis acid complexation, as in the absence of a Lewis acid catalyst, alcohols are known to be ineffective nucleophiles for this transformation.[27]

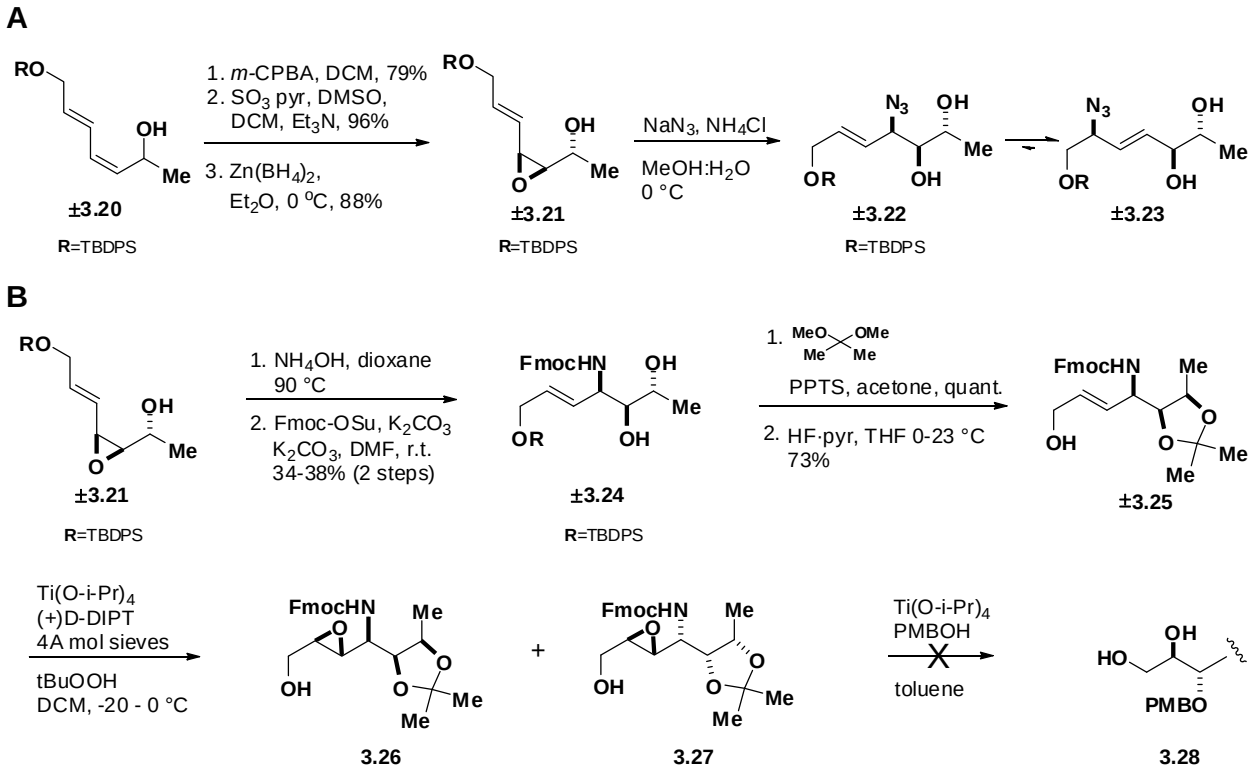

Figure 3.5. (A) Azide opening of epoxide ±**3.21** resulted in a [3,3]-sigmatropic rearrangement. (B) Substitution of Fmoc for azide enabled isolation of the desired protected amino alcohol ±**3.24**. Unfortunately, with the amine thus protected all attempts at opening epoxides **3.26** and **3.27** were unsuccessful.

3-3 2ND GENERATION MYCOSAMINE SYNTHESIS

Our inability to access **3.28** prompted us to consider alternative routes to mycosamine donor **3.6**. We were inspired by a recent publication by the White group, in which they demonstrated a streamlining of Trost and coworkers' 1987 synthesis of acosamine[28] through the use of a novel Pd-catalyzed diastereoselective allylic C-H amination reaction (Figure 3.6).[29] As acosamine differs from mycosamine only in that is lacks oxygenation at C2', we reasoned that we could adapt this new, efficient route to target **3.6**. As seen in Figure 3.6B, we reasoned that substitution of a Sharpless asymmetric dihydroxylation reaction[30] for the known hydroboration in the Trost route would afford **3.33**, which contains the necessary oxygenation at the carbon that ultimately becomes C2' in mycosamine.

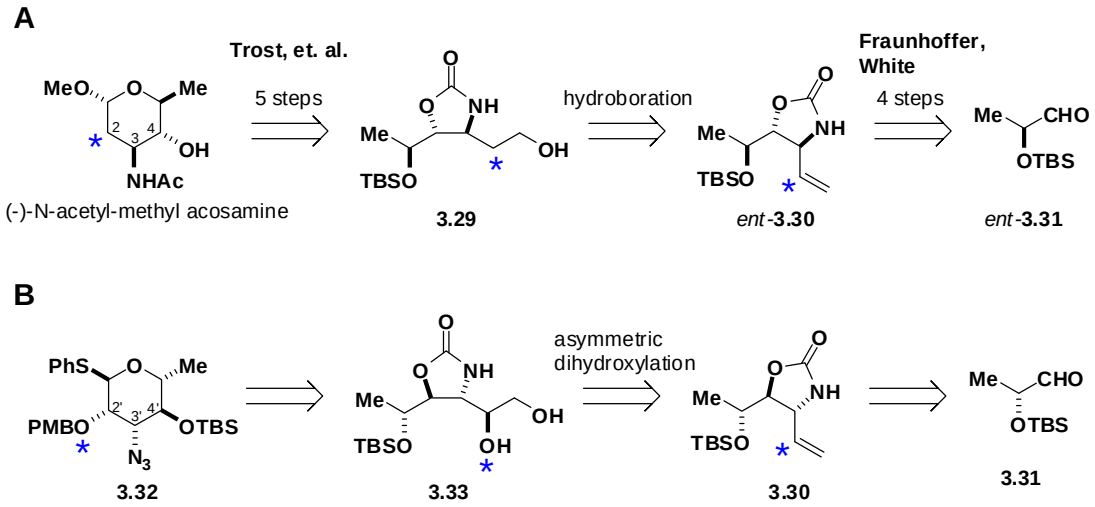

Figure 3.6. (A) A new diastereoselective C-H amination reaction allows rapid access to *ent*-**3.30**, which has been elaborated by Trost and coworkers to the sugar acosamine. (B) Substitution of a dihydroxylation reaction for the hydroboration in the Trost route was envisioned to afford a sugar, **3.32**, with the desired oxygenation at C2'.

In the forward direction, synthesis of **3.32** began with commercially available D-ethyl lactate (**3.34**) (Scheme 3.4) Protection of the alcohol as the TBS ether, followed by DIBAL-H reduction of the ethyl ester to the aldehyde set up a Brown allylation to afford homoallylic alcohol **3.35**. Subsequent formation of the N-tosylcarbamate, followed by allylic C-H oxidation with the White catalyst provided the key intermediate, oxazolidinone **3.37**, in a 9:1 d.r. and 75% yield. Column chromatography, followed by recrystallization from Et_2O provided **3.37** as a diastereomerically pure, colorless, and air-stable solid. This sequence proved not only efficient but also quite scalable, enabling the isolation of 170 g of **3.36**, and the subsequent White oxidation could be run on 25 g scale. The efficient isolation of **3.37** enabled us to test the proposed dihydroxylation.

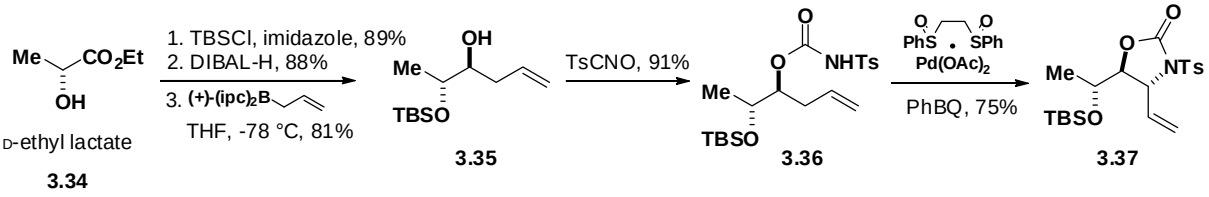

Scheme 3.4. Initial sequence toward the key intermediate, oxazolidinone **3.37**, from D-ethyl lactate.

As seen in Figure 3.7, deprotection of **3.37** with sodium naphthalide, as per the Trost route, provided oxazolidinone **3.30** in very high yield. However, subsequent dihydroxylation was

essentially unselective, giving products **3.33** and **3.38** with a d.r. of 1:1. We hypothesized that the neighboring unprotected nitrogen might be accelerating a background, ligand-free reaction, and found that performing the dihydroxylation prior to deprotection of the N-tosylate gave excellent selectivity, providing the desired diol **3.39** as a single diastereomer. The use of acetone as a co-solvent was found to be necessary due to the insolubility of both the chincona alkaloid ligand and substrate in mixtures of *t*-BuOH:H_2O. Additionally, despite literature reports of the superiority of the pyrazine-based ligands for terminal olefin substrates,[31-32] we found that the phthalazine based ligand $(DHQ)_2PHAL$ gave equally selectivity, while also being much more soluble, and giving higher yields with a substantially reduced reaction time.

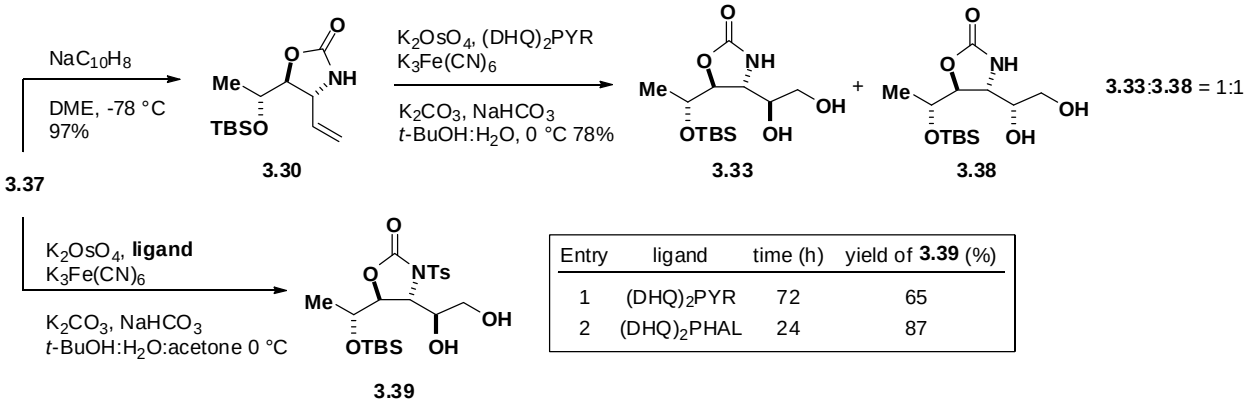

Entry	ligand	time (h)	yield of **3.39** (%)
1	$(DHQ)_2PYR$	72	65
2	$(DHQ)_2PHAL$	24	87

Figure 3.7. Dihydroxylation of **3.30** gave a 1:1 mixture of diastereomeric products **3.33** and **3.38**. Alternatively, dihydroxylation of **3.37**, prior to deprotection of the N-tosylate, gave the desired diol **3.39** as a single diastereomer, with a much faster reaction and superior yields observed using the phthalazine-based dihydroxylation catalyst.

Interestingly, unlike the corresponding reaction with olefin **3.37**, attempts to deprotect the N-tosylate of diol **3.39** with sodium naphthalide proceeded with extremely variable yields, ranging from 19–84%. Alternately as seen in Scheme 3.5, we found that **3.39** could be deprotected with magnesium powder in MeOH with much more reproducible results, though here the reaction was heavily dependent on the conditions selected. Specifically, sonication was found to be essential, and the use of 325-mesh magnesium at 0 °C maximized conversion while limiting undesired side products, allowing isolation of the product on 10 g scale in a very acceptable 90% yield (Scheme 3.5). Selective protection of the secondary alcohol as a PMB ether was effected by first forming PMP ketal **3.40**, followed by treatment of **3.40** with DIBAL-H, which opens the ketal from the less hindered terminal position, giving the desired secondary

PMB-protected alcohol (**3.41**) in 61% yield after chromatography. Oxidation of the remaining primary alcohol under Swern conditions, and subsequent reaction with CSA and trimethylformate afforded **3.42**, with the dimethyl acetal serving as a masked aldehyde. Finally, treatment of **3.42** with aqueous sodium hydroxide, which achieved hydrolysis of the oxazolidinone with concomitant deprotection of the TBS-ether, followed by protection of the resulting secondary amine with imidazolyl azide reagent **3.43**[33-34] gave the linear intermediate **3.44**, ready for acid-mediated cyclization.

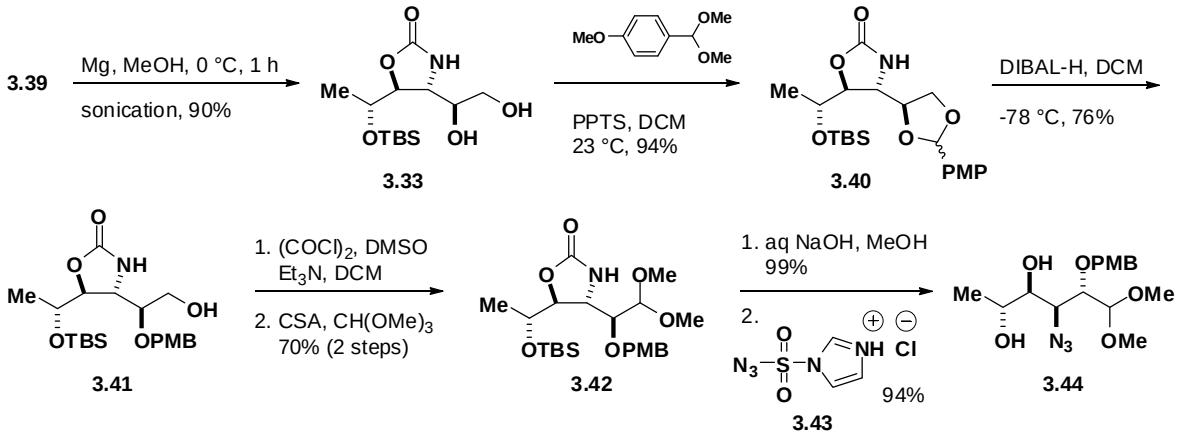

Scheme 3.5. 2nd generation synthesis of mycosamine, part 2.

Treatment of **3.44** with CSA effectively promoted cyclization (Scheme 3.6). However, after TBS-protection of the remaining alcohol and installation of the C1'-sulfide via Hanessian's conditions,[35] an X-ray crystal structure obtained for **3.46** identified it as the five-membered furanose sugar, rather than the desired pyranose. Treatment of **3.44** instead with HCl in methanol provided the desired pyranose sugar **3.47**, albeit with concomitant loss of the C2'-PMB group. After TBS protection of the C2' and C4' alcohols, installation of the sulfide at C1' was in this case found to be more efficient through the intermediacy of an acetate, which was then converted to phenylsulfide **3.48** in nearly quantitative yield. The C2' and C4' positions were then re-differentiated by desilylation with HF·pyr, followed by a selective monosilylation at C4' using 1 equivalent of TBSCl to finally provide mycosamine sugar donor **3.49**.

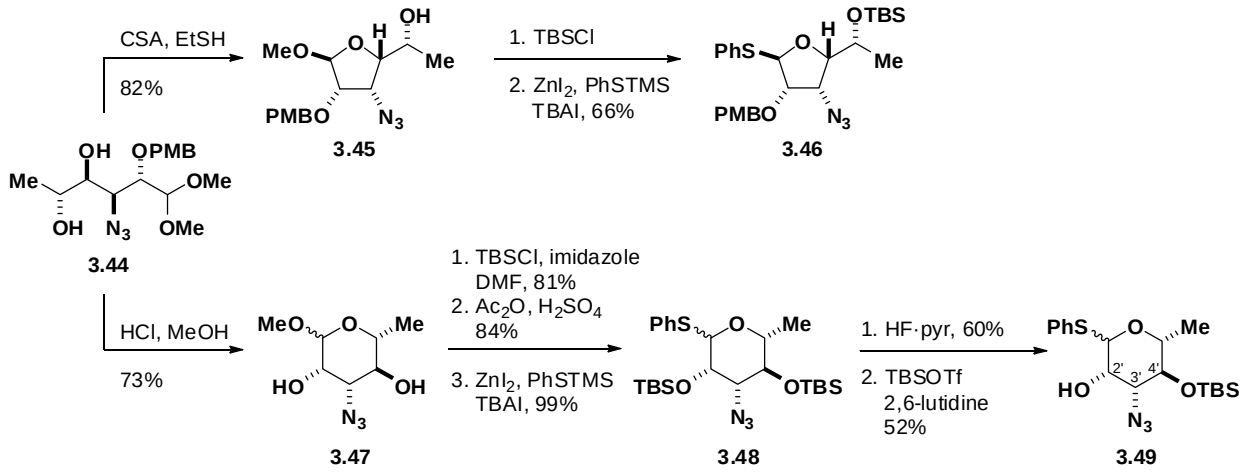

Scheme 3.6. 2nd generation synthesis of mycosamine part 3.

3-4 ATTEMPTS AT INTRAMOLECULAR AGLYCONE DELIVERY

While isolation of furanose glycosyl donor **3.46** was not useful in the long run for the synthesis of BB2 or AmB, it did provide an opportunity to initially investigate the feasibility of the IAD strategy while a route to the desired pyranose glycosyl donor was being pursued. To this end, **3.46** was exposed to BB2 aglycone **3.5** under a variety of oxidative conditions in an attempt to form the corresponding linked benzylidene acetal (Scheme 3.7). However, in no case was successful linkage observed due to the facile oxidation of the BB2 acceptor to enone **3.50**.

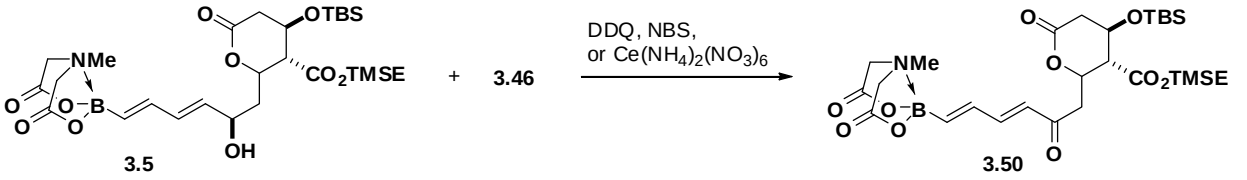

Scheme 3.7. Attempts to link **3.5** and **3.46** for IAD revealed the sensitivity of the dienyl alcohol **3.5** to oxidation.

With these results in mind, upon successful isolation of pyranose **3.49**, which contains a free hydroxyl at C2', we decided to, rather than reinstall the lost PMB group, instead attempt linkage with benzylated acceptors **3.51a**, reasoning that an allylic benzyl ether might be less prone to oxidation than **3.5**. Thus, we exposed **3.51a** to **3.49** in the presence of DDQ (Scheme 3.8). Again, none of the desired linked product was detected, though we did observe significant loss of the benzyl ether from **3.51a**. Similar results were observed with benzylated BB2 acceptor **3.51b**.

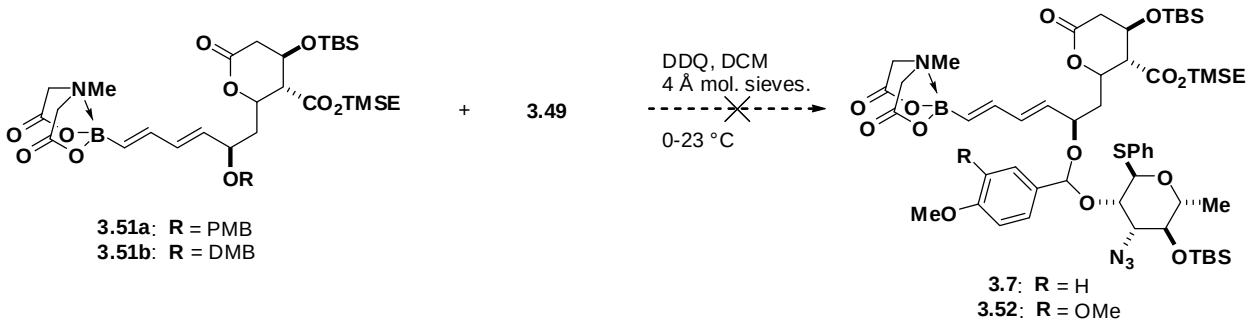

Scheme 3.8. Attempts to link mycosamine donor **3.49** to benzylated BB2 acceptors **3.51a** and **3.51b** were unsuccessful, with the primary product of the reaction being allylic alcohol **3.5** and enone **3.50**.

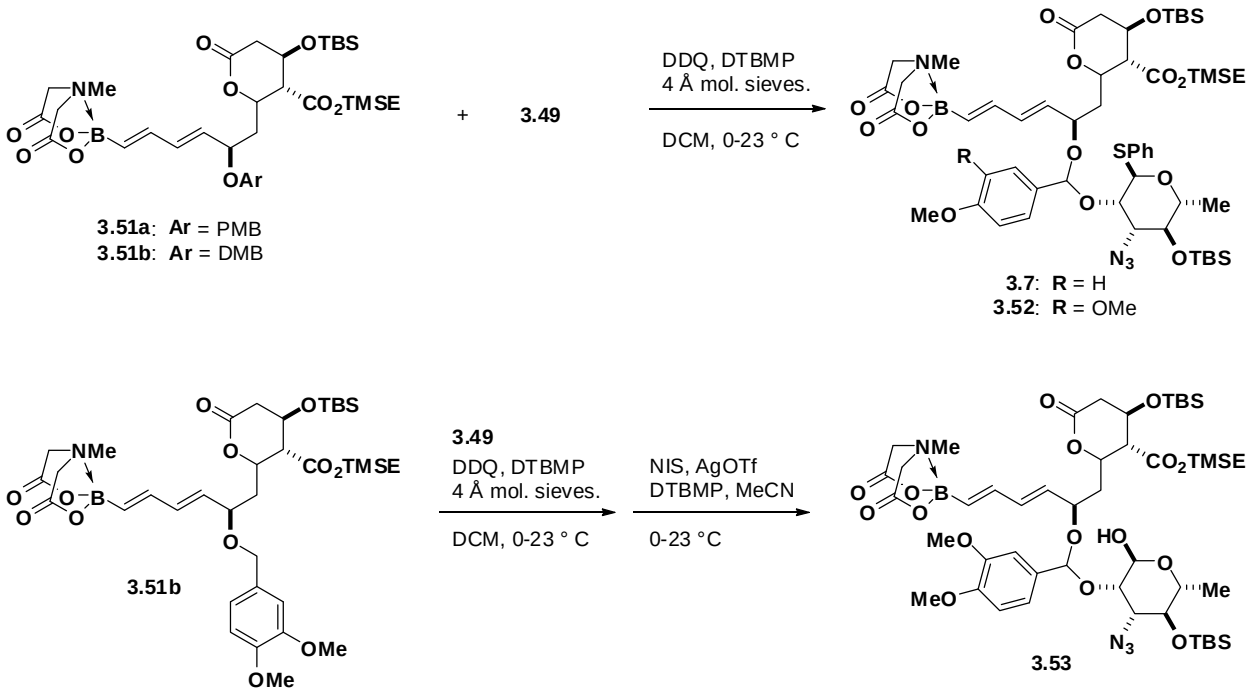

Scheme 3.9. The use of DTBMP to buffer the linkage reaction enabled formation of **3.7** and **3.52**. However, these acetals were found to be too unstable to isolate, and all attempts at glycosyl transfer on the crude linkage products were unsuccessful, only yielding hemiacetal **3.53**, suggestive of the poor nucleophilicity of **3.5**.

The observation of significant debenzylation of **3.51a** and **3.51b** suggested that activation of the benzyl ether was not the problem, and we hypothesized that the desired benzylidene acetal product might be unstable to the acidic byproducts of DDQ oxidation. Thus we investigated running these reactions in the presence of an amine base. As seen in Scheme 3.9, exposure of mycosamine donor **3.49** to benzylated BB2 donors **3.51a** and **3.51b** in the presence of DDQ and DTBMP, clean conversion to the desired benzylidene acetal was finally observed by mass

spectrometry. However, clean isolation of this intermediate was not possible due to its instability to chromatography. Further, all attempts to initiate glycosyl transfer by activation of the C1' sulfide following linkage were unsuccessful (Scheme 3.9). Isolation of hemiacetal **3.53** as a byproduct of attempted glycosylation reactions suggested that activation of the anomeric position was successful, but that transfer of the allylic alcohol was not. Collectively, these results led us to finally conclude that the IAD strategy for glycosylation of BB2 aglycone would not be possible, due to both the instability of the intermediate benzylidene acetal, and the poor nucleophilicity of the BB2 acceptor. Chapter 4 details the development of an alternative approach which ultimately enabled successful glycosylation of BB2 and the AmB aglycone.

3-5 EXPERIMENTAL SECTION

Materials.

Commercial reagents were purchased from Sigma-Aldrich, Fisher Scientific, Alfa Aesar, TCI America Frontier Scientific, Oakwood Products or Combi-Blocks and were used without further purification unless otherwise noted. Solvents were purified via passage through packed columns as described by Pangborn and coworkers[36] (THF, Et_2O, MeCN, DCM: dry neutral alumina; hexane, benzene, and toluene: dry neutral alumina and Q-5 reactant (copper(II) oxide on alumina); DMSO, DMF: activated molecular sieves). All water was deionized prior to use. Triethylamine, diisopropylamine, diethylamine, pyridine, and 2,6-lutidine were freshly distilled under an atmosphere of nitrogen from CaH_2. The following compounds were prepared according to procedures reported in the literature: **3.30**,[28] **3.35**,[29,37-38] **3.36**,[29] **3.37**,[29] **3.43**,[33-34]

General Experimental Procedures.

Unless otherwise noted, all reactions were performed in flame-dried glassware under argon. Organic solutions were concentrated via rotary evaporation under reduced pressure with a bath temperature of 35-40 ºC. Reactions were monitored by analytical thin layer chromatography (TLC) performed using the indicated solvent on E. Merck silica gel 60 F254 plates (0.25mm). Compounds were visualized by: exposure to a UV lamp (λ = 254 or 366 nm), incubation in a glass chamber containing iodine, and/or treatment with a solution of $KMnO_4$, an acidic solution of p-anisaldehyde or a solution of ceric ammonium molybdate (CAM) followed by brief heating with a Varitemp heat gun. MIDA boronates are compatible with standard silica gel

chromatography, including standard loading techniques. Column chromatography was performed using standard methods[39] or with a Teledyne-Isco CombiFlash R_f purification system. Both methods were performed using Merck silica gel grade 9385 60 Å (230-400 mesh).

Structural analysis.

^{1}H-NMR spectra were recorded at 23 °C on a Varian Unity or a Varian Unity Inova 500 MHz spectrometer. Chemical shifts (δ) are reported in parts per million (ppm) downfield from tetramethylsilane and referenced to residual protium in the NMR solvent ($CHCl_3$, δ = 7.26; CD_2HCN, δ = 1.93, center line; acetone-d_6 δ = 2.04, center line). Alternatively, NMR-solvents designated as "w/ TMS" were referenced to tetramethylsilane (δ = 0.00 ppm) added as an internal standard. Data are reported as follows: chemical shift, multiplicity (s = singlet, d = doublet, t = triplet, q = quartet, quint = quintet, sept = septet, m = multiplet, br = broad, app = apparent), coupling constant (*J*) in Hertz (Hz), and integration. ^{13}C NMR spectra were recorded at 23 °C on a Varian Unity 500 MHz spectrometer. Chemical shifts (δ) are reported in ppm downfield from tetramethylsilane and referenced to carbon resonances in the NMR solvent ($CDCl_3$, δ = 77.0, center line; CD_3CN, δ = 1.30, center line, acetone-d_6 δ = 29.80, center line) or to added tetramethylsilane (δ = 0.00). Carbons bearing boron substituents were not observed (quadrupolar relaxation). ^{11}B NMR were recorded using a General Electric GN300WB instrument and referenced to an external standard of ($BF_3 \cdot Et_2O$). High resolution mass spectra (HRMS) were acquired by Furong Sun and Dr. Steve Mullen at the University of Illinois School of Chemical Sciences Mass Spectrometry Laboratory. Infrared spectra were collected from a thin film on NaCl plates or as KBr pellets on a Perkin-Elmer Spectrum BX FT-IR spectrometer, a Mattson Galaxy Series FT-IR 5000 spectrometer or a Mattson Infinity Gold FT-IR spectrometer. Absorption maxima (ν_{max}) are reported in wavenumbers (cm^{-1}).

Synthesis of compounds.

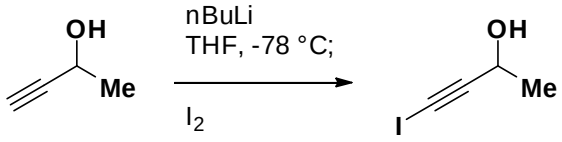

To a solution of 3-butyn-2-ol (4.11 g, 58.7 mmol) stirring in THF (125 mL) at -78 °C was added n-BuLi (1.6 M in hexanes, 76 mL, 122 mmol) dropwise. The solution was stirred at -78 °C for 30 min. Iodine (14.835 g, 58.8 mmol), dissolved in 7 mL THF was added dropwise to the stirring solution. The reaction solution was allowed to warm to r.t., and the reaction was quenched by the addition of 10 mL H_2O. The reaction was diluted with an additional 50 mL H_2O. The aqueous phase was extracted with Et_2O (2X) and the combined organic fractions were concentrated in vacuo. The resulting brown residue was taken up in Et_2O (30 mL) and washed with sat'd aq. $NaHCO_3$, aq. $NaHSO_3$ (2x) and brine. The organic phase was then dried over Na_2SO_4, filtered, and concentrated in vacuo. The resulting brown oil purified by column chromatography (SiO_2, hexanes:EtOAc 3:1 + 1% Et_3N) to give a brown oil (9.4 g, 83%) contaminated with a small amount of Et_3N.

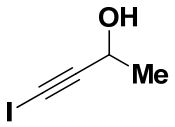

TLC (hex:EtOAc 5:1)

R_f = 0.24 visualized by p-anisaldehyde

^{1}H-NMR (400 MHz, $CDCl_3$)

δ 4.60 (q, *J* = 6.4 Hz, 1H), 1.41 (d, *J* = 6.4 Hz, 3H).

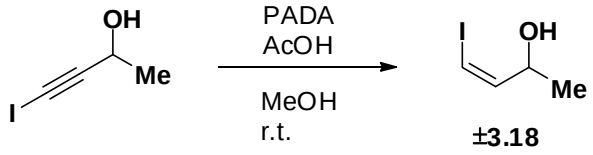

±3.18

To a solution of alkynyl iodide (8.229 g, 36.5 mmol) in MeOH (80 mL) stirring at r.t. as added potassium azodicarboxylate (PADA) (10.638 g, 54.8 mmol). AcOH (6.5 mL) was added dropwise via syringe pump over 1 h. The reaction was stirred for an additional 1 h. A second addition of PADA (10.636 g, 54.8 mmol) was made under argon flow. 6.0 mL AcOH as then added dropwise over 1 h. by syringe pump, and the reaction was allowed to stir for an additional

1 h. A third addition of PADA (10.629 g, 54.7 mmol) was made under argon flow, and an additional 6.7 mL AcOH was added dropwise over 1 h. The reaction was allowed to stir at room temp for a final 2 h. The reaction was diluted with Et_2O (100 mL) and 5% aq. HCl (100 mL). The aqueous layer as extracted with Et_2O (3 x 50 mL). The combined organic fractions were washed with brine (2 x 40 mL) and 40% aqueous Me_2NH (30 mL) The aqueous layer from the amine wash was extracted with ether, and the extract was then back washed with brine. All Et_2O fractions were dried over Na_2SO_4, filtered and conc. in vacuo to give a yellow oil. This crude material was purified by column chromatography (SiO_2, hex:acetone 5:1) to give the purified product as a pale yellow liquid (6.04 g, 84%).

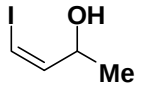

±3.18

TLC (hex:EtOAc 1:1)

R_f = 0.48 visualized by $KMnO_4$

^{1}H-NMR (400 MHz, $CDCl_3$)

δ 6.23 (m, 2H), 4.50 (m, 1H), 3.00 (d, *J* = 3.2 Hz, 1H), 1.24 (d, *J* = 6.4 Hz, 3H).

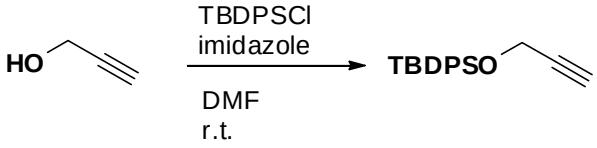

To a stirring solution of propargyl alcohol (0.963 g, 17.2 mmol) in DMF (30 mL) was added imidazole (1.841 g, 27.0 mmol), followed by *tert*-butyldiphenylchlorosilane (4.5 mL, 17.3 mmol). The resulting solution was stirred at r.t. for 17 h. The reaction was diluted with Et_2O (200 mL) and washed with water (75 mL), 5% aq. HCl (75 mL), water (75 mL), and brine (75 mL). The organic phase was then concentrated in vacuo. The resulting liquid was purified by passage through a plug of silica with hexanes (4.35 g, 86%).

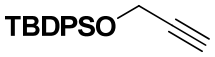

TLC (hex:EtOAc 1:1)

R_f = 0.78 visualized by $KMnO_4$

^{1}H-NMR (400 MHz, $CDCl_3$)

δ 7.78 (m, 4H), 7.46 (m, 6H), 4.37 (d, *J* = 2.4 Hz, 2H), 2.43 (t, *J* = 2.4 Hz, 1H), 1.14 (s, 9H)

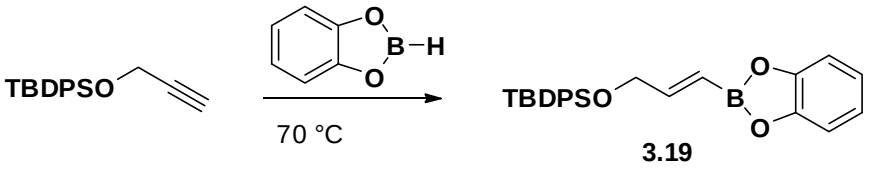

3.19

To a dry 10 mL flask equipped with a stir bar was added alkyne (1.516 g, 5.15 mmol) and catecholborane (0.66 mL, 6.19 mmol). The resulting mixture was stirred at 70 °C for 8 h. After cooling to r.t., the resulting viscous oil was used without further purification.

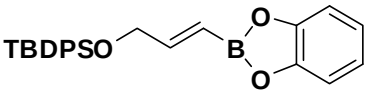

3.19

TLC (hex:EtOAc 1:1)

R_f = 0.5 (streaks) visualized by $KMnO_4$

^{1}H-NMR (400 MHz, $CDCl_3$)

δ 7.72 (m, 4H), 7.43 (m, 6H), 7.26 (m, 2H), 7.11 (m, 2H), 6.36 (dt, *J* = 18, 2.4 Hz, 1H), 4.42 (dd, *J* = 3.6, 2.4 Hz, 2H), 1.14 (s, 9H)

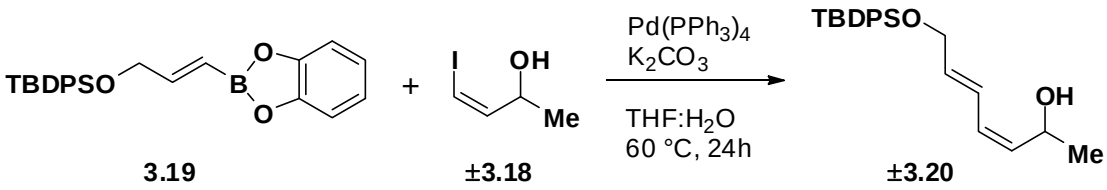

Catecholboronic ester **3.19** (1.859 g, 4.5 mmol) was transferred to a 40 mL IChem vial with 15 mL THF. Vinyl iodide **±3.18** (0.602 g, 3.0 mmol) was added to the vial by syringe, followed by K_2CO_3 (1.240 g, 9.0 mmol). The vial was thoroughly flushed with argon, sealed with a PTFE-lined septum screw cap, and brought into the glovebox. In the glovebox, $Pd(PPh_3)_4$ (0.0695 g, 0.06 mmol) was massed into a 7 mL vial, and quantitatively transferred to the reaction vial with 3 mL THF. The reaction vial was sealed, and removed from the glovebox. H_2O (15 mL) was added via syringe. The resulting mixture was maintained with stirring at 60 °C for 24 h. After cooling to r.t., the reaction was transferred to a separatory funnel and the aqueous layer was removed. The organic layer was washed with brine, and then H_2O. The organic fraction was then concentrated in vacuo, and purified by column chromatography (SiO_2, hexanes:EtOAc 3:1) to give **±3.20** as a colorless liquid (0.981 g, 94%).

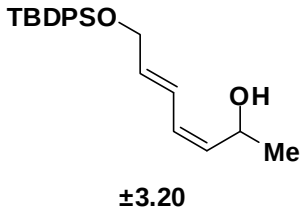

±3.20

TLC (hex:EtOAc 1:1)

R_f = 0.58 visualized by $KMnO_4$

^{1}H-NMR (400 MHz, $CDCl_3$)

δ 7.70 (m, 4H), 7.42 (m, 6H), 6.61 (m, 1H), 6.02 (t, *J* = 10.8 Hz, 1H), 5.82 (dt, *J* = 15, 4.8 Hz, 1H), 5.44 (m, 1H), 4.79 (quint, *J* = 6 Hz, 1H), 4.29 (dd, *J* = 4.8, 1.6 Hz, 1H), 1.29 (d, *J* = 6.4 Hz, 3H), 1.09 (s, 9H)

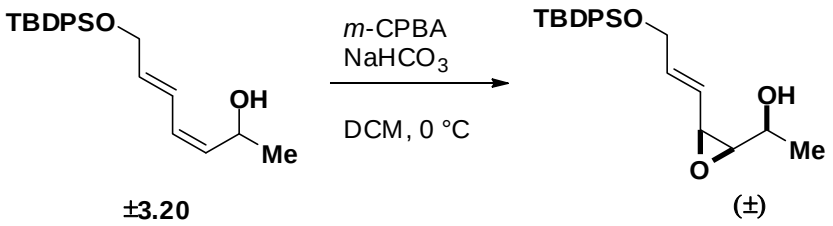

±3.20 (±)

To mixture of **±3.20** (0.689 g, 1.88 mmol), and sodium bicarbonate (0.315 g, 3.75 mmol), stirring at 0 °C in CH_2Cl_2 (12 mL) was added solid m-CPBA (0.566 g, 2.46 mmol). The reaction was stirred at 0 °C for 1 h. Me_2S (70 μL) was added, and the reaction was allowed to stir for an additional 5 min. The reaction mixture was diluted with Et_2O and sat'd aq. $NaHCO_3$. The aqueous phase was extracted once with ether. The combined organic fractions were washed with brine, dried over Na_2SO_4 and concentrated in vacuo. The resulting crude material was purified by column chromatography (SiO_2, hexanes:EtOAc 2:1 , 0.5% Et_3N) to give pure product (0.428 g, 60%).

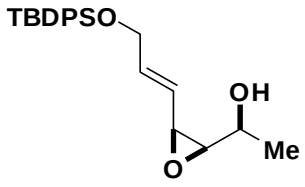

(±)

TLC (hex:EtOAc 1:1)

R_f = 0.48 visualized by p-anisaldehyde

^{1}H-NMR (500 MHz, $CDCl_3$)

δ 7.66 (m, 4H), 7.41 (m, 6H), 6.03 (dt, *J* = 16, 4 Hz, 1H), 5.70 (qt, *J* = 16, 8, 2 Hz, 1H), 4.24 (m, 2H), 3.66 (m, 1H), 3.57 (dd, *J* = 7.5, 4.5 Hz, 1H), 3.06 (dd, *J* = 8, 4.5 Hz, 1H), 2.16 (d, *J* = 3 Hz, 1H), 1.24 (d, *J* = 6.5 Hz, 3H), 1.06 (s, 9H)

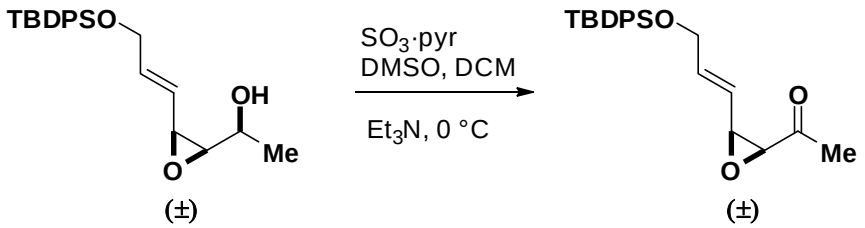

A flame dried round bottom flask was charged with DCM (4 mL), DMSO (10 mL), and alcohol epoxy alcohol substrate (0.335 g, 0.876 mmol). The solution was cooled, stirring, to 0 °C. In a separate 10 mL pear flask SO_3·pyr was suspended in DCM (2.5 mL). DMSO (5 mL) and Et_3N (0.52 mL) were added to the pear, flask, and after the suspension had become a clear solution, the contents of the pear flask were cannulated dropwise into the reaction flask. The pear flask was rinsed with DCM (2 mL) and DMSO (5 mL), and this rinse was cannulated over as well. The reaction stirred at 0 °C for 6 h. The reaction was poured into 50 mL ether:pentane 1:1 + 50 mL ½-sat'd NH_4Cl. the Aqueous layer was separated and extracted with ether:pentane 1:1 (3x). The combined organic fractions were washed with ½ sat'd NH_4Cl and with brine, and then dried over Na_2SO_4, filtered and concentrated in vacuo to give a pale yellow oil as the crude product. This crude material was purified by column chromatography (SiO_2, hexanes:EtOAc 4:1 + 0.5% Et_3N). The purified material was isolated from the column (0.197 g, 59%).

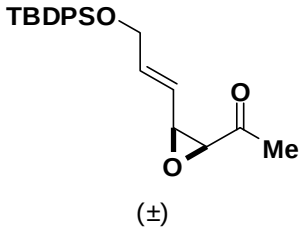

TLC (hex:EtOAc 1:1)

R_f = 0.64 visualized by p-anisaldehyde

^{1}H-NMR (400 MHz, $CDCl_3$)

δ 7.64 (m, 4H), 7.41 (m, 6H), 6.13 (dt, *J* = 15.2, 4 Hz, 1H), 5.65 (m, 1H), 4.22 (m, 2H), 3.72 (m, 2H), 2.21 (s, 3H), 1.05 (s, 9H)

HRMS (CI+)

Calculated for $C_{23}H_{29}O_3Si$ $(M+H)^+$: 381.18861

Found: 381.18891

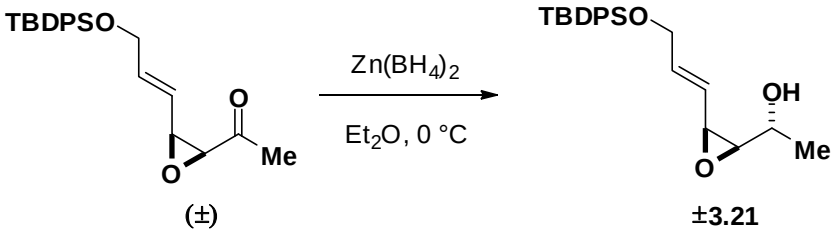

To a solution of the ketone substrate (0.1648 g, 0.433 mmol) stirring in a solution of Et_2O (10 mL) was added a dilute solution of $Zn(BH_4)_2$ dropwise until conversion was complete by TLC. H_2O (2 mL) was immediately added, dropwise via syringe, to quench the remaining reagent. The solution was allowed to stir for an additional 20 min before being poured into 10 mL each of Et_2O and sat'd NH_4Cl. The organic layer was washed with sat'd aqueous $NaHCO_3$ (1 x 10 mL) and with brine (1 × 10 mL), dried with Na_2SO_4, filtered and concentrated. the crude product was purified by column chromatography (SiO_2, gradient, hexanes:EtOAc 30:1→20:1→10:1→5:1→3:1). The pure erythro product was thusly obtained (0.146 g, 88%).

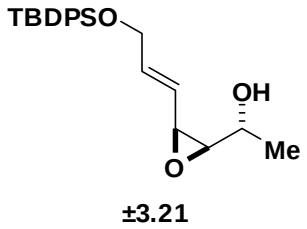

TLC (hex:EtOAc 2:1)

R_f = 0.34 visualized by p-anisaldehyde

^{1}H-NMR (400 MHz, $CDCl_3$)

δ 7.68 (m, 4H), 7.41 (m, 6H), 6.04 (dtd, *J* = 16, 4.5, 1 Hz, 1H), 5.84 (ddt, *J* = 16, 7.5, 2 Hz, 1H), 4.27 (m, 2H), 3.74 (m, 1H), 3.53 (ddd, *J* = 8, 4, 0.5 Hz, 1H), 3.01 (dd, *J* = 7.5, 4 Hz, 1H), 1.68 (d, *J* = 3.5 Hz, 1H), 1.37 (d, *J* = 6 Hz, 3H), 1.08 (s, 9H)

HRMS (ESI+)

Calculated for $C_{23}H_{31}O_3Si$ $(M+H)^+$: 383.2042

Found: 383.2052

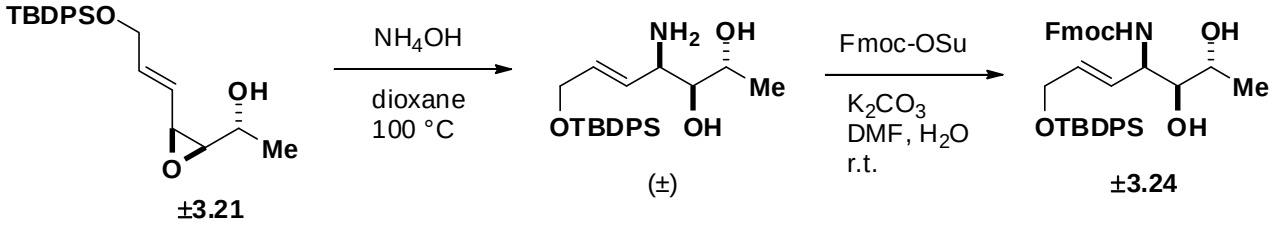

By syringe, 1.5 mL dioxane and 750 μL NH_4OH were added to 85.8 mg **±3.21** in a 7mL vial through. Under an argon funnel, the septum cap as exchanged for a Teflon lined screw cap. The reaction was maintained, with stirring, at 100 °C for 12 h. After cooling to r.t., the reaction was diluted with EtOAc and poured into 15 mL each of EtOAc and brine. The aqueous layer was extracted with EtOAc (2x), and the combined organic fractions were dried over $MgSO_4$, filtered, and concentrated in vacuo. The resulting crude material was carried forward without further purification.

To a 7 mL septum capped vial containing the crude amine and K_2CO_3 (0.0625 g, 0.45 mmol) was added 370 μL H_2O by syringe, and this solution was stirred at 0 °C. In a separate vial, Fmoc-OSu (101.6 mg) was dissolved in 1.0 mL DMF. 750 μL of this stock solution was added to the reaction vial, still at 0 °C, by syringe. Reaction was allowed to warm to room temp and stir for 5.5 h. The reaction was transferred into 15 mL each of Et_2O and 5% aq. HCl. The aqueous layer was extracted with Et_2O (3x). The combined organic fractions were washed with sat'd $NaHCO_3$, sat'd NaCl, dried over $MgSO_4$, filtered, and concentrated in vacuo. The crude product was purified by column chromatography (SiO_2, gradient, hexanes:EtOAc 5:1→1:1. From this column was isolated 47.8 mg of the purified material, a 34% yield over two steps.

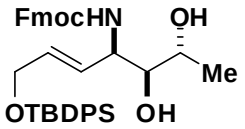

±3.24

TLC (hex:EtOAc 1:1)

R_f = 0.38 visualized by UV (254 nm)

^{1}H-NMR (400 MHz, $CDCl_3$)

δ 7.78 (d, *J* = 7.5 Hz, 2H), 7.68 (m, 4H), 7.61 (d, *J* = 7.5 Hz, 2H), 7.4 (m, 10H), 5.72 (m, 2H), 5.07 (d, *J* = 9.5 Hz, 1H), 4.58 (m, 2H), 4.47 (m, 1H), 4.24 (m, 3H), 3.51 (s, 1H), 3.41, (s, 1H), 3.31 (m, 1H), 1.76 (s, 1H), 1.27 (d, *J* = 6 Hz, 3H), 1.09 (s, 9H)

HRMS (ESI+)

Calculated for $C_{38}H_{44}NO_5Si$ $(M+H)^+$:	622.2989
Found:	622.2979

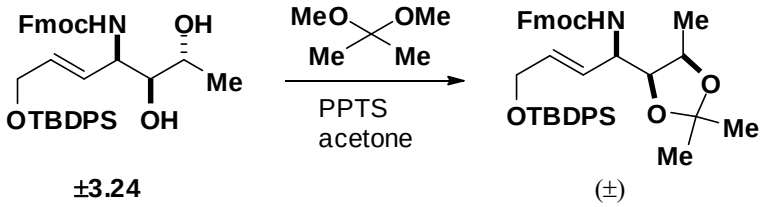

±3.24 (±)

A 7.5 mL vial was charged with **±3.24** (0.0475 g, 0.0764 mmol), 2,2-dimethoxypropane (1.15 mL, 9.35 mmol), and acetone (365 μL). A single crystal of PPTS was added, and after flushing and sealing the vial under argon flow, the reaction was stirred at r.t. for 12 h. The reaction was directly concentrated and azeotroped with DCM (3x). This crude product was purified by column chromatography (SiO_2, gradient, hexanes:EtOAc 20:1→3:1, single step with a copious 20:1 wash). The desired product was isolated (47.0 mg, 94%).

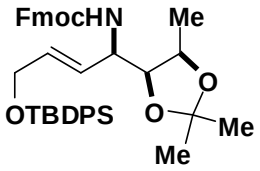

(±)

TLC (hex:EtOAc 5:1)

R_f = 0.32 visualized by UV (254 nm) and p-anisaldehyde

^{1}H-NMR (400 MHz, $CDCl_3$)

δ 7.78 (d, *J* =7.5 Hz, 2H), 7.68 (d, *J* = 8 Hz, 4H), 7.62 (d, *J* = 7 Hz, 2H), 7.40 (m, 10H), 5.75 (bs, 2H), 5.17 (bs, 1H), 4.30 (m, 9H?), 1.54 (s, 3H), 1.39 (s, 3H), 1.29 (bs, 3H), 1.08 (s, 9H)

HRMS (ESI+)

Calculated for $C_{41}H_{48}NO_5Si$ $(M+H)^+$:	662.3302
Found:	662.3307

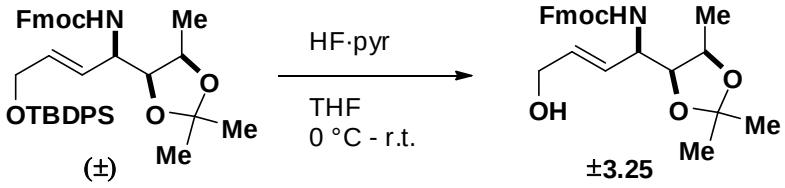

To a 7-mL polyethylene vial containing the silyl ether substrate (0.0234 g, 0.0354 mmol) was added 50 µL dry THF via syringe. The substrate was stirred at 0 °C. Into a separate identical PE vial as added 500 µL THF and 25 µL HF pyridine solution via a plastic syringe. After stirring for an additional 5 min. 150 µL of this diluted HF solution was transferred to the substrate vial. The reaction was warmed to r.t. and stirred under argon for 3 h. 1 mL sat'd aq. $NaHCO_3$ was added via syringe, and the reaction as stirred at r.t. for an additional 3 h. The reaction was poured into a mixture of Et_2O and sat'd aq. $NaHCO_3$. The aqueous layer was extracted with Et_2O (3X). The combined organic fractions were washed with brine, dried over $MgSO_4$, filtered, and

concentrated in vacuo. The crude product was purified by column chromatography (SiO_2, gradient hexanes:EtOAc 4:1→1:6). The yield for this reaction was not noted.

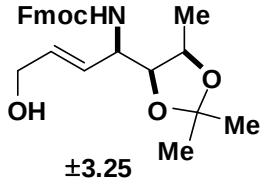

±3.25

TLC (hex:EtOAc 1:6)

R_f = 0.30 visualized by UV (254 nm)

^{1}H-NMR (400 MHz, $CDCl_3$)

δ 7.78 (d, *J* = 7, 2H), 7.61 (d, *J* = 7, 2H), 7.42 (t, *J* = 7.5, 2H), 7.33 (t, *J* = 7.5, 2H), 5.78 (m, 2H), 5.23 (bs, 1H), 4.30 (m, 9H), 1.55 (s, 3H), 1.38 (s, 3H), 1.31 (bs, 3H)

HRMS (ESI+)

Calculated for $C_{25}H_{30}NO_5$ $(M+H)^+$: 424.2124

Found: 424.2107

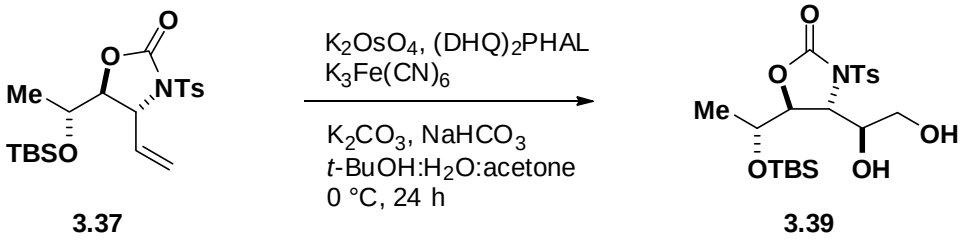

3.37 **3.39**

To a 7-mL vial equipped with a stir bar was added $(DHQ)_2PHAL$ (0.0260 g, 0.03 mmol), $K_2OsO_4 \cdot 2H_2O$ (0.0022 g, 0.0060 mmol), K_2CO_3 (0.083 g, 0,601 mmol), $NaHCO_3$, (0.050 g, 0.595 mmol), $K_3Fe(CN)_6$ (0.197 g, 0.598 mmol), t-BuOH (0.4 mL) and H_2O (0.95 mL). The resulting mixture was stirred vigorously at 23 °C for 10 min, then cooled to 0 °C and stirred an additional 10 min. **3.37** was added as a solution in t-BuOH (0.3 mL) and acetone (0.1 mL). t-BuOH (0.25 mL) was used for quantitative transfer. The reaction was thus stirred at 0 °C for 24 h. The reaction mixture was diluted with EtOAc (10 mL), and sat'd aq. Na_2SO_3 (5 mL). The

aqueous phases were extracted with EtOAc (3x), and the combined organic fractions were dried over $MgSO_4$ and concentrated in vacuo. The resulting crude product was purified by column chromatography (SiO_2, hex:EtOAc 50:50 → 0:100) to afford the title compound as a colorless solid (0.0754 g, 87% yield).

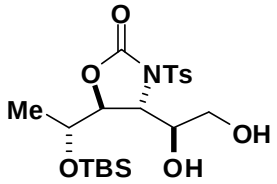

3.39

TLC (hex:EtOAc 1:1)

R_f = 0.35, stained with $KMnO_4$

^{1}H-NMR (500 MHz, $CDCl_3$)

δ 7.95 (d, *J* = 8.5 Hz, 2H), 7.33 (d, *J* = 8.5 Hz, 2H), 4.44 (app t, *J* = 2.5 Hz, 1H), 4.39 (dd, *J* = 5, 3 Hz, 1H), 4.29 (m, 1H), 3,80 (m, 1H), 3.64 (m, 2H), 3.24 (d, *J* = 5 Hz, 1H), 2.61 (dd, *J* = 7, 5 Hz, 1H), 2.43 (s, 3H), 1.13 (d, *J* = 6.5 Hz, 3H), 0.85 (s, 9H), 0.048 (s, 3H), -0.01 (s, 3H)

^{13}C-NMR (125 MHz, $CDCl_3$)

δ 152.2, 145.6, 134.9, 129.8, 128.4, 78.3, 71.3, 68.4, 62.7, 59.5, 53.4, 25.7, 21.6, 19.2, 18.0, -4.71, -4.84

HRMS (ESI+)

Calculated for $C_{20}H_{34}NO_7SSi$ $(M+H)^+$:	460.1825
Found:	460.1820

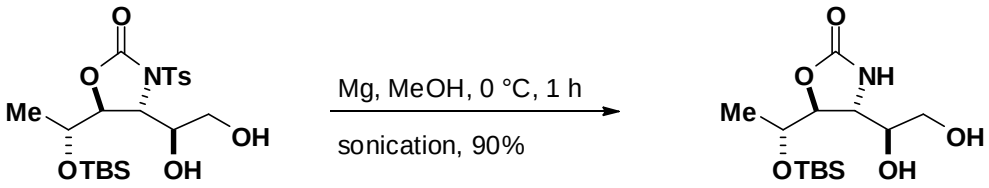

3.39 **3.33**

In a glovebox, to a 500 mL, flame dried round bottom flask was added magnesium powder (2.65 g, 109 mmol). The flask was sealed with a rubber septum and removed from the glovebox and charged with MeOH (100 mL) and **3.39** (10.8 g, 23.5 mmol) as a solution in MeOH (50 mL), and additional MeOH (50 mL) for quantitative transfer. The resulting mixture was immediately sonicated at 0 °C for 30 min. The reaction mixture was diluted with EtOAc (400 mL) and sat'd aq. NH_4Cl (200 mL). The aqueous phase was separated and extracted with EtOAc (3×100 mL). The combined organic fractions were washed with sat'd aq. $NaHCO_3$ (100 mL), and the resulting aqueous phase was separated and back extracted with EtOAc (2×50 mL). The combined organic fractions were dried over Na_2SO_4, filtered and concentrated in vacuo to give a pale yellow oil. The crude residue was purified by flash column chromatography (SiO_2, EtOAc → EtOAc + 3% i-PrOH) to afford the title compound as a colorless foam (6.44 g, 90%).

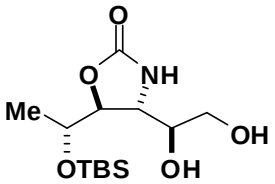

3.33

TLC (EtOAc)

$R_f = 0.18$, stained with $KMnO_4$

^{1}H-NMR (500 MHz, $CDCl_3$)

δ 7.03 (s, 1H), 4.62 (s, 1H), 4.36 (app t, *J* = 3.5 Hz, 1H), 3.99 (m, 2H), 3.79 (app t, *J* = 4 Hz, 1H), 3.71 (br s, 1H), 3.58 (m, 2H), 1.13 (d, *J* = 6.5 Hz, 3H), 0.86 (s, 9H), 0.074 (s, 3H), 0.062 (s, 3H)

^{13}C-NMR (125 MHz, $CDCl_3$)

δ 160.6, 81.7, 72.8, 68.6, 62.9, 54.6, 25.7, 18.9, 17.9, -4.6, -4.9

HRMS (ESI+)

Calculated for $C_{13}H_{28}NO_5Si$ $(M+H)^+$: 306.1737

Found: 306.1740

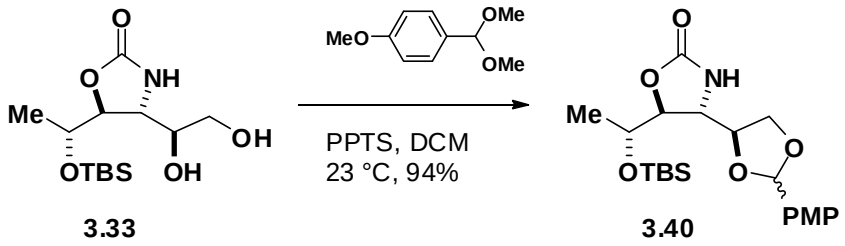

3.33 3.40

To a 1 L round bottom flask containing **3.33** (6.44 g, 21.1 mmol) and a stir bar under argon was added DCM (210 mL), *p*-anisaldehyde dimethylacetal (7.20 mL,7.20 mmol), and PPTS (1.061 g, 4.22 mmol). The resulting solution was stirred at 23 °C for 5 h. The reaction mixture was then diluted with Et_2O (400 mL) and sat'd aq. $NaHCO_3$ (200 mL). The aqueous phase was separated and extracted with Et_2O (3 ×100 mL). The combined organic fractions were dried over $MgSO_4$, filtered and concentrated in vacuo to give a yellow oil, which was purified by column chromatography (SiO_2, hex:EtOAc 3:1 → 1:1 → 1:2). Mixed fractions were concentrated and re-purified under the same conditions. The title compound was thus obtained as a mixture of acetals, and as a colorless foam (8.38 g, 94%).

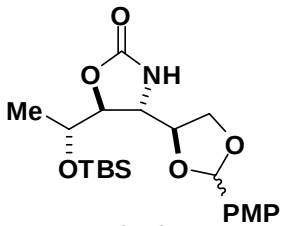

3.40

TLC (hex:EtOAc 1:1), stained with $KMnO_4$

Major diastereomer: $R_f = 0.33$

Minor diastereomer: $R_f = 0.45$

^{1}H-NMR (500 MHz, $CDCl_3$)

Major diastereomer: δ 7.39 (d, *J* = 8.5 Hz, 2H), 6.91 (d, *J* = 8.5 Hz, 2H), 5.73 (s, 1H), 4.22 (m, 2H), 4.13–4.03 (m, 4H), 3.82 (s, 3H), 1.13 (d, *J* = 6.5 Hz, 3H), 0.88 (s, 9H), 0.083 (s, 6H)

Minor diastereomer: δ 7.35 (d, *J* = 9 Hz, 2H), 6.90 (d, *J* = 7.5 Hz, 2H), 5.97 (s, 1H), 4.15 (m, 1H), 3.99 (m, 1H), 3.89 (m, 1H), 4.13–4.03 (m, 3H), 3.81 (s, 3H), 1.17 (d, *J* = 6.5 Hz, 3H), 0.88 (s, 9H), 0.098 (s, 6H)

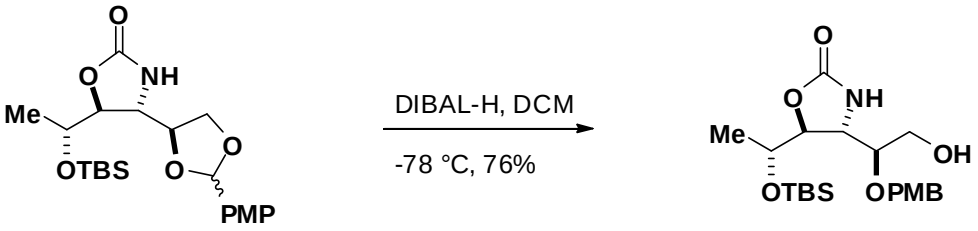

3.40 **3.41**

To a 1 L flask containing **3.40** (8.38g, 19.8 mmol) and a stir bar under argon was added DCM (100 mL) . The resulting solution was cooled, stirring, to -78 °C. DIBAL-H (1M in DCM, 100 mL, 100 mmol) was added via cannulation to the reaction mixture over 10 min. The reaction mixture was thus stirred for 8 h. Additional DIBAL-H (20 mL, 20 mmol), was added, and the reaction mixture was stirred an additional 1 h. The reaction mixture was quenched by the dropwise addition of MeOH (10 mL). The reaction mixture was then allowed to warm to room temperature, and thus stirred for 1 h, then was diluted with sat'd aq. Na, K-tartrate (200 mL). This mixture was vigorously stirred for 3 h. The aqueous phase was isolated and extracted with Et_2O (3×100 mL). The combined organic fractions were dried over $MgSO_4$, filtered and concentrated in vacuo to give a yellow oil. This crude product was purified by column chromatography (SiO_2, hex:EtOAc, 50:50 → 0:100). Mixed fractions were concentrated and re-purified under the same conditions. The pure primary alcohol **3.41**, was thus afforded (6.42 g, 76%).

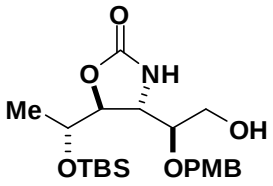

3.41

TLC (hex:EtOAc 1:1)

R_f = 0.15, stained with $KMnO_4$

^{1}H-NMR (500 MHz, $CDCl_3$)

δ 7.22 (d, *J* = 8.5 Hz, 2H), 6.86 (d, *J* = 9 Hz, 2H), 6.35 (s, 1H), 4.60 (d, *J* = 11.5 Hz, 1H), 4.46 (d, *J* = 11 Hz, 1H), 4.18 (t, *J* = 3.5 Hz, 1H), 3.95 (m, 1H), 3.89 (m, 1H), 3.79 (s, 3H), 5.91 (m, 1H), 4.47 (m, 1H), 2.63 (m, 1H), 1.08 (d, *J* = 6 Hz, 3H), 0.86 (s, 9 H), 0.061 (s, 6 H)

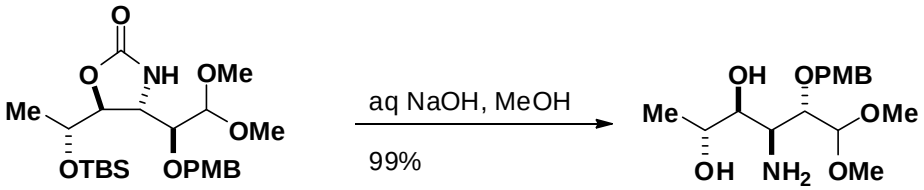

3.42

To a 25 mL round bottom flask containing **3.42** (0.2451 g, 0.690 mmol) and a stir bar, under ambient air, was added MeOH (3.5 mL). The resulting mixture was stirred to homogeneity, and then NaOH (2M aqueous solution, 3.5 mL, 7.0 mmol) was added. The flask was equipped with a reflux condenser and stirred under air at 70 °C for 18 h. The reaction was then diluted with DCM (20 mL) and brine (20 mL). The aqueous phase was separated and extracted with DCM (3×15mL). The combined organic fractions were dried over Na_2SO_4, filtered and concentrated in vacuo to give a colorless oil that was carried forward without further purification (0.2258 g, 99%).

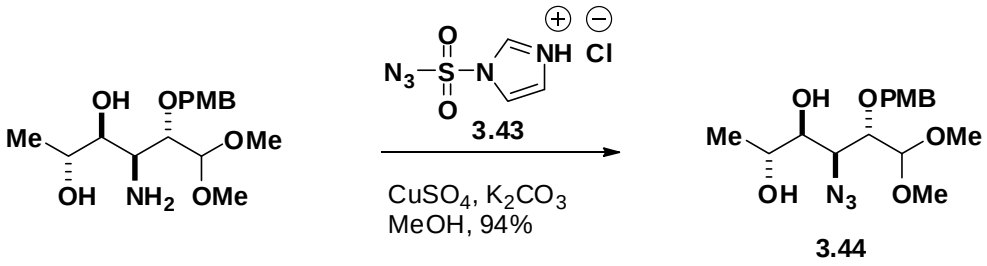

To a 20 mL vial containing **3.42** (0.2258 g, 0.76 mmol) and a stir bar was added MeOH (4.0 mL), K_2CO_3 (0.2117 g, 1.53 mmol), $CuSO_4 \cdot 5H_2O$ (0.0039 g, 0.016 mmol), and azide transfer reagent **3.43** (0.2081 g, 0.99 mmol). The resulting heterogeneous mixture was stirred at room temperature for 2 h. The reaction mixture was then diluted with EtOAc (10 mL) and H_2O (10 mL). the aqueous phase was separated and extracted with EtOAc (3x). The combined organic fractions were washed with brine (10 mL), dried over Na_2SO_4, filtered and concentrated in vacuo. The resulting crude product was purified by column chromatography (SiO_2, hex:EtOAc 2:1 → 1:1) to obtain the title compound as a colorless oil (0.1564 g, 64%).

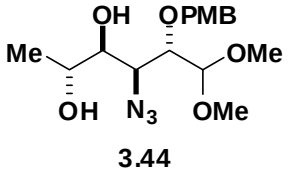

3.44

TLC (hex:EtOAc 1:1)

R_f = 0.30, stained with $KMnO_4$

^{1}H-NMR (500 MHz, $CDCl_3$)

δ 7.29 (d, *J* = 8.5 Hz, 2H), 6.87 (d, *J* = 8.5 Hz, 2H), 4.76 (d, *J* = 11 Hz, 1H), 4.63 (d, *J* = 10.5 Hz, 1H), 4.44 (d, *J* = 5.5 Hz, 1H), 3.87 (s, 1H), 3.84 (m, 2H), 3.79 (s, 3H), 3.68 (dd, *J* = 7.5, 1.5 Hz, 1H), 3.51 (s, 3H), 3.45 (s, 3H), 1.26 (d, *J* = 6.5 Hz, 3H)

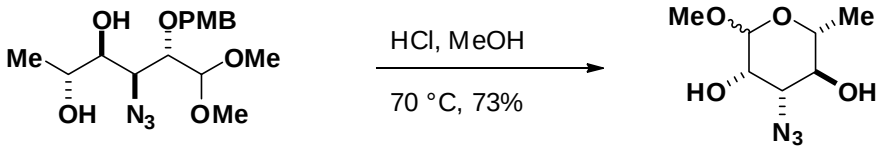

3.44 **3.47**

To a 7 mL vial containing **3.44** (0.0348 g, 0.098 mmol) under N_2 was added MeOH (1.0 mL) and HCl (3M in MeOH, 0.033 mL, 0.098 mmol) by syringe. The resulting mixture was stirred at 70 °C for 4 h. The reaction mixture was diluted with EtOAc (1 mL) and sat'd aq. $NaHCO_3$ (1mL). The aqueous phase was separated and extracted with EtOAc (3x). The combined organic fractions were dried over Na_2SO_4, filtered and concentrated in vacuo. The crude reaction product thus obtained was purified by column chromatography (hex:EtOAc 2:1 → 1:1) to afford the pyranose sugar **3.47** as a mixture of anomers (14.6 mg, 73% yield).

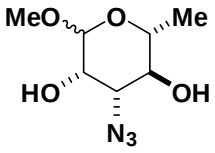

3.47

TLC (hex:EtOAc 1:1), stained with $KMnO_4$

Major anomer: $R_f = 0.37$

Minor anomer: $R_f = 0.26$

^{1}H-NMR (500 MHz, $CDCl_3$)

Major anomer: δ 4.64 (d, J = 1.5 Hz, 1H), 3.96 (m, 1H), 3.92 (s, 1H), 3.72–3.59 (m, 2H), 1.34 (d, J = 6 Hz, 3H)

Minor anomer: δ 4.39 (s, 1H), 4.08 (d, J = 2.5 Hz, 1H), 3.94 (m, 1H), 3.27 (dd, J = 9.5, 3 Hz), 1.39 (d, J = 6 Hz, 3H)

HRMS (EI+)

Calculated for $C_7H_{13}N_3O_4$ $(M+Na)^+$: 226.0800

Found: 226.0804

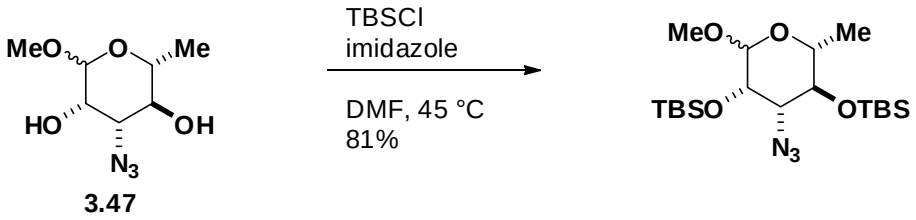

To a 2 mL vial containing **3.47** (0.0086g, 0.042 mmol) and a stir bar was added DMF (0.42 mL), imidazole (0.0638 g, 0.94 mmol), and TBSCl (0.0637 g, 0.42 mmol). The resulting mixture was stirred at 45 °C for 14 h. The reaction was diluted with Et_2O (5 mL) and H_2O (5 mL). The aqueous phase was extracted with Et_2O (5 mL). The combined organic fraction were washed with sat'd aq. $NaHCO_3$ (2 mL) and brine (2 mL), then dried with $MgSO_4$, filtered, concentrated and purified by column chromatography (SiO_2, hex:EtOAc, 20:1 isocratic) to afford the bis-TBS ether as a colorless oil (0.0148 g, 81%).

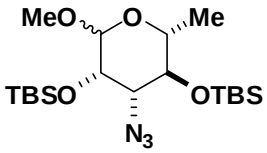

TLC (hex:EtOAc 10:1)

R_f = 0.5, stained with Anisaldehyde

^{1}H-NMR (500 MHz, $CDCl_3$)

δ 4.47 (d, *J* = 1.5 Hz, 1H), 3.97 (app t, *J* = 2 Hz, 1H), 3.58 (m, 1H), 3.50 (dd, *J* = 9, 2.5 Hz, 1H), 3.37 (s, 3H), 1.27 (d, *J* = 5.5 Hz, 3H), 0.93 (s, 18H), -0.20 (s, 3H), -0.16 (s, 3H), -0.12 (s, 3H), -0.10 (s, 3H)

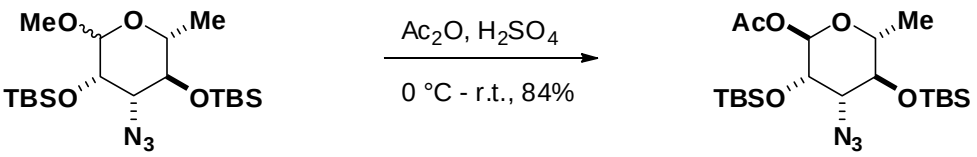

To a stirring solution of the methyl acetal substrate (0.110 g, 0.25 mmol) in Ac_2O (1.2 mL) at 0 °C was added a solution of H_2SO_4 in Ac_2O (0.020 mL, prepared by addition of 0.175 mL conc. H_2SO_4 in 0.50 mL Ac_2O). After stirring at 0 °C for 20 min, the reaction mixture was

poured into a mixture of sat'd aq. $NaHCO_3$ (50 mL) and Et_2O (50 mL). This mixture was allowed to stir at room temperature for 1 h. The aqueous phase was separated and extracted with Et_2O (30 mL). The combined organic phases were washed with sat'd aq. $NaHCO_3$ (25 mL), dried over Na_2SO_4, filtered, and concentrated in vacuo. The resulting crude product was purified by column chromatography (SiO_2 hex:EtOAc, 25:1 isocratic) to afford the anomeric acetate (0.098 g, 84% yield).

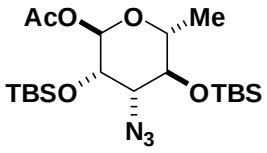

TLC (hex:EtOAc 10:1)

R_f = 0.40, stained with CAM

^{1}H-NMR (500 MHz, $CDCl_3$)

δ 5.83 (d, *J* = 2 Hz, 1H), 3.96 (t, *J* = 2.5 Hz, 1H), 3.68 (m, 1H), 3.63 (m, 1H), 3.48 (dd, *J* = 9.5, 2.5 Hz, 1H), 2.12 (s, 3H), 1.26 (d, *J* = 6 Hz, 3H), 0.923 (s, 9H), 0.915 (s, 9H), 0.197 (s, 3H), 0.151 (s, 3H), 0.119 (s, 3H), 0.113 (s, 3H)

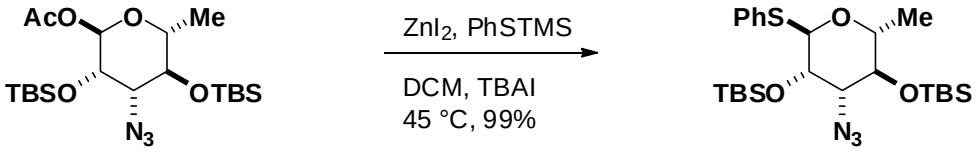

3.48

In the glovebox, o a 7 mL vial was added ZnI_2 (0.201 g, 0.63 mmol), TBAI (0.093 g, 0.25 mmol), and a stir bar. The vial was sealed with a PTFE-lined septum-cap and removed from the box. To the vial was then added the acetate substrate (0.097 g, 0.21 mmol) as a solution in DCM (2.1 mL), followed by PhSTMS (0.4 mL, 2.1 mmol). The resulting mixture was stirred at 45 °C for 15 min. The reaction mixture was diluted with Et_2O (10 mL) and sat'd aq. $NaHCO_3$ (10 mL). The aqueous phase was separated and extracted with Et_2O (3x). The combined organic fractions were dried over $MgSO_4$, filtered and concentrated in vacuo. The resulting crude product was

purified by column chromatography (hex:EtOAc 20:1 isocratic) to afford the anomeric sulfide **3.48** as a mixture of anomers (0.1072 g, 99%).

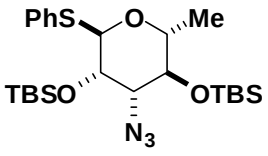

3.48

TLC (hex:EtOAc 10:1)

R_f = 0.55, stained with $KMnO_4$

^{1}H-NMR (500 MHz, $CDCl_3$)

Major anomer: δ 7.49 (m, 2H), 7.32(m, 3H), 5.24 (d, *J* = 1.5 Hz, 1H), 4.23 (dd, *J* = 2.5, 2 Hz, 1H), 4.06 (m, 1H), 3.65 (t, 9 Hz, 1H), 3.50 (dd, *J* = 9.5, 2.5 Hz, 1H), 1.27 (d, *J* = 6.5 Hz, 3H), 0.932 (s, 9H), 0.899 (s, 9H), 0.199 (s, 3H), 0.140 (s, 3H), 0.118 (s, 3H), 0.061 (s, 3H)

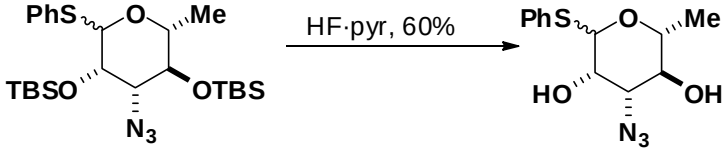

3.48

To a 12 mL PTFE vial containing **3.48** (0.158 g, 0.310 mmol) and a stir bar under N_2 was added THF (3 mL), pyridine (0.19 mL, 2.36 mmol), then HF·pyr (0.19 mL, 3.13 mmol). The vial was sealed and the solution was maintained with stirring at 50 °C for 36 h. The reaction was quenched by the addition of sat'd aq $NaHCO_3$ (added dropwise until bubbling ceased) and allowed to stir at 23 °C for an additional 30 min. The reaction was then diluted with EtOAc (10 mL) The aqueous phase was extracted with EtOAc (4x), and the combined organic fractions were dried over $MgSO_4$, filtered, and concentrated in vacuo. The resulting crude product was purified by column chromatography (SiO_2, hex:EtOAc 3:1→2:1) to afford the desired diol as a mixture of anomers (52.2 mg, 60%).

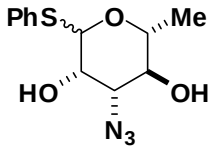

TLC (hex:EtOAc 2:1), stained with $KMnO_4$

Major anomer: $R_f = 0.26$

Minor anomer: $R_f = 0.21$

^{1}H-NMR (500 MHz, $CDCl_3$)

Major anomer: δ 7.50–7.45 (m, 2H), 7.35–7.28 (m, 3H), 5.45 (s, 1H), 4.25 (m, 1H), 4.20 (m, 1H), 3.73 (t, *J* = 9.5 Hz, 1H), 3.68 (dd, *J* = 10, 3 Hz, 1H), 1.34 (d, *J* = 6.5 Hz, 3H)

Minor anomer: δ 7.50–7.45 (m, 2H), 7.35–7.28 (m, 3H), 4.83 (d, *J* = 1 Hz, 1H), 4.22 (d, *J* = 3.5 Hz, 1H), 3.72 (t, *J* = 9.5 Hz, 1H), 3.40 (m, 1H), 3.37 (m, 1H)

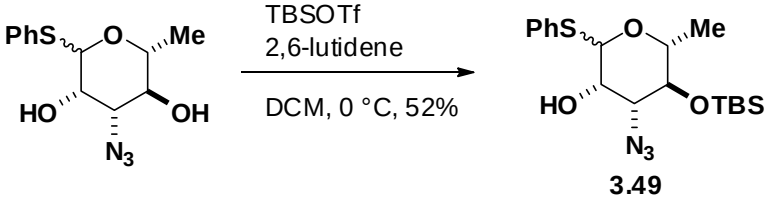

3.49

To a 7 mL vial containing the diol substrate (0.0522 g, 0.186 mmol) and a stir bar under N_2 was added DCM (1.9 mL). The resulting solution was cooled to 0 °C. 2,6-lutidene (0.032 mL, 0.275 mmol), and then TBSOTf (0.049 mL, 0.213 mmol) was added. The solution stirred at 0 °C for 3 h. The reaction was diluted with sat'd aq $NaHCO_3$ (10 mL) and Et_2O (10 mL). The aqueous phase was extracted with Et_2O (3x), and the combined organic fractions were dried over $MgSO_4$, filtered and concentrated in vacuo. The resulting crude product was purified by column chromatography (SiO_2, hex:EtOAc 5:1, isocratic) to yield **3.49** as a colorless oil (38.4 mg, 52%).

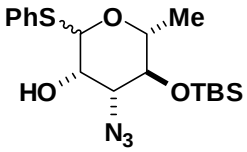

3.49

TLC (hex:EtOAc 2:1), stained with $KMnO_4$

Major anomer: $R_f = 0.58$

^{1}H-NMR (500 MHz, $CDCl_3$)

Major anomer: δ 7.47 (d, *J* = 4.5 Hz, 2H), 7.3–7.28 (m, 3H), 5.43 (d, *J* = 1 Hz, 1H), 4.28 (s, 1H), 4.13 (quint, *J* = 6 Hz, 1H), 3.59 (m, 2H), 1.28 (d, *J* = 6.5 Hz, 3H), 0.94 (s, 9H), 0.22 (s, 3H), 0.13 (s, 3H)

3-6 REFERENCES

1. Palacios, D. S.; Dailey, I.; Siebert, D. M.; Wilcock, B. C.; Burke, M. D. *Proc. Natl. Acad. Sci. U. S. A.* **2011**, *108*, 6733–6738.
2. Demchenko, A. V. *Handbook of Chemical Glycosidation*; 1 ed.; Wiley-VCH: Weinheim, 2008.
3. Ishiwata, A.; Lee, Y. J.; Ito, Y. *Org. Biomol. Chem.* **2010**, *8*, 3596–3608.
4. Koenigs, W.; Knorr, E. *Ber. Dtsch. Chem. Ges.* **1901**, *34*, 957–981.
5. Igarashi, K. In *Advances in Carbohydrate Chemistry and Biochemistry*; Tipson, R. S., Derek, H., Eds.; Academic Press: 1977; Vol. Volume 34, p 243–283.
6. Wulff, G.; Röhle, G. *Angew. Chem. Int. Ed. Engl.* **1974**, *13*, 157–170.
7. Demchenko, A. V.; Rousson, E.; Boons, G.-J. *Tetrahedron Lett.* **1999**, *40*, 6523–6526.
8. Mukaiyama, T.; Suenaga, M.; Chiba, H.; Jona, H. *Chem. Lett.* **2002**, 56–57.
9. Fei, C. P.; Chan, T. H. *Tetrahedron Lett.* **1987**, *28*, 849–852.
10. Houdier, S.; Vottero, P. J. A. *Carbohydr. Res.* **1992**, *232*, 349–352.
11. Fukase, K.; Nakai, Y.; Kanoh, T.; Kusumoto, S. *Synlett* **1998**, 84–86.
12. Barresi, F.; Hindsgaul, O. *J. Am. Chem. Soc.* **1991**, *113*, 9376–9377.
13. Barresi, F.; Hindsgaul, O. *Synlett* **1992**, 759–761.
14. Stork, G.; Kim, G. *J. Am. Chem. Soc.* **1992**, *114*, 1087–1088.
15. Stork, G.; La Clair, J. J. *J. Am. Chem. Soc.* **1996**, *118*, 247–248.
16. Fairbanks, A. J. *Synlett* **2003**, 1945–1958.
17. Nicolaou, K. C.; Daines, R. A.; Ogawa, Y.; Chakraborty, T. K. *J. Am. Chem. Soc.* **1988**, *110*, 4696–4705.
18. Szpilman, A. M.; Manthorpe, J. M.; Carreira, E. M. *Angew. Chem. Int. Ed.* **2008**, *47*, 4339–4342.
19. Packard, K. P. Synthesis of the C8 to C13 Fragment of Candidin and Construction of a Rimocidin Aglycon and β-Selective Glycosylation with Mycosamine: Efforts towards Completion of the Total Synthesis of Rimocidin. Ph.D. Dissertation, University of California Irvine, 2001.
20. Ito, Y.; Ogawa, T. *Angew. Chem. Int. Ed. Engl.* **1994**, *33*, 1765–1767.
21. Pratt, M. R.; Leigh, C. D.; Bertozzi, C. R. *Org. Lett.* **2003**, *5*, 3185–3188.
22. Nakata, T.; Tanaka, T.; Oishi, T. *Tetrahedron Lett.* **1981**, *22*, 4723–4726.
23. Lewis, M. D.; Menes, R. *Tetrahedron Lett.* **1987**, *28*, 5129–5132.
24. Awakura, D.; Fujiwara, K.; Murai, A. *Synlett* **2000**, 1733–1736.
25. Oikawa, M.; Ueno, T.; Oikawa, H.; Ichihara, A. *J. Org. Chem.* **1995**, *60*, 5048–5068.
26. Yadav, J. S.; Maiti, A. *Tetrahedron* **2002**, *58*, 4955–4961.
27. Caron, M.; Sharpless, K. B. *J. Org. Chem.* **1985**, *50*, 1557–1560.

28. Trost, B. M.; Sudhakar, A. R. *J. Am. Chem. Soc.* **1987**, *109*, 3792–3794.
29. Fraunhoffer, K. J.; White, M. C. *J. Am. Chem. Soc.* **2007**, *129*, 7274–7276.
30. Kolb, H. C.; VanNieuwenhze, M. S.; Sharpless, K. B. *Chem. Rev.* **1994**, *94*, 2483–2547.
31. Arrington, M. P.; Bennani, Y. L.; Göbel, T.; Walsh, P.; Zhao, S.-H.; Sharpless, K. B. *Tetrahedron Lett.* **1993**, *34*, 7375–7378.
32. Crispino, G. A.; Jeong, K. S.; Kolb, H. C.; Wang, Z. M.; Xu, D.; Sharpless, K. B. *J. Org. Chem.* **1993**, *58*, 3785–3786.
33. Goddard-Borger, E. D.; Stick, R. V. *Org. Lett.* **2007**, *9*, 3797–3800.
34. Goddard-Borger, E. D.; Stick, R. V. *Org. Lett.* **2011**, *13*, 2514.
35. Hanessian, S.; Guindon, Y. *Carbohydr. Res.* **1980**, *86*, C3–C6.
36. Pangborn, A. B.; Giardello, M. A.; Grubbs, R. H.; Rosen, R. K.; Timmers, F. J. *Organometallics* **1996**, *15*, 1518–1520.
37. Blonski, C.; Gefflaut, T.; Perie, J. *Bioorg. Med. Chem.* **1995**, *3*, 1247–1253.
38. Hirama, M.; Shigemoto, T.; Ito, S. *J. Org. Chem.* **1987**, *52*, 3342–3346.
39. Still, W. C.; Kahn, M.; Mitra, A. *J. Org. Chem.* **1978**, *43*, 2923–2925.

CHAPTER 4

Glycosylation of BB2 and Amphotericin B via TDMB-Mediated Anchimeric Assistance

The efforts of the previous chapter toward the application of the IAD strategy in forming the 1,2-*cis* glycosidic linkage found in BB2 reinforced our appreciation for the challenge inherent to forming this type of glycosidic bond, especially in the context of large, complex small molecules. This chapter describes the development of a different approach toward this problem, which ultimately yielded a solution in the form of the discovery of a new directing group for use in a neighboring group participation glycosylation strategy. Successful glycosylation and completion of BB2 are described, as well as application of this methodology toward an efficient glycosylation of the full amphotericin aglycone, a long-standing challenge in the chemical literature. Ian Dailey prepared **4.13** and contributed the results presented in Schemes 4.3, 4.6, and 4.7. Dr. Justin R. Struble prepared compounds **4.12** and **4.31**, contributed the results presented in Schemes 4.8 and 4.10, and contributed to the development of the mycosamine donor synthesis described below.

4-1 BACKGROUND

Our lack of success with the IAD methodology forced us to consider alternative strategies for glycosylation of BB2. A survey of the literature brought our attention back to the use of the neighboring group participation strategy developed by Nicolaou and later adapted by Carreira.[1-3] We noted that this strategy gave excellent stereoselectivity and had been shown to be compatible with large, poor nucleophiles like the AmB aglycone. Further, the necessary inversion of the C2'-hydroxyl has been shown to proceed in high yield.[1-2] The major problems were low conversion and competing ortho ester formation in the glycosyl transfer step. We therefore reasoned if these two problems could be addressed, the neighboring group participation strategy might provide an efficient route to the glycosylation of BB2 and the AmB aglycone.

4-2 SYNTHESIS OF A NEW MYCOSAMINE DONOR

The decision to pursue a neighboring group participation group strategy required us to readdress the mycosamine donor synthesis, since our existing route produced a sugar donor with the natural *S*-configuration found in AmB. Neighboring group participation would require this

carbon center to be inverted in our new proposed sugar donor, **4.1** (Figure 4.1). While **4.1** might be accessible with our current route by employing the pseudoenantiomeric $(DHQD)_2PYR$ ligands in the dihydroxylation of **3.37** (See Chapter 3, Figure 3.7), targeting a sugar donor with an inverted C2'-substituant enabled us to take advantage of substantial existing work already done in this area.[4-5] As seen in Figure 4.1, **4.1** would be accessed by opening epoxide **4.3** with sodium azide, followed by protection of the resulting C2'-hydroxyl and conversion of the anomeric PMB group to an appropriate anomeric activating group, such as the trichloroacetimidate shown. **4.3** is conveniently accessible from commercially available and relatively inexpensive 2-acetylfuran in only 6 steps.[5] This route also has the advantage of installing the C2'-substituent very late in the synthesis, which would greatly facilitate a survey of improved directing groups for neighboring group participation.

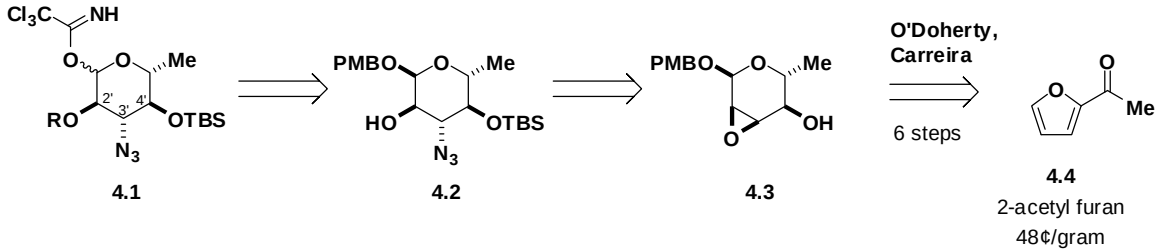

Figure 4.1. Retrosynthesis of the mycosamine donor **4.1** from commercially available 2-acetylfuran.

In the forward direction, the synthesis of **4.1** proved to very efficient (Scheme 4.1). In brief, Noyori reduction of 2-acetylfuran, followed by Achmatowicz rearrangement and diastereoselective Boc-protection provided pyranone **4.6**. Subsequent palladium-mediated installation of the anomeric OPMB, Luche reduction, and directed *m*-CPBA epoxidation provided **4.3**. This route was not only efficient step-wise, but was also found to be very scalable, enabling isolation of more than 100 g of epoxy alcohol **4.3**.

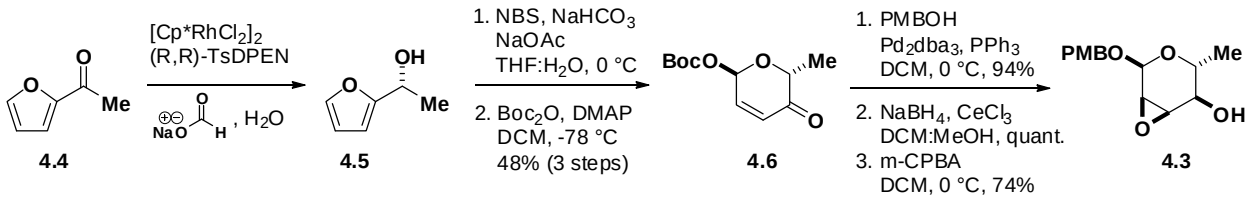

Scheme 4.1. Synthesis of epoxide **4.3** from 2-acetylfuran. This route was both efficient and scalable, enabling the isolation of more than 100 g of **4.3**.

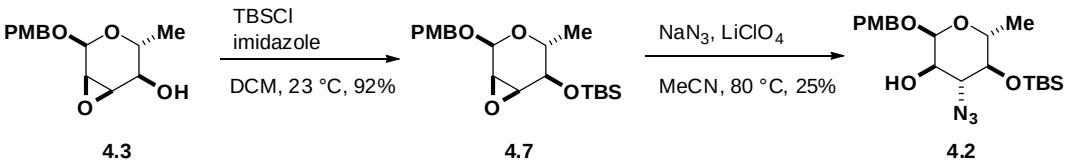

4.3 4.7 4.2

Scheme 4.2. Preparation of azido alcohol **4.2** from epoxide **4.7** proceeded via a low yielding but reliable sodium azide opening. The yield for this transformation suffered from poor regioselectivity between the two possible sites of attack on epoxide **4.7**.

Following TBS-protection of **4.3**, opening of epoxide **4.7** with NaN_3 and $LiClO_4$ proceeded in a modest 25% yield. The poor yield of this epoxide opening was not unexpected, due to the poor degree of discrimination between opening at C2' vs. the desired C3'. Similarly low yields have been observed in a very similar TES protected substrate.[5] Nevertheless, the yield for this reaction was very reproducible, and more than compensated for by the small number of steps in the synthesis to this point. Alcohol **4.2** was thus set up for acylation with our choice of directing group. For our initial attempts, the chlorodimethylacetyl group utilized by Carreira and coworkers seemed to be a logical starting point, and we were curious to see how it would perform in glycosylations with BB2. We therefore set out to synthesize **4.10** and attach it to a mycosamine sugar donor (Figure 4.2). Synthesis of the carboxylic acid was fairly straightforward, beginning with chlorination of isobutyraledhyde, followed by a Pinnick oxidation to give **4.10**. Completion of our first mycosamine donor for neighboring group participation-mediated glycosylation is shown in Figure 4.2. Briefly, acylation with **4.10**, followed by oxidation cleavage of the anomeric PMB group with DDQ, and installation of a trichloroacetimidate gave mycosamine donor **4.12.**

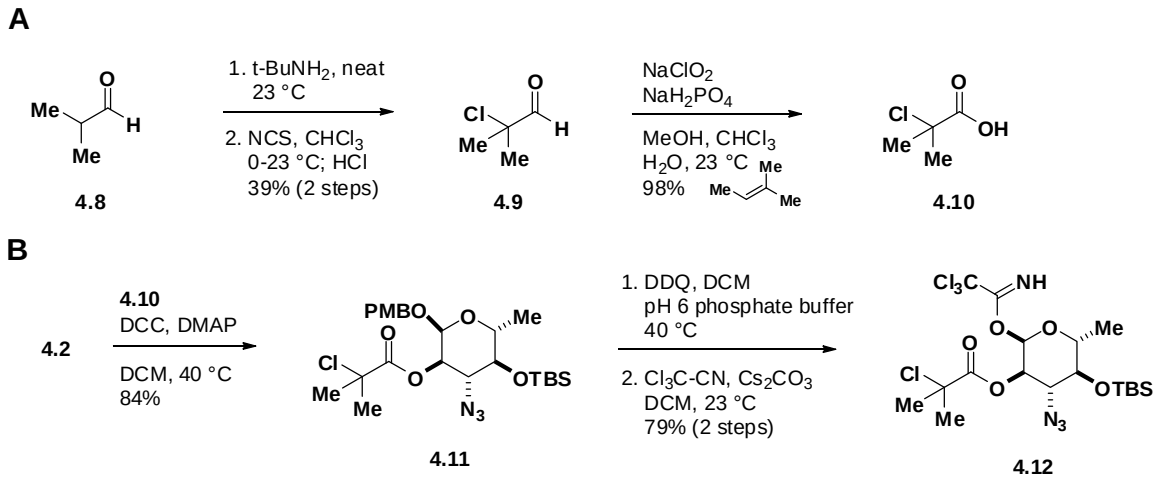

Figure 4.2. (A) Synthesis of chlorodimethylacetic acid (**4.10**) from isobutyraldehyde. (B) completion of mycosamine donor **4.12**, designed for neighboring group participation-controlled glycosylation.

For our glycosylation reactions, we chose to use BB2 aglycone **4.13**. We hypothesized that **4.13** might be a more competent nucleophile than the corresponding dienyl MIDA boronate **3.15** (See Chapter 3, Scheme 3.9). Additionally, we expected that the MIDA boronate of **3.15** would be incompatible with the strongly basic conditions necessary for removal of the C2' directing group following glycosylation. As seen in Scheme 4.3, combination of BB2 aglycone **4.13** and mycosamine donor **4.12** in the presence of CMPT/CMP in hexanes afforded the desired product in an estimated ~60% yield, along with an unidentified and inseparable byproduct. Unfortunately, subsequent removal of the chlorodimethylacetyl directing group was not possible due to the sensitivity of the BB2 lactone to base, with all attempts resulting in decomposition.

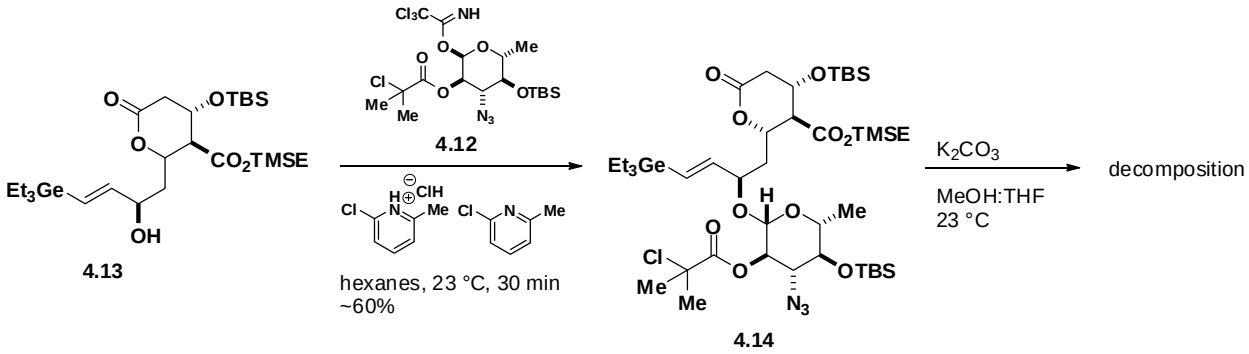

Scheme 4.3. Glycosylation of BB2 aglycone **4.13** with **4.12** enabled successful attachment of mycosamine to BB2. However, the sensitivity of the BB2 lactone to base prevented subsequent removal of the chlorodimethylacetyl directing group.

4-3 DESIGN OF A NEW DIRECTING GROUP FOR GLYCOSYLATION

Despite a less than optimal yield and an inability to remove the directing group, we were very encouraged by having finally achieved the desired glycosidic linkage. We next considered whether we could improve upon the chlorodimethylacetyl protecting group. In principle, the chlorodimethylacetate works well as a directing group because the chloride gives it a steric profile similar to a pivolate group, which helps to disfavor ortho ester formation. Inductively, the chloride withdraws electron density from the carbonyl, making subsequent deprotection of the group more facile. However, this chloride activation likely also contributes to ortho ester formation by activation of the carbonyl to nucleophilic attack in the glycosylation step. With these principles in mind, we considered several alternative directing groups which maintained a quaternary center alpha to the carbonyl, while incorporating additional functionality that would promote deprotection following glycosylation without also promoting ortho ester formation (Figure 4.3). The 2,2-dimehtylbut-3-enoate protecting group (**4.15**) developed by Crimmins,[6] can be removed by hydroboration/oxidation and subsequent lactonization. Similarly, the 4-acetoxy-2,2-dimethylbutyrate group (**4.16**) developed by Ensley is removed by acetate saponification and lactonication,[7] though we were uncertain whether a base-promoted deprotection manifold would be productive given the demonstrated instability of the BB2 lactone to base. The 4-*tert*-butyldimethylsilyloxy-2,2-dimethylbutyrate (TDMB, **4.17**) was seen as potentially the most promising, as we expected it to be labile under mildly acidic conditions (Scheme 4.4). This group had been previously employed by Trost[8] as an alcohol protecting group, but to the best of our knowledge, it had never been used in glycosylation reactions.

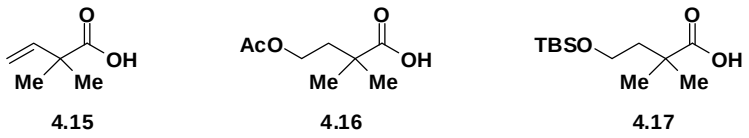

Figure 4.3. Alternative directing groups considered for use in the glycosylation of BB2.

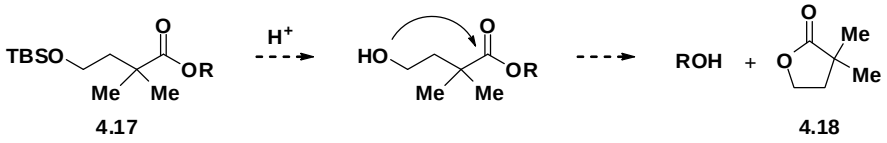

Scheme 4.4. Deprotection of the TDMB group under acidic conditions via desilylation followed by an acid catalyzed lactonization.

Between these 3 possibilities we were less confident in the compatibility of the BB2 framework to hydroboration/oxidation or base, so we proceeded initially with **4.17**, the synthesis of which was previously described.[9-10] The synthesis of a mycosamine donor, **4.20** incorporating this new directing group is shown in **Error! Reference source not found.**. In this case, functionalization of the C2' alcohol was achieved very efficiently via a DCC coupling, followed, as before, by deprotection of the anomeric PMB group and installation of, in its place, a trichloroacetimidate group. Mycosamine donor **4.20** has been shown to be stable to storage for greater than a week, though only if frozen in a benzene matrix. In contrast, the hemiketal precursor to **4.20** can be stored for greater than six months at -78 °C.

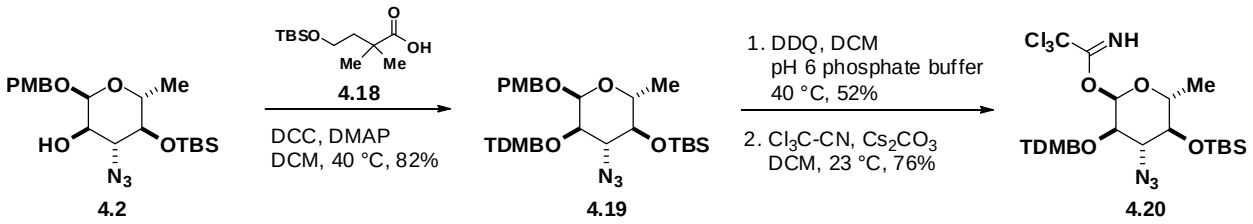

Scheme 4.5. Incorporation of the TDMB directing group into the synthesis of the mycosamine donor **4.20**.

To test this alternative directing group, mycosamine donor **4.20** was combined with BB2 aglycone **4.13** in the presence of CMPT/CMP in hexanes (Scheme 4.6). The TDMB group was very effective, providing the desired glycosylated product **4.21** in a remarkable 93% yield as a single diastereomer, with no evidence of ortho ester formation. Further, we found that the TDMB group could be removed by treatment with anhydrous CSA in MeCN. Under these conditions the desired product (**4.22**) was obtained in 60% yield. Recycling the incompletely reacted starting material a single time improved the overall yield to 72%.

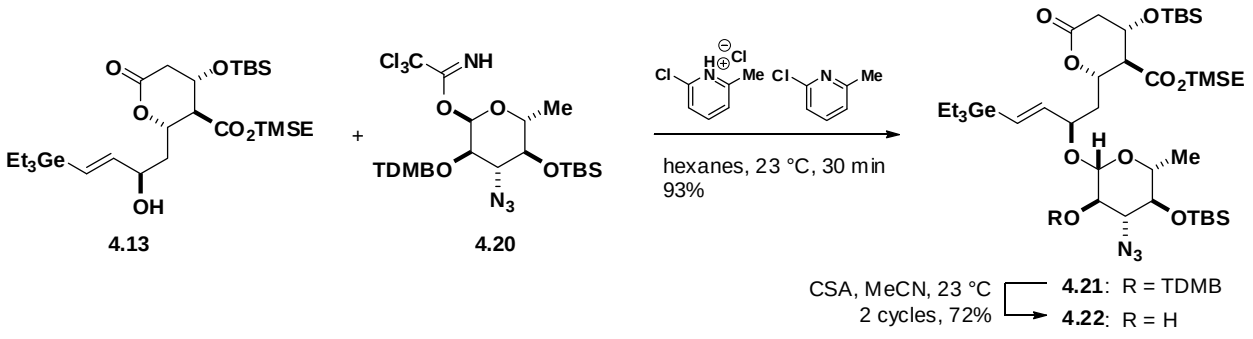

Scheme 4.6. Successful glycosylation with mycosamine donor **4.20**. The use of the TDMB group provided the desired product in 93% yield with complete stereoselectivity and no evidence of ortho ester formation. Treatment of **4.21** with CSA successfully removed the directing group to give the free alcohol **4.22**.

4-4 COMPLETION OF BB2

With the glycosylated product **4.22** in hand, we were in a position to finally finish the building block, BB2. Inversion of the C2' hydroxyl was accomplished by treatment with DMP, followed by a highly stereoselective reduction with $NaBH_4$ (Scheme 4.7).[1-2,11-12] The ketone obtained from DMP oxidation (**4.23**) was fairly unstable, both to chromatography and storage, and in the presence of water equilibrated to the hydrate, which was unreactive in the subsequent reduction. This phenomenon is consistent with a report by Rychnovsky and coworkers in their development of a β-selective glycosylation of cholesterol.[12-14] Fortunately, carrying the crude oxidation product directly into the reduction reaction allowed isolation of the *R*-alcohol **4.24** in a 67% yield over the two steps.

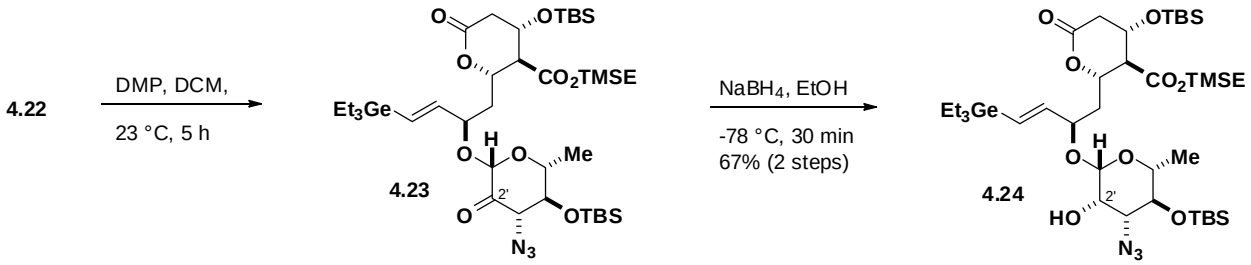

Scheme 4.7. Inversion of the C2'-hydroxyl following successful glycosylation was accomplished by oxidation with DMP, immediately followed by a selective reduction with $NaBH_4$ to give **4.24**.

With the correct configuration of the C2' position established, all that remained was extension of the olefin to a dienyl MIDA boronate, and conversion of the lactone to a ketene acetyl phosphate, thus installing each of the two cross-coupling handles of our bifunctional building block. TBS-protection of the C2'-hydroxyl, followed by iododegermylation,[15] cleanly gave vinyl iodide **4.25**. As seen in Scheme 4.8, we initially envisioned first performing a Stille coupling with bis-metallated olefin **4.26**,[16] followed phosphorylation of the lactone. While the Stille coupling proceeded smoothly, subsequent phosphorylation proceeded with concomitant hydrolysis of the MIDA boronate. This hurdle was overcome by reprotection of the boronic acid with a MIDA anhydride reagent (**4.28**) developed by Jenna Klubnick,[17] thereby completing BB2.

Although reprotection of the MIDA boronate proceeded smoothly, we wished to eliminate this step to improve the efficiency of the route. Predictably, phosphorylation of vinyl iodide **4.25** proceeded without incident to give **4.29**. We then considered whether the vinyl

iodide could be selectively coupled to bis-metallated olefin **4.26** in the presence of the ketene acetal phosphate. Indeed, when using $PdCl_2(MeCN)_2$ in DMF at 65 °C we were able to achieve complete selectivity for the iodide over the ketene acetal phosphate to again give BB2. This completed building block has been shown to be stable for greater than 2 months at -78 °C, and is ready to be incorporated into an ICC-based selective cross-coupling of the ketene acetal phosphate in the presence of the MIDA-boronate.

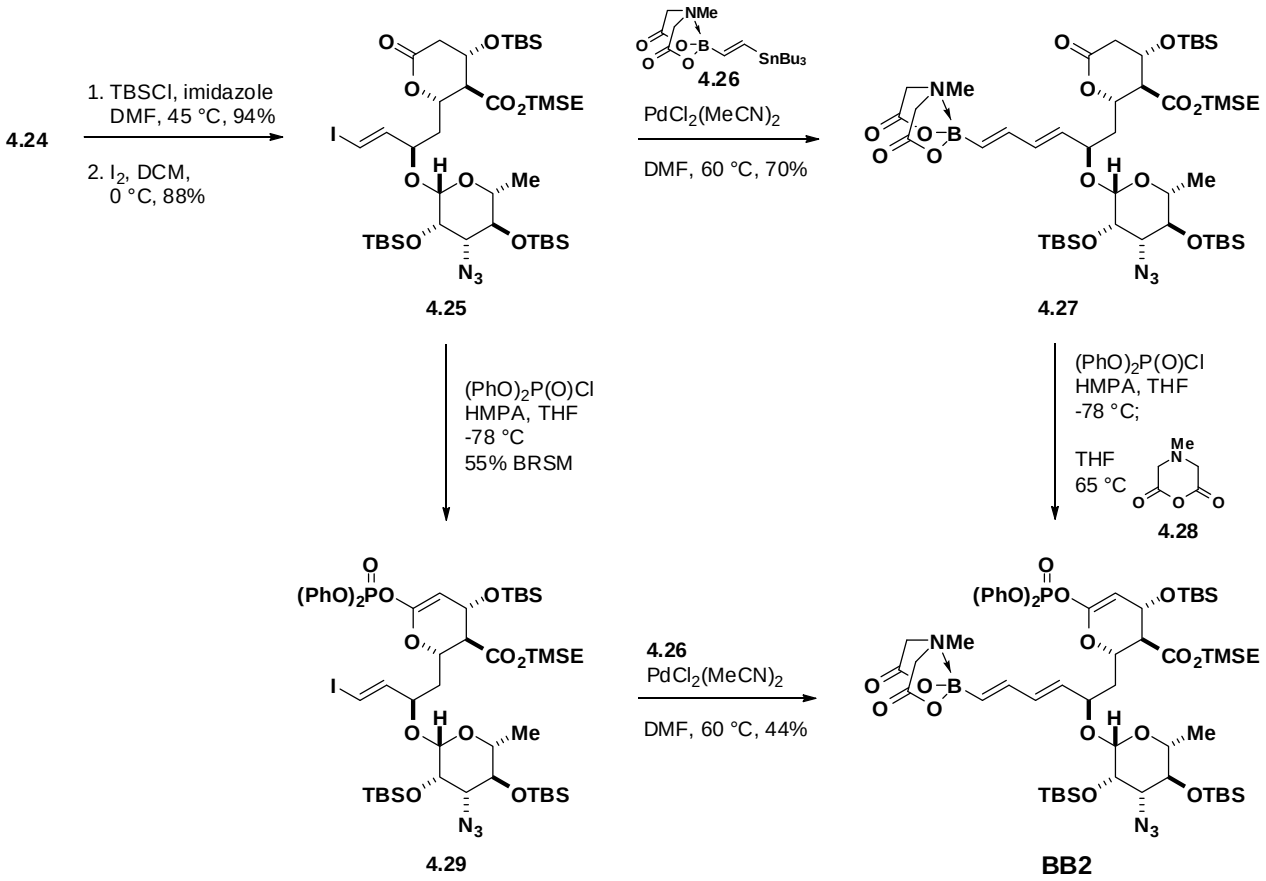

Scheme 4.8. BB2 was completed by Stille coupling of **4.25** and **4.26**, followed by phosphorylation of the BB2 lactone and subsequent reprotection of the MIDA boronate with MIDA anhydride (**4.28**). An alternative route that obviates the MIDA reprotection step was also demonstrated, whereby the lactone was phosphorylated first to give **4.29**, followed by selective Stille coupling of this iodide to **4.26**.

4-5 APPLICATION OF GLYCOSYLATION STRATEGY TO AMPHOTERICIN AGLYCONE

The successful use of the TDMB directing group in the glycosylation of BB2 prompted us to investigate whether this strategy might provide a solution to the long standing problem of glycosylating polyene macrolides. In fact, combining mycosamine donor **4.30** with protected amphotericin B aglycone, under our now standard conditions of CMPT/CMP in hexanes

provided the desired glycosylated product **4.31** in nearly quantitative yield, again with no evidence of ortho ester formation.

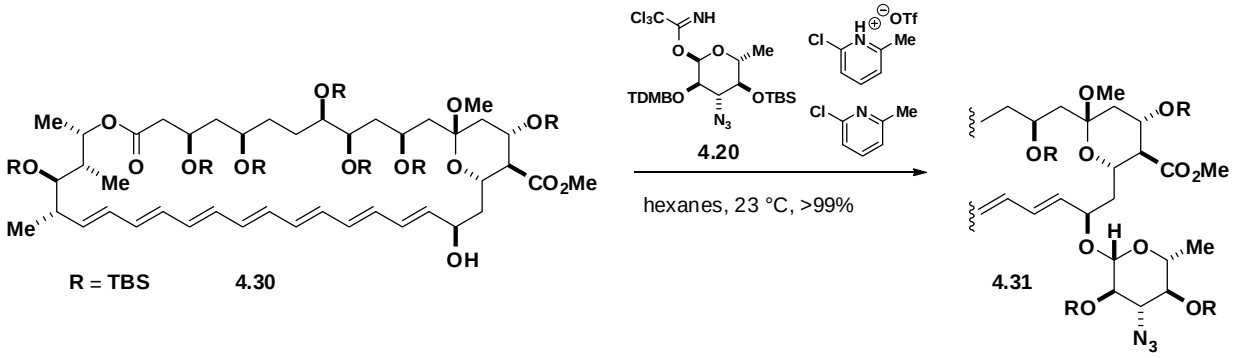

Scheme 4.9. The TDMB directing group enabled effective glycosylation of the AmB aglycone

This result represents a significant advance over existing methodology, and suggested to us an accelerated route to amphotericin derivatives containing modifications to the mycosamine sugar, since AmB aglycones like **4.30** are readily accessible via degradation of AmB.[18] As mentioned in Chapter 1, sugar-based functional group deletion derivatives are of significant interest to us, due to clear role that the mycosamine sugar plays in enabling sterol binding. To test this approach we pursued a synthesis of the C3'-deaminomycosamine donor. As seen in Scheme 4.10, beginning with intermediate **4.7** from our existing mycosamine route, opening of the epoxide with DIBAL-H afforded **4.32** in an unoptimized 10% yield, which retains the proper stereochemical configuration at C2' but lacks the nitrogen at C3'. Protection of the 2'-alcohol as a TDMB acetate via DCC coupling, deprotection of the PMB group, and subsequent installation of the anomeric trichloroacetimidate proceeded without incident to afford 3'-deaminomycosamine donor **4.33**.

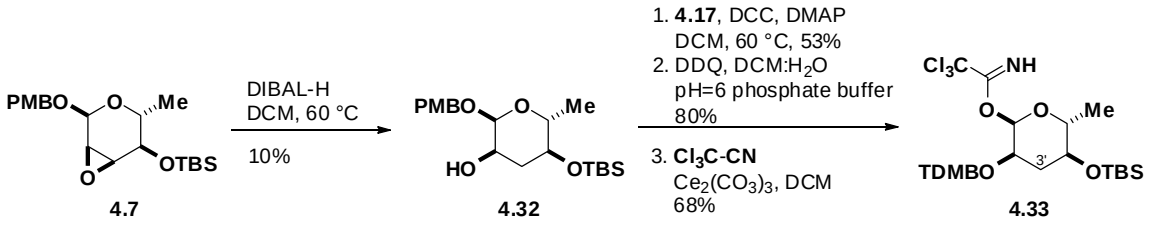

Scheme 4.10. Synthesis of a deaminomycosamine donor

Combination of **4.33** with amphotericin B aglycone **4.30** in the presence of CMPT/CMP in hexanes afforded the desired product in an excellent 97% yield. As appears to be typical for this directing group, the reaction proceeded with complete stereocontrol, and no ortho ester was observed. With the protecting group pattern chosen for amphotericin aglycone **4.30**, after inversion of the C2'-alcohol only three deprotection steps would be necessary to obtain C3'deNAmB, demonstrating the potential of this glycosylation strategy for accessing AmB derivatives containing modified sugars.

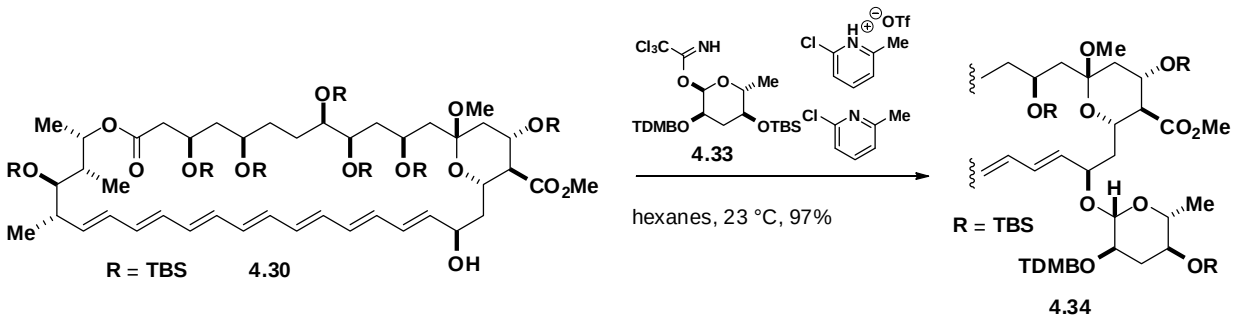

Scheme 4.11. Glycosylation of amphotericin aglycone **4.30** with deaminomycosamine donor **4.33** proceeded in an outstanding 97% yield, demonstrating the potential of this approach for accessing AmB derivatives containing modified sugars.

4-6 SUMMARY

This dissertation describes several methodological advances that were stimulated by studies toward an efficient and flexible total synthesis of AmB. In response to challenges encountered in the construction of the AmB polyene, a new cross-coupling protocol was developed whereby MIDA boronates can be used directly in SMC reactions, enabling air-stable MIDA boronates to act as surrogates for boronic acids. Additionally, conditions were identified under which MIDA boronates could be slowly hydrolyzed in the SMC reaction, enabling an in situ "slow-release" of the boronic acid. This slow-release effect enables the efficient cross-coupling of a variety of otherwise unstable boronic acids. The synthesis and isolation of 2-pyridyl MIDA boronate and its derivatives demonstrates that even the most unstable boronic acids may be rendered stable and competent cross coupling partners by conversion to the corresponding MIDA boronates. Further, the use of "fast-release" conditions enabled the construction of the AmB heptaene as well as a variety of polyenyl natural products both within and outside our research group. To overcome the challenging 1,2-*cis* glycosidic bond found in

AmB a mycosamine sugar donor synthesis was developed incorporating a new directing group for neighboring group participation. The use of this new directing group enabled efficient glycosylation of, and ultimately the completion of, BB2, a critical building block in the context of the ICC-based synthesis of AmB. The potential of this glycosylation strategy for rapidly accessing AmB derivatives was also demonstrated in the synthesis of a C3'deaminomycosamine sugar donor and its efficient attachment to a protected amphotericin aglycone.

4-7 EXPERIMENTAL SECTION

Materials.

Commercial reagents were purchased from Sigma-Aldrich, Fisher Scientific, Alfa Aesar, TCI America Frontier Scientific, Oakwood Products or Combi-Blocks and were used without further purification unless otherwise noted. Solvents were purified via passage through packed columns as described by Pangborn and coworkers[19] (THF, Et_2O, MeCN, DCM: dry neutral alumina; hexane, benzene, and toluene: dry neutral alumina and Q-5 reactant (copper(II) oxide on alumina); DMSO, DMF: activated molecular sieves). All water was deionized prior to use. Triethylamine, diisopropylamine, diethylamine, pyridine, and 2,6-lutidine were freshly distilled under an atmosphere of nitrogen from CaH_2. The following compounds were prepared according to procedures reported in the literature: **4.3**,[5] **4.5**,[4-5] **4.6**,[4-5] **4.17**[9-10].

General Experimental Procedures.

Unless otherwise noted, all reactions were performed in flame-dried glassware under argon. Organic solutions were concentrated via rotary evaporation under reduced pressure with a bath temperature of 35-40 ºC. Reactions were monitored by analytical thin layer chromatography (TLC) performed using the indicated solvent on E. Merck silica gel 60 F254 plates (0.25mm). Compounds were visualized by: exposure to a UV lamp (λ = 254 or 366 nm), incubation in a glass chamber containing iodine, and/or treatment with a solution of $KMnO_4$, an acidic solution of p-anisaldehyde or a solution of ceric ammonium molybdate (CAM) followed by brief heating with a Varitemp heat gun. MIDA boronates are compatible with standard silica gel chromatography, including standard loading techniques. Column chromatography was performed using standard methods[20] or with a Teledyne-Isco CombiFlash R_f purification system. Both methods were performed using Merck silica gel grade 9385 60 Å (230-400 mesh). For loading,

compounds were adsorbed onto non acid-washed Celite 545 (app. 10 g/mmol crude product) in vacuo from an acetone solution. Specifically, in each case the crude residue was dissolved/suspended in acetone and to the mixture was added Celite. The mixture was concentrated in vacuo to afford a free flowing powder which was then loaded on top of a silica gel column. To ensure quantitative transfer, this procedure was repeated with a small amount of acetone and Celite to transfer any remaining residue.

Structural analysis.

^{1}H-NMR spectra were recorded at 23 °C on a Varian Unity or a Varian Unity Inova 500 MHz spectrometer. Chemical shifts (δ) are reported in parts per million (ppm) downfield from tetramethylsilane and referenced to residual protium in the NMR solvent ($CHCl_3$, δ = 7.26; CD_2HCN, δ = 1.93, center line; acetone-d_6 δ = 2.04, center line). Alternatively, NMR-solvents designated as "w/ TMS" were referenced to tetramethylsilane (δ = 0.00 ppm) added as an internal standard. Data are reported as follows: chemical shift, multiplicity (s = singlet, d = doublet, t = triplet, q = quartet, quint = quintet, sept = septet, m = multiplet, br = broad, app = apparent), coupling constant (*J*) in Hertz (Hz), and integration. ^{13}C NMR spectra were recorded at 23 °C on a Varian Unity 500 MHz spectrometer. Chemical shifts (δ) are reported in ppm downfield from tetramethylsilane and referenced to carbon resonances in the NMR solvent ($CDCl_3$, δ = 77.0, center line; CD_3CN, δ = 1.30, center line, acetone-d_6 δ = 29.80, center line) or to added tetramethylsilane (δ = 0.00). Carbons bearing boron substituents were not observed (quadrupolar relaxation). ^{11}B NMR were recorded using a General Electric GN300WB instrument and referenced to an external standard of ($BF_3 \cdot Et_2O$). High resolution mass spectra (HRMS) were performed by Furong Sun and Dr. Steve Mullen at the University of Illinois School of Chemical Sciences Mass Spectrometry Laboratory. Infrared spectra were collected from a thin film on NaCl plates or as KBr pellets on a Perkin-Elmer Spectrum BX FT-IR spectrometer, a Mattson Galaxy Series FT-IR 5000 spectrometer or a Mattson Infinity Gold FT-IR spectrometer. Absorption maxima (ν_{max}) are reported in wavenumbers (cm^{-1}).

Synthesis of compounds.

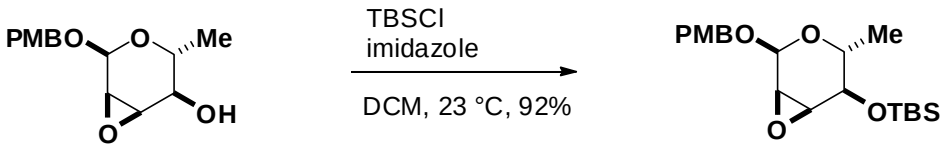

4.3 **4.7**

To a 1 L round bottom flask containing **4.3** and stir bar under argon was added DCM (325 mL) and DMF (65 mL) and the resulting mixture was stirred to homogeneity. To the mixture was then added sequentially imidazole (31.0 g, 491 mmol) and TBSCl (51.4 g, 341 mmol). The flask was fitted with a reflux condenser and, under argon maintenance, was stirred at 40 °C for 16 h. The reaction was cooled to room temperature and diluted with Et_2O (1 L) and sat'd aq $NaHCO_3$ (1 L). The aqueous layer was separated and extracted with Et_2O (500 mL). The combined organic fractions were washed with brine, dried over Na_2SO_4, filtered and concentrated in vacuo to give a white solid. The product was purified by DCVC[21] (hex:EtOAc, 20:1 → 3:1) to afford **4.7** as a white solid (40.0 g, 92%).

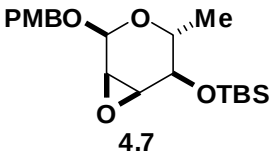

4.7

TLC (hex:EtOAc 4:1)

R_f = 0.35, stained with CAM

^{1}H-NMR (500 MHz, $CDCl_3$)

δ 7.30 (d, *J* = 8.5 Hz, 2H), 6.88 (d, *J* = 9 Hz, 2H), 4.92 (d, *J* = 3 Hz, 1H), 4.70 (d, *J* = 12 Hz, 1H), 4.54 (d, *J* = 12 Hz, 1H), 3.85 (m, 1H), 3.81 (s, 3H), 3.61 (dd, *J* = 8.5, 1.5 Hz, 1H), 3.41 (app t, *J* = 4 Hz, 1H), 3.25 (dd, *J* = 4, 1 Hz, 1H), 1.15 (d, *J* = 6 Hz, 3H), 0.911 (s, 9H), 0.140 (s, 3H), 0.110 (s, 3H)

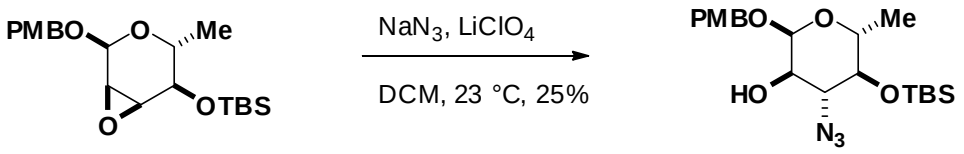

4.7 **4.2**

To a 2 L round bottom flask containing **4.7** (79.1 g, 208 mmol) and a stir bar was added MeCN. The resulting mixture was stirred to homogeneity. To the mixture was next added NaN_3 (27.05 g, 416 mmol), then $LiClO_4$ (110.67 g, 1040 mmol). The flask was fitted with a reflux condenser, and the mixture was stirred at 80 °C under argon maintenance for 24 h. The reaction was cooled to room temperature and diluted with Et_2O (2 L) and brine (1 L). The aqueous layer was separated and extracted with Et_2O (3×1 L). The combined organic fractions were dried over Na_2SO_4, filtered and concentrated in vacuo. The resulting crude material was purified in 2 batches by DCVC (hex:EtOAc 10:1 → 2:1). Mixed fractions were combined and re-purified in 3 subsequent cycles to yield the desired product as a yellow oil (22.31 g, 25%).

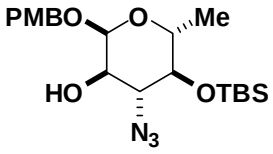

4.2

^{1}H-NMR (500 MHz, $CDCl_3$)

δ 7.28 (d, *J* = 8.5 Hz, 2H), 6.90 (d, *J* = 8.5 Hz, 2H), 4.87 (d, *J* = 4 Hz, 1H), 4.69 (d, *J* = 11.5 Hz, 1H), 4.46 (d, *J* = 11.5 Hz, 1H), 3.82 (s, 3H), 3.73 (m, 1H), 3.53 (m, 1H), 3.43 (t, *J* = 9.5 Hz, 1H), 3.02 (t, *J* = 9.5 Hz, 1H), 1.22 (d, *J* = 6.5 Hz, 3H), 0.907 (s, 9H), 0.182 (s, 3H), 0.097 (s, 3H)

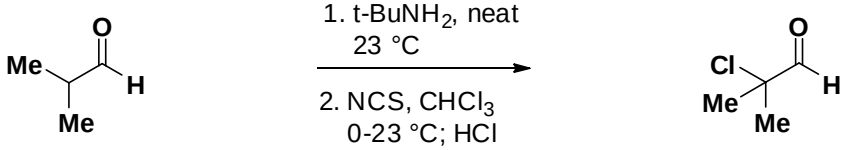

4.8 **4.9**

To a 100 mL flask equipped with a stir bar under nitrogen was added isobutyraldehyde (**4.8**) (10 mL, 110 mmol). The substrate was cooled with stirring to 0 °C, and to the flask was then added t-$BuNH_2$ (11.5 mL, 110 mmol). The resulting mixture was stirred at room temperature for 6 h. Chloroform (100 mL) and Na_2SO_4 were added, and the mixture was stirred for 15 min, then filtered into a 250 mL flask. A stir bar was added and the solution was cooled, stirring, to 0 °C. NCS (14.69 g, 110 mmol) was added in a single portion, the mixture was stirred at room temperature for 18 h. The reaction was then poured into H_2O (100 mL). The organic phase was separated and extracted with chloroform (50 mL). The combined organic fractions were washed with H_2O (50 mL), dried over Na_2SO_4, filtered and concentrated (rotovap bath at 23 °C) in vacuo. Conc. HCl (25 mL) was added, and the mixture was vigorously stirred for 6 h at room temperature. $NaHCO_3$ (ca. 30 g) was added, followed by chloroform (50 mL) and enough H_2O to dissolve the $NaHCO_3$ salts. The organic phase was separated, and aqueous phase extracted with chloroform (2×20 mL). The combined organic fractions were dried over Na_2SO_4, filtered and distilled at ambient pressure. Note: the desired product co-distills with chloroform, so 4.9 was thus isolated as a chloroform solution. 1H NMR enabled a calculation of the concentration, and thus the yield: 4.6 g, 39%. This solution of **4.9** was carried directly forward into the next reaction without further purification or characterization.

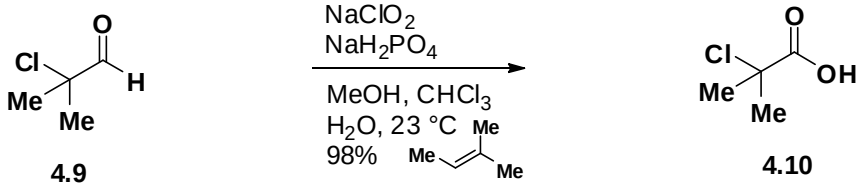

To a 1 L flask containing **4.9** (40.9 mmol in an 87 mL-solution of chloroform) and a stir bar was added MeOH (260 mL), H_2O (87 mL), 2-methyl-2-butene (43.5 mL), NaH_2PO_4 (22.588 g, 164 mmol), and $NaClO_2$ (7.409 g, 81.9 mmol). The resulting mixture was stirred briskly at room temperature for 5 h. The reaction was then diluted with 1M HCl (500 mL) and Et_2O (500 mL). The aqueous phase was separated and extracted with Et_2O (250 mL). the combined organic fractions were extracted with 1M NaOH (500 mL, then 250 mL). The combined basic aqueous fractions were then acidified with 3M aq HCl (750 mL) and extracted with Et_2O (3×500 mL). the

combined Et_2O fractions were washed with brine (500 mL), dried over Na_2SO_4, filtered and concentrated in vacuo to afford a pale yellow oil (4.92 g, 98%).

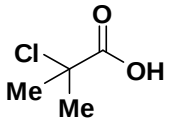

4.10

Spectroscopic characterization was consistent with literature reports.[22]

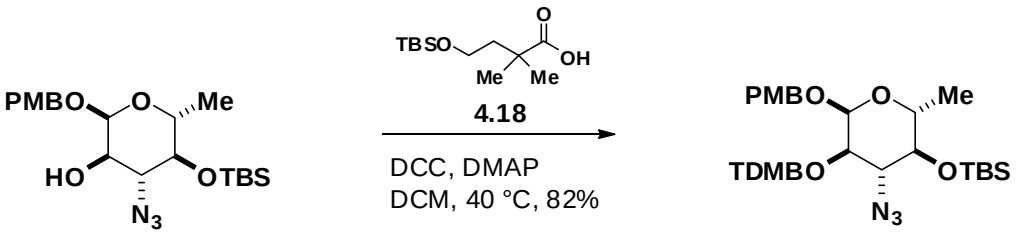

4.2 **4.19**

To a 250 mL flask containing **4.2** (4.08 g, 9.63 mmol) and a stir bar was added **4.18** (5.33 g, 19.2 mmol), DCM (32 mL), DCC (9.93 g, 48.1 mmol), and finally DMAP (2.35 g, 19.2 mmol). The flask was fitted with a reflux condenser and the mixture thus stirred at 40 °C for 36 h. The reaction was then cooled to room temperature and diluted with hexanes (ca. 250 mL) and filtered through a medium fritted glass funnel. The filtrate was washed with sat'd aq $NaHCO_3$ (50 mL). The aqueous phase was extracted with hexanes (100 mL). The combined organic fractions were dried over Na_2SO_4, filtered and concentrated in vacuo to give a yellow oil. This crude product was purified by DCVC (hex:EtOAc 50:1 → 10:1) to afford **4.19** as a colorless oil (5.18 g, 82%).

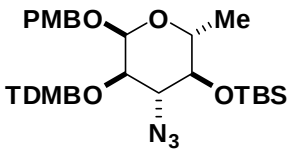

4.19

TLC (hex:EtOAc 10:1)

R_f = 0.40, stained with CAM

^{1}H-NMR (500 MHz, $CDCl_3$)

δ 7.25 (d, *J* = 9 Hz, 2H), 6.88 (d, *J* =8.5 Hz, 2H), 5.03 (d, *J* = 3.5 Hz, 1H), 4.60 (d, *J* = 11.5 Hz, 1H), 4.56 (dd, *J* = 11, 4 Hz, 1H), 4.39 (d, 11 Hz, 1H), 3.81 (s, 3H), 3.77 (dd, *J* = 10.5, 9 Hz, 1H), 3.72 (m, 1H), 3.65 (t, *J* = 7 Hz, 2H), 3.09 (t, *J* = 9 Hz, 1H), 1.82 (m, 2H), 1.22 (m, 9H), 0.905 (s, 9H), 0.873 (s, 9H), 0.171 (s, 3H), 0.098 (s, 3H), 0.029 (s, 3H)

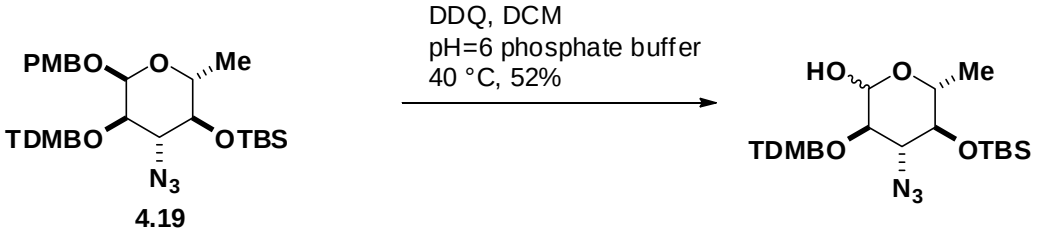

To a 1 L round bottom flask containing **4.19** (5.04 g, 7.73 mmol) and a stir bar was added DCM (135 mL), 1 M pH=6 aq phosphate buffer (27 mL), then DDQ (5.274 g, 23.2 mmol). The flask was sealed with a rubber septum and stirred vigorously at 40 °C for 36 h. Additional DDQ (1.75 g, 7.71 mmol) was added at 12 h and 24 h. The reaction was cooled to room temperature and diluted with sat'd aq $NaHCO_3$ (300 mL) and Et_2O (300 mL). The aqueous phase was separated and extracted with Et_2O (3×400 mL). The combined organic fractions were dried over Na_2SO_4, filtered, and concentrated in vacuo. The crude material thus obtained was purified by column chromatography (SiO_2, hex:EtOAc 10:1 → 4:1) to afford the hemiacetal as a mixture of anomers (2.15 g, 52%).

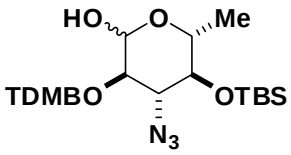

TLC (hex:EtOAc 5:1)

R_f = 0.33: Major anomer, stained with $KMnO_4$

R_f = 0.39: Minor anomer

^{1}H-NMR (500 MHz, $CDCl_3$)

Major anomer: δ 4.56 (dd, *J* = 11, 4 Hz, 1H), 4.39 (d, 11 Hz, 1H), 3.81 (s, 3H), 3.77 (dd, *J* = 10.5, 9 Hz, 1H), 3.72 (m, 1H), 3.65 (t, *J* = 7 Hz, 2H), 3.09 (t, *J* = 9 Hz, 1H), 1.82 (m,

2H), 1.22 (m, 9H), 0.905 (s, 9H), 0.873 (s, 9H), 0.171 (s, 3H), 0.098 (s, 3H), 0.029 (s, 3H)

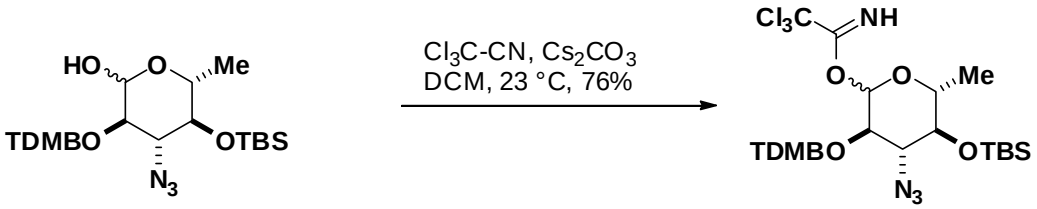

4.20

To a 250 mL round bottom flask containing the hemiacetal substrate (5.01 g, 9.42 mmol) and a stir bar under argon was added DCM (94 mL), trichloroacetonitrile (9.45 mL, 94.2 mmol) and Cs_2CO_3 (1.53 g, 4.69 mmol). The resulting mixture was stirred at room temperature for 1 h. The reaction was directly concentrated, and the resulting crude product purified by column chromatography (SiO_2, hex:EtOAc 10:1 isocratic) to yield **4.20** as a 2:1 mixture of anomers (4.83 g, 76%)

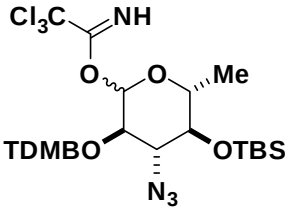

4.20

TLC (EtOAc)

R_f = 0.33, stained with $KMnO_4$

^{1}H-NMR (500 MHz, $CDCl_3$)

Major anomer: δ 8.62 9 (s, 1H), 6.42 (d, *J* = 3.5 Hz, 1H), 4.82 (dd, *J* = 10.5, 3.5 Hz, 1H), 3.87 (m, 1H), 3.78 (t, *J* = 10.5 Hz, 1H), 3.67–3.62 (m, 3H), 1.90–1.74 (m, 2H), 1.26 (d, *J* = 6 Hz, 3H), 1.21 (m, 6H), 0.91 (s, 9H), 0.87 (s, 9H), 0.10 (s, 3H), 0.03 (s, 3H)

Minor anomer: δ 8.65 (s, 1H), 5.86 (d, *J* = 8.5 Hz, 1H), 5.11 (dd, 1H), 3.55 (m, 1H), 3.45 (t, 10 Hz, 1H), 3.30 (t, *J* = 9 Hz, 1H), 3.20 (t, *J* = 9.5 Hz, 2H), 1.90–1.74 (m, 2H), 1.32 (d, *J* = 6 Hz, 3H), 1.21 (m, 6H), 0.92 (s, 9H), 0.87 (s, 9H), 0.20 (s, 3H), 0.12 (s, 3H)

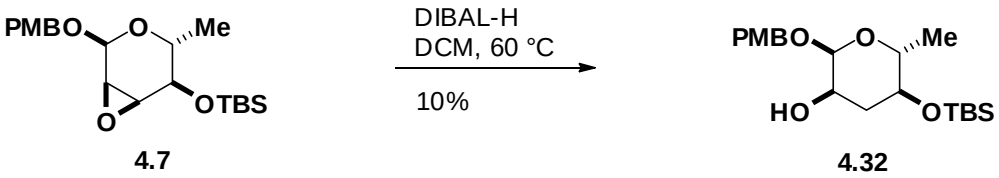

4.7 **4.32**

To a 40 mL I-Chem vial containing **4.7** (0.286 g, 0.75 mmol) and a stir bar under nitrogen was added DCM (15 mL) and DIBAL-H (1M solution in DCM, 2.25 mL, 2.25 mmol). The resulting mixture was stirred at 60 °C for 1 h. The reaction was cooled to room temperature, diluted with Et_2O (30 mL) and sat'd aq Na,K-tartrate (15 mL), then stirred for 3 h. The aq phase was separated and extracted with Et_2O (3×15 mL). The combined organic fractions were dried over $MgSO_4$, filtered, and concentrated in vacuo. The resulting crude product was purified by column chromatography (SiO_2, hex:EtOAc 5:1 → 3:1) to afford **4.32** as a colorless oil (28.7 mg, 10% yield). It should be noted that the epoxide opening appears to be completely selective under these conditions. The loss of yield is due to competitive desilylation at C4'.

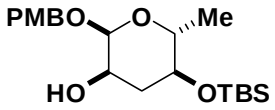

4.32

TLC (hex:EtOAc 3:1)

R_f = 0.43, stained with CAM

^{1}H-NMR (500 MHz, $CDCl_3$)

δ 7.28 (d, *J* = 10 Hz, 2H), 6.90 (d, *J* = 8.5 Hz, 2H), 4.79 (d, *J* = 3.5 Hz, 1H), 4.70 (d, *J* = 7 Hz, 1H), 4.46 (d, *J* = 11.5 Hz, 1H), 3.81 (s, 3H), 3.67 (dt, *J* = 12, 4 Hz, 1H), 3.57 (m, 1H), 3.26 (m, 1H), 2.10 (m, 1H), 1.69 (q, *J* = 11.5 Hz, 1H), 1.19 (d, *J* = 6 Hz, 3H), 0.878 (s, 9H), 0.067 (s, 6H)

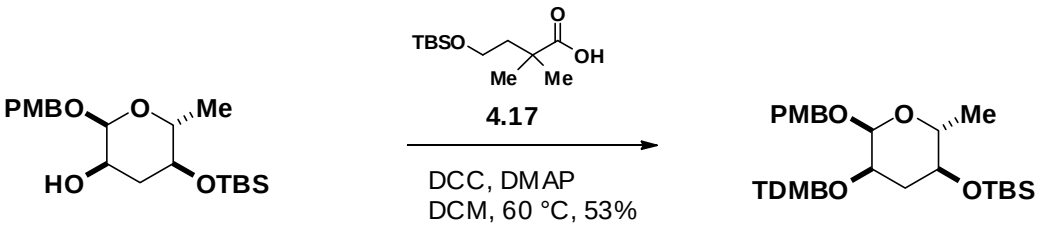

To a 7 mL vial containing **4.32** (0.0528 g, 0.138 mmol) and a stir bar was added **4.17** (0.068 g, 0.276 mmol), DCM, DCC (0.142 g, 0.688 mmol), and DMAP (0.034 g, 0.278 mmol). The resulting mixture was stirred at 40 °C for 24 h. After cooling to room temperature, the reaction was diluted with hexanes (4 mL) and filtered, then concentrated directly to a colorless oil, which was column purified (SiO_2, hex:EtOAc 40:1 → 20:1) to yield the TDMB-protected product as a colorless oil (44.8 mg, 53%).

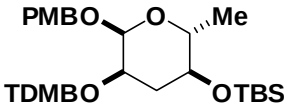

TLC (hex:EtOAc 1:1)

R_f = 0.76, stained with CAM

^{1}H-NMR (500 MHz, $CDCl_3$)

δ 7.27 (d, *J* = 9 Hz, 2H), 6.86 (d, *J* = 8.5 Hz, 2H), 4.87 (d, *J* = 3.5 Hz, 1H), 4.73 (m, 1H), 4.65 (d, *J* = 12 Hz, 1H), 4.44 (d, *J* = 11.5 Hz, 1H), 3.80 (s, 3H), 3.61 (m, 3H), 3.34 (q, 7 Hz, 1H), 1.96 (m, 2H), 1.80 (m, 2H), 1.19 (d, *J* = 6 Hz, 3H), 1.17 (d, *J* = 5 Hz, 3H), 0.874 (s, 9H), 0.865 (s, 9H), 0.067 (s, 3H), 0.063 (s, 3H), 0.015 (s, 6H)

4-8 REFERENCES

1. Nicolaou, K. C.; Daines, R. A.; Ogawa, Y.; Chakraborty, T. K. *J. Am. Chem. Soc.* **1988**, *110*, 4696–4705.
2. Szpilman, A. M.; Manthorpe, J. M.; Carreira, E. M. *Angew. Chem. Int. Ed.* **2008**, *47*, 4339–4342.
3. Szpilman, A. M.; Carreira, E. M. *Org. Lett.* **2009**, *11*, 1305–1307.
4. Guo, H.; O'Doherty, G. A. *Angew. Chem. Int. Ed.* **2007**, *46*, 5206–5208.
5. Croatt, M. P.; Carreira, E. M. *Org. Lett.* **2011**, *13*, 1390–1393.
6. Crimmins, M. T.; Carroll, C. A.; Wells, A. J. *Tetrahedron Lett.* **1998**, *39*, 7005–7008.
7. Yu, H.; Williams, D. L.; Ensley, H. E. *Tetrahedron Lett.* **2005**, *46*, 3417–3421.
8. Trost, B. M.; Hembre, E. J. *Tetrahedron Lett.* **1999**, *40*, 219–222.
9. Bartkovitz, D. J.; Chu, X.; Ding, Q.; Jiang, N.; Liu, J.; Ross, T. M.; Zhang, J. Substituted Pyrrolidine-2-Carboxamides. Patent WO2011098398 A1, 2011.
10. Berger, L.; Olson, G. L. (Hoffmann-La Roche Inc.). Pyrroloisoquinolinyl-dimethyloxoalkyl alkonoates and their use as antipsychotic agents. US Patent 4,732,902, 1988.
11. Szpilman, A. M.; Cereghetti, D. M.; Manthorpe, J. M.; Wurtz, N. R.; Carreira, E. M. *Chem.-Eur. J.* **2009**, *15*, 7117–7128.

12. Miljkovic, M.; Gligorijevic, M.; Miljkovic, D. *J. Org. Chem.* **1974**, *39*, 2118–2120.
13. Packard, K. P. Synthesis of the C8 to C13 Fragment of Candidin and Construction of a Rimocidin Aglycon and β-Selective Glycosylation with Mycosamine: Efforts towards Completion of the Total Synthesis of Rimocidin. Ph.D. Dissertation, University of California Irvine, 2001.
14. Packard, G. K.; Rychnovsky, S. D. *Org. Lett.* **2001**, *3*, 3393–3396.
15. Lee, S. J.; Anderson, T. M.; Burke, M. D. *Angew. Chem. Int. Ed.* **2010**, *49*, 8860–8863.
16. Struble, J. R.; Lee, S. J.; Burke, M. D. *Tetrahedron* **2010**, *66*, 4710–4718.
17. Klubnick, J. A., University of Illinois at Urbana-Champaign, 2011.
18. Palacios, D. S.; Anderson, T. M.; Burke, M. D. *J. Am. Chem. Soc.* **2007**, *129*, 13804–13805.
19. Pangborn, A. B.; Giardello, M. A.; Grubbs, R. H.; Rosen, R. K.; Timmers, F. J. *Organometallics* **1996**, *15*, 1518–1520.
20. Still, W. C.; Kahn, M.; Mitra, A. *J. Org. Chem.* **1978**, *43*, 2923–2925.
21. Pedersen, D. S.; Rosenbohm, C. *Synthesis* **2001**, 2431–2434.
22. Mandel, A. L.; La Clair, J. J.; Burkart, M. D. *Org. Lett.* **2004**, *6*, 4801–4803.